Progress in Oceanography 167 (2018) 164–233

Contents lists available at ScienceDirect

Progress in Oceanography

journal homepage: www.elsevier.com/locate/pocean

Wave modelling in coastal and inner seas

L. Cavaleri[a,*], S. Abdalla[b], A. Benetazzo[a], L. Bertotti[a], J.-R. Bidlot[b], Ø. Breivik[c], S. Carniel[a], R.E. Jensen[d], J. Portilla-Yandun[e], W.E. Rogers[f], A. Roland[g], A. Sanchez-Arcilla[h], J.M. Smith[d], J. Staneva[i], Y. Toledo[j], G.Ph. van Vledder[k], A.J. van der Westhuysen[l]

[a] Istituto di Scienze Marine – CNR, Venice, Italy
[b] European Centre for Medium-Range Weather Forecasts, Reading, UK
[c] Norwegian Meteorological Institute and the Geophysical Institute, University of Bergen, Norway
[d] US Army Engineer Research and Development Center, Vicksburg, MS, USA
[e] Escuela Politecnica National, Quito, Ecuador
[f] Naval Research Laboratory, Stennis Space Center, MS, USA
[g] BGS IT&E GmbH, Darmstadt, Germany
[h] Universitat Politecnica de Catalunya, Barcelona, Spain
[i] Helmholtz-Zentrum Geesthacht, Germany
[j] Tel-Aviv University, Israel
[k] Delft University of Technology, Delft, The Netherlands
[l] NWS/NCEP/Environmental Modeling Center, College Park, MD, USA

ARTICLE INFO

Keywords:
Water waves
Wave dynamics
Wind-wave interactions
Wave-current interactions
Wave forecasting
Wave measurements

ABSTRACT

In the long term development of the research on wind waves and their modelling, in particular of the inner and coastal seas, the present situation is framed with a short look at the past, a critical analysis of the present capabilities and a foresight of where the field is likely to go. After a short introduction, Chapter 2 deals with the basic processes at work and their modelling aspects. Chapter 3 highlights the interaction with wind and currents. Chapter 4 stresses the need for a more complete, spectral, approach in data assimilation. Chapter 5 summarizes the situation with a discussion on the present status in wave modelling and a look at what we can expect in the future.

1. Wave challenges in coastal and inner seas

a review of the present know-how, results, problems and expectations in this not large environment, but with a lot of connections to it

It is amply acknowledged that surface wind wave modelling has now achieved a high degree of reliability. Global modelling of the best operational centres regularly provide analyses and forecasts with an accuracy of a few percents; see, among others, http://www.ecmwf.int/en/forecasts/charts/obstat/?facets = Category,Satellite%20Data%3BParameter,Surface%20wind%20speed (wind speed) and http://www.ecmwf.int/en/forecasts/charts/obstat/?facets = Parameter,Wave%20Height (wave height) for the European Centre for Medium-Range Weather Forecasts (ECMWF, Reading, U.K.) and http://polar.ncep.noaa.gov/waves/validation/ for the National Center for Environmental Prediction (NCEP, Maryland, USA). Also in the medium range, forecasts are generally (but not always) reliable till one week in advance. This is due to the substantial improvements progressively achieved in meteorological modelling and, particularly in the middle range, to recent refinements in the physics of generation and dissipation of wind waves. Problems still exist and require attention, particularly in view of the growing acknowledgement of the role of wind waves in modulating all the exchanges at the air-sea interface (Cavaleri et al., 2012), and therefore having a basic role in determining the Earth climate. However, from the point of view of traditional wave applications, the general user can be quite satisfied.

This is not always the case in restricted (coastal and semi-enclosed) seas. The obvious affecting factors are the presence of land and associated orography, and, on purely marine terms, the presence of often extended areas of shallow waters. Land and orography substantially affect the wind fields, with immediate consequences on the evolution of the local wave fields. The presence of shallow waters, with different kinds of bottom, either rocky or sandy, and possibly covered with vegetation, mud or, in the Arctic Ocean, ice, complicates or changes which are the dominant processes at work, hence the relevance of the accuracy of the background information. In very shallow water

* Corresponding author.
E-mail address: luigi.cavaleri@ismar.cnr.it (L. Cavaleri).

https://doi.org/10.1016/j.pocean.2018.03.010
Received 27 September 2017; Received in revised form 12 February 2018; Accepted 15 March 2018
Available online 26 May 2018
0079-6611/

(kh < 0.5) the details of the bottom effects may become the dominant factors, especially with small grids with a high spatial resolution. On the application side, in limited depth areas the wave conditions may become the relevant information for, e.g., the local biological conditions, sea productivity and the corresponding proper management. At the larger end of the limited basins the so-called Arctic ocean should be included as well, its present dimensions when free of ice being comparable to some of the enclosed areas we regularly deal with, e.g., the Great Lakes of North America. The extra factor to be considered is obviously the waves-ice interactions.

An often emerging difference with respect to deep open waters is the relevance of currents. In the oceans, with the exception of well determined areas, most of the time and in most of the places the surface currents do not reach velocities as to substantially affect wave conditions (for the time being we purposely ignore the wave induced currents). Therefore also the frequent lack of accuracy in the details that characterizes most of the large scale circulation models is not likely to appreciably affect the local wave results, at least for waves of a certain dimensions, hence of general interest for most of the users. This is not the case close to the coast. Here quite often the currents (barotropic and baroclinic) are geographically enhanced reaching values that, if not considered, can lead to substantial errors in wave model results. This is more frequently the case in semi-enclosed seas, where the limited dimensions imply in general shorter wave periods than in the oceans, more sensitive to the influence of currents.

The interactions between waves and current act in both the directions, sometimes with a positive feed-back effect, forcing us on one hand to consider these interactions in their various facets, and on the other hand to pay much more attention to current modelling to achieve, as far as possible, the accuracy required for the one desired for wave model results. It is rather intuitive that, given the smaller time and spatial scales in the inner seas, the relevance of “smaller” (high resolution) details is high, and it implies a shortening of the reliable range of forecast. There are two reasons for this. On very general terms the smaller is an important detail, the more likely a forecast is to be affected by errors, because of the inaccuracies of the initial conditions and the imperfections of the model. More specifically for the coastal areas and semi-enclosed seas, the local conditions are much more sensitive than in the open sea to, e.g., a slight shift of the forcing meteorological pattern, either in space or time, with respect to the local geometry. When looking at the coastal meteorological surge, the phasing relative to astronomical tide becomes crucial, a simple time shift, of, e.g., three hours of the meteorological event possibly leading to completely different overall conditions on the coast. This implies a shortening of the useful range of forecast because the error is growing with range faster than in the open sea.

On the other hand, there is a steady growth of the already intense interest in the wave conditions in coastal areas, both at local and a more extended scale. Increasing maritime traffic, recreational activities, urban development, ecosystem restoration, renewable energy industry, offshore management, all push in this direction. The purpose of this paper is to frame the present situation in wave modelling in coastal waters and in the enclosed seas. We do not aim at a review of the existing literature (a daunting task), but rather to touch the main subjects of relevance in coastal and semi-enclosed sea wave modelling, citing sufficient examples of the relevant literature. The emphasis will be on the problems that still affect this topic. We stress the physics involved, and in turn this will imply to touch, but not to dig in, the field of meteorological and circulation modelling because of the tight coupling in a spatially limited environment. Similarly we stress the importance of wave-bottom interactions, but we do not go into details as this would open the door to sediment transport, a subject that would easily require another extensive paper to frame the related situation. All this will be complemented with an extensive range of applications, both to frame the possible accuracy and to call the attention, via the use of different models for the same event, to the differences and difficulties we still find in practical applications.

Based on this approach the paper is structured as follows.

In Chapter 2 we deal with the basic processes at work, analysing the various modelling aspects that lead to, and condition, the final results.

In particular Section 2.1 analyses the reasons why the wind model input information are likely to be less correct than in the open ocean. We also stress the higher variability and that very high wave conditions are possible also in enclosed seas.

Section 2.2 deals with the basic aspects of wave modelling in this relatively restricted environment. It explains the reasons for the greater difficulty to obtain good results compared to the open sea.

Section 2.3 focuses more on this aspect, detailing the physics involved.

In Section 2.4 we leave physics (partially) aside to discuss the crucial aspect of any numerical model, its numerics, i.e. how the various equations are integrated in space and time. Although the models are (partially) built with some self-control mechanism, we stress that every user should be aware of the approximations involved, and of the consequent likely accuracy of the final results.

Section 2.5 focuses on a crucial aspect of the validation of our model results, i.e. the accuracy of the measured data we use to compare with. While we touch most of the main instruments at use in the world, we devote quite a bit of attention to buoys. These have been for decades the almost official reference for the calibration of other instruments, especially from satellites. For this reason we devote quite a bit of space to this analysis, just to make the unaware wave modeller aware of the implied approximations.

Section 2.6 deals with applications. We have chosen a number of examples from quite different environments to highlight the various problems we (may) face in practical use and the accuracy we can expect in the various conditions.

In Chapter 3 we abandon the view of modelling waves as an isolated process, and we deal with the interaction with the two media waves involve when moving.

Section 3.1 deals with the interaction with sea currents, and how wave and currents interact with mutual and feed-back effects. We show this in a number of examples in quite different environments.

In Section 3.2 we extend this mutual interaction also to the atmosphere. This interaction can be particularly intense in coastal waters due to the enhanced effects associated to orography and limited coastal depths. The extensive citation of the existing literature is a clear proof of the complexity of these three-component interactions, exemplified in a number of cases.

Chapter 4 discusses data assimilation in enclosed seas. While the described principles are quite general, we highlight the related problems in this specific environment. In particular we stress that long term used approaches, as e.g. Optimal Interpolation, are generally not suitable for the constrained geometry of the enclosed seas. Therefore we focus our attention on a spectral approach that two examples show to be more suitable, especially for a complicated geometry.

In Chapter 5 we make an extensive summary of the situation. We discuss the quality of the present approaches, the reliability of the results, and what we must be aware of when modelling waves in enclosed seas. We also make an outlook into the future discussing the expected or likely developments, which problems are technical, hence with a foreseeable development, and which are physical, when knowledge and theory are not necessarily moving at a regular pace.

The bibliography is quite comprehensive, each Chapter and Section requiring its own share of know-how and historical and modern developments. Here below we provide a list of the most common and repetitively used acronyms with their meaning.

Being the product of multiple contributions, there is not a unique

style of writing. While an effort of homogenization has been done, unavoidably each master hand leaves a different trace. More importantly, the development of the paper follows a logical flow, in a way from relatively simple to more complicated matters. So a full reading makes sense, but it is not strictly necessary. Each Chapter and Section stand by themselves.

As expected, and being the product of a community of wave modellers, there is an ample list of authors. Different specializations and contributions are reflected into the authors of each Section. Some more names may be listed here meaning some specific limited contributions. Questions, discussion and requests can be addressed to the first author of each Section (e-mail address provided).

Acronyms

ADCP	Acoustic Current Profiler
CESM	Community Earth System Model
COAWST	Coupled Ocean Atmosphere Wave Sediment Transport
CTD	Conductivity, Temperature, Depth
DA	Data Assimilation
ECMWF	European Centre for Medium-Range Weather Forecasts
ECWAM	ECMWF WAM
ESA	European Space Agency
ISMAR	Institute of Marine Sciences
FNMOC	Fleet Numerical Meteorology and Oceanography Center
GLW	Great Lakes Wave forecasting system
GTS	Global Telecommunication System
IMLE	Iterative Maximum LikElihood
ITOP	Impact of Typhoons on the Ocean in the Pacific
JCOMM	Joint technical Commission for Oceanography and Marine Meteorology
JONSWAP	JOint North Sea Wave Project
KNMI	Koninklijk Nederlands Meteorologisch Instituut
LC	Langmuir Circulation
LTA	Lumped Triad Approximation
MEM	Maximum Entropy Method
MLM	Maximum Likelihood Method
MSE	Mild Slope Equation
NCEP	National Center for Environmental Prediction
NDBC	National Data Buoy Center
NEMO	Nucleus of European Modelling of the Ocean
NOAA-NCEP	National Ocean Atmospheric Administration – National Center for Environmental Prediction
NWP	Numerical Weather Prediction
NWPC	Numerical Weather Prediction Centres
NWPS	Nearshore Wave Prediction System
PE	Parabolic Equation
OI	Optimal Interpolation
QA	Quality Assurance
QC	Quality Control
rmse	root mean square error
RA	Radar Altimeter
ROMS	Regional Ocean Model System
SAR	Synthetic Aperture Radar
SHOWEX	SHOaling Wave EXperiment
SPB	Stochastic Parametric Boussinesq
SWADE	Surface Wave Dynamics Experiment
SWAN	Simulating WAves Nearshore
TKE	Turbulent Kinetic Energy
UKMO	U.K. Meteorological Office
USACE	United States Army Corps of Engineers
WAE	Wave Action Equation
WAM	WAM wave model
WCI	Wave-Current Interactions
WFO	Weather Forecast Office
WMO	World Meteorological Organisation
WWIII, WW3	WAVEWATCH III wave model
WRF	Weather Research and Forecasting model

2. Wave modelling

where we make a panorama of the present situation in coastal and enclosed seas, starting from meteorology, physics and numerics, ending with a keen discussion on the data we use for validation. Specific examples of application help to focus the problems we still face today

Nowadays we are used to rely heavily on weather forecast and the derived quantities. Wind, temperature and precipitation are the main relevant information of interest on land. On the contrary, granted the relevance of the overall situation, waves are the crucial factor conditioning all our sea activities, often reaching a dangerous level. It is therefore not surprising that wave analysis and forecast have received so much attention since the second world war. Starting with the physical approach by Miles (1957) and Phillips (1977), and following the basic concept of energy balance equation (Gelci and Cazalé, 1962), the last sixty or so years have witnessed a continuous intense improvement. Cavaleri et al. (2007) provided a thorough picture of the situation, also hinting at the expected further developments in the near future. As pointed out in this cited paper, there have been moments of rapid advancement followed by periods of consolidation, the new findings being quickly implemented in the operational and research models. Unavoidably the rate of improvement has decreased in time while our models are becoming better and better, slowly approaching the sort of ideal we can have in our mind (but there are almost certainly still problems to be discovered as we become more and more demanding in our search for perfection). On the whole we can be quite pleased with the results. See the statistics of, among others, ECMWF and NOAA/NCEP cited in the previous section.

In the inner seas, judging from the quality of the results, we seem to be late in this rate for improvement. Errors are more frequent in wave height, period and direction, timing is more approximate. There are two basic reasons for this. On one hand the meteorological input, the frequent culprit invoked by wave modellers, is less accurate than in the open oceans. The geometry of the coasts and the frequently complicated orography take their toll. In a limited fetch, in coastal areas, in general in an enclosed sea, a small difference of the wind direction can lead to drastically different wave results. Still on the geometrical side, small islands or shallow zones become important, but they are frequently not correspondingly well-represented, with their characteristics, in the wave model. On the other hand, while, granted the storm belts, the open ocean is characterized mainly by swell, the inner seas are often dominated by wind sea. In a general sense, swell is an established situation, and most of the times the related essential operation in wave modelling is advection. Ardhuin et al. (2010) pointed out the possible attenuation of swell over long distances mainly due to the interaction with the adjacent atmospheric surface boundary layer. However, we can call this a second order effect, probably also less relevant in the inner seas where the distances are reduced with respect to the open space of the oceans. Inner basins are characterized mainly by wind sea, that in a way can be considered as a transient situation, or at least something whose dynamical state is established by the dynamical balance of all the main “forces” (input by wind, breaking and dissipation, non-linear interactions) acting on the field. This is much more difficult for a correct quantification in space and time.

In this section we discuss the various aspects affecting the performance of our wave models in enclosed seas. After analysing (Section 2.1) the role of meteorology and the related problems, especially in coastal areas, we focus first on deep water (Section 2.2) quantifying the present accuracy in the inner seas areas compared to the oceans. Then

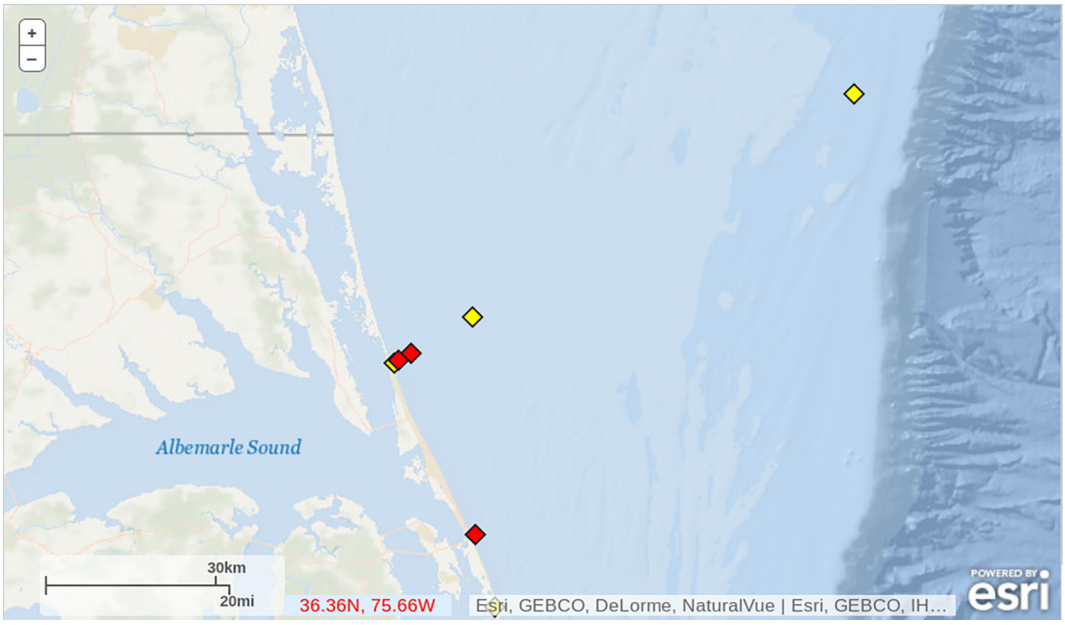

Fig. 2.1. Location of the USACE Field Research Facility on the outer banks of North Carolina, USA. The symbols show the positions of the pier (561 m long) and the measuring buoys.

we move to shallow water (Section 2.3) pointing out the additional processes that in this environment affect the energy balance of the wave systems. In (Section 2.4) we go into the details of wave modelling in these specific conditions, discussing the various approaches and the related problems and accuracy. Data availability and the associated accuracy and reliability are analysed in (Section 2.5). Finally, in (Section 2.6) we present practical applications as examples of the various mentioned aspects relevant for the accuracy of the final results.

2.1. The meteorological factor

R.E.Jensen, L.Cavaleri
Robert.E.Jensen@usace.army.mil

where we describe the differences between oceans and enclosed and coastal sea conditions, and the problems to be faced for their modelling. Specific examples are given with, wherever available, a quantification of the possible errors.

The meteorology defining winds for coastal and semi-enclosed water bodies increases in complexity from its deep water, open ocean counterpart. Synoptic-, meso- and micro-scale meteorological features have often a larger, impact on the coastal wave climate than they do in a deep, unrestricted open ocean body. Approaching the coastal domain, factors such as the land/sea interface, effects resulting from orography (differential elevation changes, e.g. mountains, cliffs), and sheltering effects (e.g. natural vegetation coverage, structures) may transform a coherent field into a complicated structure. Diurnal oscillations resulting from land-sea breezes will cause daily oscillations and directional shifts (see, among others, Stockwell et al., 2004, and Gemmrich and Garrett, 2012). In the upper latitudes *williwaws* (katabatic process) originate in the snow and ice fields of the coastal mountains where the building up of high density cold air causes the air to flow downwards warming adiabatically as it descends at increasing speed. A similar effect, although at much warmer latitudes, has been reported by Langodan et al. (2014a,b) in the Red Sea. Pierson (1983) suggested many more examples in the scaling of the motions in meteorology, while Fujita (1981) cited 14 different ways to categorize these various scales. Cavaleri et al. (2012) qualitatively summarize the processes that characterize the air-sea interface.

Unlike in the open ocean, the coastal and inner sea domains are often bounded in up to three of their four directions. These regions are bounded by land masses, by a frequently limited depth (at least close to the coast), and in some cases by large-scale current patterns, (e.g. the Gulf Stream and the Florida Current). All of these will have an impact on the air-sea interface, hence affecting the local winds or the wave conditions. Along the US east coast, Appel et al. (2005) objectively quantified the climatology of the Carolina fronts. These systems are the result of dominant high pressure systems located in the northeast of the US, the Gulf Stream providing the source of heat and moisture, and the mountains assisting the southward advance of cold air. This leads to the creation of a natural baroclinic zone near the coast, called a Cold Air Dam (Doyle and Warner, 1993). In structure these systems resemble shallow quasi-stationary or warm fronts with temperature differences that can reach 10 °C over short distances on the order of 100 km or less (Bosart, 1975). These systems provide a source of surface convergence and vorticity that often lead to the generation of cyclogenesis. The classical and most notable miss-forecast is an early degradation of the Cold Air Dam and the consequent migration of the front inland. This can result in temperature errors up to 10° and wind direction differences of up to 90°.

Apart from these “synoptic” examples, the coastal zone is frequently characterized by strong gradients of the surface wind fields. With the recent push towards wind energy resources there have been many field campaigns monitoring wind in the extended coastal zone, the related effects of atmospheric stability, and the land-sea breeze systems (Barthelmie, 1999; Smedman et al., 2003; Fredereickson and Davidson, 2003). In this respect an almost permanent study has been and is the one carried out at the USACE Field Research Facility located on the same US east coast (see Fig. 2.1). There have also been multiple field experiments carried out in the area (SWADE, Wang et al., 1994; DUCK94, Birkemeier and Thornton, 1994; SHOWEX, Graber, 2005, Plant et al., 2005). Here continuous data were obtained from two relatively close operational sites. The land-based NOS Station DUKN7 is located at the end of the pier (~561 m, at 15 m height, http://tidesandcurrents.noaa.gov/stationhome.html?id = 8651370). The offshore site is the NOAA/NDBC 44014 buoy (http://www.ndbc.noaa.gov/station_page.php?station = 44014) located approximately 95 km from the coast in about 95 m depth. The anemometer is at +5 m above the sea surface.

It is instructive to conduct a qualitative examination to see how

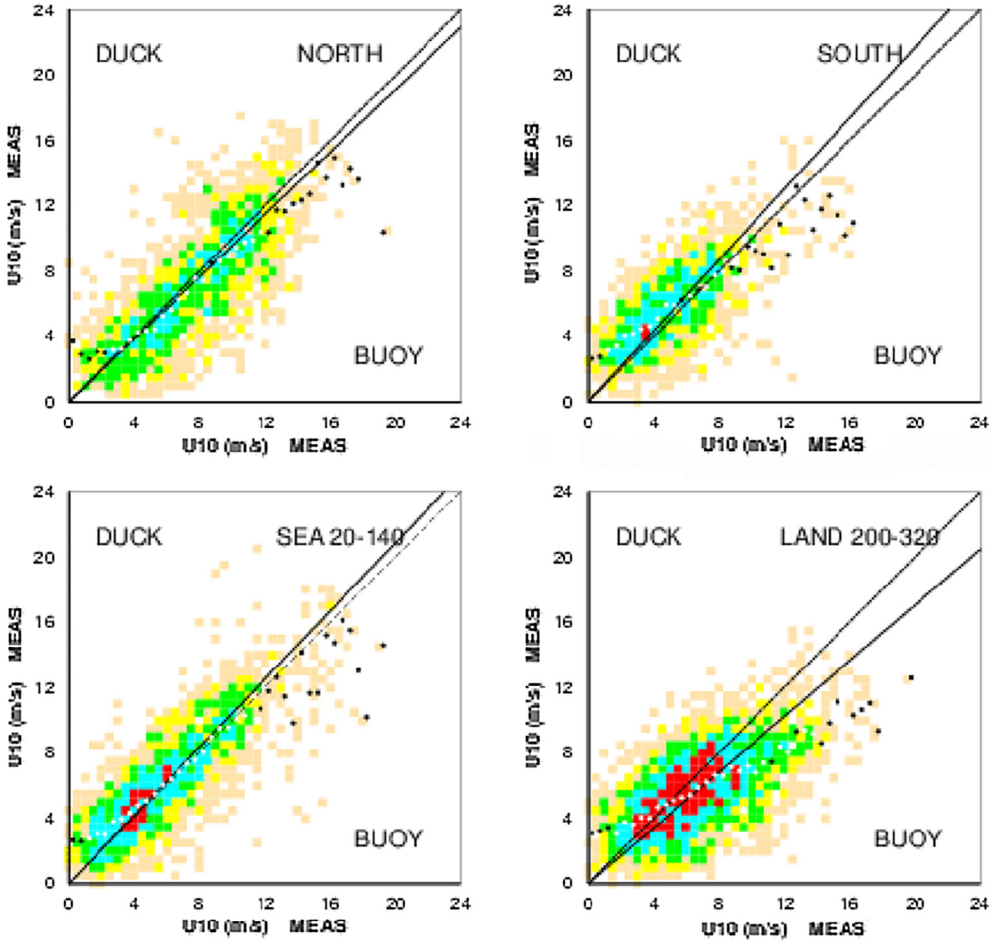

Fig. 2.2. Comparison between the wind speeds measured at the buoy 95 km off the North Carolina, US, outer banks and the meteo station at the end of the Duck 561 m long pier. The comparison is shown for different incoming directional sectors. The coast is turned about 10° counterclockwise with respect to the north–south direction. All the values moved to neutral conditions ten meter height. Incoming directions are considered.

similar or different the winds are at these two sites. Both the winds have been transformed to equivalent neutral stable 10 m wind estimates using the $z^{1/7}$ law (z height above the sea). Together with neglecting the actual air-sea stability conditions, this is a crude approximation, but that we consider suitable for some general considerations. Even looking at the sustained wind cases only, when both the recorded winds are basically depending on the general synoptic situation, we find differences that cannot be justified by the distance between the two stations. On average the offshore winds are 5% stronger. However, the situation is strongly direction dependent. In Fig. 2.2 the comparison, as wind speed scatter diagrams, is shown for four incoming directions choosing two 120° sectors centred on the perpendicular to the coast ("sea" and "land" respectively) and the two remaining 60° sectors for winds loosely parallel to the coast. Then we see that the above 5% is the average of quite different situations. For "north", "south" and "sea" there is a limited positive difference pier-buoy that however we consider within the above mentioned approximation. The large difference, 15%, buoy-pier is for offshore blowing winds. Note in particular that the differences increase for the larger value range. The possible explanation is the different surface friction on land (soon to be discussed) and the sea. This implies that, when wind enters the sea, there is the development of a new surface boundary layer and a progressive increase of the surface wind speed, reaching the new higher equilibrium value after a few tens of kilometres. Cavaleri and Bertotti (1997) provide evidence of this process, statistically analysing the winds from the meteorological model of the European Centre for Medium-Range Weather Forecasts (ECMWF, Reading, U.K.). In the case of Duck the effect is partly unexpected because Duck is on the North Carolina outer banks, with a relatively narrow strip of land enclosing a large lagoon. So there is not really land onshore of the pier. However, the much younger wind waves created by the sustained wind in the lagoon offer a much greater stress to the blowing wind, not as much as on land, but certainly more than the well-developed waves 95 km offshore. Differences exist also on direction and, remarkably, mainly for the offshore blowing wind (for the other directions the values are more similar). In this case, the most numerous one, there is on average a 20°counterclockwise turn by the time the wind reaches the buoy. Speculation into this disparity can only be made on the base of the local geography. However, the fact that we need to analyse the local reasons for the onshore-offshore differences is a strong indication that the wind characteristics in a given area are locally specific and need therefore to be carefully analysed place by place if accurate model estimates are required.

Another instructive comparison is among the winds recorded at three different stations in the Northern Adriatic Sea (Fig. 2.3). The stations are the offshore oceanographic tower of the Institute of Marine Sciences (ISMAR, Venice, Italy), 15 km from the coast in 16 m water depth, the anemometer at a local minor airport, 100 m from the beach on a narrow island bordering a large inner lagoon, and the instrument at the Venice international airport, about 10 km from the sea border, but at the inner edge of the cited lagoon. The three positions are marked in panel c. Long term experience (see Cavaleri, 2000) shows that in any wind condition the tower wind speed is substantially larger than the "land" data, with a progressive decrease towards "inland". The "." stress

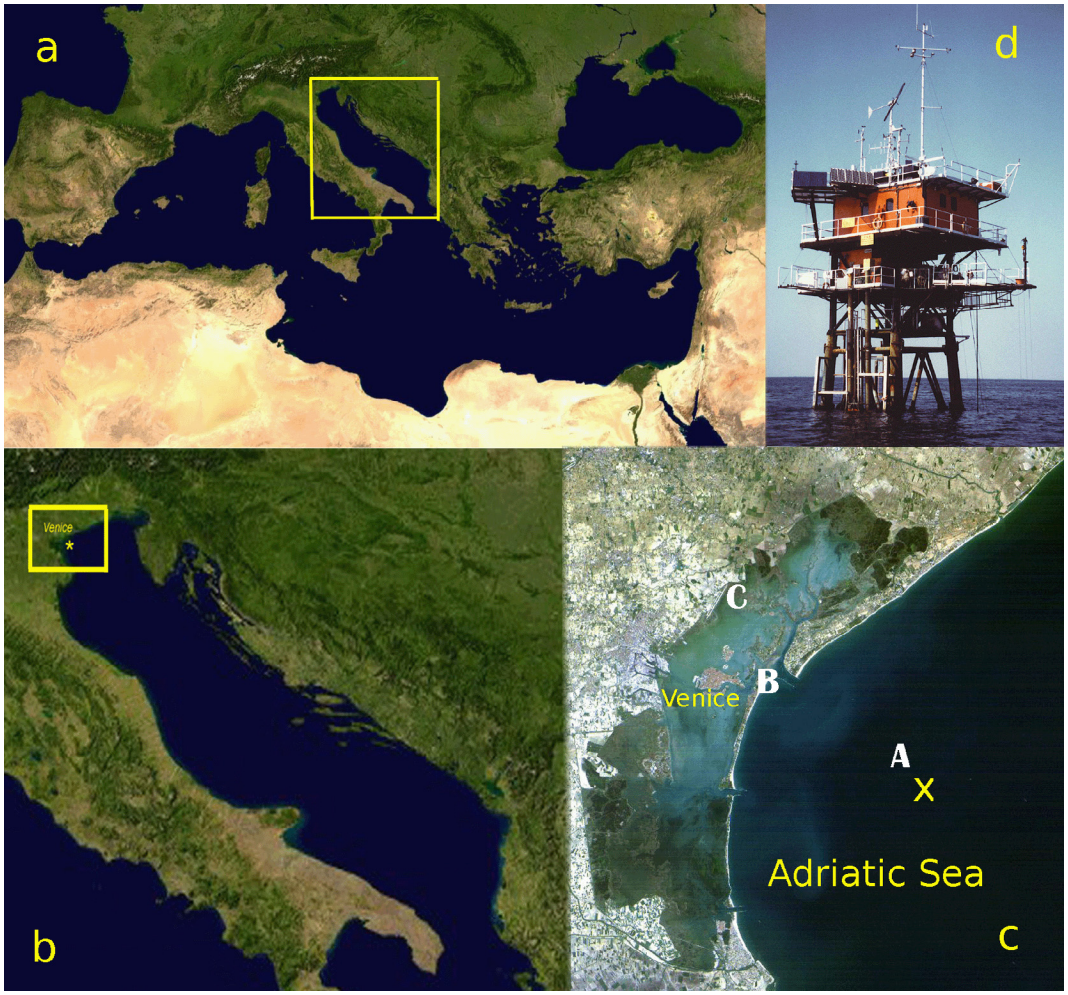

Fig. 2.3. (a) Mediterranean Sea, (b) Northern Adriatic Sea, (c) the area of, and in front of, the Venice lagoon. (b) and (c) progressive enlargements of the framed area. A, B, C mark the positions of the ISMAR oceanographic tower and the two meteo stations cited in the text. (d) The oceanographic tower.

that this is not simply due to a different surface friction on the sea and on land. Indeed, similarly to the Duck case, with the exception of the narrow island where the minor airport is located, the wind is blowing on the water of the lagoon till the international airport. The sirocco wind, the one responsible for the floods of Venice, blows perpendicularly to the local coast. Nevertheless differences up to 30% have been found with respect to the tower data. Again the point, similar to the Duck case, is that the shallow water of the lagoon (average depth $<$ 1 m) and, to a minor extent, the decreasing sea depth towards the beach imply a lot of breakers (waves in the lagoon are very young because c_p/U_{10} is small, with c_p the peak phase velocity and U_{10} the 10 m wind speed). This leads to an increased surface friction, hence slowing down of the ten meter wind speed.

The differences between offshore (at the tower position) and close to the coast become even more marked with the classical bora, a strong gusty wind blowing from north-east parallel to the coast (see Fig. 2.3). The across variability of the wind speed is also enhanced by the jet characteristics of the bora, hence showing a strong transversal gradient. This wind blows also parallel to the larger dimension of the lagoon (50×10 km). Beside the wind speed reduction, in these cases the local extended surface stresses due to the extreme very short choppy sea are manifest in the water level in the lagoon, when the level at its southern end turns up to be up to one meter higher than at the other extreme.

More in general, whenever the wind passes from land to sea, there is a progressive decrease of the surface friction felt by wind, hence an acceleration of the wind speed up to the new equilibrium value. The problem, as cited above, is that the meteorological models are too slow in reacting in this respect, with a consequent underestimate of the wind speed in the first 100 or 200 km off the coast, depending on model resolution (the higher, the better). This sorted out a long standing problem of explaining why, with offshore blowing winds, on the US east coast the offshore buoys data were showing correct model wind speeds, but underestimated wave heights. While carefully verified for ECMWF, the problem seems to be, albeit at different levels, a feature of most meteorological models. The only practical solution seems to be an increase of the model resolution, that leads to both a decrease of the spatial extent and of the level of the underestimate.

All this is evident, although not the only reason, when comparing the performance of the ECMWF global meteorological model in the ocean and in the Mediterranean Sea (an example of inner, although not small, basin). Cavaleri and Bertotti (2006) have explored how the mean and maximum values of the wind and wave fields vary on average with the resolution of the meteorological (and corresponding wave) model. Their results, updated with the latest resolutions, are shown in Fig. 2.4. The horizontal scale shows the spectral resolution TL, corresponding to 40,000/(2 * TL) km spatial resolution. (TCO is the latest model with 9 km resolution; see Malardel et al., 2016, for details). We comment here on the meteorological models. The problems with waves will be dealt with in the next section.

It is clear that, while the mean values (panel a) in the oceans (northern and southern hemispheres, plus the tropics) are practically asymptotic, the ones in the Mediterranean are still climbing (but note

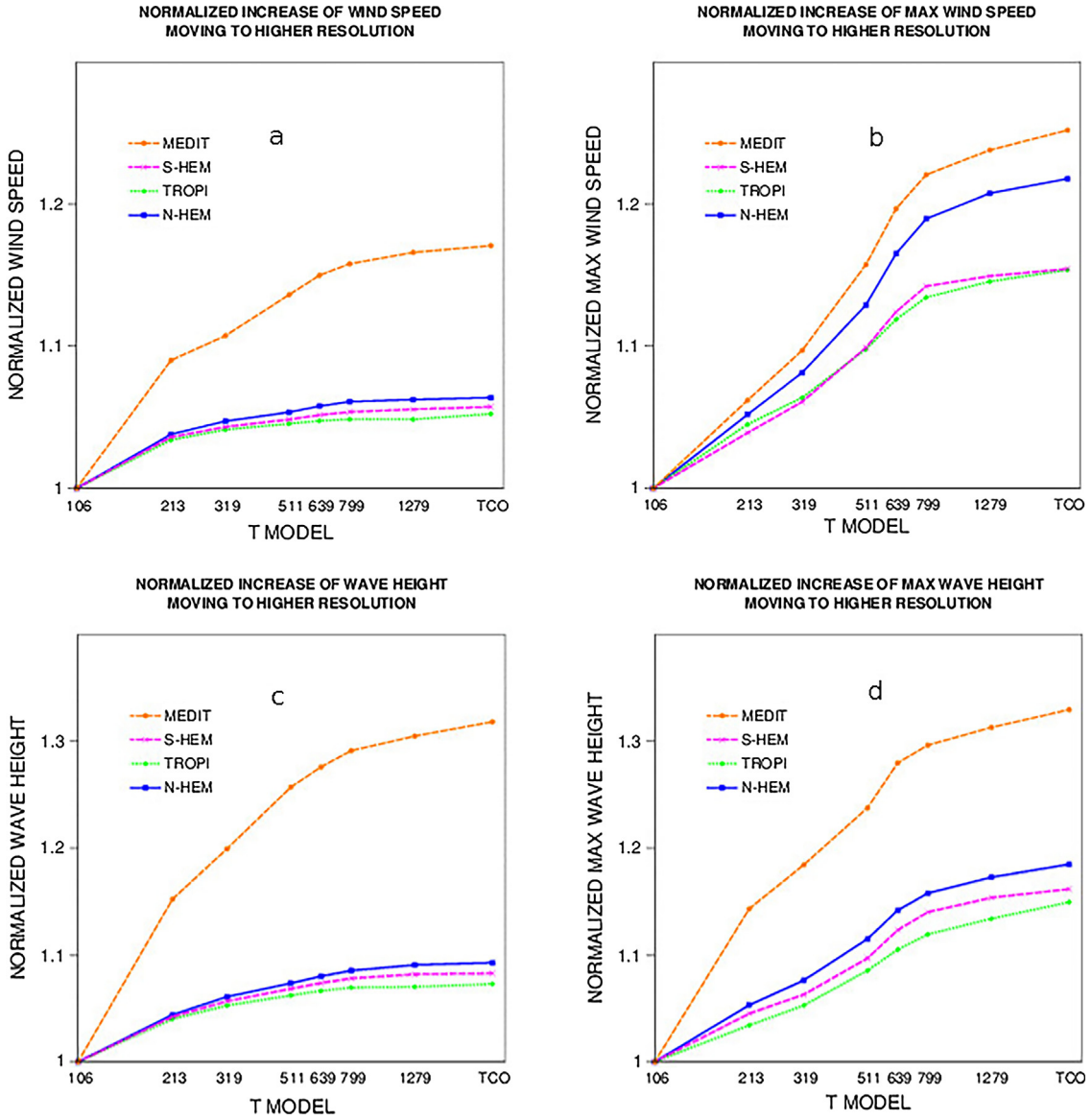

Fig. 2.4. Average increase of the (a, c) mean and (b, d) maximum wind speeds and significant wave heights in the northern and southern hemispheres, in the tropics and in the Mediterranean Sea. Upper panels for wind, lower panels for waves. The horizontal scale shows the spectral resolution of the ECMWF meteorological model (see text for details). For each resolution the results are normalized with respect to the T106 ones. The wave model resolution for these tests was the same till T511, then progressively increased parallel to the resolution of the meteorological model, up to the present 14 km.

the compressed horizontal scale in the upper resolution range). This strongly indicates that we are still not close to a fully satisfactory solution for the inner seas.

The conclusions are slightly different for the maximum values in the field (panel b). Here, although different from basin to basin, all the maxima were 'exploding' moving to higher resolution, a strong indication that till T799 (25 km resolution) we were not yet able to pick up the physics and the processes at the heart of the storms and hurricanes. Beyond this resolution we seem to be approaching the solution, although we still see an evident increase when, as done in March 2016, the ECMWF resolution passed from 16 to 9 km.

On a more local scale the orography of the coast can have dramatic effects on the local wind field. A classical case is the presence of a coastal jet running parallel to a coast. Barrier jets occur when a stable onshore flow interacts with a mountain barrier, but the flow is too stable to rise over the barrier. The dynamic response is for the ascending air to cool and generate a hydrostatic positive pressure perturbation which forces a turning of the wind (to the left) along the barrier (in the northern hemisphere – the other way around in the south). This flow is then rotationally trapped against the barrier and a barrier jet results (Winstead et al., 2004; Loescher et al., 2006).

In the case of an offshore flow the local mountains and valleys lead easily to strong jets that exit the coast as strong concentrated flows. Classical examples are the Tehuano winds in the gulf of Tehuantepec (Mexico, see Garcia-Nava et al., 2009), the mistral on the Mediterranean French coast, the mentioned bora in the Adriatic Sea along the valleys that cut the Dinaric Alps of Croatia, and the Panama jet in the Colombia Pacific (Portilla et al., 2015). Most of these winds have been studied for many decades. Gap winds, coastal wind jets, or Bernoulli winds have been studied, among others, by Mass et al. (2014), Isoguchi and Kawamura (2007) and Zingone and Hufford (2006) using Synthetic Aperture Radar (SAR) images. These complex features can extend outward in the ocean for hundreds of kilometres, resulting not only in lobes of intense wind speeds, but also in large transversal gradients in the wind speed distribution.

Embedded in coastal wind records is a diurnal oscillation in the winds caused by land-sea breeze effects. These cells originate from the differential temperature gradient caused by the land and water heating

or cooling at different rates. During the day sea breezes (onshore flow) will result; during the night land breezes (offshore flow) will be in control. It has been documented that the seaward extent of these cells ranges from kilometres to over 100 km, see, e.g., for a large extent example Langodan et al. (2014a,b). Gille et al. (2005) found that the strength of the diurnal wind cycle is statistically significant reaching far into the deep oceanic basins of the world. This phenomenon has been studied, modelled (Jiang, 2012; Steele et al., 2013; Colby, 2004), and quantified in point source measurements (Tsujimoto and Koike, 2013; Barthelmie et al., 1996; Zhu and Atkinson, 2004), or mining daily satellite wind observations (Gille et al., 2005). The intensity of the sea breezes, up to 10 m s^{-1}, and their extent in the coastal seas imply that they should be properly represented in meteorological models. For the more limited extents, of the order of ten kilometres or so, the global models have an obvious problem of resolution. While the solution is in local high resolution modelling, care is required in choosing the optimal balance (for what breezes are concerned). Indeed the effects of grid resolution have been estimated by Colby (2004). The surprising conclusion from this study is that beyond a certain resolution a smaller grid spacing produced larger errors when compared to observations. This is due to the so-called 'double penalty effect', i.e. when the details represented by the model are not supported by sufficient measured data. In practice the model is physically sound, but not deterministically correct.

We have cited above how the local wave characteristics can affect the local wind conditions. More in general, the land/sea interface has been studied to determine changes in surface roughness, momentum transfers, and ultimately leading to a net change in the growth characteristics of wind-generated waves. The transfers of momentum across this interface is very complex (see, e.g., Janssen, 1991, 2004), varying on temporal and spatial scales spanning orders of magnitudes. Wave age (defined as c_p/u_* or c_p/U_{10}, where u_* is the friction velocity) is the key parameter in establishing the kind and level of interaction across the interface. This is particularly intense, in both directions, between a generating wind and a young wind-sea. Therefore the related complexities are further increased in the coastal and inner seas. In arbitrary water depth (defined as non-deep water), wave related mechanisms, like shoaling, refraction and depth-induced wave breaking will change the wind characteristics. Sun et al. (2001) found that in an offshore blowing wind the stress over the coastal water can be influenced by a strong turbulence advected from land. Further studies on coastal air-sea fluxes (Frederickson and Davidson, 2003) found these regions to be far more complex than their deep water open ocean counterparts.

The possible interaction with the underlying wind fields opens a full perspective of possible interactions, that we will partly deal with in the section on coupling. A cause of concern when working on a coastal area facing a large enough expanse of water is the possible presence of swell propagating towards the coast and against the local wind and wind-sea. These conditions have been well illustrated by both Flamant et al. (2003) and Garcia-Nava et al. (2009), working respectively in the Gulf of Lion with mistral wind (North-Western Mediterranean Sea) and the Gulf of Tehuantepec (Pacific Mexican coast) with the mentioned Tehuano winds. Both the studies have highlighted the role of swell in affecting the local roughness length evolution with fetch, the growth rate of the wind sea, and consequently the spatial evolution of the offshore directed young wind sea.

All the mentioned effects, related to coast or to the interaction with especially young waves, become more and more relevant the more enclosed is the basin under consideration, in the limit considering a fully enclosed basin, as for instance the Black Sea in Europe or the Great Lakes of North America (Michigan, Superior, Huron, Erie, Ontario). One could think of these lakes as being small-scale deep ocean bodies. The net effects of these systems on a wave climate are visually evident. The coastal boundary layer and the land-sea breeze now surround the entire domain effectively altering the wave climate. These fluctuations are more difficult to detect when masked by larger-scale synoptic systems. Although a substantial number of studies have been performed on wind and waves in lakes, most of them have been focused on wind-wave growth (Bretschneider, 1958; Donelan et al., 1992; Young and Verhagen, 1996) and not on the atmospheric forcing.

Because of the related strong economic interest, the Great Lakes have been and continue to be a viable region to study. Point source buoy sites (approximately 15 sites, NOAA/NDBC and Canada/MEDS) and shore based meteorological stations surround the perimeter of the lakes making them a very practical region to study winds and wave generation. As a whole, they also encompass many different meteorological events. Apart from the conditions associated to large scale synoptic systems, one of the characteristics observed in these enclosed systems is the rapid acceleration of cyclogenesis. This happens when there is a strong positive difference between the water and air temperature, typically in the Fall, leading to an intense exchange of heat, in so doing fuelling the possible rapid development of the storm. Typical examples happen in the North-Western Mediterranean Sea and also in the Great Lakes. An example, among the many available, is given by the storm of 23 September 1989 when, according to both model and measurements, over a four hour duration the wind speed increased from about 6 to nearly 20 m s^{-1} with a significant wave height increase of nearly 5 m over a similar period. Also, during a sailboat race from Port Huron (Lake Huron) to Mackinac a similar situation occurred (Burke, 2008), forcing almost half of the boats to withdraw because of a rapidly developing storm system that was miss-forecast, (http://www.bycmack.com/history/1985_Port_Huron_to_Mack_Race_by_John_Burke_(2008).pdf). Neither of these cases were associated to frontal systems. They were both local, rapidly developing storms. This makes them much more difficult to forecast, as repetitive experience has clearly shown.

One of the characteristics of more or less isolated bodies of water is their immediate reactivity to the changing meteorological conditions. Of course this holds for waves, an enclosed sea lacking the longer term memory of the oceanic sites. For instance, this is again typical of the Great Lakes. Jensen et al. (2012) quote a 22 day period during which in Lake Michigan fourteen wind shifts of 180° occurred, none of them associated to sea or land breezes. Each time the wave system reacted accordingly, with practically no memory of the previous conditions.

Still about waves (that we will discuss more in the next sections), there is a diffused tendency to believe that the stormy wave conditions possible in an enclosed sea or a lake are much lower than in the ocean. While this is true for the most extreme ocean storms, we should not forget that it does not take 1000 km or more to build a severe storm. In the two documented (for their consequences) storms in the Adriatic Sea, 4 November 1966 and 22 December 1979, that led to the two most disastrous floods of Venice, Cavaleri et al. (2010) have estimated significant wave heights up to 12 m on a mere few hundreds of km fetch, reduced to "only" 8 m when approaching the Venice coastline, mostly because of bottom induced breaking. While no measured wave data exist for either storm, the damage to the tower (see Fig. 2.3) present after the 1979 event (not there in 1966) was a clear proof that during the storm the wave crests had repetitively passed above 9 m above the mean sea surface. In Lake Superior the well documented sinking of the Edmond Fitzgerald (Hultquistet al., 2006) during a November 1975 storm exemplifies the effect of rapid intensification of cyclogenesis and the consequent wave conditions occurring in the Great Lakes that proved to be very deadly. No available buoy data were available to quantify the degree of accuracy in the model estimate (7 m, Hultquist et al., 2006). However, twenty-three years later a near identical storm entered the Great Lakes basin. Also this time only one measurement site was in operation during the event, located in the southern part of Lake Michigan. Still not on the most intense area of the storm, peak significant wave height conditions of over 6 m were measured (Jensen et al., 2012).

Having listed the problems we encounter when modelling wind and wave conditions in the coastal and enclosed seas, it is fair to recall the

Table 2.1
Performance of the distributed NCEP wave forecast system versus 50 NDBC coastal buoys in the Gulf of Mexico and US East coast. rmse is root mean square error, SI scatter index. Error metrics are for significant wave height.

Forecast (h)	24	48	72	96
Rel bias (%)	−5.6	−4.3	−4.2	−4.2
rmse (m)	0.24	0.27	0.31	0.42
SI	0.20	0.22	0.26	0.35
Best-fit slope	0.88	0.88	0.88	0.86

accuracy (see Chapter 1) presently achieved in the global models. However, the cited statistics hold on a global basis. In enclosed seas, particularly if affected by local orography, the performance is appreciably inferior. For instance, in the Adriatic Sea Cavaleri and Bertotti (2004) must regularly enhance the ECMWF wind speed to get the correct corresponding values (compared with satellite data) to be used with the local wave modelling system. The wind enhancement factor, decreasing with the progressively improving resolution, is still at 1.16 notwithstanding the 9 km resolution of the present ECMWF model. The obvious solution is high resolution limited area modelling. The system Nettuno (wind and wave forecast, a cooperative effort of the Italian Meteorological Service and ISMAR) with 7 km resolution in the Mediterranean Sea, boasts a 1.00 best-fit slope for the model U_{10} versus measured data. However, under close analysis the corresponding figure for the various sub-basins varies from 0.92 to 1.09 (Bertotti et al., 2013). These are typical figures for enclosed seas, showing the difficulty of properly modelling the various effects and coastal influence we have rapidly described.

As a summary of this section, meteorological effects in coastal and enclosed water bodies can and do often become quite complex. It is as if we had a synoptic-scale (cyclogeneses, pressure systems, frontal passages) on top of which smaller scale features keep adding or subtracting from the existing conditions. We enter a regime where land/sea boundaries actively affect the flow patterns, and orographic effects from large- (mountains) to small-scale (buildings and vegetation) play an important role in the overall wind field. In addition to this, daily heating of the land can produce diurnal oscillations in the very local winds or land-sea breezes. Thermal effects can generate small scale sea surface temperature gradients resulting in transient surface roughness regions. This in turn will affect the estimates in the frictional velocity and very local scale wind-wave generation. Field, laboratory and modelling studies have been performed isolating these mechanisms. In semi- or fully enclosed water bodies, one could identify the meteorological conditions as a microcosm of its open ocean counterpart. The meteorology and the mechanisms are identical; but what could appear as small-scale in the deep open ocean, in limited coastal areas will effectively impact the winds themselves. In part the modelling capability of some of these situations has been greatly improved in our present day forecasting efforts, particularly with high resolution local modelling, but we still have a long way to go.

2.2. Open seas versus enclosed basins

L.Cavaleri, J.-R.Bidlot, W.E.Rogers
luigi.cavaleri@ismar.cnr.it

where we point out the problems with modelling waves in enclosed and coastal seas and the basic reasons for this condition. A deeper look into the related physics is in the following Section 2.3

In the previous Section 2.1 we have highlighted the difficulties we encounter with properly defining the meteorological conditions in coastal areas and enclosed seas. As expected, this is not the only problem. Also wave, and more in general oceanographic, modelling faces new challenges. In this section we give a brief overview of the conditions that give rise to the differences between wave modelling in the open ocean versus the coastal and enclosed seas, highlighting the implications and the consequent limitations. A more physical interpretation of the various aspects implied is given in the next Section 2.3.

In Chapter 1 we have pointed out the high level of accuracy of wave modelling in the oceans. Performances with a few percent errors in the significant wave height, scatter indices of 10% or slightly more are what is expected for the first day or few days of forecast from the best meteo-oceanographic operational centres. Of course this is the general view, and errors occur, for example with exceptional events where the physics of the meteorological and wave models may be pushed to their limits. Also, considering the evolution of a storm, the error can be less related to the estimation of modelled quantities than to where and when the storm occurs. A 5% error in the speed of a cold front will misplace it by about 100 km and three hours during the course of a three-day forecast. While on the whole the statistics will be good, at specific times and locations the evidence will be quite different.

One difficulty in the open ocean is the full specification of the wave conditions, generally characterized by a wind sea and one, or more often a few, swell(s). While the H_s statistics may be favourable, we may find large differences in the spectral distribution of energy (this subject is discussed also in Section 2.5, and more extensively in Chapter 4). In a way the accuracy depends on the purpose. For instance, a ten-day towing of an oil rig across a large expanse of ocean may judge as dangerous (or at least relevant) certain errors in H_s and swell forecast, while the same errors may be considered irrelevant for an oil tanker. In any case the fact that we indeed consider as usable ten-day forecasts is in itself a marvel. Having become accustomed to the almost constant high quality, we should not forget that at a given time, what in ten days will be the crucial meteorological factors for the local conditions may be at the moment almost half a globe away.

Once we move to the coastal and inner seas, the statistics of the global model results are not so good. See for example Table 2.1, reporting the performance of NOAA operational WAVEWATCH III Multi_1 model (soon to be described in Section 2.6) at all coastal NDBC buoys in the Gulf of Mexico and the US East Coast. The performance can be considered good for coastal waters, but certainly not up to the level of the global model results. The persistence of the underestimate (on average 4.5%) with the extent of the forecast shows the consistency of the global meteorological model that is not letting the atmosphere gain or lose energy with time. However, the specific errors of the details, e.g. the mentioned ones in space and time, are evident in the progressive substantial increase of the scatter index. This is already relatively large, 0.20, at 24 h forecast (compare with the 0.10 of the global model on the oceans from the statistics cited in Chapter 1), and then growing with what one could judge almost an exponential rate.

Following the above argument, because in enclosed seas the dominant condition is wind sea, with swell more rarely, if ever, present depending on the local geometry, any error in the driving wind field implies a direct corresponding error in the wave conditions. This considerably shortens the extent of the useful forecast. But there are other reasons. Still referring to the global models, the resolution may, and in general will, not be sufficient to carve out the necessary details, both in the driving winds (think of orography) as in the geometry of the local basin. The common problem of a too slow catch up of the surface wind when passing from land to sea implies that the smaller the basin the stronger the corresponding underestimates will be (see Cavaleri and Bertotti, 2004, for a clear picture of the situation).

The obvious solution is to move to nested modelling, something useful both for (meteorological) better describing the wind field as a function of the local orography and geometry, and (waves) providing the correct geometry and bathymetry of the basin. Because there is a direct relationship between the resolution of a model and the scale of the processes that we will be able to describe, a higher resolution will make it possible to follow in greater detail the small scale events often associated to enclosed seas. However, this higher sensitivity is not without cost. Nested models are very sensitive to errors in the initial

and boundary conditions. The cited (see above) error in timing and location in the global models cannot be corrected by the nested grids that will inherit errors from the larger grids. In some cases, as the Nettuno system in the Mediterranean Sea (Bertotti et al., 2013), an independent data assimilation system can be used. This avoids the influence of the global model in the initial conditions, but, if the sea is not fully enclosed, the local model is still dependent on the global one for the boundary conditions. A large local area can be chosen to extend the independence, but at the expense of the required computer time. In practice nested models do not usually go further than three or four days, because on a longer forecast range they will be completely dependent on the accuracy of the global model.

By increasing the resolution, we may be able to see many more details, and visualize more processes at work, in the wave models, but more so especially in the meteorological models. These details, as the small scale (order of kilometres) turbulence in the field, may look, and possibly are, physically sound. However, this does not mean they are deterministically correct. The key point is that simply we do not have the information for driving this, e.g. turbulence, with data assimilation. Luckily, being integrated in space and time over the driving wind fields, waves typically low-pass filter these oscillations, providing the output that duly reflects the larger scale pattern. Note however that the obtained wave energy may duly and correctly represent the integrated effect of small scale turbulence (think of the effect of gustiness explored by Abdalla and Cavaleri, 2002).

On the fetch-limited conditions typical of the enclosed seas, the significant wave height H_s is proportional to U_{10} (see, e.g., Kahma and Calkoen, 1992), hence the H_s errors associated with wind speed error are not so large as in the ocean, where for well-developed conditions H_s tends to approach a square dependence on wind speed. On the other hand, the typical generative conditions are the most complicated ones for a model because of the various processes at work (generation, nonlinear interactions, dissipation, plus all the shallow water ones). This is immediately evident when, instead of the classical case of a straight coast and a perpendicular offshore blowing wind, we have a curved coast and possibly slanting (oblique) fetch generation. This also gives rise to the need for expanding the global and shelf sea operational observing networks to these near-shore locations, to be able to develop and validate operational models at these scales (see more on this in Section 2.5). As it will be discussed in Chapter 3, interactions with currents becomes a common issue in near-shore water where the wind and wave action leads often to currents of much larger intensity than what we usually find offshore, or also of different type, e.g. rip currents.

Summarizing the general view, to be detailed in the following sections, and particular in the examples of Section 2.6, perhaps the most critical information for wave modelling in the inner seas is the meteorological input that sets substantial limits to the extent of the usable forecast range. The statistics of the model performance are not as good as in the open sea, but still at a high usable level. This is on average. Detailed values for specific areas vary from almost perfect (best-fit slope close to 1.0) to large errors, the latter often depending on errors of the large scale model to which nesting can be extremely sensitive. As is the case on a global scale, a useful approach to establish the confidence in the forecast and the related uncertainty is the ensemble forecast, see Pezzutto et al. (2016) and Bunney and Saulter (2016) for a detailed related study in the Mediterranean Sea. However, all these results seem to vary amply with the application and the specific area. This is clearly exemplified in Fig. 2.4 (see the previous section) where we show the progressive increase, in the oceans and the Mediterranean Sea, of the ECMWF mean and maximum wind speeds and significant wave heights with the resolution of the operational meteorological model. Note that for these tests the wave model resolution was the same till T511 (see Section 2.1), then progressively increased with the meteorological one till the present 14 km.

While the ocean mean wave heights are asymptotic to what (see the statistics of ECMWF and NCEP cited in Chapter 1) appears to be an almost correct value, it is interesting to note how the corresponding maxima are still climbing. This suggests that indeed the peaks of some storms are characterized by very high spatial gradients. For our present purposes all this is exacerbated in the Mediterranean Sea where we see that both the mean and maxima values are still climbing, a strong indication that, as shown by repeated comparisons with satellite data, even at 9 and 14 km resolution (for wind and wave respectively) we are still not close to the correct solution.

Though not specifically pertaining to the coastal situation, it is useful to consider the impact of sea ice on waves and wave predictions. There are two different aspects where this impact is felt. One is the variability in time of the extent of sea ice, hence in reverse the one of free sea where waves can develop. The second one is the impact of ice in its various forms, from its early formation (grease ice) to more or less dense ice floes and further to a compact pack, on the waves themselves. To envisage the importance of sea ice, one need only imagine the implications of disregarding sea ice when modelling regions where ice occupies some fraction of the basin. We do not need to think of the retreating Arctic Ocean ice. Even inner or limited seas as, e.g., the Baltic Sea, Beaufort Sea, Caspian Sea, or Nordic Sea show, and have shown in the past, ample seasonal variations. Neglecting this would of course result in excessive wave generation, among other problems. On top of the implied ‘free’ geometry of the basin, sea ice has a number of implications for wave modelling in the ice environment. This will be dealt with in the next Section 2.3.

We close this quick and general survey of the “open seas versus enclosed basins” line of discussion with a figure that beautifully summarizes the situation, making clear the level of performance in the two different environments. An old saying goes as “a picture is worth a thousand words”. This is indeed the case here. Fig. 2.5 shows the global distribution of the ECMWF scatter index (SI) for the significant wave height first guess (i.e. before any data assimilation) compared to the Jason-2, Cryosat-2, and Saral altimeters. Looking at the picture, we see at once how, with respect to the open oceans, the higher SI are practically a drawing of the continental borders. Note in particular the inner seas, as the Great Lakes, the Gulf of Mexico, the Mediterranean, the Red Sea, the whole area between the Asia South-East and Australia, the area between Japan, Korea and China. Note the large SI along the whole US North-East coast and, in contrast, how the west coasts fare in general better. The obvious reason is the general west to east motion in the storm belts. There are exceptions. One is the Somalia coast, on the Horn of Africa, because the area is dominated by the south-west to north-east monsoon in summer and the opposite direction one in winter. The other exception is the North Sea, between U.K. and Scandinavia. Although subject to violent storms and acting as a semi-enclosed basin, the area is amply exposed to the North-Atlantic storms and swell, this link giving a higher reliability to the local forecasts, at least for waves entering the sea from north-west. This example will be further exploited when discussing data assimilation in Chapter 4. Fig. 2.5 has been obtained comparing with altimeter data. It could be argued that these data are not fully reliable close to coast, in so doing disqualifying the overall result. This is not the case. Firstly, ubiquitous altimeter data have been chosen to highlight the difference between ocean and coastal water. Then, of course with less data, similar results (Bidlot, 2017) have been obtained also, where available, for buoys.

At this stage the message is clear. We have a problem in the inner and coastal seas. The reasons why and the physics behind is what we deal with in the next and following sections.

2.3. Coastal areas and enclosed seas

G.Ph.van Vledder, L.Cavaleri, W.E.Rogers, J.M.Smith, Y.Toledo
G.P.vanVledder@tudelft.nl

where we discuss in more detail the physics of the most important processes that govern the evolution of wave fields in enclosed and coastal

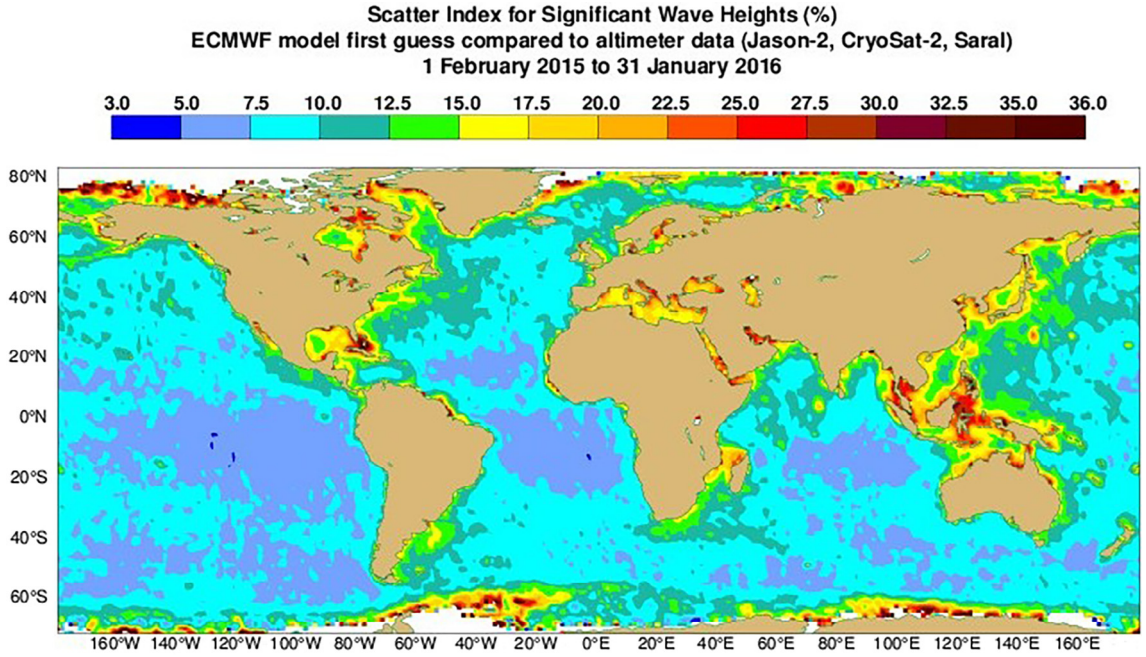

Fig. 2.5. Global distribution of the scatter index for the validation of the ECMWF significant wave height first guess versus altimeter data. Note how all the coasts (especially those facing east) and inner seas are characterized by much higher scatter values than in the open oceans.

seas

Leaving the large space of the oceans we release the difficulty of correctly identifying large currents and gyres, and their consequent effects on waves. However, when modelling waves in coastal areas or enclosed seas additional challenges emerge in comparison to open ocean wave modelling. The common factor of these two kinds of areas is the proximity of land resulting in relatively small-scale changes in bathymetry, currents and winds, whereas differences are mostly related to the amount of sheltering from externally generated waves. The interplay of all these factors requires a careful assessment of the significance of these processes on wave evolution. This knowledge can then be used to make proper choices in setting up a wave model for coastal applications, which become increasingly important in view of, e.g., the development of renewable energy resources or coping with coastal hazards due to sea level rise and climate change.

Good examples of complicated areas for wave modelling are the North Sea, the Gulf of Mexico, the Bothnian Sea (part of the Baltic Sea) and the Adriatic Sea (a sub-basin of the Mediterranean Sea, see Fig. 2.3). The North Sea is a partially enclosed sea with a decreasing depth while moving from north to south. Along the Danish and Dutch coast the water depth slowly decreases up to the coast-line, but along the east coast of England and along the Belgium coast many shallow ridges exist causing small-scale variations in wave characteristics. As the North Sea is connected to the Norwegian Sea and the Atlantic Ocean, occasional swell systems may also penetrate south-wards providing mixed sea states. Of particular interest for the Gulf of Mexico is the shelf break, and Gulf Stream-related currents. Both areas are also known for their violent storms or hurricanes causing storm surges and dangerously wave conditions of which the 1953 and 1961 storm surges in the North Sea and hurricane Katrina of 2005 are well-known examples. The Adriatic Sea is unique in its shape, a rectangular basin in which strong southerly sirocco winds may create large waves and dangerous storm surges at its northern end.

Of further interest is the transition to smaller spatial and temporal scales in coastal regions. This is particularly true for the North Sea which in its southern part is bordered by many shallow estuaries and tidal inlets of which the Wadden Sea is the most prominent feature. In these areas water level variations and current effects play an important role on wave evolution. A special feature of the Wadden Sea is the tide induced flooding and drying of sand banks and the occurrence of various muddy areas. Different spatial scales also occur in the southern part of the Bothnian Sea where thousands of islands ranging from a few meters to several kilometres in diameter make any modelling a real challenge. This wide range of spatial scales results in strongly varying wave conditions in relatively small geographical areas.

All these effects have implications for the proper choice of the physical processes to be modelled, the specification of external factors involved in forcing the wave model, the spatial resolution and numerical techniques in solving the wave (action balance) equation and the validation of model predictions. In the following sub-sections each of these aspects and their mutual interactions are discussed.

2.3.1. *Depth effects*

A key difference between open ocean and coastal areas is water depth. As the water becomes shallower, depth effects influence the evolution of the wave field. On the one hand depth effects influence the propagation of wave energy while on the other hand they affect the physical processes of wave generation, wave reflection and refraction, dissipation, and non-linear interactions exchanging wave energy between different wave components.

Spatial variations in depth influence the kinematics of the waves causing changes in the phase velocity producing wave refraction, while changes in group velocity lead to a steepening of individual waves. The spatial scale of depth changes is of importance for choosing stable and accurate numerical methods for wave propagation. A good example is the treatment of areas with steep gradients in bathymetry that are poorly-resolved by the model spatial resolution. Such situations may require limiters to prevent unrealistic solutions, see for instance Dietrich et al. (2013). This subject is discussed more thoroughly in the following Section 2.4. Though computationally more expensive, applying sufficiently fine higher spatial resolution is still the best option to properly resolve the gradients in the wave field (e.g. due to spatial changes in bathymetry or currents). In case of explicit propagation schemes, this inflation of computational expense is doubly true, because these schemes require that the time step size decreases in tandem with the smallest geographic grid spacing. These limitations can be

overcome by applying unstructured grid techniques in conjunction with implicit schemes of which those by, e.g., Roland (2008), Zijlema (2010) and Huchet et al. (2015a,b) are good examples.

Depth effects have also consequences for the physical processes of wave generation by wind, dissipation due to steepness or by depth limitations, and non-linear triad or quadruplet wave-wave interactions. From the wave side point of view, shallow water effects may cause waves to become steeper invoking breaking. Such sea state dependencies on wave evolution were discussed by Makin (2002) and Babanin and Makin (2008) based on a field study in Lake George, Australia. They identify various effects of which depth-induced wave breaking and steepening of individual waves are most important for wind wave growth. Background swells may also affect the sea drag through hydro-dynamic interactions in which shorter waves may experience enhanced breaking. This issue is still not settled as found by Ardhuin et al. (2007) who did not find any effect of incoming swells on local wave growth near Duck, North Carolina.

In deep water, breaking is associated with steepness. As waves enter shallow water, traditional deep-water parameterizations for steepness-induced breaking are generally unable to predict the strong enhancement of breaking rate by depth effects, so some "engineering solutions" are needed to predict, for example, the variation of wave height across a beach profile. One of the most popular approaches to this family of so-called "depth-induced" wave breaking formulations is the empirical bore-based model of Battjes and Janssen (1978). The actual water depth is a key parameter in this model and its performance is still surprisingly good (Salmon et al., 2015; Salmon and Holthuijsen, 2015). Progress in improving this model is slow as the physics of breaking is still poorly understood. Ruessink et al. (2003) introduced the dimensionless depth kh, and Westhuysen (2010) introduced the bi-phase to scale the dissipation rate. Salmon et al. (2015) suggest another local scaling method by including depth, bottom slope and directional spreading. It is evident that an accurate estimate of the total water depth is essential for a proper application of such breaker formulations. Lastly, Filipot et al. (2010) proposed a so-called "universal" treatment of breaking which would, in principle, making it unnecessary to separately specify source terms for open-ocean breaking ("whitecapping") and surf zone ("depth-induced") breaking.

Note that in all these formulations the local effect of wind is ignored. Indeed, an order of magnitude estimate of the amount of energy involved by the local wind input shows this to be much lower than the one associated to the dissipation for depth effects. However, the problem is not in the amount of energy involved. Rather, there is the distinct possibility that wind, if properly aligned, may favour the local shallow water breaking. The opposite situation is also possible. A sufficiently strong reverse wind, i.e. blowing towards offshore, hence against the incoming 'ready to break' waves, may lead to a reverse breaking, in so doing possibly counteracting the "wish" of the wave to break shoreward. An example of this situation is in Fig. 2.6. The next sub-section provides a compact view of the general situation in whitecapping.

As shown by Herterich and Hasselmann (1980), the strength and spectral shape of the resonant non-linear quadruplet transfer rate change as water becomes shallower. The consequences for wave modelling in shallow water have hardly been explored as an accurate calculation of these interactions is still not feasible for operational applications. A simple parameterisation of depth effects has been included in the WAM model (WAMDI, 1988) based on an analysis of peak values of the transfer rate as computed by Hasselmann and Hasselmann (1981). This simple method neglects the change in spectral shape, hence in the non-linear transfer rate. A deeper problem is the applicability of presently used formulation of the quadruplets, as strictly speaking they were derived assuming homogeneity of the media in which the waves evolve (see, e.g., Rasmussen, 1998). Moreover, Willebrand (1975) pointed to inconsistencies in the wave action balance equation in inhomogeneous media. Smit (2014) developed new methods to handle these issues more accurately in which the coherence of the wave field is taken into account by also keeping a balance of wave phases. Both points of concern need further attention to improve model application in coastal areas.

Fig. 2.6. Reverse breaking in shoaling waves due to adverse wind (photo by Luigi Cavaleri).

In very shallow water non-linear triad wave interactions become important. These interactions generate both lower and higher harmonics in the wave spectrum. These interactions can properly be modelled in phase-resolving time domain model, like Boussinesq models (e.g. Madsen and Sørensen, 1992; Kirby, 2003; Sørensen et al., 2004) or non-linear non-hydrostatic wave models (e.g., Zijlema et al., 2011). In phase-averaged models only approximate methods have been developed to redistribute energy within the wave spectrum. A well-known example is the Lumped Triad Approximation (LTA) of Eldeberky and Battjes (1995), but its accuracy is poor. A fully directional model has been described by Becq-Girard et al. (1999) known as the Stochastic Parametric Boussinesq (SPB) model. A collinear implementation of the SPB model was developed by Salmon et al. (2016) showing improved behaviour in comparison with the LTA method. A fundamental problem occurs in phase-averaged models as the generated harmonics are treated as free surface waves whereas they are linked with the primary peak of the spectrum. However, these harmonics can become permanent as, e.g., in the case of a barred beach where, beyond a certain deformation, past the bar energy cannot move back to the fundamental wave period.

2.3.2. White-capping and breaking

Although not a process confined to shallow or enclosed seas, whitecapping is still a challenge for wave modelling. Granted some new insights and improved versions in the recent years, by and large whitecapping is still the tuning knob of most operational wave models. In framing the situation for enclosed seas, it is therefore convenient to summarize the related modelling situation.

In the early formulations by Komen et al. (1984, 1994) the whitecapping dissipation was associated to the spectral mean wave steepness. Implicitly the approach assumed a wind sea where the mean steepness has a well-defined physical meaning. However, this parameter, once defined from the whole spectrum, loses its original meaning, hence its usefulness, if, as commonly the case in the oceans, different wave systems, in practice including one or more swells, are present. Indeed, although with some limitations, this can be the case in coastal and/or shallow seas.

The situation can be summarized as follows. The use of a mean-wave steepness causes problems in mixed sea states (wind sea plus swell), as the dissipation rate is too high for the swell part and too low for the wind sea part, causing an over-prediction of the wind sea part and an under-prediction of the swell part. Rogers et al. (2003) proposed an alternative weighting of the mean wave steepness to ameliorate the

negative side effects, but this can only be regarded as a temporarily fix. More recent whitecapping formulations like those of Ardhuin et al. (2010), Rogers et al. (2012), and Zieger et al. (2015) consist of a mix of a saturation based whitecapping formulation and a cumulative wave steepness effect on the whitecapping dissipation rate and, more importantly, swell dissipation is treated separately.

A fundamental, but still ignored, problem is the relationship between white-capping and wind speed. White-capping is strictly related to the energy and momentum input by wind on an actively generated sea. As mentioned above, so far whitecapping formulations neglect the effect of wind on the process. There is, however, accumulating evidence that wind effects cannot be disregarded for this type of dissipation.

2.3.3. Bottom processes

In shallow water the orbital motion of the water particles extends down to the sea floor. This leads to interactions between the surface waves and bottom roughness elements of length scales associated with sediment size and the characteristics of the wave orbital velocity, down to the scale of the bed forms. One of these interactions is bottom Bragg scattering resulting in a local redistribution of wave energy (Ardhuin and Herbers, 2002). A dissipative interaction is based on friction in the turbulent boundary layer whose strength depends on the bottom conditions. Hasselmann et al. (1973) suggested using an empirically based constant with different values for wind seas and swell. Zijlema et al. (2012), however, argue that one value suffices in conjunction with a proper choice of a wind drag formulation. A nonlinear formulations based on drag was proposed by Hasselmann and Collins (1968) then simplified by Collins (1972). A more sophisticated eddy viscosity model was developed by Madsen et al. (1988). A complication is that in many circumstances the bottom ripples characteristics may changes depending on the wave and current conditions. This requires movable bed formulations which were addressed by Tolman (1992) and Smith et al. (2011). In practice, the variations in bottom conditions in coastal areas make the a priori selection of friction parameters problematic. As a consequence bottom friction is commonly part of the tuning procedure, often specific for a given area, and spatial variations within a model grid are commonly ignored.

In many coastal areas muddy bottoms exists. These consist of cohesive sediment or fluidized mud. A problem with such a bottom type is that it presents a rather different mode of wave dissipation which is difficult to represent (e.g. Winterwerp et al., 2007; Holland and Elmore, 2008; Rogers and Holland, 2009; Engelstad et al., 2013). Idealized models have been derived that are based on a two-layer description of the water column in which surface waves drive internal waves at the interface between the nearly inviscid water and the highly viscous (and therefore dissipative) muddy bottom layer. Muddy areas may also affect the growth of short waves (Trainor, 2009) or lead to extensive sediment plumes (Engelstad et al., 2013). Mud rheology (characteristics including thickness, viscosity, density, elasticity, and plasticity) is difficult to estimate even from in situ data, since the mud changes when it is extracted from the water, and the depth of fluidization is highly non-stationary, even when overall mud thickness does not change. Mud can also be transported of course, and thickness is not uniform spatially, making this an intimidating problem for a modeller, see the recent work by Shynu et al. (2017) and Samiksha et al. (2017). Coupled wave-sediment models are one approach for dealing with this, and can be applied to both cohesive and non-cohesive sediments (Carniel et al., 2016a). The reliability of bottom boundary layer modelling is not well established, however.

A recent field of interest is dissipation by vegetation such as mangrove forests or salt-marshes (Suzuki et al., 2011, Anderson and Smith, 2014; see also Samiksha et al., 2017). Such vegetation grows in the inter-tidal zones along tropical and temperate coasts. Such areas may help protect vulnerable coastal areas against wave attack and there is a recent trend to artificially create such areas, being an example of "building with nature". The hydro-dynamics of vegetation fields are different from bottom roughness elements. Still, the earliest attempts tried to model the dissipation using an equivalent bottom friction value tuned to local circumstances. A more advanced approach is to consider the vegetation as structural elements. A commonly method is to determine the drag by a field of cylinders with a certain diameter and density (Dalrymple et al., 1984). This approach was extended by Mendez and Losada (2004) to include specification of vegetation characteristics, but also bottom slope and breaking waves. Suzuki et al. (2011) implemented this extended approach in the SWAN model.

2.3.4. Sea ice

In the previous section we have highlighted the importance of sea ice for the geometry of a basin where waves can actually be generated. However, this is a simplified view because the different forms under which ice is present on the sea imply different physical interactions with ocean waves. Here we give a brief overview of the problems involved.

Historically, sea ice was treated in phase-averaged wave models by simplistic methods. In early versions of WW3 and WAM, sea ice was treated as either open water or land, with the binary selection based on ice concentration (e.g., Tuomi et al., 2011). In WW3, this was updated by Tolman (2003) to a "continuous treatment" to allow partial blocking for partial ice cover. These methods do not treat the effect as "dissipation" via the S_{ice} term, but rather as a feature of the propagation scheme. Further, they do not permit variation of dissipation rate with frequency, which is a clear defect given the intuitively obvious existence of such variation in the real ocean. High frequency waves are rapidly attenuated, while long period swell can penetrate hundreds of kilometres under a solid ice pack. More recently, WAM and WW3 have been updated to treat the sea ice as part of the physics (see Doble and Bidlot, 2013, and Rogers and Orzech, 2013), a concept which was in fact proposed much earlier (Komen et al., 1994), but never implemented outside of academic studies.

Sea ice can have a number of effects on the waves. The first, and perhaps most obvious, one is the dissipation of wave energy. This depends strongly on the characteristics of the ice and on wave frequency. The tail of the spectrum is rapidly attenuated also by small ice floes. Long period swell propagating under the pack is attenuated by the strain induced into the undulating ice and the orbital motion under the ice bottom (see Wadhams, 1973, for an early estimate of the involved process). The second impact is the scattering and reflection of wave energy. In the context of a third generation wave model, this is an energy-conserving process, directionally redistributing energy within the spectrum, again in a way strongly dependent on the ice characteristics and the wavelength. See Masson and LeBlond (1989) for an early approach to this aspect of the interaction. The third impact is the modification of the phase speed and group velocity consequent to the strain in the ice, hence its resistance to the motion induced by waves. This produces effects analogous to refraction and shoaling (respectively) by bathymetry. The fourth effect is the modification of open water source functions such as the wind input to waves, which is of course dramatically reduced under rigid ice cover or even under grease ice that changes the microstructure of the sea surface. These four effects can be more or less important for differing types of ice cover, and of course the primary challenge today for modelling waves in ice is that the modeller typically has very little information about ice cover, e.g. perhaps only the concentration is known, and possibly not well, since it may be based on a satellite observation that is a few days old. Moreover, the ice conditions may be dynamically linked to the waves themselves, suggesting a complex two-way coupled nonlinear problem (Collins et al., 2015a). Lastly, some of these issues, such as the reduction of wind input by pliable ice cover, has hardly been given any attention by experimentalists, and so the modeller can only make an educated guess of this effect.

2.3.5. Input fields

This section provides an overview of the various input fields and the related consequences for modelling waves in coastal and semi-enclosed areas. These include bathymetry, bottom type, water levels, currents and wind. Wave initial and boundary conditions must also be provided. On ocean scale wind is the most crucial input field for large-scale wave models, as the source of energy and momentum of surface gravity waves. Ocean currents can also produce significant impacts on the wave field in areas like the Gulf Stream or Agulhas current (Holthuijsen and Tolman, 1991). In coastal areas and semi-enclosed seas additional effects and external variables start to play a role. As discussed in Section 2.1 the specification of proper wind fields in such areas is a difficult task as the surrounding land masses may cause strong temporal and spatial variations in wind speed and direction. In general wind blowing offshore increases with fetch and neglecting these variations can degrade model performance. In some areas strong wind jets may locally cause severe wind seas. Examples are the bora winds in the Adriatic Sea (Cavaleri and Bertotti, 2004), mistral winds in the western Mediterranean, strong wind jets near the Catalan coast as reported by Pallares et al. (2014), Tokar Gap winds in the Red Sea (Langodan et al., 2014a,b), and the Tehuanos near the gap of Tehuantepec in Mexico (Steenburgh et al., 1998).

In coastal areas tidal (astronomical) and wind effects may generate currents and water level variations. These currents can be very strong in narrow straits or in tidal inlets requiring locally high resolution grids (e.g. Westhuysen et al., 2012; Ardhuin et al., 2012a,b). Currents also affect the kinematics of the waves causing refraction and focussing of waves. In a strong opposing current wave blocking may lead to enhanced dissipation. Waves travelling on a current also change the apparent wind speed. In addition, temporal variations of water level and bottom level may affect the propagation of waves resulting in tide-induced modulations of wave height and wave period measures (e.g., Tolman, 1991a). Current and water levels need to be computed by dedicated flow models, driven by astronomical constituents and by wind. In many applications they are applied as a stand-alone model and their results are fed into the wave model. In many circumstances, however, waves will also affect the coastal currents and water levels which require a two-way coupled wave-flow modelling approach., see e.g. Dietrich at al. (2011) for the Gulf of Mexico, Roland et al. (2012), and Brown and Wolf (2009) for the Irish Sea (more on this in Chapter 3). Especially in the relatively shallow coastal zone an accurate prediction of water levels and currents is important for depth-limited wave breaking and the propagation of swell waves.

The spatial distribution of bottom characteristics is required to scale dissipation processes due to bottom friction, mud layers and vegetation. In many coastal areas these fields are either sparsely known or they vary in time (on time scales larger than those associated with movable beds, see the Kerala case in Samiksha et al. (2017) and Shynu et al. (2017)). Acquisition of accurate bathymetry is, in fact, often a primary challenge for operational nearshore modelling, especially for military applications where the region in question is typically not easily accessible. Further, within what engineers call the “depth of closure”, sediment transport is active, and beach profiles can be strongly affected by the activity of storms (or the lack thereof). During and after storms, bathymetries may be much different than they were when surveyed, making it difficult to perform an accurate hindcast. This implies that bottom surveys should be carried out regularly to retain accurate bathymetries. A practical problem is that information on the spatial variation of bottom characteristics, like grain size, is often difficult to obtain. A common practice, then, is to neglect the spatial variation of bottom characteristics and to select a constant value for the whole computational domain, despite the well-established heterogeneity of the seafloor (e.g. Holland and Elmore; 2008).

In semi-enclosed seas wave boundary conditions need to be specified, most often obtained from a larger-scale ocean wave model. Specification of these conditions is especially relevant for the lower-frequency wave components like swell waves, as these may penetrate through the whole computational domain independently of local wind conditions. In fully enclosed seas like the Black Sea, wave boundary conditions are not required as all waves are locally generated. Nesting is also required when modelling a coastal area bordering a large inner basin or an open ocean. Nesting of wave model grids may sometimes lead to consistency problem in cases where different types of wave models are nested in each other. For instance, when the SWAN model is nested into the WAVEWATCH III model, different physical packages may lead to changes in total energy and spectral shape along the grid boundary. In addition, subsequent nesting to finer grids should be carried out with resolution ratios small enough to retain the spatial variation along the grid boundaries (a resolution ratio of about 5:1 is often suitable, in our experience). Boundary forcing can affect the skill of a nest in ways that are not always obvious. For example, Rogers et al. (2007) found that while total energy may be well-predicted near the boundaries in a nest, inaccuracies in the directional distribution of its boundary forcing translate to poor prediction of total energy in the interior of the nest, since the impact of islands and bathymetry within the nest is strongly dependent on the swell directions.

2.3.6. Spatial resolution

There is an interplay between the resolution of the computational grid of the wave model and the resolution of the input fields. If all input fields (including bathymetry) are coarsely defined, there will often be limited benefit from a highly resolved computational grid. Conversely, a coarse wave model cannot benefit from highly resolved forcing. Spatial resolution is also connected to the accuracy with which the underlying equations are solved. As a general rule the spatial resolution should be sufficiently fine where accurate results are required. An optimal way to achieve this is to apply either nested telescoping grids with increasing resolution or to apply unstructured grids (e.g. Benoit et al., 1996; Roland, 2008; Zijlema, 2010; Huchet et al., 2015a,b; see also Section 2.4). Higher spatial resolutions are required where high gradients in wave conditions occur. As this is difficult to determine a priori, a commonly applied approach is to link the density of grid points to depth and gradients in bathymetry. A particular example is the cited archipelago sea located in the southern part of the Bothnian Sea (Tuomi et al., 2012; Björkvist et al., 2016). One of the problems is associated with identifying the start of the fetch. In cases where the wave model is run in combination with a flow model, also (expected) gradients in flow conditions should be taken into account. In the context of non-stationary eddies within a flow prediction, the strategy of “higher resolution where needed” requires a so-called “adaptive grid”, i.e. a grid which changes with time. This type of approach, while common within other disciplines, is relatively new and has seen limited use (so far) in wave modelling. One example is provided by Popinet et al. (2010).

2.3.7. Spectral resolution

Spectral resolution applies to both the frequency (or wavenumber) range and direction. For ocean applications a frequency range of 0.03–0.6 Hz and a directional resolution of 10° have been considered to be sufficient, but note that proper evaluation of the air-sea interactions, in particular between waves and the forcing wind, may require a higher upper frequency limit. In high-resolution coastal applications with initial wave growth starting from land, a higher upper model frequency may be required to properly resolve the spectrum as in fetch-limited situations peak frequencies close to shore are about 1 Hz, especially for low wind speeds. Bottema and Van Vledder (2008) report an upper value of 1.9 Hz being required for hindcasting waves in inland lakes. Additionally, higher directional resolutions, of say 5°, may be required to accurately resolve swell propagation with a narrow directional spread.

2.3.8. Validation

Validation is an important part of coastal wave modelling, just as

with modelling of larger scales. One major challenge to such validation exercises is that, as we have discussed, the wave field tends to be relatively inhomogeneous in the nearshore, making sparse or isolated point measurements less useful. This is especially true in tidal inlets where strong gradients in both bathymetry and current field exist. In very shallow water, validation can be reliably done only when both the bottom level and the water level are accurately known. Radar data can be especially useful for providing spatial variation (e.g., Kleijweg et al., 2005), but unfortunately, such data tends to be less reliable (more noisy, etc.) than in situ data. Altimeter data close to the coast is part of the product of the most recent satellites, e.g. Sentinel 3. However, these products still lack a thorough validation. See Section 2.5 in this respect.

2.3.9. Nonlinear shallow water effects

2.3.9.1. Bottom reflection. Wave forecasting models are based on the wave action equation (WAE). This equation was derived using a variational approach by Bretherton and Garrett (1968) for linear wavetrains in the presence of vertical mean currents. The WAE is essentially an advection equation. As such it does not account for wave reflections from the sea bottom. When waves shoals over a changing sea bottom, some of their energy is reflected from the seabed and creates a reflected wave in the opposite direction. Steeper bottom slopes and shallower water conditions are expected to increase wave reflection. This process can be linear, which results in a reflected wave of the same harmonic and relates to linear Bragg resonances (e.g., class I and II), or nonlinear, which can transfer energy to other backward propagating wave harmonics and relates to nonlinear Bragg resonances (e.g., class III), see Liu and Yue (1998) and Agnon (1999). In the linear case, bottom reflection may increase wave amplitude as much as 20% in extreme cases, and ~5–10% for more common cases, (see Tatavarti et al., 1988; Mahony and Pritchard, 1980; Elgar et al., 1994).

The main approach used nowadays for calculating linear wave reflection in WAE based models was pioneered by Miche (1951), where a semi-empirical reflection coefficient was derived for monochromatic waves shoaling towards a sloped shore. This reflection coefficient was tested by Elgar et al. (1994) and later approximated more accurately by Ardhuin and Roland (2012), to produce a reflection source term. Another form of bottom reflection source term was derived in Ardhuin and Herbers (2002) and Magne et al. (2005), where the bottom topography was described through a discrete Fourier transform. This source term accounts for bottom reflection due to class I Bragg scattering, and is currently used to describe sub-grid bottom ripples, but may have the potential to account for bottom reflection in larger scale. There are currently no source terms for calculating nonlinear wave reflection.

Ambient currents can also impose reflection as they also change the medium in which the wave propagate. Moreover, they can even block waves from propagation when the group velocity of the waves is slower than an adverse current's magnitude. Such blocking will also cause wave reflection (see Smith, 1975; Suastika, 2012). An implementation to the WAE of such effects is yet to be provided.

2.3.9.2. Diffraction and higher order bottom/current effects. Bretherton and Garrett's WAE can be derived from the time-dependent Mild Slope Equation (MSE) (see Jonsson, 1981; Kirby, 1984). This procedure consisted of neglecting the diffraction and higher-order refraction components of the MSE as well as bottom and current reflection. In the nearshore region, such effects many times cannot be neglected (see, e.g., Chamberlain and Porter, 1995). Applications of improved frequency-direction spectrum WAEs without an ambient flow were presented by Mase (2001) and Holthuijsen et al. (2003) using the parabolic approximation of Berkhoff (1972) time-harmonic MSE and the same MSE without this approximation respectively. Both presented good improvements in their numerical results for steady problems. Liu (1990) used the same method taking into account also ambient current effects, but did not derive it also to the frequency-direction spectrum that should allow its use in wave forecasting models. The MSE was extended to the time-dependent case with higher order bottom and current components by Toledo et al. (2012). Its WAE form in frequency-direction coordinates was also formulated, but it is yet to be implemented to operational wave forecasting models. Another direction for advancing the capabilities of WAE models in the nearshore region was given by Smit et al. (2015). They altered the spectrum definition and added a quasi-coherent structure source term to provide the coherent wave interferences in the nearshore region showing good results in comparison to laboratory and field measurements.

The above-mentioned models all relate to the linear wave problem with a vertically averaged current. A linear wave action conservation equation for surface gravity waves in the presence of vertically-structured currents were presented in the mostly overlooked work of Voronovich (1976). Both derivations yielded a WAE but without giving its specific definition. The formulation process uses the so-called WKBJ method. The zeroth order solution yields the Rayleigh equation. Its solution describes the local vertical profile of the wave flow. The next order of the approximation yields a conservation equation. In order to actually use the resulting formulation, the Rayleigh equation first needs to be solved to yield the eigenvalues (frequencies/wave celebrities) and eigenfunctions (vertical profiles). Then, its solution can be substituted into the conservation equation to create the WAE. As Rayleigh equation does not have an analytical solution, a WAE using Voronovich's implicit formulation is problematic for implementation. By the use of perturbation solutions of the Rayleigh equation (Skop, 1987) and an approximation of Voronovich's formulation, a WAE was formulated by Quinn et al. (2017). It is yet to be transferred to the frequency-direction formulation and implemented in an operational wave forecasting model.

Few works also discussed the extensions of these models to account for quadratic nonlinearity wave-current interactions. Kaihatu and Kirby (1995) presented in an appendix a quadratic nonlinear model without an investigation or numerical results. It extended the MSE of Kirby (1984) to consist of quadratic nonlinear terms, and was simplified, as in the case of no currents, using a parabolic approximation. It was later used for investigation of nonlinear wave-current interactions in a 1D problem of waves propagating over a flat bottom by Kaihatu (2009). Janssen and Herbers (2009) constructed a quadratic nonlinear parabolic model for investigating horizontally shearing currents in deep water and Shrira and Slunyaev (2014) investigated trapped wave modes. In an earlier work, Willebrand (1975) presented a nonlinear extension of the wave propagation (i.e. the wave rays are dependent on each other). In all of the above works nonlinear wave-current interactions were shown to have significant effects on the spectral shape (see, e.g., Saprykina et al., 2015). Nevertheless, at present WAE models do not have appropriate mathematical formulations to take these effects into account.

2.3.10. Nonlinear triad interactions

Nonlinear energy transfer is a dominant process that affects the evolution of wave spectra both in the deep and shoaling region. Nonlinear interactions in deep water consist of wave quartet interactions at leading order. Wave quartets, which act at cubic nonlinearity in wave steepness, satisfy resonant conditions of the wave frequencies and wave numbers. This type of evolution is rather a weak one that requires large spatial distances (time spans) of thousands of wave lengths (wave periods) in order to have a considerable effect. In intermediate to shallow water, the nonlinear interactions act much faster with significant energy transfers between triads of waves. This is possible due to the influence of the bottom that enables to satisfy the resonant conditions already in quadratic nonlinearity. Furthermore, when waves shoal, their steepness increases significantly, and as nonlinear interactions are proportional to the wave steepness, the nonlinear energy transfer becomes even larger in this region. Hence, this phenomenon is a main mechanism for energy transfer between the different wave

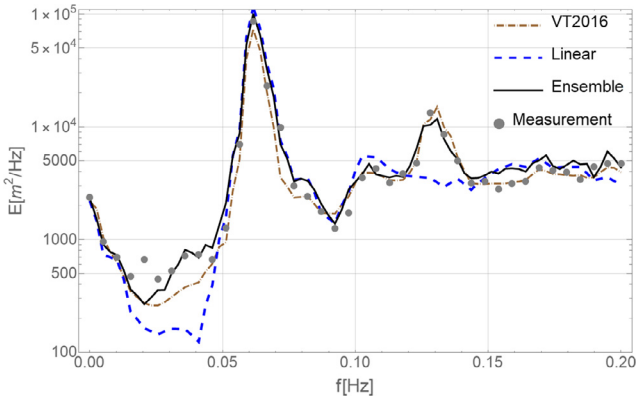

Fig. 2.7. Measured and modelled wave spectrum in depth of 4.1 m after shoaling over a mildly sloping beach. Dots: the field measurement results of Freilich and Guza (1984); Dot-dashed brown line: Vrecica & Toledo (2016) localized stochastic model (with a minor correction in the numerical implementation); black line: ensemble-averaged results of the deterministic model of Bredmose et al. (2005); dashed blue line: the WAE model solution. The models show the evolution from the 14 m depth measurements input, where the nonlinear triad source term is required for providing the higher second harmonic peak and the low infra-gravity wave evolution. The difference between linear and nonlinear formulations in the infra-gravity range should be even more pronounced for deep to shallow water evolution.

frequencies in the near-shore region. The most pronounce energy transfers are the generation of a second harmonic spectral peak and energy transfers to the infra-gravity wave regime (see Fig. 2.7).

The field of frequency-domain quadratic nonlinear deterministic models consists of several approaches. Agnon et al. (1993) constructed a set of quasi-2D quadratic nonlinear hyperbolic equations to account for triad interactions. Based on the linear Mild Slope Equation of Berkhoff (1972), Kaihatu and Kirby (1995) followed the method of Agnon et al. (1993) and constructed a model consisting of a set of elliptic MSEs coupled by quadratic nonlinear terms. An extension of this work to the complementary MSE was presented by Toledo and Agnon (2009) using a stream-function formulation. In order to reduce computational complexities, Kaihatu and Kirby (1995) applied a parabolic approximation to their MSE formulation yielding a quadratic nonlinear parabolic equation (PE) model (Kaihatu, 2001). Bredmose et al. (2005) advanced the accuracy of the nonlinear interaction terms by employing infinite pseudo-differential operators. Another nonlinear PE, which improves the accuracy of the formulation of Kaihatu and Kirby (1995), was constructed by Janssen et al. (2008). Commonly, PE models have the mathematical limitation to deal with waves that approach the shore under large attack angles. Janssen and Herbers (2009) later solved this problem using a Fourier transform in the lateral direction. Toledo (2013) advanced the PE modelling approach and resolved its direct incidence wave approximation for both linear and nonlinear cases by facilitating an oblique parabolic approximation, which can account for wave input with any attack angle. Using this model, it was identified that energy can be transferred from two monochromatic incident waves approaching in different angles to waves with larger attack angles in the same harmonic. This counter-intuitive result shows that unlike the case of linear wave shoaling, where waves reduce their attack angle in the refraction process, in the nonlinear shoaling process the attack angle can increase and explain the observed broadening of the wave spectrum (see Groeneweg et al., 2015, for the effect on wave penetration to channels). This presents the need of formulating a two-dimensional triad interaction source term.

In WAE models, quadratic nonlinearities are represented as bispectral terms, which are composed by combinations of three wave energy spectral components. Evolution equations for bispectral terms can also be written, resulting in dependence on higher-order terms. As in the turbulence problem, a stochastic closure relation is applied in order to relate higher-order terms (trispectra, etc.) to the lower-order ones (wave energy and the bispectra). Owing to the vast amount of permutations, the bispectral evolution equations induce a heavy computational load, which makes these two-equation models less applicable for operational wave forecasting models. Various works have addressed this limitation. Eldeberky and Battjes (1995) simplified the one-dimensional (co-linear) bispectral equations by assuming negligible bispectral changes, a flat bottom and energy transfer to higher harmonics for each spectral component (self-interactions) without accounting for other energy transfers between different triad combinations and energy that is transferred to lower harmonics. Becq-Girard et al. (1999) relaxed some of these assumptions by accounting for all one-dimensional triad interactions. A recent advancement for better consistency is given by Salmon et al. (2016). In their approach they made use of an algebraic solution of the bispectra, which allowed its substitution in the energy evolution equation and hence the construction of a one-equation model.

Agnon et al. (1993) presented a full representation of the bi-spectral model (see also Kofoed-Hansen and Rasmussen, 1998; Eldeberky and Madsen, 1999). They also provided an analytical solution of the bispectra ordinary differential equation. This allowed for constructing a more accurate one-equation model. Still, due to this operation the resulting interaction coefficients became non-local (i.e., containing integrals over the space), and therefore difficult in their application to forecasting models. This difficulty was overcome in the works of Stiassnie and Drimer (2006) and Toledo and Agnon (2009, 2012), where the nonlocal operator was separated to a mean energy transfer component and an oscillatory integral one, which was neglected. In these works, changes in the bottom depth were shown to have a significant effect and without it the nonlinear mechanism inflicts no mean energy transfer. Nevertheless, once the water depth became shallower, the nonlinear transfer coefficients became too large and on flat bottom the method provides no energy transfer.

The apparent contradiction between these two branches of models, where one assumes a flat bottom while the other one shows mean energy transfer only over sloped bottom, was settled in Vrecica and Toledo (2016). They showed that the class III Bragg mechanism, which requires bottom changes, is dominant in intermediate water, but in shallow water one-dimensional shoaling ($kh < 1$) there is a direct nonlinear resonance providing strong energy transfers even on flat bottom. Vrecica and Toledo (2016) constructed a consistent localisation procedure that accounts for the deep to shallow problem. The model was evaluated with respect to deterministic ensembles, laboratory experiments and field measurements with very good agreement.

The formulation of the two-dimensional triad interactions in WAE model still needs to be further investigated. Currently, Vrecica and Toledo one-equation model has quasi-two-dimensional capabilities, and Smit and Janssen (2016) two-equation model has a full two-dimensional formulation. Nevertheless, no comparisons of these works to accurate deterministic models or measurements are currently provided.

2.3.11. Discussion

The requirement of providing sufficient accurate input fields has already been discussed in the context of resolution. However, it is worthwhile this to discuss also in the more general sense of uncertainty. As resolution increases, the relative importance of different physics changes. A good review is found in Battjes (1994), then reproduced in Young (1999). Ardhuin and Roland (2013) present an overview of the various challenges when predicting waves in coastal environments. They also present a hierarchy of factors affecting the overall model performance. In decreasing order of importance they note that the accuracy of forcing fields is usually the most important, i.e. wind, wave boundary conditions, currents, bathymetry and water level. Hereafter, the quality of the source term parameterisations is important. Finally, the quality of the numerical schemes is of importance. It is noted, however, that this hierarchy does not always hold as this may depend

on the type of application, see also Roland and Ardhuin (2014). For instance, in case one is interested in the propagation of a pure swell system through the North Sea, then the quality of the numerical propagation scheme and geographic resolution are probably the most important. Conversely one can readily identify cases where the accuracy of the source functions is arguably the primary source of error.

2.4. Numerics

A.Roland, G.Ph.van Vledder, W.E.Rogers, L.Cavaleri
aaronroland@gmx.de

recalling that for practical solutions we live in a discrete world

Most of the discussion in previous sections has focused on the physical aspects of the problem of wave modelling in semi-enclosed seas. There is no doubt that indeed this must be our first approach in understanding the related processes to derive the equations that express the evolution in time and space. However, while the derived physics, still with all its approximations, hold for any “point” in space-time dimensions, in practical applications we aim at evaluating the related evolution only at a limited number of “points”. Therefore, the governing equations need to be discretized and numerically solved. This is far from straightforward because many processes are non-linear, interdependent, and often exhibit short scales in time and space. These problems are felt more, for different reasons, in enclosed seas. This is due on one hand to the geometry of the coastlines, the presence of islands, currents and to the frequent shallow water we come across, on the other hand to the limited dimensions of the enclosed basin characterized mainly by young and active seas. In addition, ocean swells may occasionally penetrate from an open boundary (a classical example is the North Sea between U.K. and Scandinavia). These characteristic make the numerical modelling a challenging exercise. In this section we describe and discuss the various numerical approaches that have been devised and are used to provide the best solution in the various possible situations.

2.4.1. Framing the problem

where we outline the basic reasons for different approaches in coastal and shallow area

When efficient numerical wave modelling in enclosed and coastal seas is of concern, the problems involved stem from the variety of spatial and temporal scales we need to resolve within our simulation. We not only have to deal with the fractal geometry of our coastlines and with bathymetries littered with small scale structures. We also come across submarine and tidal channels, reefs, bars, river outlets, wetlands, marshes, vegetation and/or bed forms, which need to be properly resolved within the utilized numerical model if the related scales are of interest. The proper numerical treatment of all the involved processes, spatial and temporal scales still bears a significant challenge in wind wave modelling. To arrive at a practical approach, balancing computational requirements and required accuracy, we need to be aware of the possible approaches and the required assumptions and shortcuts we make to reach our goal. Indeed, acting after the physics of the model has been defined, the numerical solution of the various equations needs to take into account, at a certain level, of the approximations present in our description of some of the physical processes.

In establishing the grid where to solve numerically our equations the first and most natural solution in deep water has been the regular structured grid. A drawback of this approach is that spatial gradients of the processes we deal with cannot always be properly resolved. Classical examples are explosive cyclogeneses and typhoons/hurricanes in the open ocean, and strong localised wind jets from the coast as for mistral (French Mediterranean coast) or bora (in the Adriatic Sea). So in coastal and shallow water, the main crux of a structured grid is that it relies on a fixed resolution in geographical scale. We may relax this resolution a little by employing curvilinear grids. However, this approach is computationally inefficient to resolve small scale features, since the smallest resolution radiates through the whole domain along the grid lines. In order to overcome the strangulation of a fixed discretization, a number of different approaches have been introduced in the past two decades, ranging from nesting techniques to multigrid approaches (Tolman, 2007), or quad-tree techniques (Popinet et al., 2010). However, nesting, multi-grid and quad-tree techniques efficiently relax the constraint of a structured grid only to a limited extent. An alternative way to overcome the fixed discretization length in geographical space is given by the numerical methods based on unstructured grids. Mostly based on triangles, this approach has been pioneered in wind wave modelling by Benoit et al. (1996) based on semi-lagrangian methods, whereas the first Eulerian discretization on unstructured grids was done by Liau (2001) followed by many others (e.g. Sørensen et al., 2004; Roland et al., 2006; Roland, 2008, Qi et al., 2009; Zijlema, 2009a). When compared to structured grids, all these approaches have shown significant improvements in terms of efficiency with respect to structured grids (Hsu et al., 2005b, Zijlema, 2009a, Zijlema, 2009b, Roland et al., 2005).

By introducing the variability of the geographical discretization, the spatial scales in which the wave spectra change as waves approach the coast can be more flexibly adopted in spectral wave models. As illustrative examples in Fig. 2.8, panel a shows an unstructured grid of Lake Michigan. The grid resolution varies from 2.5 km in deep water (actual operational setting at NCEP) down to 200 m at the coastline. The grid is generated based on the CFL (Courant et al., 1928) number of the dominant wave frequency. An adaptive depth refinement is effectively limiting the total depth variations in a given triangle. In this way the characteristics of the bathymetry as well as the temporal and spatial scales of the wave physics in the near shore area can be properly resolved without increasing significantly the number of computational points as it would be the case for structured grids. The second example, panel 2.8b, is the extremely high resolution and real multiscale application of the fully coupled wave-current modelling of the Albufeira lagoon, Portugal. Here the resolution varies from the 2 km off-shore down to 2 m in the wave-current interaction region of the lagoon inlet (Dodet et al., 2013) using SCHISM:SELFE and SWAN. These examples illustrate the ability to represent different spatial scales in one computational grid. The benefit of this approach is having high resolution only where required, in so doing making the number of points of the unstructured grid much lower than on the corresponding structured one.

This additional degree of freedom of having the possibility to choose the location where the equations will be solved does not come free of charge. The fees to be paid are inherently greater computational requirements per grid point (but balanced by less grid points), and the mathematical and computational complexity associated to the use of unstructured grid methods. Besides the freedom of placing the points in the domain of interest is not only a blessing: it is also a non-trivial task with respect to the grid generation process. However, present numerical methods on unstructured grids easily allow three to four orders of magnitude variation of the discretization length (the so called multi-scale applications) within one numerical grid. Examples are provided, among others, by Zijlema (2009b), Babanin et al. (2011), Dietrich et al. (2011), and Dodet et al. (2013).

Spectral wave models based on unstructured grid have become a quasi-standard solution in the last decade. These developments have also paved the way making feasible the full coupling with circulation models. This is one of the most important tools, particularly in the

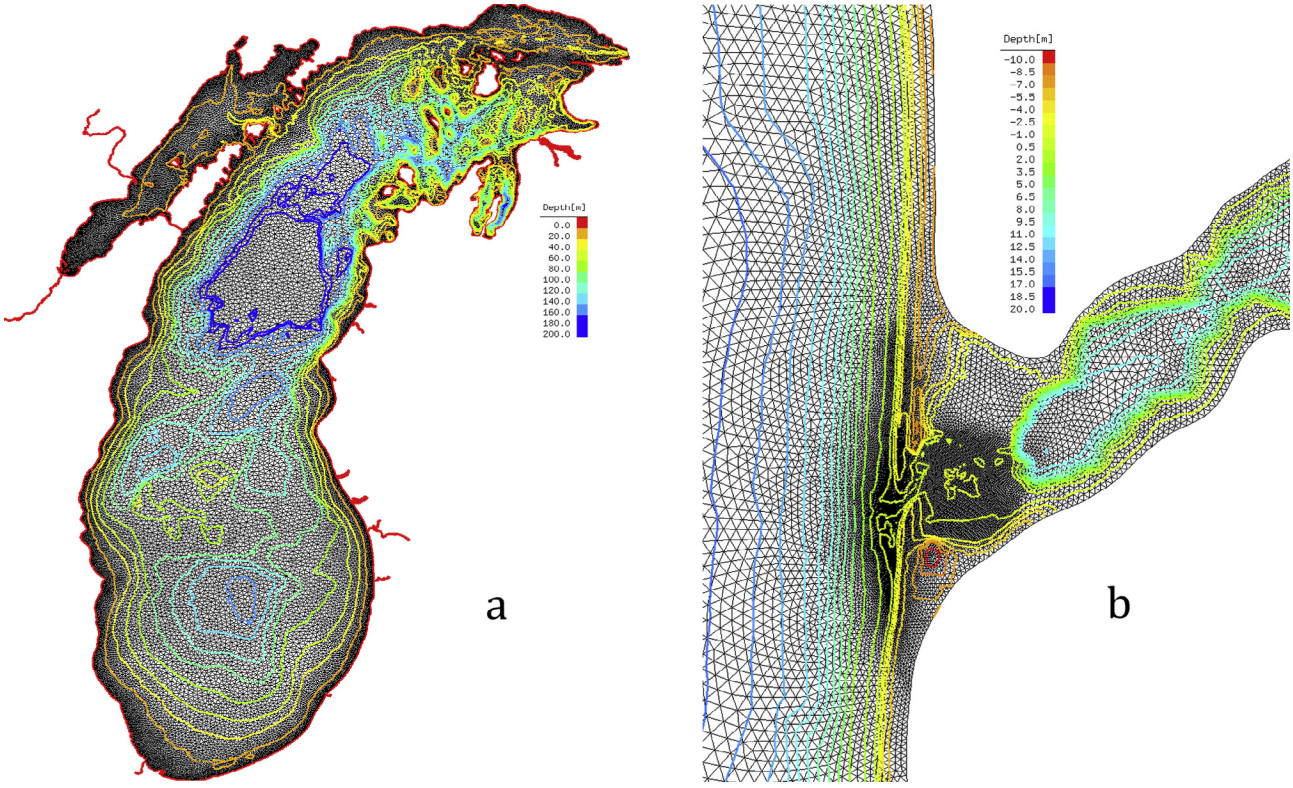

Fig. 2.8. (a) Unstructured grid of Lake Michigan (Great Lakes, USA). The resolution varies from 2 km to 250 m. The latitudinal extent is 500 km. (b) Numerical grid used for the coupled modelling of the Albufeira lagoon in Portugal (Dodet et al., 2013), with resolution ranging from 2 km offshore down to 2 m. The colour scales indicate the water depth. Note the extremely complicated, and time variable, bathymetry and emerged sand banks. The plotted latitudinal extent is 2.5 km. (For interpretation of the references to colour in this figure legend, the reader is referred to the web version of this article.)

forecasting chain of storm surges (see Westerink et al., 2008; Roland et al., 2009; Roland, 2014; Dietrich et al., 2011; Beardsley et al., 2013; Ferrarin et al., 2013; Hope et al., 2013; Bertin et al., 2015), coastal hazard mitigation and for environmental studies (e.g., Ferrarin et al., 2008).

2.4.2. *A brief outline of the available numerical approaches where we briefly describe the various approaches that can be used for the solution of the equations with which we describe the processes of interest*

The solution of the wave action balance equation is in itself a formidable task as the equation not only has four dimensions (two spatial, two spectral) varying in time, but also because the described physics cover multiple scales of processes amply varying in time and space. The application of this kind of models has been at its beginning largely linked to operational centres, but the large computational resources that became available in the last two decades have made these models attractive to oceanographers and engineers. A thing to note is that the present scales of interest are far below the operational ones (~10–50 km or more) at which the models have been originally developed. With increasing computational power, finer spatial and spectral resolutions are possible and with more reliable measurements more demands are posed on the accuracy of the solution. The challenge therefore is to balance these requirements with the desired accuracy.

Originally, and still with structured grids, downscaling in wind wave modelling became feasible with the development of nesting methods. The application of nesting, or so-called telescoping methods is at the end limited to a small region for the highest resolution grid, which may have the same constraints as any structured grid itself. As done by Tolman (2007), the idea of nesting can be generalized in the multigrid approach, where various structured grids can be combined, and also moving grids can be utilized. The latter one is a particular solution where at each time step the resolution of the structured grid can be locally increased, e.g. doubling the resolution where the gradients are above a threshold value. This approach appears useful where, like in hurricanes, the area where a higher resolution is required may and does change in time. However, although pursued for a number of years by, e.g., Popinet et al. (2010), this approach has not yet taken off, on one hand for the greater numerical complexity (e.g. book keeping), on the other hand for the continuous interpolations it requires with a consequent tendency to smooth the profile of the various variables. However, interest continues in such approaches.

The benefit of the multigrid approach was the seamless two-way nesting of various grids (see the later example in Fig. 2.15). However, the limitations of structured grids remain inherently the same because the highest resolution grid can only cover a limited region of interest. More recently numerical schemes have been developed that achieve higher resolution by subdividing each computation cell in a certain way (e.g., Popinet et al., 2010; Li, 2012). These so-called Quad-Tree or spherical multi cell (SMC) grid methods are much more flexible than their structured counterparts, but still the location of each node is constrained by the geometry of the grid and it does not allow a free placement. Moreover, the grid subdivision cannot be efficiently used in real multi-scale applications where in the domain of interest the geographical scale varies by several orders of magnitude.

All the present wave models, as MIKE21-SW, FVCOM-SWAVE, SWAN, ECWAM, WW3 or WWM, have introduced unstructured grids as an alternative to their structured approach. Different unstructured discretization methods in geographical space have been applied to solve

the hyperbolic problem of wave propagation. These include explicit finite volume methods (e.g. Sørensen et al., 2004; Qi et al., 2009), implicit finite element methods (e.g., Hsu et al., 2005a), implicit finite difference schemes (Zijlema, 2010), and implicit/explicit residual distribution schemes (Roland, 2008), as given in Ricchiuto et al. (2005), These numerical schemes do relax the downscaling problem massively, but they unleash a variety of new problems, which have not been of the due concern so far. For instance at their best they are up to second order accurate in geographical space and third order in spectral space (e.g., Roland, 2008; Zijlema, 2010). For unstructured grid methods the approximation of the time derivative is at best first order accurate. See the next sub-section for a more extensive discussion on the accuracy of the various approaches.

The time stepping methods used for (un)structured grids in spectral wave modelling follow two different approaches. The explicit methods are based on simple Euler time stepping or the Lax-Wendroff approach (Lax and Wendroff, 1960) applied within different kinds of operator splitting techniques (see, among others, Tolman, 2002a; Sørensen et al., 2004; Roland, 2008; Qi et al., 2009). This approach suffers from severe time step constraints given by the CFL number. As an example, the integration time step for a shallow water 13 s wave in 10 m water depth and 10 m grid resolution is limited to one second. To circumvent these limitations Booij et al. (1999) and Ris et al. (1999) included the use of implicit methods on structured grids. Originally used in the SWAN model, this new approach met with immense success, and SWAN quickly became the most used model among the users community for coastal applications. The implicit methods were then implemented also on unstructured grids (Roland, 2008; Zijlema, 2010; Huchet et al., 2015a,b).

When the unconditionally stable implicit method of SWAN was presented, it was at that time the most efficient approach for solving the wave action balance equation in shallow water and it pioneered the use of this model class in shallow water, paving the way for future developments. Indeed at the time this appeared as an extremely good and the long lasting solution. However, the steadily increasing computer power and the efficient parallelization now introduced in the models have largely expanded the field of application of explicit methods in unstructured grids, leading to some sort of subdivision of the respective areas of application. So the explicit approach may become the convenient solution down to 200 m resolution, if larger regions and operational applications are of concern (e.g., Ardhuin et al., 2012a,b, http://marc.ifremer.fr/). Conversely, implicit time stepping schemes are the convenient choice if efficient multiscale applications are of concern, especially when the variations of the grid resolution, starting from the tens of kilometres offshore, span up to four orders of magnitude down to a few meters, and if spectral wave models are coupled to shallow water phase resolving wave models.

As it is obviously the case, all these discrete numerical approaches are approximations to nature. They imply errors, of which we need to be aware if we want to make a meaningful use of these no doubt very sophisticated instruments. This is the subject of the next sub-section.

2.4.3. Numerical methods, their characteristics and errors

where we indicate the possible sources of error in wave modelling, how these depend on the situation and the used method, and which are the most common solutions for the daily problems

Having briefly described the possible basic approaches, here we want to dig into them to quantify the errors and the limitations each of them implies.

By and large the basic types of numerical errors for unstructured grid schemes are similar to those already discussed in Cavaleri (2006) and Cavaleri et al. (2007) for numerical schemes on structured grids. However, moving to shallow water, more processes become active, nonlinearities play a relevant role, scales becomes smaller, and errors may become larger.

In the following discussion we will consider three basic distinctions of the possible approaches:

- linear (1), nonlinear (2) [a scheme is linear in the sense that the new solution is a linear combination of the old and new ones in different grid points],
- first order (1), higher order (2) [in accuracy],
- explicit (1), implicit (2) [time integration method].

In the above order, each approach will be classified as, e.g., (1,2,1), i.e. linear, higher order, explicit. Beside its numerical characteristics, every approach can also be classified on the base of the average (situation dependent) characteristics of the obtained results. The schemes should preferably obey certain design principles that ideally fulfil the below criteria. The scheme is:

(P) positive and (M) monotonic – it does not produce unnatural negative results, e.g. for energy, and it does not generate new extrema in the solution,
(LP) linear preserving – it guarantees higher order when the solution is smooth, and first order in the vicinity of very strong gradients,
(C1) conservative – e.g., overall energy is not numerically created or destroyed along wave rays (Whitham, 1974), but it varies only according to physical processes (generation and dissipation),
(R) robust – it is stable, and it does not depend strongly on the chosen discretization lengths in space and time as long as they make physical sense,
(C2) convergent – the solution converges to a unique solution with decreasing resolution,
(E) efficient – it can be run efficiently when strong downscaling is of concern (multiscale applications) and it does not significantly depend on resolution and time step if chosen in physical reasonable ranges,
(A) accurate – how close the numerical solution is to the true value of the considered variable.

One key point of numerics is that, on the base of the relevant background theory, all these characteristics, in particular P, M, C and LP, are not easily obtained at once (the interested reader may refer to the various theorems by Godunov, 1959, Lax and Wendroff, 1960, and Lax and Richtmyer, 1956). This will be better described in the following discussion.

Starting with linear first order methods (1,1,1), the classical objection is that they imply significant numerical diffusion with consequent artificial (non-physical) dissipation when adherent to coast (see Cavaleri and Sclavo, 1998). One solution is to move to linear higher order methods (1,2,1) with the intent of reducing numerical diffusion. However, these linear higher order methods, no matter explicit or implicit (e.g., Hsu et al., 2005a; Qi et al., 2009; Rogers et al., 2002), do not fulfil positivity, monotonicity and linear preservation, producing in this way negative wave action and oscillations in the solution. This kind of behaviour occurs especially in regions where steep gradients in the solution are present. To treat this negative wave action, certain heuristic methods have been considered, an example being the conservative rescaling used in WWI (Tolman, 1992) and SWAN. However, this artificial redistribution of wave action in the directional space transfers some energy in other areas of the spectra, which can be seen as numerical diffusion in theta space. The magnitude of the possible negative

wave action depends hereby on the gradient of the wave action in the various dimensions and the CFL number. Besides, it is clear that, albeit (but not always) at a limited extent, not all the directional conservation properties of the schemes are then fulfilled.

As a consequence, this behaviour of higher order schemes imposes a constraint on the chosen time step with respect to model convergence rather than due to stability problems. Refining the mesh may alleviate these problems, but this may also increase them since it may lead to even higher gradients as it is often the case when using unstructured grids. Basically unstructured grids are intended to do so by construction, and therefore linear higher order methods are hard to control.

A fundamental approach to this problem is to construct nonlinear higher order schemes (2,2,∗) that are globally positive and flux-conservative (Godunov, 1959). The nonlinearity is essential to jump over the Godunov theorem and fulfil P, M, C1 and LP at the same time. However, implicit nonlinear higher order schemes (2,2,2) are not yet available to the spectral wave modelling community since this would involve the solution of a nonlinear equation system, which is very costly. Only non-linear explicit schemes (2,2,1) have been successfully employed so far, mostly on structured grids (WW3, see Tolman, 2009), showing significant benefits when swell propagation over long distances is of concern.

The conditions change drastically in coastal seas. Here the use of higher order propagation schemes can even have surprising undesired consequences. For instance, in nature, in the lee region of not well resolved islands, refraction, diffraction and nonlinear propagation will result in wave energy transport in the shadowed regions of the islands (see, e.g., Holthuijsen et al., 2003; Liau et al., 2011; Willebrand, 1975; Toledo et al., 2012). However, higher order numerical schemes indicate a perfect sheltering of waves, a fact not seen by first-order schemes where the implicit diffusion helps to compensate, up to a certain point, for the lack of, e.g., diffraction, nonlinear propagation, swell decay, scattering, and all the processes we have only begun to take into account in spectral wave modelling. However, this is a case of getting the right answer for the wrong reasons. For higher order schemes the related problems can be alleviated by explicitly adding diffusion as proposed by Booij and Holthuijsen (1987). Moreover, as e.g. pointed out in Cavaleri (2006), one reason for the success of first order schemes is that wave action gradients in geographical space are usually not strongly pronounced (see also Janssen, 2008).

The lesson is that when we increase the order of our schemes, we need also to increase the number of physical processes we take into account, processes that are now partly mimicked by the numerical diffusion. As a matter of fact, most of the published results on unstructured grids apply first order schemes with good results even in complicated environments (e.g. Ardhuin et al., 2012a,b), even if the numerical errors in terms of diffusion are known to be significant.

Still about spatial resolution, when decreasing (i.e. improving) it is of concern, the numerical schemes should be efficient, robust and accurate even if the resolution varies over several orders of magnitude. The maximum possible time step should not depend significantly on the CFL number as it is the case for, e.g., non-monotone schemes. The scheme should also not have a significant time step dependency (robustness). The computational cost should not increase exponentially as function of unknowns and the scheme should perform efficiently also when parallelizing the program (efficiency). Moreover, the scheme should converge (C2) as fast as possible to a weak (i.e. pragmatically, but not formally, correct) solution if we reduce the time step and increase the resolution (accuracy).

Another class of numerical errors, the so called splitting errors, arises in e.g. the fractional step method (Yanenko, 1971). They follow the separate numerical treatment in various dimensions of the advection and source terms (e.g. Tolman, 2002b). The splitting error becomes significant when the operators do not commute and the global (i.e. large scale) time step is much bigger than the one locally used for each of the sub-problems (source terms or spectral advection – see, e.g., LeVeque and Yee, 1990; Lanser and Verwer, 1999; Sportisse, 2000; Geiser, 2012). The splitting error between source terms and geographical advection, as well as with spectral advection, may become significant for large global time steps when a large number of sub-iterations are required. The optimal case would be that each of the various spaces has unity sub- or just some few sub-steps in the various dimensions. For splitting schemes, however, it can be shown that in hard cases (i.e. cases for which a small time step is required for stability) there is a severe order reduction of the scheme. It must be noted that splitting methods that use implicit schemes for geographical advection are much more prone to splitting errors since large global time steps are possible. This leads to significant splitting errors, especially if for the purpose higher order linear schemes are used (see, e.g., Roland, 2008; Roland and Ardhuin, 2014). Consequently, for numerical schemes which have a pronounced dependency on the integration time step it is advisable to carry out a convergence analysis by reducing the time step and increasing the resolution up to the point where the resulting difference are in the acceptable range for the specific purposes. This mainly involves splitting methods and higher order linear schemes. To summarize, in order to be able to judge the results, it is advisable (a) when applying higher order linear schemes, to either carry out convergence studies (e.g. by refining the mesh and/or reducing the time step) or (b) even to apply first order schemes, which are more predictable in how they characterize the solution.

To frame the situation, usefully summarised in Table 2.2, we can say that suitable nonlinear higher order schemes are not yet available for the extensive daily activity, and implicit first order methods on unstructured grids are probably at this time the best approach while having a sufficiently resolved grid/mesh, especially in applications that consider coastal and enclosed seas with multiscale characteristics. However, if new physics is to be investigated, using first order schemes it will remain difficult to properly quantify the numerical errors versus the ones arising from the investigated physical description of the processes. Here it is important to design test cases, where the physical phenomena of interest are isolated and the effects of numerics significantly reduced, something that can only be achieved by higher order

Table 2.2
Numerical characteristics of the different solutions adopted in the various approaches.

Discretization			Properties			Downscaling performance		
Linear/nonlinear	First/higher order	Time-stepping method	Conservative-convergent	Linear preserving	Positive	Efficiency	Robustness	Accuracy
Linear	First	Explicit	Yes	No	Yes	Average	High	Low
Linear	First	Implicit	Yes	No	Yes	Highest	Highest	Lower
Linear	Higher	Explicit	Yes	No	No	Average	Low	Low
Linear	Higher	Implicit	Yes	No	No	Low	Low	Low
Non-linear	Higher	Explicit	Yes	Yes	Yes	Average	High	High
Non-linear	Higher	Implicit	Yes	Yes	Yes	High	High	High

schemes or high spatial resolution.

2.4.4. Limiter effects

where, after describing the possible errors, we indicate the most common used solutions

Notwithstanding the problems we have briefly described in the previous sub-sections, we need (1) to produce results, (2) to be aware of the possible errors, (3) to devise methods to limit these errors as much as possible. Knowing by theory and experience where the problems may arise, we can use some pragmatic approaches to limit the undesired consequences. This leads us to the subject of limiters.

Limiters are required in operational wave modelling for the sake of robustness and efficiency and act as a safeguard in many situations. The limiters are designed to (a) limit instabilities arising in stiff systems, e.g. related to the nonlinear four-wave interactions if operating with a large time step, (b) limit spectral space advection velocities (viz., c_θ and c_σ) if they become too high, and (c) limit the maximum wave height when depth induced wave breaking is of concern (see the classical paper by Battjes and Janssen (1978)). This happens, e.g., when the integration time step is chosen to be too large for the problem of interest, or if the advection velocities, e.g. due to steep and under-resolved bathymetry, are too large (see Komen et al., 1994; Booij et al., 1999; Hersbach and Janssen, 1999; Tolman, 2002b; Monbaliu et al., 2000; Zijlema and Van der Westhuysen, 2005; Tolman, 2009; Roland and Ardhuin, 2014). In the (c) case above, the wave breaking limiter acts as a safeguard with respect to the physical value of wave heights in shallow waters. In practice we need to be sure that, based on numerical and discretization errors or the wrong use of the physical formulation, the wave model does not produce obviously unphysical results (e.g., wave heights far greater than the water depth or other non-physical artefacts). All numerical forecasting methods rely on the above summarized limiters as a pragmatic safeguard.

The problem with limiters is that, once embedded in the program, they may appear and virtually become part of its physics. However, ideally these limiters should not have a big influence on the solution. In this respect we should not forget that most of these limiters have been originally designed for global wave forecasts and for operational needs (see, e.g., Monbaliu et al., 2000). In most of the cases they appear in their original form in the present models. For instance Hersbach and Janssen (1999) and also Tolman (1992) have shown that, especially in the initial growth stages, the results depend strongly on the integration time step. This is of special significance for enclosed basins where the typical conditions of a (fetch-limited) developing wind sea with high spatial and temporal gradients may impose restrictions on the integration time step. If limiters are active for a large part of the model integration, it should be remembered that they are effectively negating the physical solution which is being sought and can affect conservation.

Apart from playing with the resolution, to circumvent this problem we could also redesign the numerical methods (Tolman, 2009) or reformulate the wave action limiter with the aim to reduce their impact on the solution. The alternative limiter suggested by Hersbach and Janssen (1999) reduces significantly the time step dependency of the solution showing very good results in operational forecasting, but it has also shown oscillations for small time steps (Monbaliu et al., 2000) and has not yet been significantly tested in shallow waters. Actually, the Phillips limiter by Komen et al. (1994), acting on the rate of change in the spectral tail, is presently used in most wave models, also when applied in shallow water modelling (Booij et al., 1999). In these circumstances the integration time step is the crucial parameter, especially if transient solutions are of concern. Further research is needed to design a limiter formulation for implicit schemes in shallow waters, a (wave action) limiter which does not introduce such a significant time step dependency in the solution and makes in this way more efficient modelling possible, both in terms of computer time and accuracy.

In many approaches limiters have been applied also to the propagation velocities in spectral space (refraction and frequency shifting) in terms of bottom slope, spatial resolution or other parameters. Some models allow the user to limit the amount of refraction for under-resolved bathymetries. This is true for most of the models, either acting on the code (WAM, WW3 or WWM) or on the SWAN input file. The consequences depend on the situation and require attention by the user (see later). Another compromise solution is to further reduce the time step in spectral space, put a maximum value to the bottom slope in each grid step, in so doing effectively placing a limit to the refraction term c_θ and spreading the change of depth on a higher number of steps. In this respect it is interesting to note that, in contrast to the action density limiter, the limiters on spectral advection velocities are not required for model stability (the overall energy, i.e. H_s, is not varied), but for efficiency or accuracy reasons (we do not want to change too much the distribution of energy in the spectrum). However, at the end of the day, whichever the accuracy we can use in our action, the relevant point is that the application of these limiters may have significant effects on the results. Therefore their implications must be investigated in terms of convergence studies (e.g., Roland and Ardhuin, 2014). It is highly advisable to explore the convergence of our model and, e.g. depending on the grid resolution, (1) how necessary is indeed a limiter, (2) if its use is prone to substantial local errors.

2.4.5. Summary and outlook

where we summarize where we are today, but then look forward to the future problems and numerical possibilities

The discrete description of the natural world we are forced to use in practical applications requires its fee, and we have seen this is paid in terms of both computer time and accuracy, the latter depending again on resolution and errors of the results. All this is enhanced in the enclosed seas: the limited dimensions of the basins imply shorter waves, frequently under active wind generation conditions. We also have complicated geometry of the coasts, shallow water conditions, steep gradients both in, e.g., the bathymetry and in the values of the variables (significant wave height, periods, directions, spectral distribution) we care about and need to know.

As expected, this has stimulated the development of a variety of methods (linear and nonlinear, first or higher order, explicit or implicit, regular and unstructured grids) that time and experience have helped to frame with respect to their characteristics and applicability in the different environments and situations.

Talking about the last one of the just mentioned characterizations, there is no doubt that unstructured grids have gained much ground in applications in the inner seas and coastal water. When approaching a complicated coastline and a highly varying bathymetry, a flexible and adaptable grid (although not yet dynamically varying) is the desired and obvious solution. Of course the same situations that lead to this choice imply more complications in the numerical solution of the (partial differential) equations with which we describe the physics we care about. This may range from the “simple” problem of wind waves to the complex ones of coastal flooding or environmental studies dealing with sediment transport and water quality.

The choice between explicit and implicit methods seems to depend on the scale of the area of interest and the situation. Implicit schemes offer advantages and are the best choice if at the coast we go for resolution of the order of $\sim$100 m or less. Indeed examples of implementations in WW3, WWM-III and WAM, besides the obvious SWAN, exist. At a higher scale, if computer power is available and thanks to parallelization, the explicit approach has still its place up to a certain extent, say 200 m resolution, provided points in higher depth, like e.g. shipping channels, are not considered. In the latter case one “bad point” can destroy the whole performance of the explicit scheme, which means that much more time in grid generation needs to be spent in order to have an efficient mesh in contrast to implicit schemes where this would not matter in terms of performance. The situation is flexible

to a certain extent.

Much effort has been put in developing explicit nonlinear higher order schemes, ideally to avoid some of the apparent limitations present in linear first and higher order ones. However, the results are debatable, and there are indications that first order schemes are still a valuable solution. This is also connected to a lack of knowledge and to the discrete use of the physics of the many processes that appear with a potentially relevant role in shallow water. We compromise this with the use of numerical limiters to avoid either unphysical values of physical parameters, or excessive fluxes either in space or spectral terms. Apart from the actual physical or flux value, from the numerical point of view these limiters may imply problems in the convergence to the right solution. Therefore convergence studies are highly recommended to establish a priori if and when a limiter is needed, and, if so, its most suitable value. Future developments should be aimed at designing schemes in such a way that the effects of heuristic measures on the solutions vanish or are strongly reduced, in so doing reducing also the numerical uncertainty in wave prediction in shallow water conditions. This will imply some basic steps in the extension of the first order schemes towards higher orders, particularly nonlinear implicit ones.

With this in a way we are still on the “traditional” ground of the energy or action balance equation. However, the new frontier opened by pushing, e.g., the models closer and closer to coast, in shallower and shallower water, practically in the breakers zone, implies extremely strong spatial and temporal gradients, hence new physics and new interactions to be considered. If, but still we do not know how, we want to model this area in an effective way, obviously new approaches, equations, numerical methods need to be developed.

More generally, we should never assume that the ground we firmly stand on and that has been there for a while will be our permanent solution. New openings, not only numerical, but certainly related to numerics, are presently explored. Already in 1975 Willebrand had worked on a nonlinear scattering relationship, which implies the extension of the equations to inhomogeneous media. Toledo et al. (2012) have explored the extension of the energy balance equation to higher order bottom slopes and shear currents, an extension that results in a nonlinear, amplitude dependent equation and a new definition of the conserved variables since wave action is no longer conserved anymore under such conditions. In terms of efficiency the extension to wave models based on these innovative approaches will imply a significant breakdown of our forecasting range, demanding a complete revision of our numerical approaches before operational applications are even thinkable.

Further problems, still related to coastal or, e.g., harbour features, concern wave interference and diffraction that cannot be dealt with by a homogeneous, Gaussian statistics. Recently Smit and Janssen (2013) and Smit et al. (2015) have developed a generalized evolution equation for the transport of the complete second order wave statistics of the surface elevation, including cross-correlation. Specifically, this equation generalizes the action balance equation by including the evolution of the cross-correlation terms. This approach will improve the physical basis of e.g. computing the sheltering and spreading of waves behind an island, as discussed in Section 2.4.3.

We have repeatedly mentioned the basic problem of representing in a discrete way the natural continuum. In meteorological modelling the spectral approach solves this issue by representing the fields as two-dimensional Fourier series (see, e.g., the Integrated Forecast System, IFS, of the European Centre for Medium-Range Weather Forecasts, Reading, U.K., www.ecmwf.int). Yildirim and Karniadakis (2012) did so in wave modelling using a spectral approach in spectral space. More recently, Adam et al. (2016) introduced the so-called adaptive Haar wavelets, which is even more promising. How effective this approaches can be in strongly non-periodic fields is to be seen.

Possible future developments will be further commented upon in the general look to the future in Chapter 5.

2.5. Data availability

R.E.Jensen, S.Abdalla, A.Bemetao, L.Cavaleri
Robert.E.Jensen@usace.army.mil

where, contrarily to the common attitude of wave modellers, we make an extensive critical analysis of the wave measuring instruments, hence of the accuracy we can expect on the data we use for the validation of our modelling work. We also stress the need to go further than the usual integrated parameters to have a detailed and more meaningful validation of the model results.

Availability of the sea truth, of wave conditions in particular, is a key element for the validation, and consequent improvement, of model results. In this section we provide an overview of the commonly used technologies to provide those data, highlighting their advantages and limitations, and what to expect for the immediate future. Unavoidably the various arguments will not be valid only for coastal or shallow waters, or for inner seas. However, we also mention specific problems generally typical of this environment.

2.5.1. Generals

where we outline the importance of measured data and their accuracy

We have been directly measuring wind-generated surface gravity waves (henceforth ‘waves’) for over 60 years and continue to operate and maintain an array of measurement platforms around the world to this day. Wave measurements in the context of enclosed, semi-enclosed bodies of water or the coastal domain have and continue to be a necessity in all aspects of wind-generated surface gravity wave studies. Wave measurements have been, are and will continue to be used in evaluations, model testing/improvements, source-term specification, climate trend analyses.

Our roots in the development of wind wave growth rate expressions are based on field measurements in enclosed bodies of water such as Lake Okeechobee, Florida (Bretschneider, 1952), Lake Ontario, US-Canada (Donelan et al., 1985), Lake St Clair, US-Canada (Donelan et al., 1992), Lake George, Australia (Young and Verhagen, 1996). Even JONSWAP (Joint North Sea Wave Project, Hasselmann et al., 1973) was conducted in what would be classified as a coastal region in the North Sea. The Surface Dynamics Experiment (SWADE, Weller et al., 1991) and the Shoaling Waves Experiment (SHOWEX, Ardhuin et al., 2007) were conducted along the US Atlantic Ocean operating on the continental shelf, investigating wind-wave growth, and transformation processes. These field campaigns highlight the need of accurate data in coastal and enclosed seas. Before discussing the characteristics of the main instruments in use, we make a brief panorama of the different approaches.

Waves have been measured using various measurement platforms from point-source sites, such as surface buoys, bottom mounted systems (pressure), acoustic profilers, to fixed systems as in the case of continuous wire gauges, step resistance, to downward looking radar and laser. Each system has a well-defined range of application, placed at a site with the general purpose of monitoring local conditions. Problems occur of course. As a first hint we mention that wave measurement systems used in enclosed, semi-enclosed water bodies and coastal waters have to consider the frequency range of the wave climate, the water depth where the devices are placed that can vary based on tides, surges, seiching of the free surface as well as changes in the bottom, and the breaker zone where the free surface cannot be distinguished any more. For bottom mounted gauges, the water depth acts as a low-pass filter, reducing the ability to measure high frequency wave energy. Wave-current interaction effects from the diurnal oscillation of tides, wind generated, or in shallow water wave-induced ones can and will modulate the measurements and produce erroneous results (see in this respect Chapter 3). It is clear that we need a thorough look at what wave measurements can really provide. Most of all, wave modellers need to

Table 2.3
Satellite missions with reliable radar altimeter instruments.

Satellite	Launch	End of Life	Altitude	Repeat Cycle
SEASAT	1978	1978	800 km	17 days
Geosat	1985	1990	800 km	17 days
ERS-1	1991	1996	785 km	35 days [+]
TOPEX/Poseidon	1992	2006	1336 km	10 days
ERS-2	1995	2011 [#]	785 km	35 days [*]
GFO	1998	2008	800 km	17 days
Jason-1	2001	2013	1336 km	10 days [*]
ENVISAT	2002	2012	800 km	35 days [*]
Jason-2	2008	–	1336 km	10 days [*]
CryoSat-2	2009	–	720 km	369 days
HY-2	2011	–	963 km	14 days
SARAL/AltiKa	2013	–	800 km	35 days [*]
Jason-3	2016	–	1336 km	10 days
Sntinel-3A	2016	–	815 km	27 days

[+] Followed other orbits with repeat cycles of 3 days and 168 days.
[#] Limited coverage from 2003 onwards.
[*] Different orbit followed towards the end of its life.

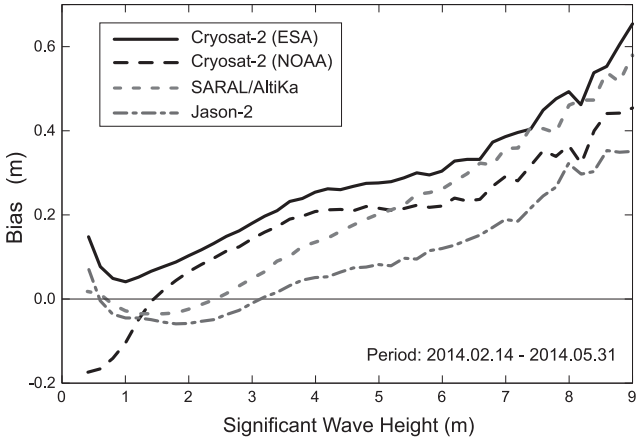

Fig. 2.9. The significant wave height difference (bias) between various altimeters and the ECMWF operational wave model first-guess as functions of significant wave height.

realize that, contrary to the use often done, measured data are not that perfect piece of information we would like to have. Rather, they have statistical and intrinsic errors that we elucidate further in this section where we briefly describe the main methodologies used to measure waves and the related implications for accuracy.

2.5.2. *Types of measurements*

where we mention the main systems for measuring waves and their respective characteristics

There are two primary types of instruments to measure waves: wide scope measurements, using remote sensing including satellites, aircraft equipped or land-based systems, and point-source measurements i.e. focusing attention on a very limited area, most of the time a single point. Both have strengths and weaknesses. Satellite systems provide large-scale, repetitive spatial coverage, but with discontinuities in time. Land based radar systems cover with continuity a certain area, but they lack details and accuracy. Applications to land-based radar systems measuring waves have been questioned and require further testing and evaluation of historical ones. Point measurements provide data continuity, but of course limited at a single location.

2.5.2.1. *Remote sensing*

2.5.2.1.1. Altimeters. Numerical Weather Prediction Centres (NWPC) as ECMWF, NOAA/NCEP, UKMO, and FNMOC forecast wave conditions for the entire ocean covering the world. Prior to launch of the short living SEASAT (1978) and GEOSAT (1985) and the consequent availability of altimeter wave height estimates, assessing the quality of large scale model results was impossible to achieve. Satellite based remote sensing, using altimeters such as those on-board TOPEX/Poseidon, Jason-1, Jason-2, Jason-3, ERS-1, ERS-2, ENVISAT and Sentinel-3 (see Table 2.3 for a longer list) and using synthetic aperture radar (SAR) such as those on-board ERS-1, ERS-2, ENVISAT and Sentinel-1, has provided and provides useful data in remote locations of the world's ocean basins up to a few tens of kilometres off the coast (but see the recent advances with Sentinel-1, e.g. by Ardhuin et al., 2015). NWPC's routinely use these results to evaluate the wave forecasting performance (Romeiser, 1993; Janssen et al., 1997; Bidlot et al., 1997; Janssen et al., 2003; Li and Holt, 2009), or, via the assimilation into a first-guess wave fields, to improve the wave forecast quality (see Abdalla and Janssen, 2017, for an extensive discussion on the subject). Note that using the same data for both purposes does not have much significance unless the model forecast (rather than analysis) is being evaluated using data that were assimilated at earlier times.

The radar altimeter (RA), or just altimeter, is a nadir looking active microwave instrument. This instrument emits pulses and measures the characteristics of the returned signal from the ground. The travel time, the power and the shape of the return pulse are used to estimate several geophysical parameters including the marine surface wind speed and the significant wave height. Typically, an altimeter provides one measurement every 1/20th of a second (20 Hz). About 20 individual 20-Hz values are averaged to form one measurement every second (1 Hz). Depending on the satellite altitude, the distance covered will be typically between 6 and 7 km along the satellite track. Table 2.3 shows an extensive list of radar altimeter instruments with some of their basic characteristics.

Altimeter significant wave height measurements are very robust and of very good quality. The errors in such measurements can be attributed mainly to the algorithms used in deriving the wave heights from the altimeter raw measurements. It was shown by several authors (see for example Abdalla and Janssen, 2017) that altimeter significant wave height compares quite well with in-situ measurements as well as model predictions. Based on the triple collocation technique, which makes use of three independent sources of wave height data sets at the same time and same locations and assuming linear error model, Janssen et al. (2007) and Abdalla et al. (2011) showed that at the scale of the ECMWF model (~75 km) the random error in altimeter wave height is about 6% of measured values.

In general, specific altimeter instruments can be quite different from each other. Indeed measurements by various altimeters are not consistent, but they may differ by few percent. Besides the calibration of these instruments is usually done in the 2 to 4-m wave height range, while the ones on the lower and higher ranges can be, and usually are, different. Finally most of these calibrations have been done based on measurements by open ocean buoys (see Fig. 2.8, but also the later discussion about buoy data) where the usual wave conditions are different from the enclosed seas, and this affects the calibration.

Fig. 2.9 shows the difference between the significant wave height from various altimeters (CyoSat-2, SARAL/AltiKa and Jason-2) and the ECMWF operational wave model first-guess as functions of the wave height itself. It is clear that altimeter measurements deviate from each other by 0.10–0.30 m depending on the wave height regime (typically more than 10%). Of course, the model is not the truth but it is taken here as the reference against which altimeter wave heights were compared due to the absence of the "truth". One of the altimeters or even the in-situ measurements could have been selected as the reference as well but this does not matter apart from reducing the sample size (all altimeter measurements can be collocated with corresponding model predictions but the collocations among the altimeters is not very common).

An interesting observation in Fig. 2.9 is the difference between

CryoSat-2 wave heights as produced by ESA (the European Space Agency), which is the owner and operator of the spacecraft, and those produced by NOAA (the National Oceanic and Atmospheric Administration) using different algorithms. Therefore, the differences among various measurements from various altimeters do not originate only from the measuring instruments themselves but also from the algorithms used to derive measurements.

Combining measurements from different altimeters or replacing a dead or degraded altimeter with another one cause some challenge on which one to trust. In any case, an inter-calibration of the different instruments is required in order to achieve a rather consistent dataset. This is inevitable since satellites are usually designed to serve for a few years (around 3–7 years). Although, they usually last twice as long on average (see Table 2.3), none of them was able to survive more than a decade without serious issues.

Before using the altimeter measurements, one needs to consider few limitations. The first is related to the spatial and temporal sampling. Although space-borne altimeters cover the whole globe, this is done in a form of a mesh with spacing of few tens to hundreds of kilometres depending on the satellite orbit. The satellite repeat cycle is the time duration it takes the satellite to revisit the same point on the earth surface. The repeat cycles are typically 10–35 days (see Table 2.3). ERS-1 followed few repeat cycles of 3 and 168 days for experimental purposes while CryoSat-2 has a cycle of 369 days. The longer the repeat cycle the narrower the separation between the satellite tracks. This has some consequences regarding the availability of altimeter data in smaller water bodies or some coastal areas as they may fall in altimeter-blind zones. Furthermore, if the area of interest is visited by an altimeter, the temporal separation between nearby measurements within the repeat cycle is not regular.

Another limitation affects small significant wave heights as most of altimeter wave heights are typically not reliable below about 0.50 m. This arise from the fact that the altimeter signal is digitised using a finite number of bins (called gates). Significant wave height is derived from the slope of the returned signal and the finite separation between the gates does not allow proper slope measurements. Furthermore, altimeter measurements are not well-calibrated at high wave heights. The coincidence of having an altimeter pass in the vicinity of an in-situ wave measuring device during high sea state is not very common. The comparison against models provide longer validation data sets but it is not clear how reliable wave models (even buoys) during extreme wave height conditions.

Another issue to be aware of is the (horizontal) scale of the altimeter measurements. It is well known that altimeters sample the ocean surface at a rate of 1 Hz, which is in fact an average of around 20 individual measurements obtained at a rate of 20 Hz (those 20-Hz data started to be released by altimeter data providers recently). During 1 s, the satellite moves along its track by 6 km (for satellites at high altitudes like the Jason family) to 7 km (for satellites at lower altitudes like Sentinel-3). However, this is different that the scale of the altimeter measurements. The altimeter beam illuminates the sea-surface as a growing circular footprint which, while growing, turns into a ring. The returned signal, which is received by the altimeter, is composed from all reflections from the surface. If the surface is flat, the returned signal would come from the illuminated circle at a specific instant. However, the roughened surface (due to surface waves) causes reflections from larger area increasing the altimeter footprint. In other words, the size of the altimeter footprint, and thus the horizontal spatial scale, is a function of the significant wave height with smaller footprints/scales for smaller wave heights and larger footprints/scales for higher wave heights. The 1-Hz averaged measurement covers an oval footprint that measures for significant wave heights of 1, 2.5 and 5 m, in the respective order, around 9, 10 and 12 km in the along-track direction and about 3, 4 and 5 km in the cross-track direction (see Chelton et al., 2001).

The variance of the “random error” can be estimated even in the absence of an absolute truth using the triple collocation technique which was first introduced by Stoffelen (1998) to estimate the random error in Scatterometer wind data. This technique can be summarized as follows (see Janssen et al., 2007 for details): given three independent estimates of the truth, T, with unknown random errors it is possible to show that the error variance in each estimate can be found using the total variances and covariances of the three data sets in addition to the “unknown” covariances of the errors. Further assumptions are needed to estimate the error covariances. The assumption of uncorrelated errors, for example, nullifies the error covariance terms. For an extensive discussion of this approach and a number of applications see Janssen et al. (2007) and Abdalla and De Chiara (2017).

Janssen et al. (2007) used the triple collocation technique (and its extension for quadruple and quintuple collocations) to estimate the random errors of the ENVISAT and the ERS-2 altimeter wave heights at a scale of about 75 km (average of 11 1-Hz measurements) during the period from 2000 (2003 for ENVISAT) to 2004. They used various combination of measurement sources including both altimeters, in-situ and ECMWF model analysis, first-guess and hindcasts. Error correlations were estimated and were taken into account to estimate the significant wave height random error variances. The errors normalized by the mean significant wave heights are respectively 6%, 6.5%, 8%, 9% and 5% for ENVISAT, ERS-2, buoys, ECMWF model first-guess and ECMWF wave analysis.

Abdalla et al. (2011) used the technique to estimate the variances of random errors of ENVISAT, Jason-1 and Jason-2 significant wave height during a different time period (from 1 August 2009 till 31 July 2010). In order to avoid the complications of assimilating altimeter wave height in the wave model, two options were considered. The first was the operational model 1–day forecast which is a compromise between very close to analysis to represent the model accuracy and too far from analysis to eliminate a large portion of the error correlation which complicates the triple collocation technique. The second was a wave model stand-alone hindcast run without any data assimilation was carried out. The model was forced the operational ECMWF wind fields. For the period preceded the ECMWF IFS model change in resolution on 26 January 2010, the wind fields were obtained from the output of the parallel ECMWF model run with the same version of the model that was operationally implemented on 26 January 2010. The NRT significant wave height observations from each altimeter were collocated with the model hindcast and buoy independently producing three different data sets. All data sets with effective scales of lower than 75 km (altimeters and in-situ) were averaged over windows corresponding to the 75 km. The random significant wave height errors of Jason-1, Jason-2, and ENVISAT altimeters together with the model 1-day forecast and in-situ (buoy) are shown in Fig. 2.10 as functions of the wave height regime. It is clear that the altimeter wave heights has the lowest errors followed

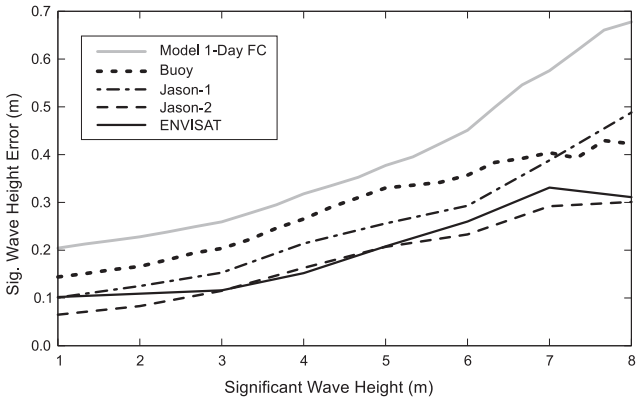

Fig. 2.10. The variation of the random error in significant wave height (as estimated using triple collocation technique) with respect to the significant wave height.

by the in-situ measurements and finally the model 1-day forecast. It is important to stress that the error in ECMWF model should be much lower than the forecast. It is well-known that the error in analysis is lower than the lowest error of the model first-guess and the data used in the assimilation for optimal data assimilation technique. It is also important to note that the validity of the results is restricted to the areas where buoy measurements exist which is mainly offshore along the coasts of Northern America and Europe.

Despite the resounding success of using altimeter data for assimilation and validation purposes (but see Chapter 4 in the former respect), there are in fact degrees of uncertainty in these records. The statistical uncertainty of sampling a random sea is generally reduced by the ample (a few kilometre diameter) sample area at each radar shot (typically available at a rate of 20 per second) and by providing one a second data averaged over the 20 shots. However, thinking especially of coastal and inner waters, if strong spatial gradients are present, it is clear that providing one datum every six to seven kilometres has a strong tendency to smooth the field.

The mentioned difficulties close to coast are connected to the discontinuity felt in passing from land to sea and vice versa. The European Space Agency funded COASTALT, a study on the development of altimetry in the coastal zone for ENVISAT, which started in 2008 and has reached completion a few years ago (COASTALT, 2011; see http://www.coastalaltimetry.org/). A similar study, PISTACH (see https://www.aviso.altimetry.fr/fileadmin/documents/data/tools/hdbk_Pistach.pdf) was commissioned by CNES. Pilot studies have been undertaken with the goal of developing algorithms that can adequately and accurately recover altimeter information in coastal waters (e.g. Cipollini et al., 2009; Vignudelli et al., 2012).

A strong effort has been performed to improve data recovery and accuracy in coastal areas with the launch of the first and third ones of the Sentinel satellite array. While the first results suggest some optimism, calls have been issued by the European Union for projects assessing the quality of, and finding optimal ways to interpret, raw altimeter data. In particular the attempt to use the data from each single radar shot could provide data closer to coast, but at the price of a much larger uncertainty (up to 0.5 m error). See in this respect the well summarizing ppt available at https://owncloud.ve.ismar.cnr.it/owncloud/index.php/S/NcbmkTWQjKMIulr.

There are two recent developments in the altimeter measurements which are relevant to inner sea and coastal areas. The first is the development of SARAL/AltiKa which is an altimeter that makes use of the shorter electromagnetic wave known as Ka-band. Ka-band has a wavelength of about 0.8 cm compared to the Ku-band used by conventional altimeters which has a wavelength of about 2.5 cm. This reduces the altimeter ground footprint by a factor of 1/4. Furthermore, it allowed to have higher repetition rate of 40 Hz rather than 20 Hz used by conventional Ku-band altimeters. Such an improvement enables SARAL/AltiKa to measure closer to the coast. An assessment of significant wave heights from SARAL/AltiKa can be found in Abdalla (2015).

The other development is the implementation of delay Doppler shift (also called SAR altimetry) to achieve ground footprints that are still few kilometres wide across the track (as for conventional altimeters) but only ~300 m "long" along the track. This was first used for CryoSat and followed by Sentinel-3 SRAL (SAR Radar Altimeter). This is expected to be the future trend. All future Sentinel-3 satellites (B, C, D, etc.) and Jason-CS will carry a similar instrument. An assessment of significant wave heights from CryoSat-2 SAR altimeter can be found in Abdalla et al. (in press).

2.5.2.1.2. Radars and lasers. Given that waves, as a geometric feature of the sea surface, reflect radar waves, it is only natural to use this instrument to measure waves. Remote sensing systems have also been used on board fixed winged aircrafts. In particular, airborne scanning LIDAR systems (Hwang et al., 2000), Scanning Radar Altimeter (Walsh et al., 2002), airborne radar RESSAC (an a C-band radar with a scanning beam antenna, Pettersson et al., 2003) have been used for specific short-term missions mapping the spatial variability in the wave climate over short time periods, particularly in coastal areas. Hwang et al. (2000) investigated quasi-steady state wave fields under active generation, and a decaying wave field following slacking winds. The uses of these data, as they generally occur in a near coastal region, are specific to either a large-scale field experiment or a unique meteorological situation, and are of high directional resolution.

Closer to surface, X-band marine radars have been used transmitting and receiving pulses of microwaves at grazing incidence. The radar pulses interact with the centimetre-scale sea surface roughness through Bragg scattering. 3D backscatter data are processed with well-established Fourier Transform-based technique to retrieve directional wave spectra. The processing involves a series of filters and the application of an empirical Modulation Transfer Function to account for the radar image formation nonlinear mechanisms. Radar coverage of the sea surface is up to few km from the antenna, even though the backscatter signal decays super-linearly with the range and has a strong dependence on the azimuth. From radar data, the surface current (an extra information) is determined by means of a least-squares regression method that exploits the dispersion relation for gravity waves. While the X-band signal needs the centimetric waves, hence some wind, to be reflected, the HF-band radar, mainly used to measured currents, has the capability to interact directly with the wavelengths (10–200 m) we mostly care about. Note that HF radars provide only direction-of-looking information, hence they need either two separate sources or to look, progressively or with multiple antennas, in different directions. In the very near-shore HF and X-Band radar systems have been used to map the spatial and temporal variability for a specified patch of the free surface. These systems (e.g. CODAR, OSCR, WERA, and Pisces, see Wyatt et al., 2009) continue to operate at various coastal locations, however work continues to better interpret and improve their estimates of wave characteristics (see, among others, Prandle and Wyatt, 1999, and Wyatt et al., 2003). These systems have also been plagued with operational constraints (dependent on individual system applications, Wyatt et al., 2003, 2005, 2009), especially in a coastal environment.

2.5.2.1.3. Stereo. Stereo imaging systems allow the 3D sea surface to be measured using digital images acquired from (at least) two distinct points of view. For typical applications, stereo imaging captures short- to mid-size wavelengths, in the range: 0.2–80 m, with high frequency resolution. The accuracy of the observations is of few centimetres along the 3D axes. The pre-processing involves the calibration of camera parameters and the determination of the pose between the stereo cameras. Then, the coordinates of 3D points of the sea surface are recovered via triangulation of the corresponding pixels. Stereo wave imaging was proved to provide accurate wave fields for investigating different aspects of the oceanic waves, such as extreme (freak) waves, the shape of the directional spectrum, the phase speed of the largest waves. Benetazzo et al. (2015) provide an extensive view of this powerful system that no doubt will become more popular in the future. Fig. 2.11 provides an enlightening view (one image from a 20 min record) taken from the ISMAR oceanographic tower (see Fig. 2.3 for its position).

2.5.2.2. Point-source measurements. Point-source measurements have been operationally used to measure the ocean surface for the past six decades (e.g., Tucker, 1991). Most of these gauges were operated in the coastal domain. Wire capacitance and resistance gauges both effectively use depth of submergence in water to complete a circuit. Originally these gauges were affixed to piers (Thompson, 1977) and offshore platforms (e.g., Hamilton, 1972; Cavaleri and Zecchetto, 1987; Cavaleri, 2000), but they have also been modified for their use on vessels (Drennan et al., 1994) and integrated into a spar surface buoy (Graber et al., 2000). Downward looking laser altimeters (Magnusson and Donelan, 2013) are used as the baseline for an intra-measurement evaluation in the North Sea (Allender et al., 1989), and have also been

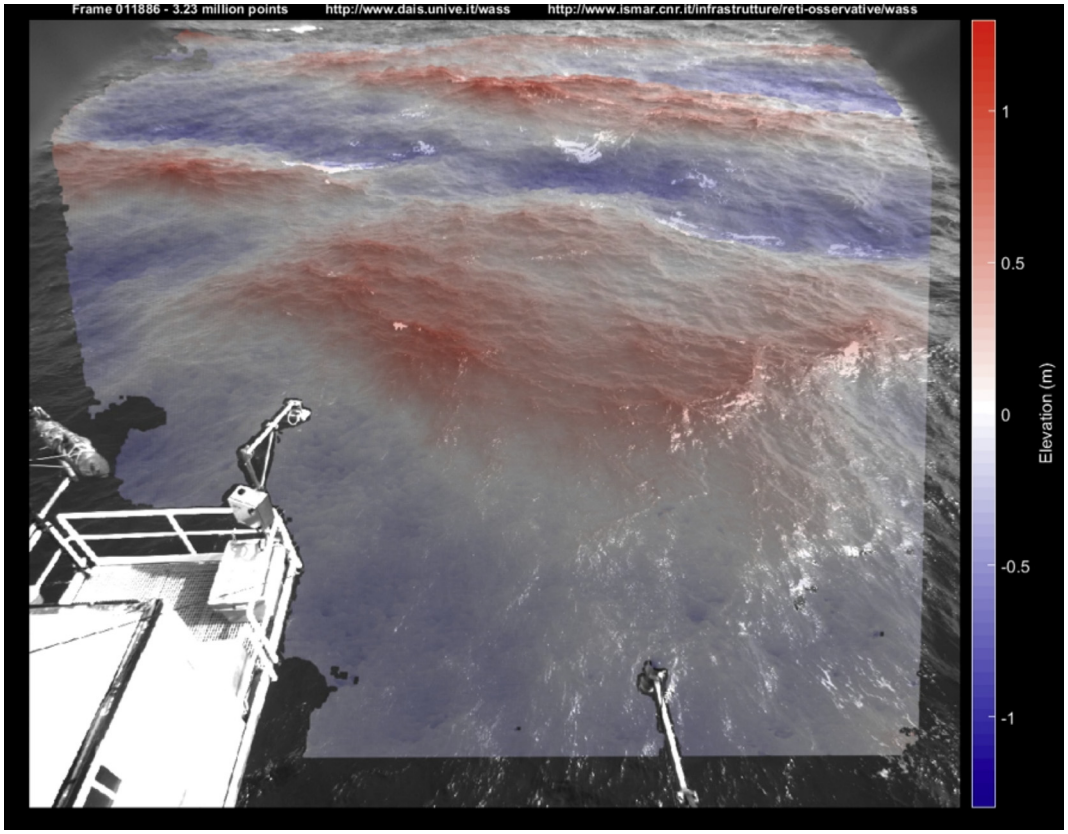

Fig. 2.11. 3D field of wind waves as measured by stereo system at the ISMAR oceanographic tower. See Fig. 2.3 for its position and Benetazzo et al. (2015) for the description of the system.

affixed to a moving research vessel (Donelan et al., 2005). Nadir-looking radars are another popular solution on rigs to measure, as with laser, the mean sea level and the waving surface. The combination of three, often four, instruments provides directional information. Three transducers provide, for directional distribution, the same amount of information that we will soon discuss in buoys.

The second class of devices used again in the coastal area, are bottom mounted sensors. Bottom mounted sensors fall into two categories: pressure transducers and upward looking acoustic current profilers. Measuring waves with pressure transducers have been operationally used for nearly six decades (Bishop and Donelan, 1987; Pomaro et al., 2017). The ease of deployment, relative cost and survivability make these systems highly popular. Apart from the problems related to fouling, usually more intense in coastal waters and enclosed seas, one of the impediments using a pressure transducer are the assumptions governing the relationship to translate a pressure response to the corresponding free surface oscillation. The reason is the amplification factor from the submerged measurement point to the surface that increases pretty rapidly with increasing frequency (the inverse of the attenuation with depth). For example, in 8 m water depth the amplification ranges from about 1.05 for 0.054 Hz signals to 13.1 for 0.318 Hz. Any noise in the pressure response will be amplified according to the frequency dependent factor. It is essential to minimize the noise or the wave estimates will be heavily contaminated.

Currents, nonlinearities, spectral analysis versus wave-by-wave approaches do affect the estimates in significant wave heights. Bishop and Donelan (1987) summarized the two principal approaches to prevent contamination of the wave signal by noise. The first would be to subtract an assumed noise level from the pressure spectrum prior to translating it to a surface displacement spectrum. The second would be to truncate the pressure spectrum where noise dominates. Smith (2002) summarized the techniques to compensate pressure responses under an active current. She showed that in a coastal inlet neglecting currents can lead to order-one errors in wave heights. Cavaleri (1980) showed how to avoid the dynamical effects of current and wave motion measuring only the signal due to wave pressure. Herbers et al. (2000) built an array of bottom mounted pressure sensors in water depths ranging from 12 to 87 m studying the transformation of swell energy (0.07–0.1-Hz). In all these cases the investigators relied on specific analysis procedures to remove noise and/or compensate for currents and nonlinear effects.

With respect to the classical three sensors for directional information, more is possible with more dense arrays. A multiple pressure array (two six-pressure arrays) used in the Southern California Bight (Torrey Pines, California) was capable of resolving bi-directional wave systems at one frequency separated by only 8-deg in direction (Freilich et al., 1990). The complex cross-spectral matrix between all sensors in an array was averaged over eight frequency bands, resulting in a frequency resolution of 0.0078 Hz. The cross spectra were then ensemble averaged over 20 records, producing 320 degrees of freedom. An iterative maximum likelihood (IMLE) method (Pawka, 1983, Oltman-Shay and Guza, 1984) was used converging on a possible true directional wave spectrum. The results produced extremely high resolution, high quality estimates in shallow water. A similar system using IMLE has been in operation at the USACE's Field Research Facility for nearly forty years (Long and Oltman-Shay, 1991). As in a single pressure gauge, the system assumes linear theory to recover the pressure response factor converting to estimates of the free surface, that are functionally related to the water depth and frequency.

Upward looking acoustic current profilers (ADCP) have been used in the coastal environment to estimate wave characteristics. Herbers and Lentz (2010), among others, summarize the various systems identifying the limitations of each system in correctly interpreting the recorded data. Under severe wave conditions, in a limited depth coastal

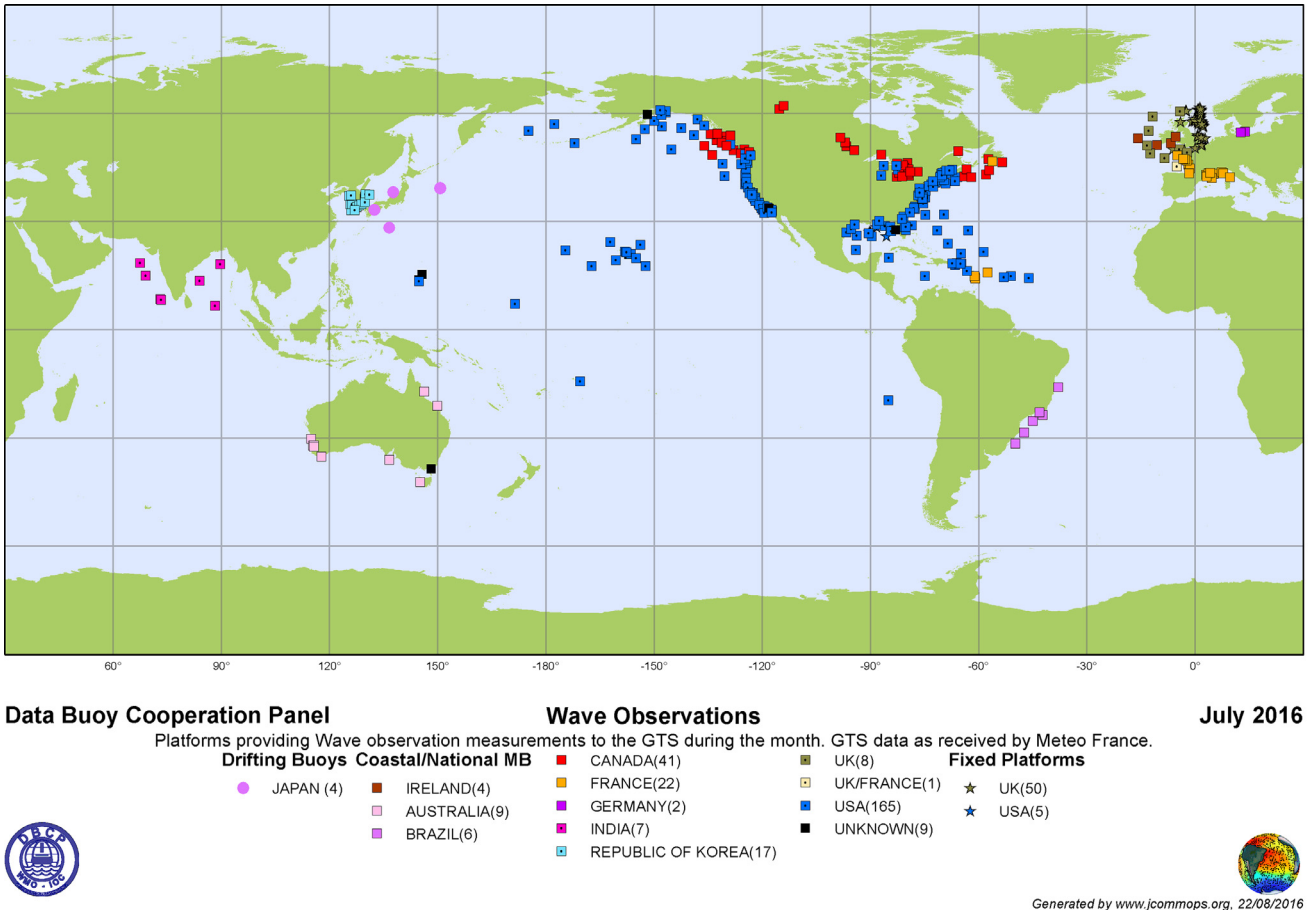

Fig. 2.12. Location of 348, available via GTS, wave measurement sites (July 2016), from JCOMM Data Buoy Collaboration Panel, http://www.jcommops.org/dbcp/network/maps.html.

environment breaking can be frequent and the presence of large air bubbles just below the surface can interfere with the acoustic measurement of the surface. It is therefore convenient to shift in this case to pressure measurements, as done for instance at the ISMAR oceanographic tower (see Fig. 2.3 for its position). Working in a low wave energy environment, dominated by long-period swells (Southern California), creates finite bounds to assess the reliability of ADCP wave estimates. It is then customary to define a simple parametric estimation technique capable of providing a robust estimate of the gross directional wave properties even when the quality of the data is marginal.

What just given is a short summary of the main instruments used to measure waves. We still miss what is probably the most popular one, i.e. buoys. Taking advantage of the extensive experience available with this instrument, we will discuss extensively the related problems as a detailed example of the ones that affect all wave measurements.

2.5.2.3. Buoys. Wave measurements across the world's oceans have been increasing, and in general the vast majority of these assets are surface wave buoys (see Fig. 2.12 for a distribution). Most of these sites are located within about 200 km of the coasts, deployed on a continental shelf, and in water depths less than 200 m. This distribution (plus the fixed platforms) does not reflect all operational wave measurement sites, only the ones that transmit data directly through the Global Telecommunication System (GTS).

Differences exist in the type of wave measurement system occupying a site, and need to be considered when using a set of wave data. The world's data providers use Quality Assurance and Quality Control (QA/QC) protocols prior to release to the GTS. However, there is no universal criteria under which the data are considered as error free. QA/QC flags are also contained in the data records, but seldom interrogated by a user. And thus, if the quality of the data were independently related to the wave system there would be no need to consider the existence of errors in the measurements. Unfortunately this is not the case and there are well defined differences. It is not to say there is one wave measurement system superior to all other known platforms. It is to have documented knowledge where and when a given wave measurement does not contain the quality required for a particular problem. Valid for buoys, of course these statements hold for every measuring system.

There are three major components in a buoy wave measurement system: (1) the platform, the hull, shape, composition, super-structure, and mooring; (2) the sensor; (3) the payload or on-board analysis package. Each group has its own unique characteristics that necessitate specific attention, requiring very explicit information and guidance. Surface buoys can be spherical, discus, boat-shaped (e.g. NOMAD, Timpe and Van de Voorde, 1995), with extended super-structures generally housing meteorological sensor packages, solar panels for supplemental power, cages to prevent access by sea mammals. The size of discus buoys ranges from slightly more than one meter up to 12 m in diameter (but see the two paragraphs at the end of next Section 2.5.3). The composition of the hull has been evolving from aluminum to foam. Moorings (and bridling systems) can be open link chain, polypropylene, and shock cord, permitting the buoy to be free-floating and actively revolving within a well-defined watch circle. The sensor systems have changed over the past three decades. HIPPY (see http://www.datawell.nl/Products/Motionsensors.aspx) sensors have been used operationally in the early 1970s (Steele et al., 1992, 1998). The configuration was a mechanical gimbaled sensor used to directly determine the pitch and roll angles (or to measure the accelerations in x, y, and z as in the case

of a Datawell wave buoy). As in the case of NOAA/NDBC, the trend over the past two decades has been to migrate from HIPPY sensors to electronic motion packages housing tri-axial accelerometers combined with digital magnetometers and compass packages to measure the buoys motion and translate it to the free surface.

Most of the existing (e. g. AXYS, http://axystechnologies.com/: NOMAD, TRIAXYS, WatchKeeper, WatchMaster, WatchMate; Fugro, http://www.oceanor.com/systems/seawatch/buoys-and-sensor/ WAVESCAN, and SEAWATCH) and new companies (TIDAS 900 http://www.nortekusa.com/usa/news/new-tidas-900-monitoring-buoy) now market wave measurement systems capable of providing directional estimates of the free surface. Testing and evaluations of the buoy technologies, old and new, need to be addressed to better understand the differences in the wave measurement from one buoy system to the other.

Using their recent advancements, Global Positioning Systems (GPS) have been used as sensors in wave buoys. The evaluation of the integral wave parameters and frequency spectra was made with respect to a Datawell Directional Waverider off the California coast (Herbers et al., 2012) and to a high resolution pressure array located along the outer banks of North Carolina (Thomson, 2012). In both cases the tests were conducted in a low wave energy environment. These GPS wave buoys use a specialized sensor package that measures the horizontal and vertical buoy velocities based on the Doppler shift in received GPS signals providing a more accurate estimate of the free surface.

2.5.3. *The truth about wave measurements from buoys*

where we analyse the performance of buoys as measuring systems pointing out advantages, disadvantages and what we can and cannot get from their records

Surface buoys are the most common and largest number of point source wave measurement systems occupying enclosed, semi-enclosed water bodies and the coastal waters of the world. Because of this and the interplay between point-source measurements and altimeter data sets, and their use in NWP's forecast evaluation, our attention focuses on these systems. This requires a steady effort by wave modellers to resist the pressing request by forecast management to assimilate the buoy data in the daily analysis, in so doing improving both analysis and forecast, especially close to the coast, where most of the buoys are. However, wave modellers want independent non-assimilated wave data to be able to get an objective judgment of the quality of the model results.

One of the primary objectives is to obtain accurate estimates of the two-dimensional distribution of energy S in frequency f and direction θ shown in Eq. (1) below.

$$S(f,\theta) = S(f)\left[a_1\cos\theta + b_1\sin\theta + a_2\cos 2\theta + b_2\sin 2\theta + \sum_{n=3}^{\infty} a_n\cos n\theta + b_n\sin n\theta\right] \quad (1)$$

This is crucial information, absolutely necessary to be able to evaluate a wave model's performance for any meteorological event(s) at as many measurements sites as possible. Second, a wave buoy containing a sensor measures the buoy response in the presence of free surface waves. Thus, the measured buoy response requires a mathematical transfer function that will allow estimating the free surface. Each buoy configuration should have its own unique transfer function dependent on the physical factors influencing the buoy motion. It is clear this may not be the case in our existing global wave buoy array.

No matter what defines the sensor, the payload (i.e. analysis package) acquires the raw signal and transforms it to an estimate (x,y,z) of the free surface from which ultimately directional estimators (the lowest Fourier coefficients $a_1(f)$, $b_1(f)$, $a_2(f)$, $b_2(f)$ in the above equation), frequency spectra, and integral wave parameters are derived. For example the Datawell is a particle follower buoy; its estimate of the Fourier coefficients follows directly from the measured accelerations and linear wave theory (O'Reilly et al., 1996), whereas the NOAA/NDBC is a slope following system, and the estimates of a_1, b_1 incorporate various corrections for hull-mooring response (Steele et al., 1992, noted that translational buoys use α_1 α_2, r_1 and r_2 that are trigonometrically related to the four Fourier directional coefficients). TRIAXYS systems (MacIsaac and Naeth, 2013) are based on strapped down accelerometers and three strap down rate gyros.

In general, only the first four moments of the directional distribution can be resolved, the mean wave direction, the directional spread, the skewness and kurtosis (Jensen et al., 2011). Directional estimators like the Maximum Likelihood (MLM) and Maximum Entropy Methods (MEM) approximate the series expansion (the summation in Eq. (1)) to rectify the directional distribution (e.g., Benoit, 1992). Inverting the spectral estimates using MEM will reproduce the four directional Fourier coefficients exactly. MLM will not. Hence, any graphical representation (Fig. 2.13) of the directional shape or 2-dimensional directional wave spectrum is an interpretation of nature, and should not be construed as exact. The only exception would be a multi-component linear array where the number of degrees of freedom permits the direct estimation of the directional wave spectrum (e.g. Long and Oltman-Shay, 1991).

All wave buoys monitoring the ocean surface contain noise in the time series record, similar to that encountered for pressure gauge, or velocities derived from acoustic profilers in shallow water. It is the level of that noise compared to the real wave energy or in the directional coefficients that can contaminate any wave record. Noise is generally relevant in the less energetic part, i.e. the low and high frequency range of a spectrum. For the same reason noise is also more apparent in wave records when the natural energy level is small. The signal-to-noise level provides the measure to determine the quality of the wave sensor output. O'Reilly (2007) equated directional wave instruments to audio equipment, defining what we can call *fidelity*. Instruments with high fidelity can be used to resolve some of the finer details of the directional wave spectrum, like the directional width at a particular frequency and can often determine if the directional characteristics at that frequency are bi-modal. Low fidelity instruments will generally return reasonable estimates of the mean wave direction, but will over-estimate the directional spread and under-estimate skewness and kurtosis (O'Reilly et al., 1996). A common assessment of the signal-to-noise levels is that sea surface displacement has a larger signal than the sea surface slope signals. Similarly, while an increased wave energy will result in a larger signal, the lower the frequency the lower the acceleration, slope, and velocity signals and thus the higher the potential for contamination from noise. It is a controlled balance between removing noise without removing *real* energy. Following a better assessment of the tapering off of low frequency noise in an acceleration spectrum, NOAA/NDBC has modified their noise correction algorithms (Riley et al., 2011). This can have non-trivial consequences.

Noise in wave records in the coastal area may also be manifested in larger scale physical processes such as near-inertial surface currents. Gemmrich and Garrett (2012) investigated long-term wave height records (hourly estimates over a 20-yr period of record) along the Canadian coast, ranging from near coastal observations to about 700 km from shore. They found a distinct peak in the H_{mo} power spectra by periodic currents. Given a clearly defined peak, the contribution to the overall variance in H_{mo} was small, on the order of 0.03-percent in the variance at the inertial peak compared to the background variance of the wave climate. The average root-mean-square modulation of the wave height by near-inertial currents was 2-percent.

The most dramatic study of buoy records was performed by Bender et al. (2009, 2010). A 3-m discus buoy (similar to the standard NOAA/NDBC 3-m buoy), containing multiple sensor packages, was deployed during Hurricane Katrina in the Gulf of Mexico. This study found large differences (26–56%!) in significant wave height estimates as the wave heights increased from 6 to 8 m, the differences depending on the

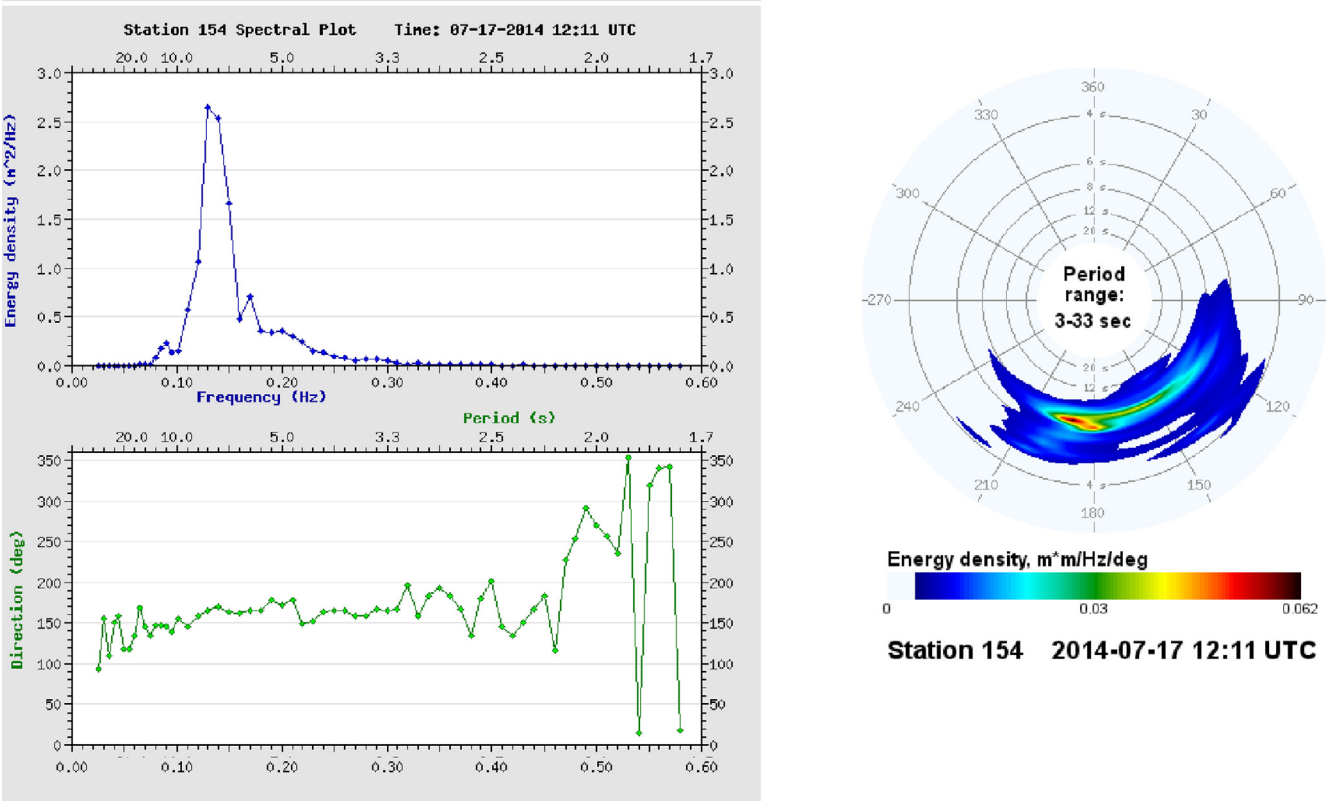

Fig. 2.13. (Left panel) frequency spectra and vector mean wave direction, and (right panel) estimate of directional wave spectra, for H_{mo}1.43 m from http://cdip.ucsd.edu/?&nav=recent&sub=observed (Station 44097).

analysis methods used. Strapped down accelerometers commonly used by the world's wave measurement providers would be affected by this work. It would also have a dramatic impact on measuring extreme wave conditions not only from tropical cyclone forcing, but also large extra-tropical events.

The sustained heeling of the buoy due to wind forcing on the superstructure was cited as the likely cause of the bias. NOAA/NDBC is now implementing a suggested corrections of Bender et al. (2010) on their 3-m buoy systems to remove this effect in extreme situations that on the other hand are the most interesting ones to have data about (Jensen et al., 2011). Collins et al. (2014) applied the tilt correction suggested by Bender et al. (2010) during the Impact of Typhoons on the Ocean in the Pacific (ITOP) experiment for wave data measured from a 6 N buoy. The tilt correction surprisingly resulted in decreasing and increasing the calculated surface elevation signal from wave to wave. However, in the extreme case the tilt correction did in fact reduce the individual wave height estimates. The 6 N buoy used in ITOP (Drennen et al., 2014) was deployed in a water depth of 5600 m, with an approximate watch circle of 1.45 km. Wind and wave loading derived from the passing of four typhoons with wind speeds of 25 m/s and H_{mo} values of 10 m may not push the buoy to its mooring limit reducing the tilt. Results from Bender et al. (2010) 3D buoy were based on a deployment in a depth of 19 m and most likely a very small watch circle. It seems likely Bender's buoy would be more susceptible to adverse tilt because of the mooring length compared to that of IOP. From the two cases it is apparent that the problem of tilt is mostly felt in coastal water, often shallow enough for the mooring force components to act on a more horizontal direction and, if shallow enough, waves to be more frequently breaking.

We have purposely focused our attention on the "traditional" buoys, i.e. the ones with diameter ≥ 1 m. However, the progresses in electronics, data storage and energy supply have led in the latest years to a drastic reduction of the related volume and weight. The obvious consequence has been a reduction of also the hull (dimensions and weight) and cost, making these buoys easily handable from a small boat.

A number of these buoys is now on the market, as the SCRIPPS buoy (http://iprc.soest.hawaii.edu/NASA_WS_MD2016/pdf/Centurioni2016.pdf), SWIFT by the University of Washington (http://www.apl.washington.edu/project/project.php?id = swift), and Spotter by Spoondrift (https://spoondrift.co). The problem is that these buoys have not been extensively tested in all the possible conditions. A test concerning the electronics would be straightforward, putting them on the same hull as done (see above) by Bender et al. (2009, 2010). However, the main concern with these light buoys is their hydrodynamic response. For instance, it is natural to expect that a steep, or even breaking, wave crest will tend to move horizontally the buoy at a non-trivial extent, the more so when the buoy is drifting. The point is that the limited cost makes the buoys expendable, letting them drift (while transmitting data) till when they last or run aground. Tests can be organised mooring them to one of the "traditional" buoys or another wave recording system. However, the limited weight suggests that their behaviour when moored or drifting can be quite different.

2.5.4. *Importance of wave measurement evaluations where we stress the importance of assessing the data accuracy and describe the efforts done in this respect*

The increasing quality of wave modelling results and the need for more accurate forecasts force buoys, and the other measuring systems, to a continuous improvement of their performance. In particular there is an acute need for an improved convergence of the data from the various data providers. In 2007 a meeting was held (ACT, 2007) to discuss sensor technologies and evaluations. This meeting consisted of numerous private sector manufacturers, data providers and data users. The primary objectives of this workshop were to define the present state of wave measurement technologies, to identify the major impediments to their advancement, and to make strategic recommendations for future developments, and the necessary steps to integrate wave

measurements sensors into operation coastal ocean observing systems. Two recurring themes of the discussions were a disparity between user requirements, and to what degree existing and new technologies should be adequately tested. The concept of "First 5" was introduced (O'Reilly, 2007) to nominally evaluate directional estimates in wave measurement systems. As discussed earlier (Eq. (1)), the "First 5" define the first four directional Fourier coefficients in the infinite series expansion quantifying the directional resolution. The ideas initiated at this meeting were elevated to an international forum through the World Meteorological Organization (WMO) and the Joint Technical Commission for Oceanography and Marine Meteorology (JCOMM) at a meeting held in 2008 (JCOMM, 2008). Ultimately this carried forward resulting in the Integrated Ocean Observing System Report entitled *A National Operational Wave Observation Plan* (IOOS, 2009, and the related summary by Birkemeier et al. (2012)). Swail et al. (2009) summarized the need for high quality directional wave measurements and further acknowledged the protocols for intra-measurement evaluations. These procedures were summarized in Jensen et al. (2011), where a *relative reference* (a Datawell Directional Waverider buoy) was selected to serve as the baseline for the evaluations, and a methodology was introduced (WavEval Tools, see http://cdip.ucsd.edu/?nav = documents&sub = index&xitem = product&xdoc = cdiptool) to serve as the method for the evaluations. ACT (2012) followed their original workshop establishing a plan, later summarized by Luther et al. (2013), for the execution of the intra-measurement investigations, and the procedures to follow.

The concept of an intra-measurement evaluation is not new. Over the past twenty-five years there have been a series of experiments at various locations focusing on the evaluation of wave measurement systems (e.g. WADIC, Allender et al., 1989; Harvest Platform, O'Reilly et al., 1996; Wacsis, van Unen et al., 1998; FETCH, Pettersson et al., 2003; NDBC Sensor Systems, Teng and Bouchard, 2005; ITOP, Collins et al. (2014) and analysis methods to use in the evaluation process, Krogstad et al. (1999). As new sensor and wave measurement systems mature, the need for more intra-measurement evaluations will emerge.

One study, the Field Laboratory for Ocean Sea State Investigation and Experimentation (FLOSSIE) located in Monterey Canyon off the California coast, was initiated in July 2015 (Jensen, et al., 2015). The wave buoy array consisted of three buoys, a NOMAD containing five wave sensor/payload packages, a 3D aluminum buoy with two onboard sensor/payload systems, and one Datawell Directional Waverider buoy used as the *relative reference*. Waves were recorded every 30-min or 1-h intervals returning the data for over two years. One of the most important outcomes of this study is that despite consistency in the wave height, period and direction (only relative to the 3D buoy) measurements (Jensen et al., 2015), there is a substantial variation in the frequency spectra and frequency dependent directional components (mean wave direction, spread, skewness and kurtosis).

Despite FLOSSIE residing in deep water, the information gained from an experiment like this can be applied to the coastal domain, including continental shelves and near-shore regions, as well as semi-enclosed and enclosed water bodies. In general, for coastal applications the water depth will influence any wave measurement. A buoy is deployed at a unique site defined by a latitude longitude pair, however there is a defined watch circle (based on the mooring configuration), the buoy will meander while it measures the local meteorological, oceanographic and waves conditions. In the coastal domain, the importance of where the buoy is stationed relative to the local bathymetry becomes extremely important. Finite depth mechanisms such as shoaling and refraction will affect the measurements and are frequency dependent affecting the energy and directional attributes. Provided that the transfer function relating the buoy motion to the free surface is well composed, the quality in the data will be retained. Water level variations based on tides and surge effect as well as currents will impact the wave measurements more so in the coastal region, and could contaminate the data. Performing a FLOSSIE type experiment in finite depths would most likely yield larger differences in the five Fourier directional variables. In semi- and enclosed bodies of water the only external factor affecting the wave measurements is the marine/land boundary. The wave climate will be dictated by the size of the domain; the smaller this is the more the applicable frequency range will be translated towards higher frequencies. Sampling rates will have to be shorter to compensate for the high frequency waves. Noise levels for the high frequency range of observable conditions needs to be reduced. And finally measuring high frequency range common to small water bodies requires the buoy size be small enough to adequately resolve those conditions.

One other aspect found in the examples shown illustrates the need to better evaluate intra-wave measurements as well as model to measurements. Defining the wave conditions using only the significant wave height, period and mean direction only answers the basic tendencies at a site. The details found in the frequency spectra and, if provided, the directional attributes defined by the four Fourier directional parameters result in a better picture of the existing wave conditions. Two examples illustrate the similarities and differences between sensor systems, hull types and analysis packages that lay behind a set of standard values of $H_{mo}T_{pp}$, and θ_{wave}. For multiple wave systems one system will be ignored. The energy will be combined into the larger of the two. Partitioning into a wind-sea and swell wave system is a better method than using only one (see in this respect Chapter 4). Unfortunately the wave community continues to be steadfast in the use of a three variable system. Whether it is reporting the quality in our ability to accurately forecast waves, or a wave model performance evaluated for a single or series of storm events, or intra-measurement evaluations time, scatter graphics along with statistical tests based on the height, period and wave direction are usually presented. Even standard statistical tests as in the case of the root mean square error (and normalized), scatter index used in evaluation of waves has recently been questioned, (Mentaschi et al., 2013).

One year of hourly wave directional wave measurements define a population over 8500 individual observations. Considering the number of frequencies in our present measurement capabilities of about 50, where energy density and four directional moments (or four Fourier directional parameters) are defined, the amount of data to investigate becomes large, but not insurmountable. However, that information defines better what exists at a given site. Over the years attempts have been made to reduce the number of independent variables, and yet provide results to quantify the details in the directional wave spectra. Spectral partitioning was introduced to the wave community by Gerling (1992) with follow-on studies by Hanson and Phillips (2001), and more recently by Portilla et al. (2009, 2015). The requirement for these methods is to define directional wave spectra. As previously noted, other than possibly a high resolution (up to 10 sensors) linear array, the best a buoy or current profiler can provide is the energy density and four Fourier directional parameters as a function of frequency. Hence, spectral partitioning is dependent on an estimate of the directional distribution that approximates the infinite series found in Eq. (1). Gerling (1992) and Hanson and Phillips (2001) assumed a directional distribution, whereas Portilla et al. (2015) interrogated the frequency spectra defining energy peaks and a filter consisting of a two-dimensional discrete convolution operation between the spectrum and an equally weighted convolution kernel. WavEval Tools (Jensen et al., 2011; ACT, 2007) take a different approach. The four Fourier directional parameters are used to calculate the four moments of the directional distribution at each frequency band: the mean direction, spread, skewness and kurtosis. Partitioning is performed on each discrete frequency band, and a discrete energy level. A bias and root mean square error percentage is determined from averaging the differences between two data sets. The result is a qualitative graphic displaying defined range of the per cent deviations.

An example of the WavEval Tools is provided in Fig. 2.14, displaying the average energy bias (this as also H_{rms} the right scale)

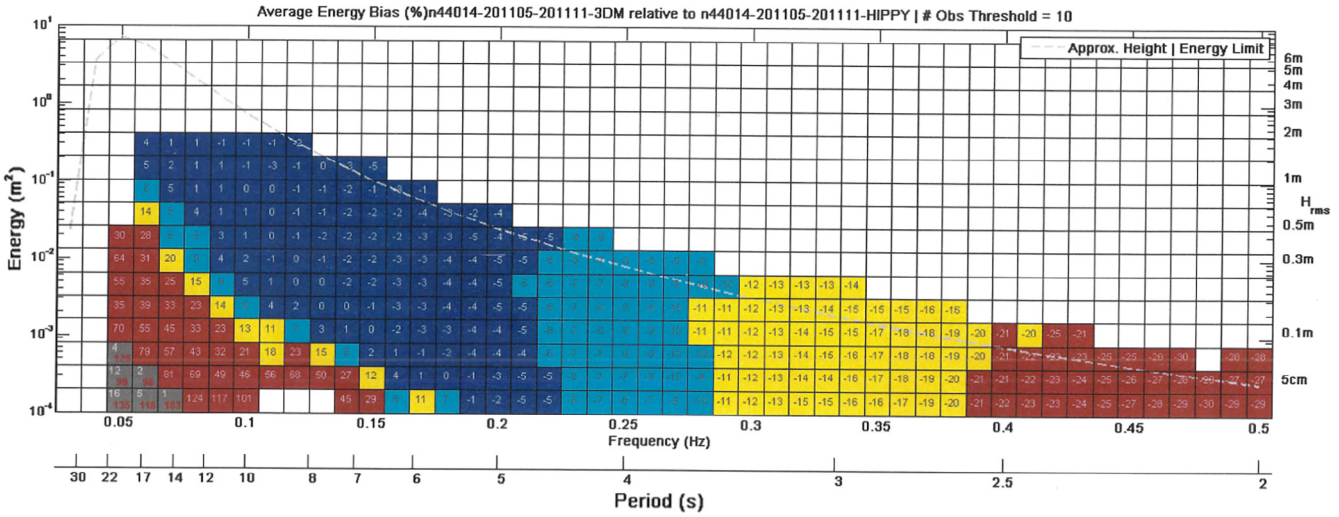

Fig. 2.14. Different performance of the two measuring systems, 3DM and HIPPY. The figure provides their average per cent difference (with respect to the latter) as a function of frequency f and energy E (this as also H_{rms} on the right scale). The specific figure is written in each (f-E) pixel, the pixels then grouped with different colors in the sequential ranges provided in Table 2.4.

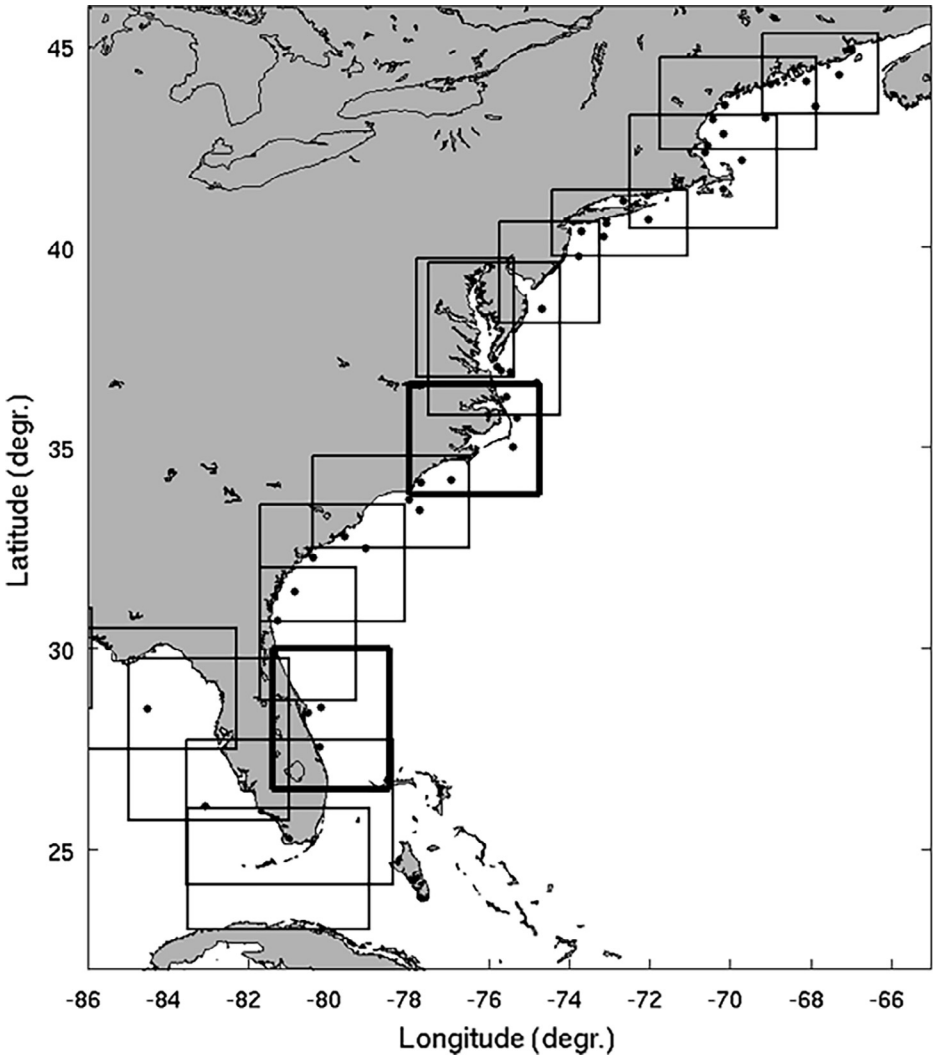

Fig. 2.15. Distribution of the various sub-zones in the modulational approach to wave forecast on the US East coast.

Table 2.4
Colour to range identification.

Color	Range (percent)
Dark blue	0% to ± 5%
Light blue	± 5% to ± 10%
Yellow	± 10% to ± 20%
Red	> ± 20%
Grey	Number of observations below threshold
White	No data

Table 4.1
Specification of the areas considered in Fig. 4.1 panel a.

ALL	All
HW	Hawaii
NPC	North Pacific Coast
USWC	US West Coast
INDIA	India
ASWC	Australia South West Coast
CRB	Caribbean Sea
ASEC	Australia East Coast
NEATL	North-East Atlantic
JAPAN	Japan
NRDIC	Nordic (North Atlantic and Norwegian Sea)
USEC	US East Coast
CANEC	Canadian East Coast
GM	Gulf of Mexico
NSEA	North Sea
CHNIS	English Channel and Irish Sea
MDSEA	Mediterranean Sea
BLTIC	Baltic Sea
KOREA	Korea
GRTLK	Great Lakes

between a HIPPY and 3DM sensor contained in a 3D buoy consisting of results during a six-month deployment period. The specific figure is written in each (f-E) pixel, the pixels then grouped with four primary colors in the sequence ranges found in Table 2.4. The results are clear. The two systems, HIPPY and 3DM, provide on average the same energy (within 10% difference) for wave periods longer than 3 s, but from 6 s upwards only if there is sufficient energy in the system. HIPPY is much lower in energy for long period but not large waves. Conversely its energy is always larger in the upper frequency range.

These techniques can provide useful information that is quantitative as well as qualitative reducing the assessment in directional properties to a reasonable number of products. Recently, two new methods evaluating frequency spectra (Dabbi et al., 2015), and correlating paired wave spectra (Collins et al., 2015b) have been used. The work by Dabbi et al. (2015) introduced a seven pair estimator to better define unimodal wave spectra. Although somewhat limited to unimodal spectra, it does provide an alternative to using the bulk wave height, period and direction estimates. On the other hand, Collins et al. (2015b) used a canonical correlation analysis to investigate the correlation structure of the matrix of spectral correlations. They found the method was effective to understand the degree of correlation between sets of paired spectral observations.

There is no lack of trying to develop new methods to evaluate large spectral data sets to determine similarities, differences, quality or deficiencies in measurement to measurement systems, model to model results or model to measurements. However, we cling tightly to the bulk wave parameters because we know what they represent. For example two data sets produce a bias of 0.5 m out of 4 m. We know what that represents; we know how large a 0.5 m H_{mo} looks like. Now consider a difference in the frequency spectra of 10 m^2 s out of 125 m^2 s. The ratio is the same as in the case of the H_{mo}, but what does it represent? That may be the only impediment holding the wave community back from progressing into the future. An intermediate solution is the use of partitions (see more in Chapter 4) where we split a full spectrum into the single composing, and at a large extent independent, wave systems. Then the use of integral parameters makes more physical sense, and it is much more intuitive to mentally combine different and well defined wave systems coming together at the considered point.

Establishing a “First 5” criterion and a well sought analysis procedure to evaluate present and future directional wave measurements is a lofty goal, and will impact nearly every facet in the study of wind generated surface gravity waves from a physics based standpoint, to model improvements and daily performance of our weather prediction forecast centres. To have some quantifiable standard for all wave measurements would be highly beneficial to the user, and thus remove existing uncertainties, generally dismissed to the level where all data are at a uniform quality level, something far from the truth.

2.6. Applications

L.Cavaleri, J.-H.Alves, L.Bertotti, S.Langodan, A.J.R.Padilla-Hernande, S.V.Samiksha, A.H.van der Westhuysen
luigi.cavaleri@ismar.cnr.it

where we provide examples of wave modelling application in coastal and enclosed seas environments, showing a sample of the different problems/situations we have to face compared to the open ocean.

In the previous sections we have listed and discussed the characteristics that, for a certain range of problems, make wave modelling in coastal and enclosed seas different from the open oceans. These concern, possibly most of all, the meteorological input due to a potentially strong influence of land and its orography. Given that the inner seas are more dominated by wind sea than in the ocean, the wind is often the crucial aspect of an application. The other relevant aspect is the presence of a variegated coastline and the limited depths waves have to deal with. This leads to a number of complications concerning both physics (for the correct representation of the processes involved) and numerics. The latter derives for large part from the frequent strong spatial gradients of the fields that imply particular limitations, hence attention, in the methods we use to integrate the model equations to obtain what we would like to be reliable and accurate results. All these problems have been analysed and discussed in the first four sections of this chapter. Then of course we wish to know how correct our results are, and this is achieved comparing them with the measured truth. Unluckily (Section 2.5) measured data turn out not to be (within limits) the solid reference we would like to have. Different instruments, also of the same kind, have different problems and accuracy, and this has to be considered in the validation of model results.

Having framed the spirit of the problem, in this section we provide examples dealing with different aspects:

2.6.1 – the NOAA/NCEP multiple system for the whole US coastline,
2.6.2 – the Adriatic Sea and the enhancement of wind speed,
2.6.3 – wave forecast for the Rotterdam channel,
2.6.4 – the fractal coastline of the Botthnia Sea,
2.6.5 – the peculiar meteorology and opposing wave conditions of the Red Sea,
2.6.6 – the muddy bottom off the Kerala coast of India.

2.6.1. The NOAA-NCEP multiple system for the whole US coastline

The US coast, facing two oceans and with an often articulated coastline, is a classic example of how to combine large scale and inner/coastal seas approaches into a sensible and effective working machine. While the two different scales naturally involve different spatial resolutions, it is also obvious that the extent and different characteristics of the coastline imply a modulational approach and, to be effective, a distribution of the responsibilities. The solution is shown for the Atlantic coast in Fig. 2.15 (NCEP). Granted the global ocean model and the availability of its results as boundary conditions, the coastline is subdivided into a number of sub-zones, each one with a different model

unit and under the responsibility of a local office. For operational purposes NOAA currently uses implementations of the WAVEWATCH III (Tolman, 1991b) and SWAN (Booij et al., 1999) models driven by atmospheric fields provided by its coastal Weather Forecast Offices (WFOs). A SWAN-based modelling system, the Nearshore Wave Prediction System (Westhuysen et al., 2013, 2014), provides downscaled guidance for open-ocean coastal areas relative to the Global WAVEWATCH III model. Parallel to this, a high-resolution WAVEWATCH III system, the Great Lakes Waves Forecasting System (GLW), is used for operational forecasts in the North American Great Lakes (Alves et al., 2014).

The challenges of the complex orography and associated flow fields in these coastal areas are addressed by allowing coastal WFOs to force the wave model at these scales with forecaster-consensus winds, as opposed to one or more raw atmospheric models. Those forecaster-consensus winds are compiled from ensembles of individual atmospheric models, and adjusted for biases or other known deficiencies using available observations. As such, they constitute the official atmospheric forecast in these complex regions.

Due to the routine human intervention in the forcing applied, the NWPS runs are conducted in an on-demand fashion, with forecasters from 36 WFOs triggering the runs over their individual domains, which are computed on NOAA's operational supercomputer. The GLW system is forecast-driven, whereby marine forecasters from 11 WFOs provide consensus winds for their areas of responsibility. Wind fields are modified by the forecasters and are stitched into a coherent wind field covering the wave model domain (Fig. 2.15), which are sent to NOAA's operational computer on an hourly basis. GLW model runs are made in four daily cycles using the latest consensus wind fields.

The operational NWPS applies SWAN v40.81, using the wind input and white-capping dissipation expressions recommended by Rogers et al. (2003), and default settings for the remaining shallow water physics. Wave boundary conditions are taken from NOAA's Global WAVEWATCH III model discussed in Chawla et al. (2013). This global model, driven by NOAA's Global Forecast System (GFS) atmospheric model, features a two-way nesting with a resolution of 4 nmi over the US shelf seas. NWPS downscales this coastal resolution to nominally 1 nmi, and where required by local features to 500 m or less, in deterministic forecasts out to 102 h. At present, this is achieved with a regular grid for each WFO domain, followed by smaller-scale nesting, to be replaced in the future by variable-resolution unstructured meshes.

At these resolutions, it becomes necessary to include the interaction of wind waves with coastal currents. Closer to the shore, accurate estimates of the total water depth including tides and storm surge, and its effect on the wave evolution, become essential. This has been illustrated in recent events such as superstorm Sandy (2012) and Winter Storm Jonas (2016), which featured large coastal surges, and significant sustained damage due to wave action. Under these conditions, the greater water depth due to the combined effect of tides and surge allows larger waves to reach the coast. These effects and the related modelling approach are described in Section 3.1.

A direct action of the local WFOs is obviously more useful in now- or very short term fore-cast, the system being active four times per day. In the medium range the local forecast is fully dependent on the global one and following nesting, with all the related implications. This is clearly shown by the performance statistics versus buoy data. Table 2.1 summarizes the performance of the NOAA/NCEP multiple system against the significant wave heights measured by 50 NDBC coastal buoys in the Gulf of Mexico and along the US East coast. 24, 48, 72 and 96 h forecast horizons are considered. It is quite remarkable that the limited bias, between −4 and 6%, and the best-fit slope do not change with increasing range.

One example of the advantage of the NWPS was given by the passing at Duck (N.C., see Fig. 2.1) of hurricane Joaquin which traversed the North Atlantic between 27 September and 7 October 2015. Three buoys were locally in operation at different distance from the coast, respectively on 47.6 m (the most offshore one), 26 m, and 17.4 m depth. While the differences between the global wave model and the local NWPS were practically absent offshore and limited at the intermediate buoy, they were dramatic at the nearshore one, the two models providing respectively 2 and 4.5 m maximum significant wave height, the latter close to the actual measured value.

Although facing similar challenges, the GLW runs as a separate system at NCEP, focusing on the particular environment given by the Great Lakes of North America. The complex meteorological scenarios that develop in this area forced the local development of the GLW already in 2004, a precursor of the then general system for all the US coasts. The local conditions, with mid-latitude cyclones, Artic air mass intrusions, and organized intense convective systems, has forced an early shift to a higher resolution (from 12 to 4 km) of the forcing winds, with a marked improvement of the final results. GLW uses WAVEWATCH III on a 2.5 km curvilinear spatial grid, with an expected shift to an unstructured grid in 2017.

2.6.2. The Adriatic Sea and the enhancement of wind speed

In Section 2.1 we have hinted at the need, but also to the difficulty, of having sufficiently correct winds in an enclosed sea. When passing from land to sea surface, winds experience a suddenly decreased surface drag. The reason is that, although the local wave age is often very young, nevertheless the surface drag is substantially lower than on land. Under the action of the overall meteorological situation and in correspondence to the high above geostrophic wind, surface wind tends to a new, higher dynamical equilibrium. A new marine surface boundary layer is developed, and U_{10} keeps increasing while blowing towards offshore till reaching the new equilibrium condition. The time, hence distance, required vary with the situation, always in the order of a few tens of kilometres. This is not so for modelled wind. Partly because of the not fully correct representation of the physics involved, more so because of spatial resolution, the time and space required by a modelled wind to reach a new equilibrium are larger. The practical consequence, relevant for wave modelling in these areas, is that the modelled U_{10} is underestimated in the coastal area until, when and where, the model achieves the new equilibrium. Of course this has practical consequences. The first one is that for an offshore blowing wind the locally generated wave conditions are underestimated for a longer extent than for wind (wave growth takes time). This explanation sorted out a long standing problem concerning wind and wave modelling on the US East coast. As measured by NOAA buoys, moored till many tens of (up to 200) kilometres offshore, modelled wind speeds appeared correct, but not so the wave heights, always too low (with an offshore blowing wind of course, there a common situation). The explanation is what said above, and the problem has been progressively attenuated with the progressive increase of spatial resolution of the meteorological models.

Moving from the oceanic coastal waters to the enclosed ones, it is clear that, depending on the size of the basin, wind from all the directions can be affected, leading to a permanent underestimate. When the MEDATLAS Group (see Sclavo et al., 2002) produced the Mediterranean atlas of the local wind and waves using the ECMWF archive, they first enhanced the modelled data using distributed altimeter data. Consistently with the dominant direction of the storms from the North-West quadrant moving towards the South-East sector, the enhancement factors (see Fig. 2.2, panel a) were higher close to Spain and France, progressively decreasing and approaching unity getting close to the African coast.

A more complete case is the Adriatic Sea (see panel b), practically enclosed, whose dimensions, 200 × 700 km, make it deal with the wind underestimate for practically all the possible conditions. Indeed Cavaleri and Bertotti, starting with their 1997 paper, using the ECMWF wind for the local wave forecast system (Bertotti et al., 2011), have been forced to enhance the surface wind speed to get the correct wind (versus scatterometers) and wave (versus altimeters and buoys) results. While on a more approximate approach a uniform correction factor

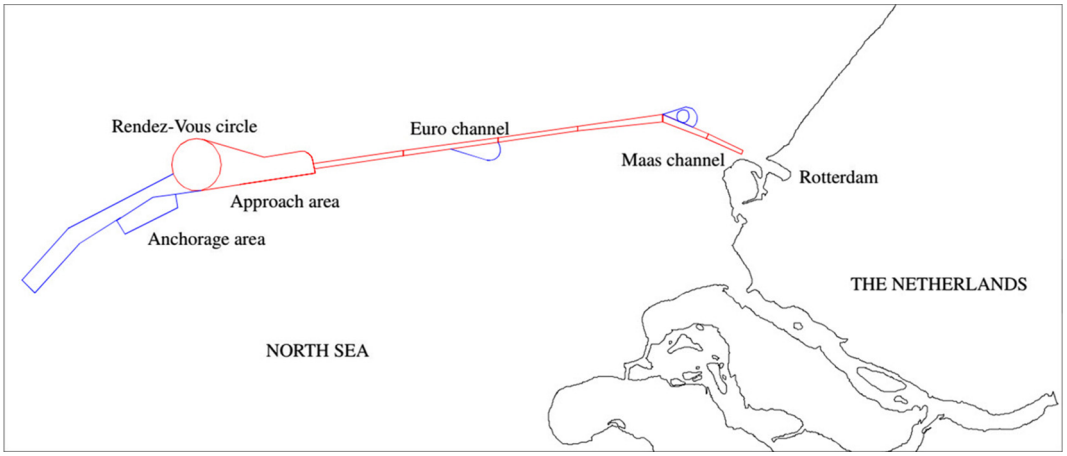

Fig. 2.16. Structure of the channel leading to the Rotterdam (Netherlands) harbour in the southern North Sea.

could be used, a further improvement could be reached using coefficients area (north, central, south) and quadrant (0°–90°–180°–270°–360°) dependent. This was associated to the different longitudinal and transversal dimensions (700 vs 200 km), but also to the dominant mountain ridges that characterize both the long sides of the basin.

The progressive increase of resolution of the ECMWF model has led to a parallel decrease of the "fetch" required by wind to reach its sea equilibrium, hence correspondingly of the wind enhancement factors from the original 1.50 (for T213, with nominal 90 km resolution) till the present 1.16 (for TCo1279, with 9 km resolution).

Although the local quantified experience is mainly based on ECMWF winds, parallel tests have shown this to be, possibly to a different extent, a feature of all the meteorological models.

2.6.3. *Wave forecast for the Rotterdam channel*

Rotterdam harbour is the busiest one in Europe and competing to be the most one in the world. Located at the south end of the North Sea, on the Dutch coast, it is not in principle in the most favourable position. The progressively shallowing North Sea ends at the Dutch coast with a very limited depth, largely unsuitable for the present large oil and container ships. The problem has been solved dredging a 76 km long channel, now 800 m wide, 26 m deep, until a similar depth is naturally found. Fig. 2.16 shows a scheme of the channel. Of course the sandy bottom and the sea storms imply an almost permanent dredging to keep the channel in the desired conditions. We focus here on the local wave forecast system.

Given the cost of maintaining the channel geometry, its depth is not larger than necessary. One meter clearance is accepted between the bottom and the keel of the ships. This implies that, beside tide, also the wave conditions are critical for making the passage of a big ship possible or not. Once a ship has entered the channel, it takes a few hours to reach the other end; given also the consequences of an accident, it is mandatory to have a reliable estimate of the incoming wave conditions. Mandatory for the next few hours, its forecast for the days ahead allows an optimization of the future activity.

With these needs in mind, a tidal and wave forecast system has been set up (Gautier and Caires, 2015). The system is based on the SWAN model (Booij et al., 1999) with two different grids. The first, coarse one, called SWAN-DCSM, covers a large area (−12° to +9°E, 48° to 64°N) and computes boundary conditions for the detailed nested model domain. The resolution is 1/20° × 1/30° (which is circa 3.6 × 3.6 km). The nested model, SWAN-ZUNO, has a curvilinear grid with resolution varying from 2 km offshore to circa 200 m close to the coast. HIRLAM wind fields from the Dutch meteorological institute (KNMI) and large scale boundary conditions from the ECMWF global model are used. Water level and currents are similarly forecast.

For the ship motion, in particular heave and pitch, while in the channel, there is special interest in the low frequency wave energy (0.03–0.1 Hz). Therefore, beside the standard integral parameters H_{m0} and $T_{m-1,0}$, the so-called low frequency wave height H_{E10} is considered, defined as the wave height corresponding to the energy in the 0.03–0.1 Hz range.

Fig. 2.17 shows the performance of the above model system versus measured data. While the results are satisfactory for H_{m0}, it is evident there is, beside the large scatter, a substantial underestimate of H_{E10} and, although at a smaller extent, also of the mean period. Of course the last two results are related because an underestimate of $T_{m-1,0}$ implies that on average the model places the (on average) right amount of energy too much towards the higher frequencies. Unavoidably this leads to an underestimate of the energy in the 0.03–0.1 Hz range, hence of H_{E10}. The reasons for this are still unknown and, apart from specific tuning, research is on the way to find the culprit (or culprits) for this. The possibilities range from the large scale (wind and wave input, wave model, etc.) to the very local ones. For instance, zooming on the local scale, Groeneweg et al. (2015) have pointed out how, considering the interaction of the waves with the channel, the absence of various sub- and super-harmonic interactions in SWAN causes an unrealistic amount of energy to be trapped on the channel slopes owing to wave refraction.

In more general terms it has been pointed out that the H_{E10} concept, conceived 20 or 30 years ago, at a time when first hand solutions were required, should be abandoned in favour of a more rigorous solution. Granted that the full 2D spectrum is available, a specific estimate should be provided for each vessel on the base of the its response function. Of course we still have the general model energy shift towards higher frequency, but in a busy and economical world where accident probabilities and ensemble consequences are carefully evaluated, this is clearly the way to go.

2.6.4. *The fractal coastline of the Bothnia Sea*

Few places in the world, if any, can be compared as complexity of the local geometry and bathymetry to the Bothnia Sea in the central part of the Baltic Sea. Fig. 2.18 shows a progressive zooming on the area. Even at the 100 m scale it is impossible to resolve all the minor islands and tiny rocks that emerge from the surface. The submerged part and the convoluted shape of the shoals add to the complexity of the archipelago. There is no doubt that wave modelling here is a challenge because the scale of the relevant processes, as refraction and depth induced breaking, is beyond the practical resolution of even experimental runs.

The Finnish Meteorological Institute has been very active in improving the wind and wave modelling in the area, both for navigation purposes (ship routes do pass through the archipelago) and also for estimating the conditions out of, but relatively close to, the archipelago.

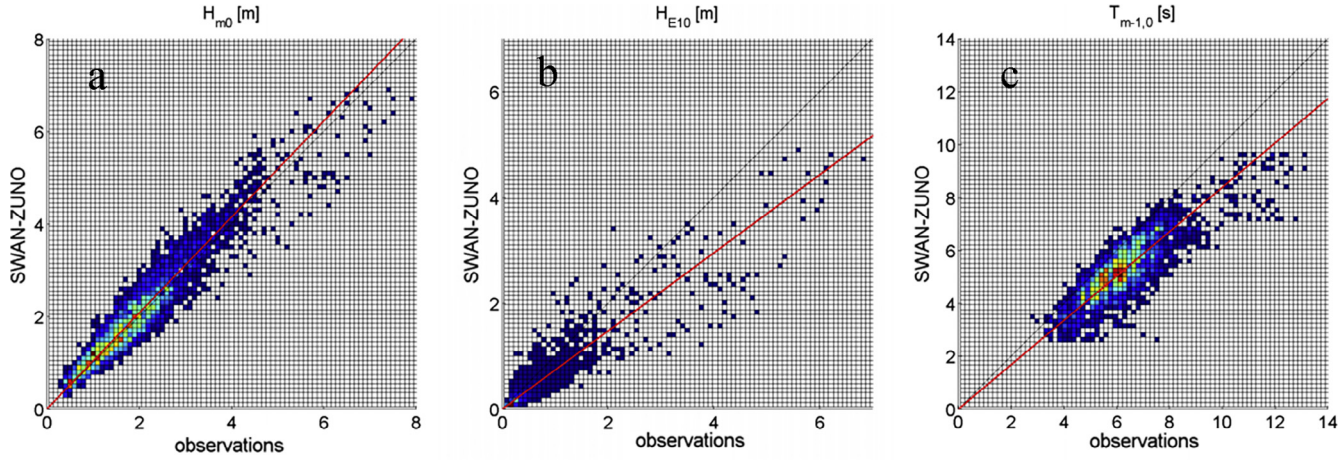

Fig. 2.17. Performance of the wave forecast system for the Rotterdam channel (see Fig. 2.16). Model comparison vs buoy. (a) Significant wave height, (b) H_{E10}, (c) mean period T_{m-10}.

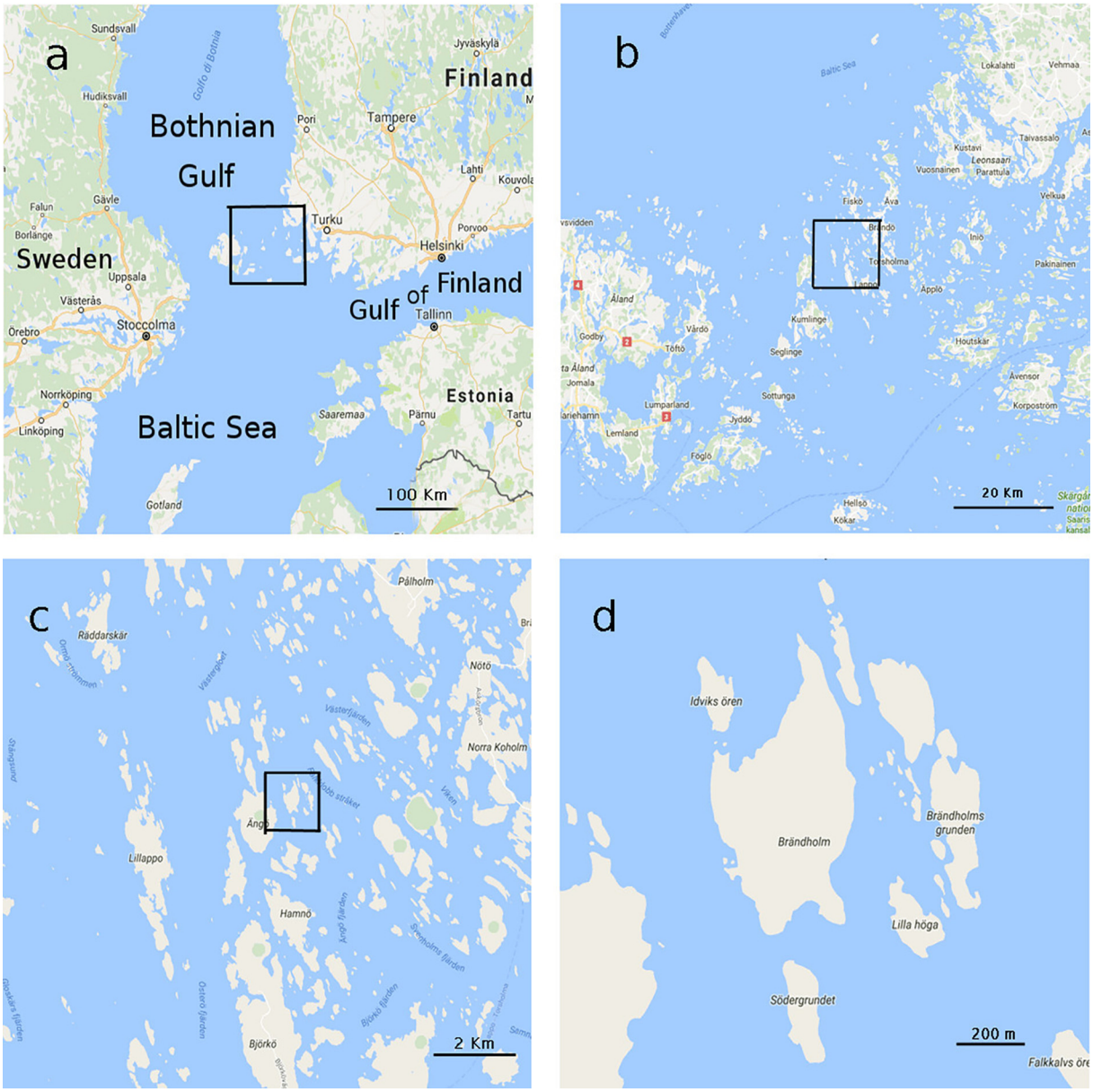

Fig. 2.18. Progressive zooming on the archipelago in the Baltic Sea. Each panel is, in the order, the enlargement of the little square in the previous panel.

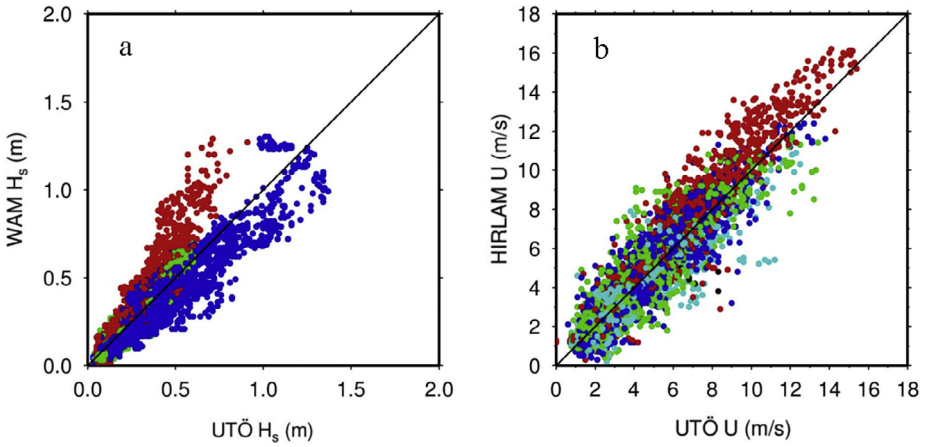

Fig. 2.19. Comparison between model and Utö buoy data. Location just South of the archipelago shown in Fig. 2.18. (a) Significant wave height, blue North going, red South going, (b) corresponding wind speeds. (For interpretation of the references to colour in this figure legend, the reader is referred to the web version of this article.)

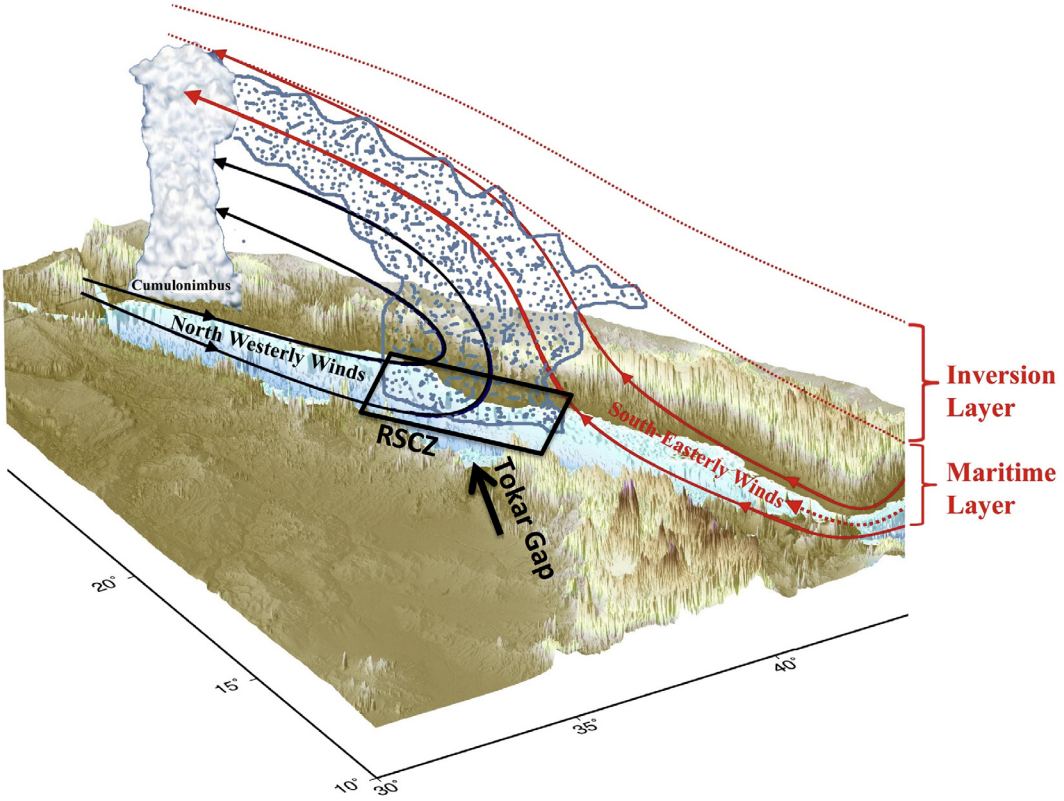

Fig. 2.20. Red Sea. Encounter between the cold north-westerly wind and the warm south-easterly one. The scale is provided by the geographical coordinates.

Ten different detailed grids were generated based on coastal nautical charts with horizontal resolutions of 0.1 and 0.5 nmi, also using different methods. Running the WAM model with locally produced high resolution winds, Pettersson et al. (2014) found that the minimal, 0.1 nmi, resolution was essential even only to obtain meaningful results. However, even at this resolution problems still exist. Model data have been compared with the data (wind and wave) recorded at the Utö buoy, located slightly south of the archipelago. The results are in Fig. 2.19. The blue dots refer to southerly wind conditions (hence blowing from the open water towards the archipelago). The red ones refer to the opposite direction. It is clear that, granted the usual and expected scatter, the wind has no particular problem. However, while waves coming from the South are slightly underestimated, there is a substantial overestimate of the waves coming from the archipelago. This suggests that the model does not succeed in reproducing the true conditions among, and due to, the islands. Possible reasons are a still insufficient resolution or the complexity of the large and small scale generation and dissipation that take place among and along the islands. One wonders if a solution, however pragmatic, is possible. This will be further discussed in the final Chapter 5.

2.6.5. *The peculiar meteorological and wave conditions of the Red Sea*

The Red Sea is the narrow (200 km) and long (2200 km) almost closed basin between Africa and the Arabian peninsula. Its borderline can be seen in Fig. 2.21. The orography is pronounced on both the sides, with cutting valleys aiming directly to the sea. Two opposite wind regimes dominate the situation. The periodic storms moving eastwards in the Eastern Mediterranean (just off the northern part of the map) lead to relatively cold inflows from the North that move then to the South channelled by the coastal orography. Alternatively during the winter months the East-North-East monsoon in the gulf of Aden (just out of the lower-right corner of the map) forces strong winds through the Bab-el-Mandeb strait (the only opening of the Red Sea). These winds are then again channelled by orography in the longitudinal direction of the

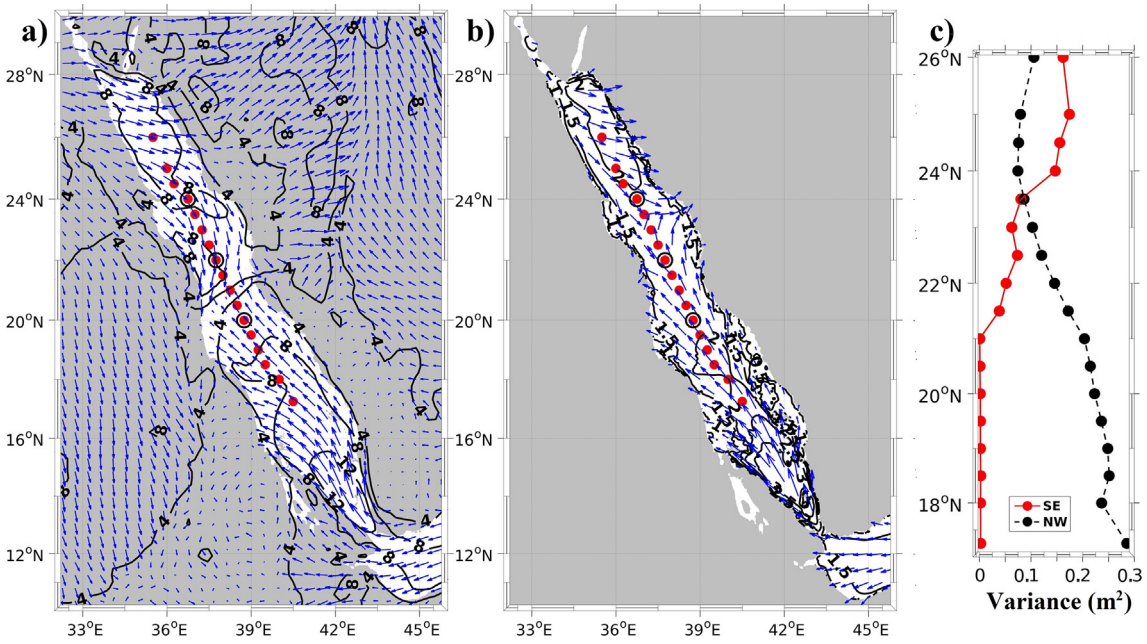

Fig. 2.21. Red Sea. (a) Surface wind speeds corresponding to the situation in Fig. 2.20. Isotachs at 4 m s^{-1} interval. (b) Significant wave height distribution corresponding to the situation in panel a. Isolines at 0.5 m interval. (c) Distribution of the wave energy (at the dots in panel b) for the two North and South going systems. Black moving to North-West, red to South-East. (For interpretation of the references to colour in this figure legend, the reader is referred to the web version of this article.)

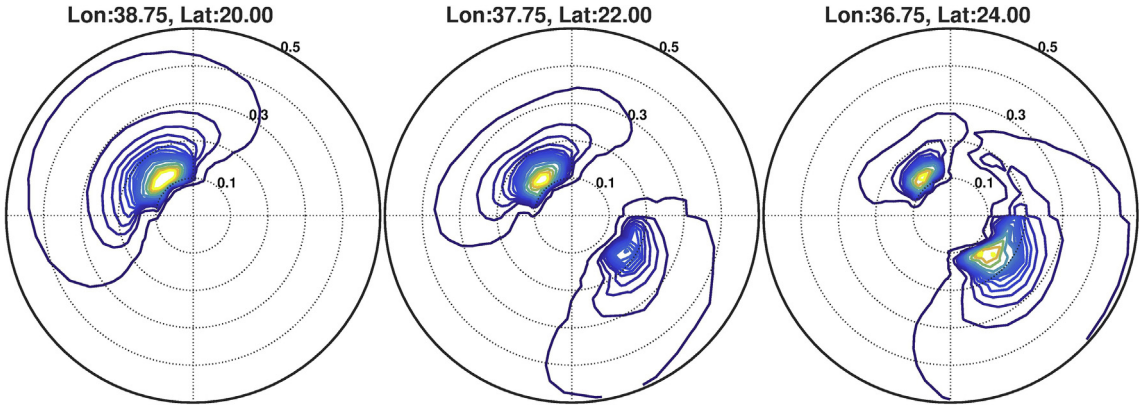

Fig. 2.22. 2D wave spectra corresponding to three points in panel a (see coordinates). Note the presence of the two opposite wave systems.

basin, in so doing being exactly opposite to the ones coming from the Mediterranean Sea. When, as it happens in winter, both the conditions are present, a peculiar, rather unique situation arises in the basin. The two winds, colder from the North, warm from the South, meet somewhere, forcing the South coming lighter air mass (see Fig. 2.20) to raise above the incoming northern air. This gives raise to local clouds and precipitation (drizzles) in the middle of an otherwise fully sunny area. The corresponding wind (panel a) and wave (panel b) conditions are shown in Fig. 2.21. Panel c reproduces the distribution along the Red Sea of the energy of the two wave systems, the red one moving to South, hence decreasing in this direction, the black one to the North. The wave spectra at three separate positions (see also their geographical coordinates in Fig. 2.22) provide a clear evidence of the simultaneous presence of the two systems.

From the wave modelling point of view the unique situation is the one of two opposite winds blowing against each other, hence two opposite wind seas clashing together. The physical aspect of interest is that in this situation many of the implicit assumptions underpinning the wave model physics are no longer true. In the standard situation of a generative sea, wind and waves move more or less in the same direction, and, with some theoretical background and a sufficient level of tuning, we have suitable formulas for energy input by wind and dissipation by white-capping. However, in the described situation the physics is, partly at least, different. This forced Langodan et al. (2015) to propose, in what they define “a preliminary crude attempt”, and use a modified version of the two corresponding approaches. Given E_A and E_B as the energy of the two opposing systems, the modified source functions appear as

$$S_{inA} = [.....](1-\alpha(E_B/E_A)(L_{short}/L_{long}))$$

$$S_{disA} = [.....](1 + \beta(E_B/E_A)(L_{short}/L_{long}))$$

where […] indicate the presently used source functions. L_{short} and L_{long} are the wavelength of the two systems, the shorter and longer one respectively, independently of which system the source function refers to. Langodan et al. (2015) report a marked improvement of the quality of the results using $\alpha = 0.08$ and $\beta = 0.20$, the different values reflecting the also physical perception that white-capping is the most affected process in the described situation. Of course problems exist also for the DIA approximation. Conceived for and sufficiently fitting the classical case of a single generative sea, obviously, as also shown in the cited

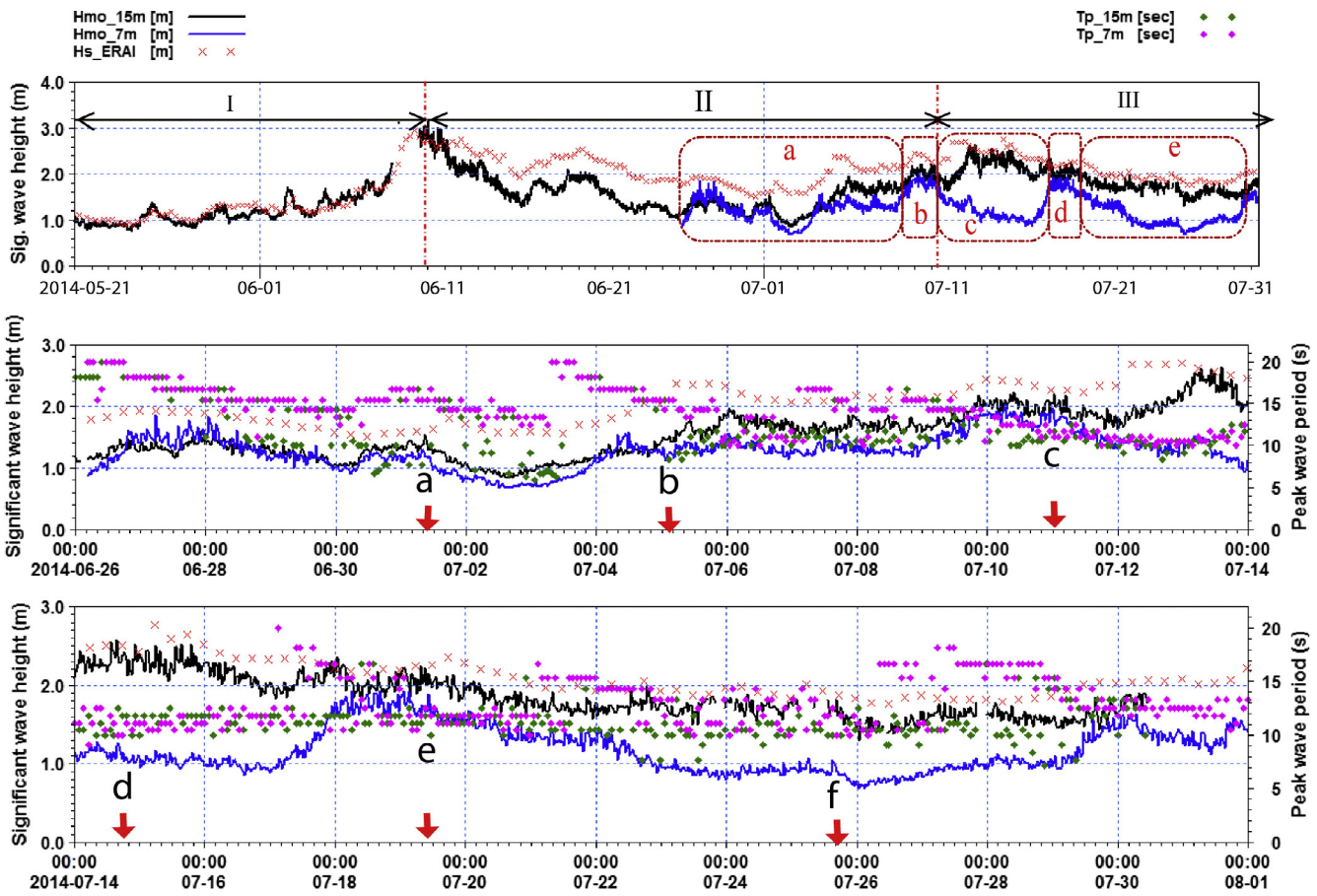

Fig. 2.23. Significant wave heights recorded off Alleppey (Kerala, India) from two buoys at 15 m (black) and 7 m depth (blue) water depths. Red line shows the corresponding ERA-Interim values. The dots (pink and green) show peak wave periods at the two locations. The upper panel is H_s during May to July 2014. Its right parts (II & III) are expanded in the central and lower panels respectively. Here the a to f letters refer to the time of the spectra in Fig. 2.24. Days are given as yyyy-mm-dd. Please disregard the a to e letters in the top panel, written there for a different purpose not part of this paper. We apologize for the confusion. (Derived from Samiksha et al. (2017) and Shynu et al. (2017)).

paper, it cannot cope with the “encounter” situation. We stress that this “encounter” is substantially different from the common case in the ocean of a wind sea superimposed to a background swell, this typically with different (lower) frequency and direction. In the Red Sea case the two systems have more similar frequencies, albeit varying along the respective fetch. The “preliminary crude attempt” of Langodan et al. (2015) is only a patch, although physically in the right direction, hinting to the fact that the physics we presently use in wave modelling is based on idealized conditions that often (we wonder, e.g., about the much simpler case of a wind sea plus a non-small swell) do not properly represent the truth of nature.

2.6.6. *The muddy bottom off the Kerala coast of India*

Kerala is the southernmost state on the west coast of India. Wave climate is dominated by the long swells coming from the Southern Ocean and by the southwest monsoon waves (predominantly wind seas). A peculiar phenomenon existing off Kerala is the non-permanent presence of a thick layer of viscous mud (mud-banks) in an extended shallow area just off the coast. Locally known as 'Chakara', the dimensions of the mud-banks are not yet known. The mud, whose origin and transport have not yet been fully determined, has the peculiar characteristic of leading to an area of relatively calm zone (soon to be quantified); off the periphery of this calm zone, rough conditions prevail because of the southwest monsoon waves (June–Sept). During this time the significant wave height off the periphery of this mud-bank would be up to 3–4 m, with the highest values frequently above these figures. On the contrary in the mudbank area the wave heights are highly attenuated. Fig. 2.23 shows the H_s recorded by two Waverider buoys at two water depths (15 m and 7 m) off Alleppey (Kerala). The two buoys are located at 10 km and 5 km off the coast, respectively. The mudbank and its periphery are known for their very high biological productivity, leading to a flourishing fishing activity. In practice, the mud is an important factor for, and a driver of, the local economy.

The fact that mud in shallow water attenuates waves is not new. Spectacular attenuations have been reported in the Gulf of Mexico when large waves come across narrow gulleys with a thick layer of viscous mud. Forristal and Reece (1985) and Forristal et al. (1990) made an extensive study of the situation. When the mud is distributed along elongated gullies, the effect is in a way rather local. On the contrary, along the Kerala coast the mud is distributed over a large area, leading, where present, to a progressive attenuation of the waves while approaching the coast. An excellent aerial view of mud accumulation has been provided by Holland et al. (2009), and a summary of the mud attenuation related studies is found in Komen et al. (1994, 169–171). The CSIR-NIO (Goa, India) initiated a multi-disciplinary oceanographic program, “Alleppey Mud-bank Process Studies (AMPS)” in 2014 (still continuing) to study the various aspects of the Alleppey mud-banks, including also a high resolution wave forecast system. An extensive description of the Alleppey mud-banks and its local phenomenology is provided by Samiksha et al. (2017) and Shynu et al. (2017). Although a number of studies/hypotheses have been conducted/proposed for the origin, the formation and disappearance of the mud-banks still remain a mystery. Granted that they are related to the waves and currents associated with the southwest monsoon, not enough

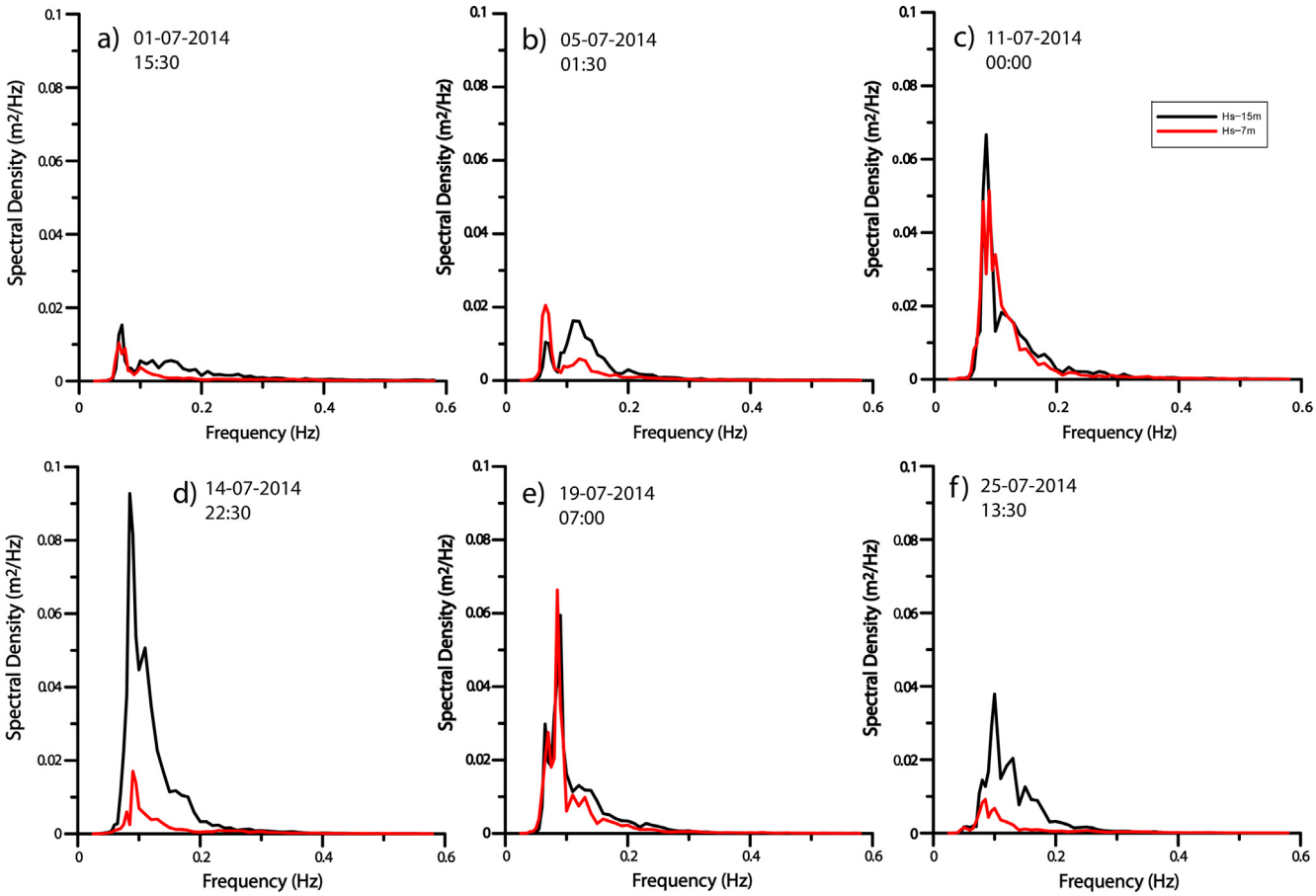

Fig. 2.24. Wave spectra at 15 and 7 m water depth locations, at the six times (a to f) shown in the central and lower panels of Fig. 2.23. Days are given as dd-mm-yyyy (a different format from Fig. 2.23).

data are available to predict with sufficient accuracy the formation of the mud-banks.

The two above cited studies provide a detailed description of the wave attenuation due to mud-banks. The wave heights recorded at the two cited buoys are compared are compared to the corresponding estimates derived from ERA-Interim (Dee et al., 2011) as well as model results. Here, we reproduce two figures taken from the above work, that offer a spectrum of the possible situations. The upper panel of Fig. 2.3 (derived from the above works) shows the H_s time series from the two buoys (the offshore buoy is denoted by B, black, and the onshore buoy by C, blue) measured during May to July 2014, and the corresponding (close to the offshore buoy) ERA-Interim H_s (red, A). Sections II and III (Fig. 2.23, upper panel) are then expanded in the respectively central and lower panels, wherein peak wave periods are also provided (but not discussed). In these two panels six specific times are identified (a to f) and the corresponding spectra from the two buoys are shown in Fig. 2.24. We offer only a qualitative analysis that however suffices to make evident the difficulty of local wave modelling.

Until the first 3 m peak around the middle of May, (the) A, B, C (H_s) coincide, an indication (of the quality of ERA-Interim data, but for our present purposes) that mud has not yet reached the area. After this episode A > B = C, (suggesting that) mud has reached the area, but still offshore B, hence the limited differences (only in the higher frequency range) between the two spectra. Further in section II, time b, mud is also between B and C (hence A > B > C). The two spectra show a more marked attenuation at C. At c the mud is back offshore B, hence A > B = C, and the two spectra practically coincide. The situation changes completely in section III (lower panel) when the mud is now shoreward of B. At time d it is between B and C. Note the attenuation of the corresponding C spectrum with respect to B. At e most of the mud is shoreward of even C, so that A ≈ B ≈ C and the spectra are again the same. At time f the mud is moving towards offshore, now between B and C, so that A = B > C with a highly reduced spectrum at C. To close the cycle note how at the end of III the two buoys are again the same, but both B,C < A, i.e. the mud is now offshore B.

In other areas of the world, where present, the mud-banks are permanent (the Amazon being a classical example), generally at the mouth of rivers, and the formation mechanism is clear. It may be noted that in case of mud-banks off Alleppey, there is no presence of a river. Off Alleppey (where by the way no river exit is present)) and the Kerala coast in general, the mud is moving in with the monsoon waves and currents. With such variable conditions, it is difficult to predict/forecast waves accurately, when the mud distribution of this area is not known.

3. Interactions and coupling

where we describe the physics and the applications of fully coupled systems, first waves with currents, and then with also the atmosphere

In the previous chapter we have done a general, occasionally deeper, survey of the meteorology and wind waves that characterize the enclosed and coastal seas. We have highlighted the main differences with respect to how the same processes act and where they lead in the great open oceans. Oceans do cover most of the earth surface, but large part of the human population lives along the coasts, and most of our economic activity is concentrated in this area.

The shorter wavelengths and the younger and steeper waves that characterize the inner seas make waves more sensitive to the interaction with currents and also with the atmosphere. Some of the physics involved is similar, but often enhanced, with respect to the open oceans.

In particular the steeper waves and the shallow water processes imply a higher level of non-linearity in the system. Of course this makes the analysis and, more so, the forecast more “delicate”, in the sense that limited differences in the input information may lead to substantial ones in the final results.

Different processes arise, typically in shallow water. Indeed the costal time scale where waves and current interact can be of the order of 10 or 100 m. All this poses new challenges to the corresponding modelling, both as physics and numerics. While in the previous chapter we have considered the single aspects of the problem, e.g. the meteorological and waves ones, each one on its own, it is now time to go closer to the true world discussing the thin layers of air and water that surrounds our planet as a single unit and exploring what this implies. However, given the purpose of this paper, we will not take the grand view of the climate. Rather, our, perhaps biased, focus will be mainly on the inner seas, although some general discussion on the physics involved will imply describing the parallel processes in the wider open seas. For a progressive approach to the problem we will first deal (Section 3.1) with the wave-current interactions, that we will then expand in Section 3.2 with some consideration of the role of atmosphere in the coupling of the full system.

3.1. Wave-circulation interactions

J.M.Smith, A.Benetazzo, S.Carniel, L.Cavaleri, A.J.-R.Padilla-Hernandez, J.Staneva, G.Ph.van Vledder, A.J.van Westhuysen
Jane.M.Smith@usace.army.mil

with the physics of the interactions between waves and current and illustrative examples on the various aspects of interaction

Interaction between wind-generated surface gravity waves and current represents one of the important driving forces in coastal and offshore areas. Waves and circulation (partly the latter) are dominantly governed by the same driving factor (the atmospheric wind) and propagate in the same medium (the oceanic water). Waves and currents form a complex system which has usually been discussed assuming distinctly the influence of waves on hydrodynamics and the influence of currents on waves, a reductionist approach that, despite having merits, should be overcome by an integrated holistic approach. This broad topic is usually referred to as wave-current interactions (WCI) which traces back to the pioneering work of Longuet-Higgins and Stewart (1960, 1961).

Before discussing the problems related to practical applications, it is useful to frame the problem from a very general point of view. From this perspective the overall problem of WCI could be dealt with in a complete way by solving the non-linear shallow-water equations including the non-hydrostatic picture of the local environment. The basic ideas can be found, among others, in Zijlema and Stelling (2008) and Smit et al. (2014). However rigorous in principle, this approach is not pursuable in practical applications for various reasons ranging from the availability of all the necessary information to, most of all, the enormous volume of the implied computer resources. Hence a different approach is required.

To make the problem manageable, surface gravity waves are usually averaged out of numerical circulation models by integrating the governing equations of continuity and momentum over the time scale of the short wave motions. Circulation varies slowly in space and time at a scale that for most applications is large compared with typical wave lengths and periods. In spite of the separation in frequency space (minutes to weeks for circulation versus 1–30 s for wind generated waves), the interactions between circulation and waves have first-order impacts on both processes in key coastal locations such as coastal inlets, channels, and surf zones.

The general circulation near the coast and in estuaries or bays affects surface gravity waves through refraction, shoaling, and breaking. The latter occurs where the currents are strong (generally in the range of 1 m/s or more) or due to wave-water depth interactions, where tides or storm surges significantly alter the water depth (Jonsson, 1990). In turn waves impact the circulation through momentum transfers that drive currents, including Stokes-Coriolis force and wave setup (Longuet-Higgins and Stewart, 1960, 1961, 1962, 1964; Hasselmann, 1971; McWilliams et al., 2004). Additional interactions take place through wave mass transport, enhanced bottom friction, and turbulence enhanced mixing, besides the normal component of the wind stress.

Although circulation models often consider only the direct momentum transfer from wind to currents via surface wind stress, waves have their role as well in the process, with important implications, in particular for the mixing in the upper layer. The transfer of energy and momentum from the wind to the ocean via ocean surface waves influences the mixing dynamics through several ways (Ardhuin and Jenkins, 2006). The most intuitive one is wave breaking (Kantha and Clayson, 2004), that inputs momentum and turbulent kinetic energy within a depth comparable with the order of magnitude of the wave height. The second way is via Langmuir cell generation or circulation effects, resulting from the interaction of turbulent vorticity with wave-induced Stokes drift, and that propagates in the whole mixed layer (McWilliams et al., 1997; Babanin et al., 2009). Last, the Coriolis-Stokes forcing needs to be accounted for, resulting from the interaction of large-scale planetary vorticity with Stokes drift associated with ocean surface waves (Polton et al., 2005).

3.1.1. A short review of coastal circulation modelling where we outline the general accuracy of modelling coastal currents

Circulation models take many numerical forms, but produce fields of water levels and currents in either 2D horizontal (depth integrated) or 3D. Computational model grids may be structured or unstructured and the solution techniques may be explicit or implicit. Circulation models typically have time steps of seconds or smaller for accuracy and stability. Their inputs include bathymetry/topography, bottom friction coefficients, tidal forcing, atmospheric forcing (wind, pressure, air temperature, relative humidity, and more generally heat fluxes), Coriolis, river discharges, and short wave stresses. Turbulent shear stresses are expressed in the form of an eddy viscosity term. Circulation models generally give excellent results for idealized problems with analytical solutions (within a few percent) (e.g., Gerritsen et al., 2007). In coastal applications, however, simple approaches using constant vertical mixing are now generally substituted with more sophisticated approaches, e.g., two-equation turbulence closure models that account for wave breaking and Langmuir mixing induced processes (Sullivan and McWilliams, 2010; Kantha and Clayson, 2004). Inclusion of these processes are critical to reproduce the distribution of momentum fluxes within the mixed layer.

Solutions to field applications are more challenging. Circulation models rely on accurate bathymetric specification which can be difficult to obtain for complex coastal sites (e.g., tidal inlets, shoal complexes, tidal flats, and wetlands). The bathymetry is also often assumed to be stationary, even though it may change significantly on the time scale of a storm (surge) or of a tidal cycle. Narrow channels and steep bathymetry require locally a high grid resolution, which results in reduced time steps and longer computational times. To improve model stability, bathymetry features may be smoothed, reducing local accuracy. Accurate wind and pressure fields for complex storms, such as tropical cyclones, are also a challenge for accurate circulation modelling, especially in coastal areas. Circulation models focused on a certain area are very sensitive to the boundary conditions set in the model, and inaccuracies in radiating long waves at the boundaries can result in improperly reflected long waves being trapped in the domain. Another frequent issue in circulation models is flooding and drying of land during tide cycles or surge events. Flooding and drying algorithms are often ad hoc and can cause model instabilities and leave thin pockets of water on dry land during recession. Warner et al. (2010) and Lesser

et al. (2004) describe procedures to account for morphological updating in coupled flow-wave model systems. Some recent efforts have included the moveable-bed feature (Warner et al., 2008a, 2010).

Despite these challenges, modern circulation models generally provide accurate representation of water levels. Modelling tides at 101 tidal stations on the US East and Gulf coasts and the Caribbean, the ADCIRC model (Luettich and Westerink, 2004) reproduced tidal constituent amplitudes within 6–13% (Mukai et al., 2002), with the lower range of error in the dominant components. Errors in tidal constituent phases were 7–13°. Approximately half of these errors can be attributed to measurement errors. Dietrich et al. (2012) modelled four recent hurricanes in the Gulf of Mexico (Katrina, Rita, Gustav and Ike) with ADCIRC tightly coupled to the spectral wave model SWAN (Booij et al., 1999), where tight coupling refers to the passing of water levels and depth-averaged currents directly in memory from ADCIRC to SWAN and radiation stress from SWAN to ADCIRC as the models run on the same grid (Dietrich et al., 2011, 2012). The modelled surge was evaluated with an unprecedented data set of measured water levels and high water marks (approximately 1500 data sets over the four storms). The mean error for all four storms ranged from −0.07 m to 0.15 m, which is remarkable given the complexity of the modelling domains. Scatter Indices ranged from 0.16 to 0.28.

Water levels are a driver, but can also be considered an integrated product, of circulation. The key point is that limited differences in level between two locations can lead to substantial currents. This implies that modelling of currents within circulation models is generally more challenging, and errors vary significantly with the location. Blain et al. (2010) validated ADCIRC for tidal currents at eight gauge locations in Delaware Bay (USA). Relative mean absolute errors ranged from 1 to 35% for 2D and 3D simulations. The 3D model exhibited improvements in the estuarine region where there is complex stratification and mixing due to tides and river fluxes. Sutherland et al. (2004) evaluated two circulation models (DELFT3D and PISCES) at the mouth of the Teign estuary (UK). Waves were included in the simulations, but only water levels were fed back to the waves, not currents. Measured currents during the experiment ranged within ± 0.5 m s^{-1}. Relative mean absolute errors averaged over eight current meter measurements were approximately 70%. However, current measurements are prone to errors (more than a tide gauge). Thus removing the estimated measurement error of 0.05 m s^{-1} reduced errors to 3%, a clear proof of the need to take instrumental errors into account (see Section 2.5 for the similar problem with waves). Hsu et al. (2008) evaluated DELFT3D for wave-driven longshore currents with data from two US beaches (Duck, North Carolina, and Santa Barbara, California). Normalized root-mean-square errors ranged from 21 to 30%.

3.1.2. *The interaction with waves*

where we describe how currents affect waves

Coastal currents and water levels impact oceanic waves by changing the wave length, speed, height and direction. Changes in the shape of the waves can also make them more nonlinear. Wave-current interaction is a “problem of wave propagation in an inhomogeneous, non-isotropic, dispersive, dissipative, and moving medium, which also interacts with the wave” (Jonsson, 1990). Wave-current interactions are calculated on the basis of conservation of wave action. Phase-averaged spectral wave models calculate wave-current interaction based on linear wave theory with currents that are assumed homogeneous over depth, although solutions of the dispersion equation for weakly sheared currents are available (e.g., Kirby and Chen, 1989). Depth-integrated currents are generally applied in modelling, but surface or wave orbital–weighted currents may also be applied in stratified environments (e.g., Elias et al., 2012).

Waves entering a following current lengthen and reduce in height. Waves entering an opposing current shorten and steepen and may break. Tolman (1991a) investigated the effect of spatial and temporal variations of currents in the Southern North Sea on wind generated waves, showing that these effects can significantly alter both the significant wave height and period measures. If opposing currents are of sufficient strength, they may completely block the waves (Lai et al., 1989). In tidal inlets with strong currents, wave heights may double or triple on ebb currents, and the increased height and steepness, with the consequent frequent breaking, can be a hazard to navigation. Wave-current interaction also impacts refraction and diffraction. In addition to constricted tidal inlets, strong coastal currents such as the Agulhas current off the east coast of South Africa, the Kuroshiro off the east coasts of Taiwan and Japan, and the Gulf Stream off the southeast coast of the US interact strongly with waves. Examples of such interactions are nicely illustrated in Holthuijsen and Tolman (1991).

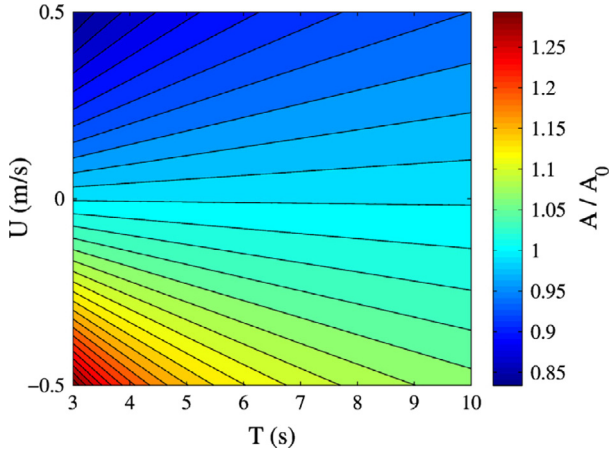

Fig. 3.1. How a following or opposing current (U) affects the amplitude (A; A0 is the amplitude in still water) of a monochromatic wave of period T.

The change of wave amplitude when entering a current is well summarized in Fig. 3.1, providing the result for a range of current velocity (± 0.5 m s^{-1}) and wave period (3–10 s). Of course we are implicitly assuming that waves and current move in the same direction. If waves and current are at an angle, only the current component in the wave direction needs to be considered. However, the transversal current too has implications, in particular on the wave direction. The smaller the group speed, the stronger the effect will be.

A more interesting example, because it is actually measured, is shown in Fig. 3.2. One of the several wave measuring systems on the oceanographic tower seen in Fig. 2.3, panel d, is a stereo wave imaging system capable of providing a high-resolution ‘3D + time’ history of a large span of the sea surface upwind from the tower for a bora event (from North-East). Similarly to a case described in Section 3.1.4, bora waves are generally associated with a relevant current in the same direction. The stereo system provides high-resolution spectra both in frequency and direction (see Benetazzo et al., 2012, 2015). Fig. 3.2 is quite rich in information. In the left panel, we plot the (k_x,k_y) distribution of energy at absolute frequency 0.926 Hz. What is shown is a section, at the indicated frequency, of the 3D distribution of energy (k_x,k_y,f) (see Holthuijsen, 2007, p. 51, 3.5.38 for a description of this approach). The dashed circle shows the expected energy distribution according to the linear dispersion relationship. However, current was present with average speed 0.20 m s^{-1}, in the indicated direction. This implies that the actual waves moving in the same direction are seen at a higher frequency by a fixed observer. Conversely, in the opposite direction, upward in the panel, the frequency is smaller and waves are delayed by the current with respect to the observer. The full circle shows the actual wave number distribution of the waves, in all the directions, seen as f = 0.926 Hz by the fixed stereo system. The comparison between the two circles provides a clear depiction of the current-induced Doppler effect on waves. However, there is much more in panel a. The distribution of energy in the main wave direction

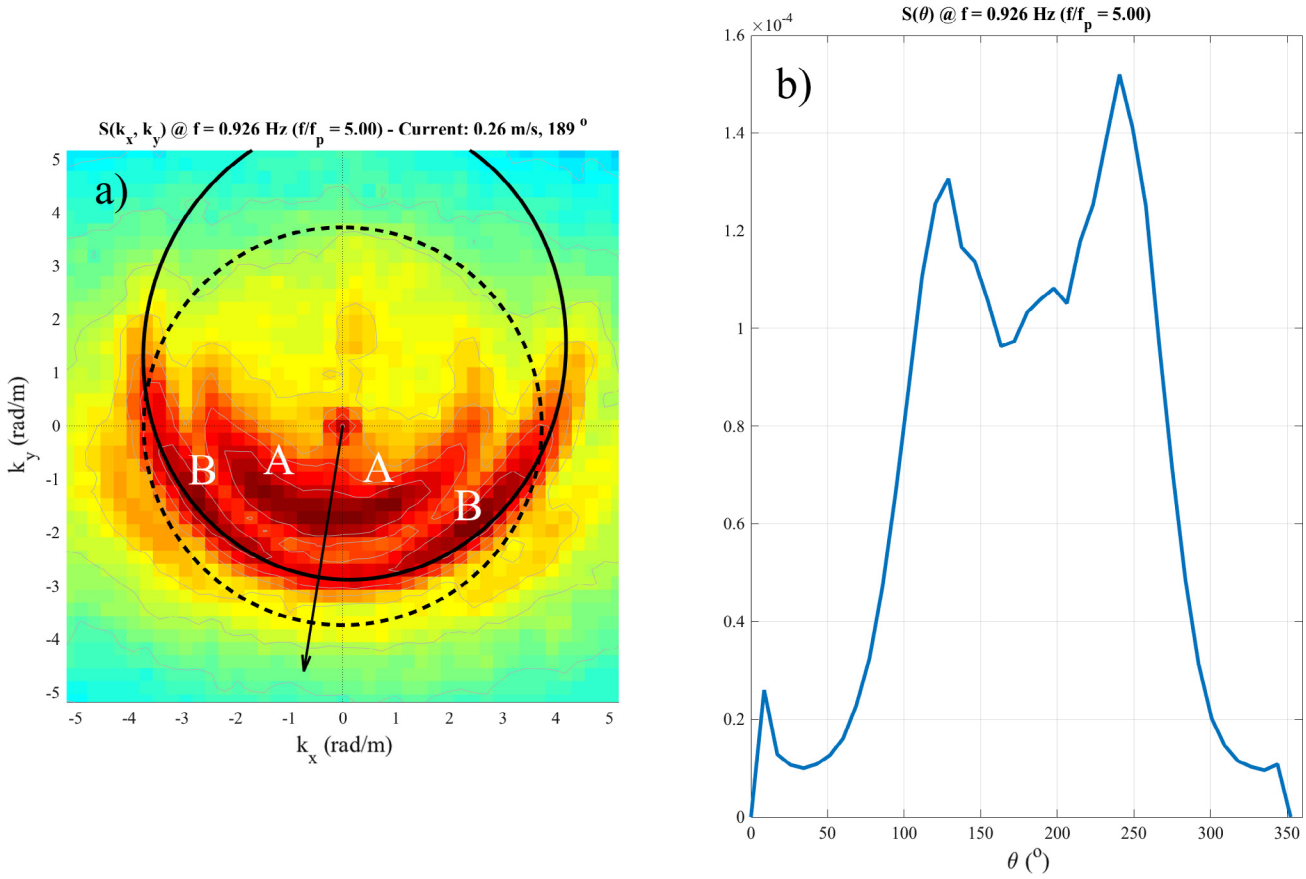

Fig. 3.2. (a) Section, at measured frequency 0.926 Hz, of a (k_x,k_y,f) 3D spectrum derived from stereo measurements of the sea surface. Dash circle: energy distribution according to the linear dispersion relationship. Continuous circle: actual energy distribution with respect to current. Arrow indicates the flow direction. (b) Directional distribution of energy along the continuous circle. Note the bimodality of the distribution associated to the non-linear interactions (see text for the full details). f_p is the peak frequency of the spectrum.

(practically coincident with the current) is evident, but evident are also the superharmonics, A-A as the arc of energy internal to the full circle. Not only that, along the full circle, at about ± 45° with respect to the main direction, are two peaks of energy B, better seen in the right panel providing the energy density along the circle, i.e., at 0.926 Hz (with respect to the current). The obvious remarkable feature is the two just mentioned peaks that represent the effect of non-linear interactions in the frequency range just above the 1D peak.

If steepening of waves in sufficiently intense, then the opposing currents has the double implication of increasing their non-linearity and, as cited, leading possibly to breaking. Chawla and Kirby (2002) found that wave breaking criteria based on steepness work well for this situation, but require coefficient modifications compared to the standard breaking case. Also, they found that the significant steepening of the waves requires that nonlinear terms in the dispersion relation become important and must be included. Ardhuin et al. (2012a,b) evaluated dissipation rates proportional to wave steepness to the fourth power, but found none of the parameterization to be fully satisfactory. This points to the need for more measurements and improvements to parameterizations.

As waves on an opposing current become steeper, hence possibly strongly nonlinear and near blocking, sideband instabilities develop that play a crucial role in the dynamics close to the blocking region (Lai et al., 1989). In this situation energy shifts from the peak frequency to both higher and lower sidebands. If blocking occurs at the peak frequency and above, energy in the lower sideband may still penetrate the current. Spectral wave models do not account for this nonlinear frequency downshifting due to wave modulation, and thus would predict total wave blocking, when downshifted energy exists. Like Chawla and Kirby (2002), Dodet et al. (2013) suggest that the application of a higher-order dispersion relationship would improve modelled wave heights on strong currents.

Water level variation from tides or surge impact waves in an expected way. Increases in water levels allow larger waves to penetrate deeper into estuaries at high tide or even larger distances inland with large storm surge. Indeed waves riding on storm surge do much of the destruction of infrastructure during hurricanes (Kennedy et al., 2011). One of the unresolved difficulties of modelling this “overland” wave propagation is a good parameterization of wave dissipation for interaction with buildings, urban infrastructure, and terrestrial vegetation. Waves propagating over shallow shoals are modulated based on the local wave height to water depth ratio. In this respect, see the recent thesis and related publications by Salmon (2016) and Salmon et al. (2015). For example, Smith et al. (2000) applied STWAVE and ADCIRC to model waves, currents, and water levels at the entrance to Willapa Bay (see Section 3.1.4 for more details). The results demonstrated that the dominant transformation process for waves in the bay was wave breaking over the Willapa bar, and the energy dissipation was controlled by the tide elevation.

From the above it is obvious that waves are particularly sensitive to strong current gradients, and indeed most of the impact is found in areas downwave of the gradient zones. For larger scale variations the impact is less extreme, and Ardhuin et al. (2012a,b) found that for larger scale current variations, the observed modifications of the sea state are mostly explained by refraction of waves over currents and relative wind effects (wind speed relevant for wave generation is the speed in the frame of reference moving with the near-surface current). Introducing currents in wave models can reduce the errors in wave

heights by more than 30 percent in some macrotidal environments, such as the Brittany coast in France.

In Section 3.1.1 we mentioned the possibility, and eventually the need, to model currents with a 3D approach. Sheared currents are a frequent reality, especially in shallow areas if considering the implications for their interaction with waves. Indeed in these conditions an improvement of the mean period is reached by considering the 3D Doppler shift as formulated by Kirby and Chen (1989). This process is important in sheared flows where the use of a depth-averaged current induces errors on the wave-current interaction estimation for the different wave components. The influence of bathymetry is also seen to be stronger on the wave field when considering the 3D Doppler shift.

Expanding our look to wave measurements, in addition to modelling waves, wave-current interaction needs to be considered in the analysis of wave information derived from subsurface pressure and currents or radar measurements. Waves ride a current according to their dispersion relationship. However, seen from the static point of view of an instrument at a fix position, their phase speed is apparently different, larger or smaller depending if waves follow or move against the current. A one point fixed gauge measures the period of the waves, therefore current is necessary information to derive the correct wave period, hence spectrum. The higher the frequency, the more crucial this is, not only because of the stronger relative frequency shift due to current, but also for the higher amplification of the signal once transformed to the surface (Smith, 2002).

3.1.3. Two-way coupling

where we point out the reciprocal and conditioning actions between waves and currents

Granted that waves may generate currents and the latter affect the former in various ways, it is obvious that the actual truth hides a continuous interplay with reciprocal interactions. These can be more manifest in certain areas and require specific numerical approaches.

As waves break under the action of wind or in near coastal regions, momentum is transferred from the wave field to the mean circulation. Near coast longshore currents and cross-shore water level variations are generated. In bathymetrically complex nearshore regions, strong circulations including rip currents may be generated. These current and water level patterns can feedback into the modification of the wave field through wave-current and wave-water level interaction. Kumar et al. (2012) and Uchiyama et al. (2010) compare radiation stress and vortex flux formulations for wave effects on 3D currents (including 3D wave stresses). Non-conservative wave effects on currents include wave-enhanced vertical mixing due to wave breaking and surface rollers, bottom streaming stress due to near-bed wave drag, and wave-enhanced bed shear stress (e.g., Soulsby, 1995). Formulations for wave breaking enhanced mixing are generally empirical.

On the sea bottom, the wave-enhanced turbulence in the Bottom Boundary Layer (BBL) modifies the boundary conditions for momentum in the Reynolds-averaged Navier–Stokes equations and determines the rate of sediment bedload and resuspension. Locally, the non-linearities involved in combined wave and current dynamics may produce a relevant increase in bottom shear stress and thus in sediment mobilization (Soulsby, 1995). State-of-the-art BBL sub-models include current velocities at a reference elevation close to the bed, bottom wave period, bottom wave orbital velocity, and wave direction, in order to account for the combined effects of waves and currents (Soulsby, 1995). WCI has a twofold influence on sediment transport: on one hand, the presence of a flow field modifies the geometric features of waves, while on the other hand the wave contribution to the water column momentum can generate relevant modifications in the local circulation features. This implies that both bottom stress and advective flow fields may be affected by WCI, in turn affecting both sediment suspension and transport (Sclavo et al., 2013).

The incorporation of wave effects (subgrid scale) in the form of wave-averaged bottom stresses and wave-averaged sediment transport rates remains a challenge. The wave boundary layer thickness is small compared to the layer thicknesses usually applied over the vertical in practical applications. This will remain a challenge for modelling systems that integrate hydrodynamics, waves, and sediment transport to predict morphological changes.

From the numerical point of view, wave-circulation coupling has been approached in a number of previous studies that consider two-way coupling between currents and waves (see, among others, Bolanos et al., 2011; Malhadas et al., 2010; Dietrich et al., 2011; Benetazzo et al., 2013; Benetazzo et al., 2014). The coupling may be achieved via direct connections within the codes or using couplers that provide efficient interpolation methods and message passing routines, but make communication of parameters less transparent and more difficult to debug. For this purpose, appropriate coupling software must be adopted (see e.g., Larson et al., 2004; Jacob et al., 2005; Warner et al., 2008b) which exchanges matrices between the different modules and interpolates between different coordinate systems.

Additionally, we should recall that parameterizations for most state-of-art models have been calibrated and consolidated to mimic observed dynamics in the absence of an explicit coupling within a complete coupled wave-current-atmosphere system. Besides improvement in the physical insight, the benefits of a shift towards a coupled approach in terms of model performances are therefore expected to appear progressively, as further fine-tuning is carried out based on the new modelling framework (Carniel et al., 2016b). For this reason, it is not straightforward to generalize evaluations of coupled versus uncoupled model skill, and a systematic comparison against field and laboratory observations is still required.

3.1.4. Practical examples

where we describe cases where waves and currents interact at various levels of complexity

Having provided the background for the possible interactions between waves and currents, it is useful and mandatory to provide examples where this happens and, where available, to quantify the implications. We consider examples at different scales, from the relatively small one of the exit of a river to the still enclosed, but wider span of the Gulf of Mexico.

3.1.4.1. Dee Estuary. The Dee Estuary, close to Liverpool, U.K., provides a good example of the impact of currents on waves. The river flow is not big in itself, but the remarkable range of the local tide, up to several meters in spring conditions, leads to currents exceeding $1\,m\,s^{-1}$. Exposed to the active and potentially violent Irish Sea, full consideration of the effects of currents and local changing depth on the wave characteristics is a mandatory condition. Brown et al. (2013) have implemented a tide-set-up-surge-current-wave coupled system in the whole Irish Sea with a nested high-resolution version in Liverpool Bay. The much stronger gradients in the bay require a much reduced integration time step (30 s instead of 200 s). To illustrate how careful we need to be in coupling, we quote the difficulty Brown et al. (2013) report with radiation stress. Initially a 3D method (Mellor 2005) was coded (Bolanos et al., 2011). However, in shallow water this approach (Mellor 2011) led occasionally to spurious accelerations, in particular just outside the surf zone. In turn this implied unrealistic coastal circulation. In the end, a 2D radiation stress approach was preferred (Mastenbroek et al., 1993), leading to quite realistic results for wave set-up and induced circulation. See also Bolanos et al. (2014) for a discussion of details of WCI.

3.1.4.2. Frisian Islands. The combination of a former ice age, lower and then rising sea level, tide, and wind led in the millennia to the formation of the Frisian Islands, a 500 km line of dunes off the coast, cut through by the sea at several locations, and extending from The

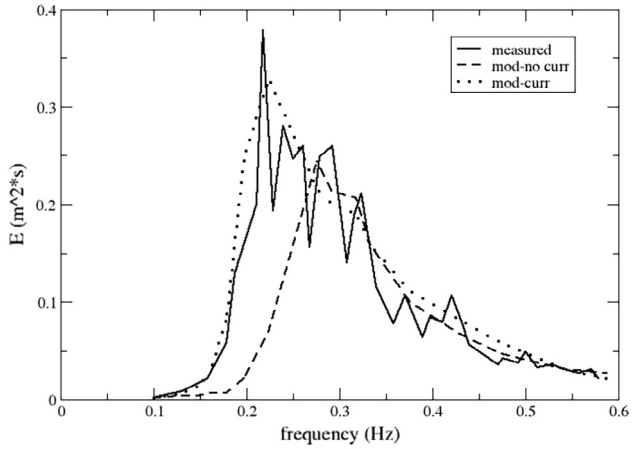

Fig. 3.3. Wave spectrum modification by an opposing current, as seen by a stationary observer.

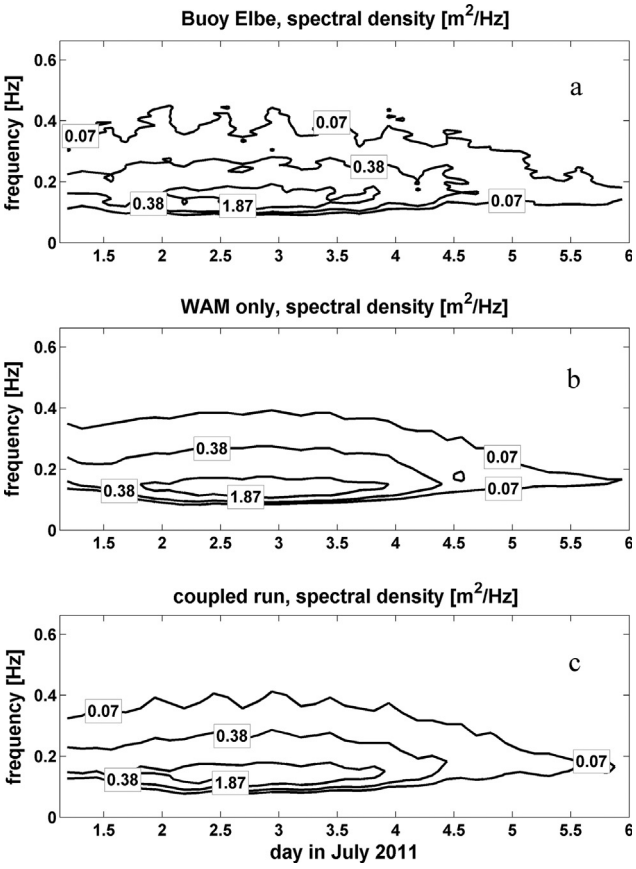

Fig. 3.4. German Bight, Southern North Sea. Sequence of spectra as measured and estimated at the local Elbe buoy (f vertical, time horizontal). Isolines of 1D energy density are shown. (a) Note the modulation by tidal current in the measured spectra. (b) and c) Uncoupled and coupled run respectively. The only slight modulations in (b) are due to a modulation of the driving wind.

Netherlands to Germany and Denmark. This leads to remarkable currents in the various inlets between successive islands. These currents interact with the frequent, potentially violent, storms of the North Sea. Groeneweg et al. (2008) used the SWAN model to estimate the wave conditions in the inlets. As expected, they found that taking local currents into account is a necessary condition to get reasonable wave results. The local environment is particularly difficult because of the local strong spatial gradients for both waves and currents. Fig. 3.3 provides a nice example of the need of coupling for meaningful results. Compared to the measured spectrum (Hs ≈ 0.7 m), we see the model spectra without and with consideration of current. When compared to measurements, the better fit with current is evident.

3.1.4.3. Southern North Sea. The southeastern North Sea (the German Bight) is dominated by strong tidal currents exceeding in some areas 1 m s^{-1}. Therefore the feedback between currents and waves plays an important role in this area, and wind wave–circulation coupling needs to be accounted for, especially during extreme events. Fig. 3.4, panel a, shows how the locally measured spectra at the Elbe buoy station varied during a mild storm (maximum H_s 2.5 m) during the first five days of July 2011. There is an obvious modulation of the spectra at half a day interval, i.e. with the semi-diurnal tide. Note, as expected, how the modulation is stronger in the high frequency range (up in the panel) due to their lower group speed with respect to the current. The uncoupled wave model results in panel b show only a very slight modulation, expected to depend on the variable wind forcing, because wind too varies with tide and temperature. It is only in the coupled model (panel c) that we recognize the full 12-h cycle in the modulation of the spectra with a good fit to the results in panel a. The tidal currents are mainly affecting the tail of the spectra, whereas the energy around the peak is not much different in all three panels. The statistical analysis of the results (see Staneva et al., 2016) confirms what is already evident from the figure.

3.1.4.4. Willapa Bay. The entrance to Willapa Bay (Washington, USA, see Fig. 3.5) includes a complex of shoals and a meandering channel. The mean tide range is 2.7 m with peak currents of over 2 m s^{-1}. The average yearly wave height is 2 m with storm heights up to 9 m. In the entrance channel, Smith et al. (2000) found that the effect of currents on waves was most significant in the outer entrance channel, where wave heights on the ebb increased up to 80 percent and on the flood decreased up to 20%. A remarkable fact is that the modulation of the waves in the upper part of the bay (points 2, 3, 4), affected by the conditions offshore (point 1), depend strongly on the tide via the shoal at the entrance and the consequent variable bottom induced wave breaking. Olabarrieta et al. (2011) found that also the locally generated waves in the bay (point 5) are strongly modulated by the transversally non-uniform tidal flow via the tunneling or detunneling effect. If the flow is stronger at the center of the local channel, opposite moving waves will tend to focus at the center of the channel. The opposite is true for following waves.

3.1.4.5. North Adriatic Sea. The North Adriatic Sea (see Fig. 2.3, panel a for its location) has the double advantage of (a) strong bursts of bora wind with consequent high locally generated waves and resulting currents, and (b) the availability of a fully instrumented oceanographic tower (panel d) located 15 km off the coast of Venice. Benetazzo et al. (2013) implemented the first fully coupled wave-ocean 3D model (COAWST suite) in the Adriatic sea region, where the current passed from the ocean model to the wave model was based on the Kirby and Chen (1989) formulation (see above), which computes a weighted depth-averaged velocity accounting for the vertical current structure and the dispersion relation of surface gravity waves. The importance of vertically averaging the currents over a depth controlled by the spectral wave numbers was found to be important in shallow waters, where almost the entire vertical current shear affects wave dynamics. With this approach Benetazzo et al. (2013) were able to show that the presence of current, up to 0.6 m s^{-1}, led to 0.6 m H_s reduction with respect to the “only waves” case. At the same time it turned out that 10–15% of the current speed was due to the presence of waves. We will go into more details for this storm in Section 3.2, discussing the interaction with the atmosphere.

Fig. 3.5. Willapa Bay (Washington State, USA). The dimensions (see scale) are about 40 × 10 km. Numbers indicate the location of the measuring buoys.

3.1.4.6. Hurricane Isabel. Warner et al. (2010) developed and applied the COAWST system to a hurricane scenario, forced with the atmosphere Weather Research and Forecasting model (WRF) (Skamarock et al., 2005). They showed that in certain conditions the significant wave height increases by as much as 20% when a wave system meets an opposing current. Similar results were obtained by Fan et al. (2009) who found a reduction in the wave energy when including an oceanic current following the waves. The authors also highlight that wave-current interaction improves hindcasts and forecasts of wave energy and, as a consequence, significant wave height. Fig. 3.6, left

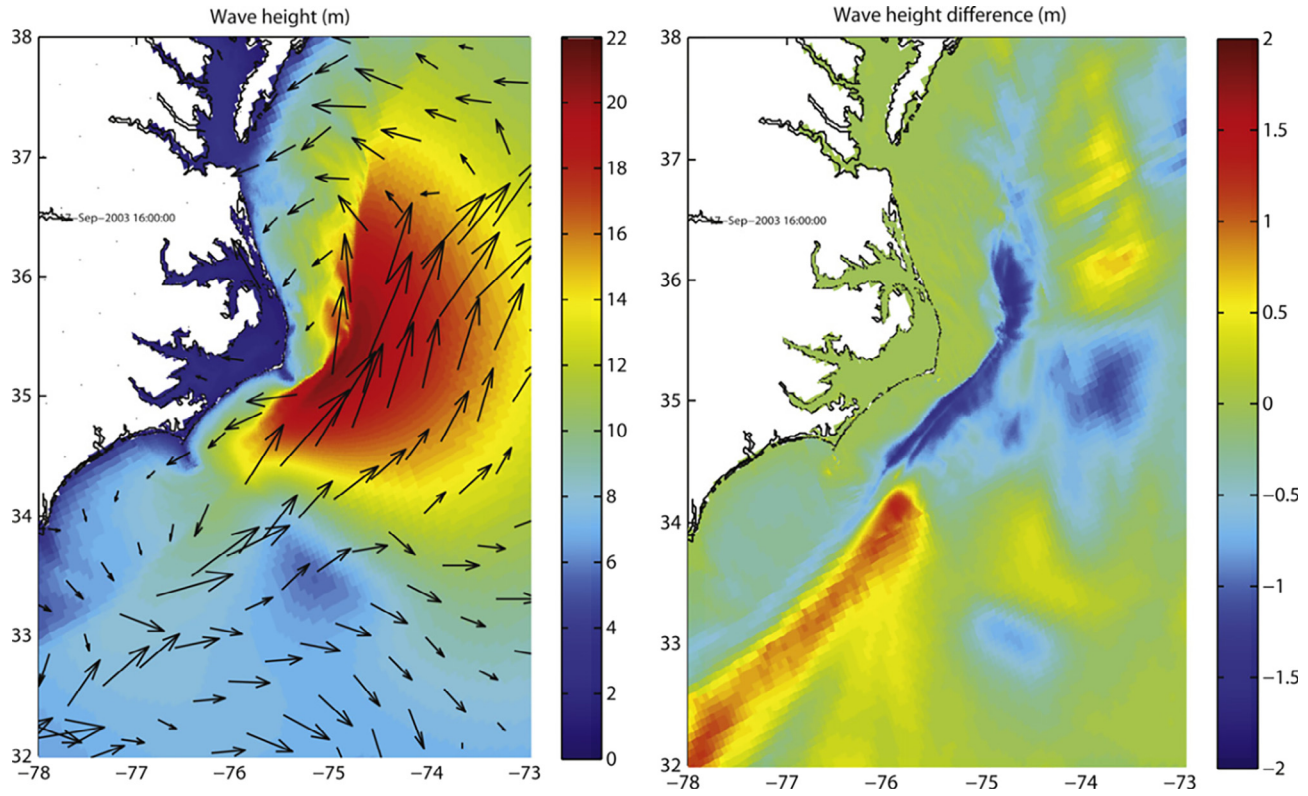

Fig. 3.6. Hurricane Isabel, 18 September 2003. (a) Interaction between the hurricane generated waves (colors) and the Gulf Stream (arrows) around Cape Hatteras. At the time of the plot the eye was located in the lower central part of the figure. (b) Wave height differences with-without wave-current interaction. (For interpretation of the references to colour in this figure legend, the reader is referred to the web version of this article.)

panel, shows the Gulf Stream off Cape Hatteras interacting heavily with the waves produced by Hurricane Isabel (18 September 2003, 12 UTC) whose eye at this time is in the lower central part of the panel. In the right panel we see the wave height differences due to the interaction with the current field. To the left of the eye, waves move against the current, hence the line of increased heights along the border of the continental shelf. On the contrary, just east of the cape, the maximum estimated wave heights at this stage of the hurricane, up to more than 18 m H_s, are locally decreased by a strong component in the direction of the current.

3.1.4.7. Northern storm on the Gulf Stream. A similar case, but in less extreme conditions, is shown in Fig. 3.7. The left panel shows large wave heights, 5–6 m H_s, from a northerly storm along the coastline of Melbourne (Florida, USA), estimated without considering the interaction with the local current field. When the Gulf Stream (panel b) is taken into account, the overall H_s field is substantially enhanced (panel c). Note the elongated shape of the enhanced area, practically superimposed on the Gulf Stream. Note in particular in panel c the lateral convergence of wave energy towards the enhanced area following the wave refraction due to the transversal current gradient of the Gulf Stream. .

Moving closer to coast, we report now the results for two events of completely different magnitude, but both showing the reciprocal role of

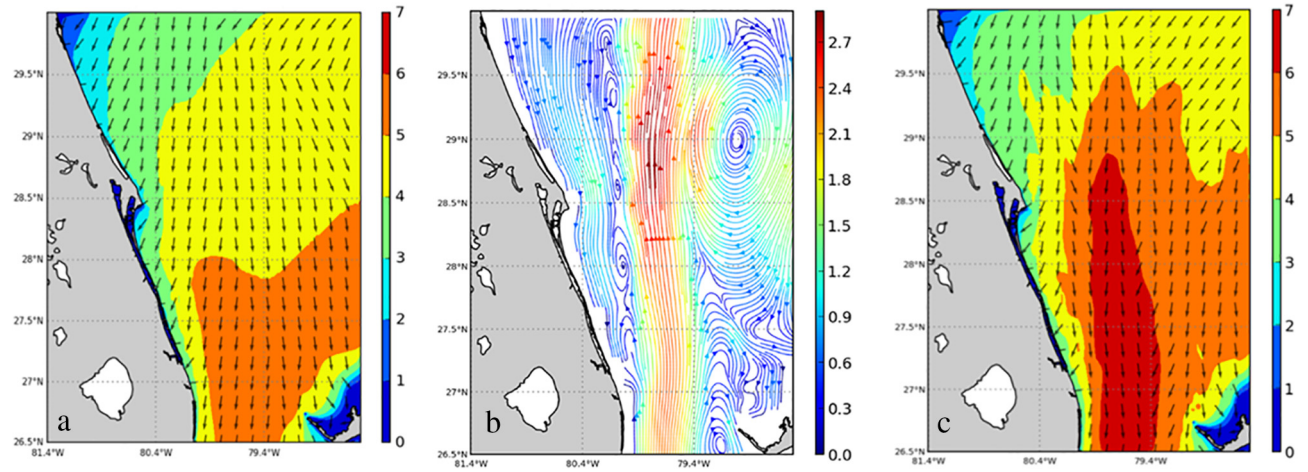

Fig. 3.7. Interaction between the Gulf Stream and a northerly storm off Melbourne (Florida, USA). (a) The uncoupled wave field, (b) the Gulf Stream distribution, (c) the coupled wave field. Note the much increased wave heights and the wave lateral convergence towards the Gulf Stream due to current induced refraction.

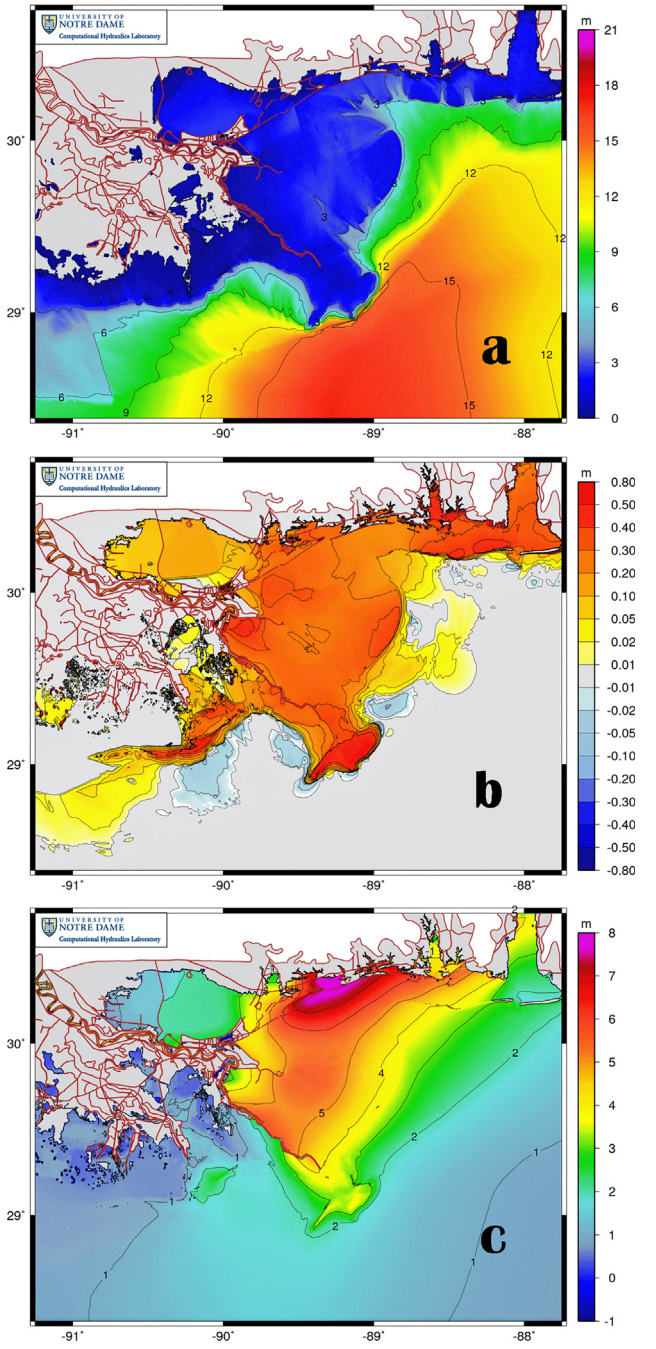

Fig. 3.8. Hurricane Katrina, August 2005. Area around and to the East of the Mississippi delta. Distributions of maximum (a) significant wave height, (b) wave set-up, (c) water level (courtesy of Casey Dietrich, North Carolina State University).

waves and water level in determining the conditions at the coast.

3.1.4.8. Hurricane Katrina. Katrina, August 2005, was the costliest natural disaster, and one of the five deadliest hurricanes, in the USA documented history. Reaching peak strength in the Gulf of Mexico, Katrina landed just east of New Orleans. Much of the damage on the coast and the inland area (up to several kilometres) was due to the increased level of water and the consequent action of waves. Fig. 3.8, three panels, show respectively: (a) the maximum significant wave height reached in the area around the delta of the Mississippi river, (b) the maximum wave set-up, (c) the maximum water level elevation. Of course all these quantities are reciprocally related. Large wave heights

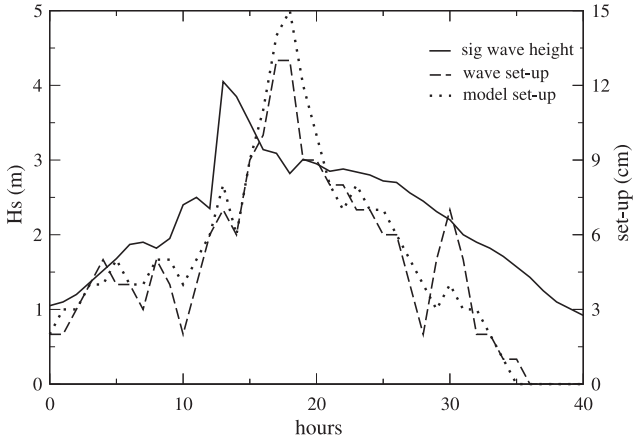

Fig. 3.9. Wave set-up on the Venice coast during the storm of 22 November 1979. The set-up is between a tide gauge 2 km offshore (at the end of a jetty, 6 m depth) and the one on the oceanographic tower 15 km offshore. See Fig. 2.3 for details. The significant wave heights are referred at the tower position (16 m depth).

arriving at, and breaking on the shallow areas of the delta leads to wave set-up in a positive loop involving both these quantities. All this is further enhanced by the overall storm surge (note the 8 m coastal surge about 70 km east of New Orleans). We will come back to this last point, more specifically panel c, in Section 3.2 dealing with the reciprocal interaction with the atmosphere.

3.1.4.9. Wave set-up at Venice coast. Much smaller wave heights and surge were involved in the storm that hit the Northern Adriatic Sea (Fig. 2.3) on 22 December 1979. The flood ranked as the second most severe in Venice history, with 1.66 m above the nominal local sea level. The availability of tidal data at the oceanographic tower (panels c, d) and at the jetties at the entrance of the lagoon made it possible to measure the different sea levels. Fig. 3.9 shows the H_s values at the tower and how the difference varies through the storm. We point out that after the nominal 20 h, the wind had changed direction so that it was not blowing any more towards the coast. Therefore after this time the difference was due only to wave set-up, duly decreasing in time with the wave height. Bertotti and Cavaleri (1985) estimated the set-up with a wave-sea level coupled model starting from a general hindcast of the storm and the conditions at the tower where, according to the hindcast, waves were already limited by depth-induced breaking, hence we were already in a set-up regime. The shown differences are not with respect to the coast, but to almost two kilometres offshore, at the end of the jetty at 6 m depth. The maximum coastal set-up was estimated at more than 0.5 m with respect to the tower.

3.1.4.10. Catalan coast. We end this section with a formally negative example that will open the way to the next section of interaction with the atmosphere.

The Catalan coast is at the north-western end of the Mediterranean Sea (Fig. 2.3, panel a). It is exposed to mainly easterly winds, but with often sustained wind storms from inland. Fig. 3.10 shows the along-shelf, depth-averaged flow component just off the coast as measured by local current meters. The three color lines show the results of the local circulation modelling at 1 km (SHECAT) and (two-step nesting) 50-m resolution. Finally the corresponding results for the fully coupled (WRF, SWAN, ROMS) system are shown. In general the three simulations do not differ dramatically, although occasional larger differences associated with coupling appear. However, the main message comes from the comparison with the measured data. There are repeated, also extended, occasions when the measured data are completely different, well off the set of the modelled data. Sanchez-Arcilla et al. (2014) attribute this to transient forcings of the atmospheric driver. The lesson to

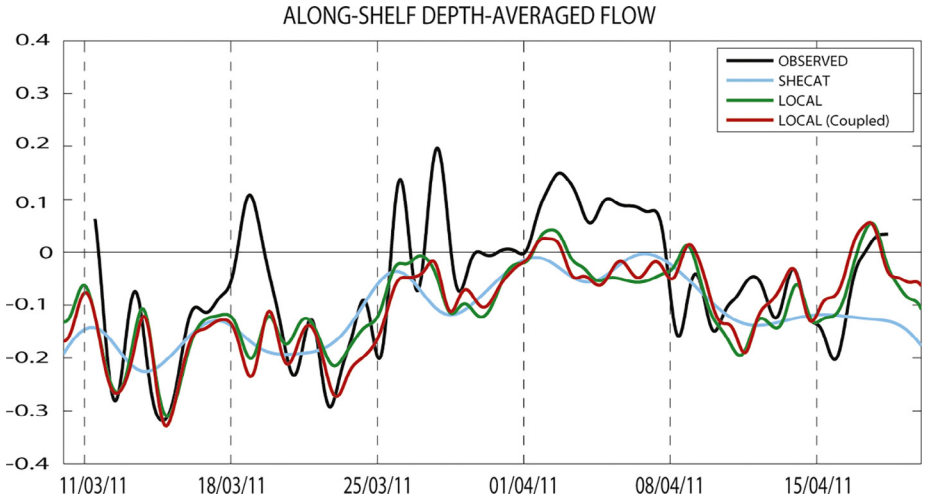

Fig. 3.10. Currents measured and estimated just off the Catalan coast. The Shecat model has 1 km resolution. Local, uncoupled and coupled, 50 m resolution. Observed data from local currentmeters.

be derived has been known for decades: we can have all the possible sophisticated approaches in our model, however, if the atmospheric input is not sufficiently correct, all the couplings we consider will not necessarily move the final result in the right direction. Still with much attention, this encourages us to move to full coupling with the atmosphere.

3.2. The coupling of ocean waves with the oceanic and atmospheric boundary layers

Ø.Breivik, J.-R.Bidlot, L.Cavaleri
oyvind.breivik@met.no

where we involve the atmosphere in the interplay between ocean and waves

Until recently, the oceanic wave field and the interior ocean were modelled as separate entities, each forced independently and inconsistently by atmospheric fluxes of momentum, heat and latent heat with no feedback to the atmospheric boundary layer. Climate models were naturally the first to delve into coupling of the ocean and the atmosphere, but also these models refrained from including the oceanic wave field. Except for the coupled atmosphere-wave forecasts issued by ECMWF since 1998 (Janssen, 2004), no attempt was made at coupling operational atmosphere-wave forecasts, let alone fully coupled atmosphere-wave-ocean forecasts. Only very recently Breivik et al. (2015) acted in this direction.

Interestingly, the most active part of the sea is its surface, and ocean waves play a key role in modulating, in a direct or indirect way, all the exchanges at the surface. Because in turn some of the effects feed back to the wave field and the upper ocean, all this is of interest also for our present purpose.

In this section we deal with the full coupling of the ocean–wave-atmosphere system. This requires a clear view on the processes in the ocean mixed layer. Unavoidably, in dealing with this, we release momentarily the coastal-only perspective (but most of what we will say is valid also there), only to converge again when going into the details of specific processes. Also, although the number of specific examples at a limited scale may be less abundant than in the previous Section 3.1, they will also show the crucial role of the full coupling in some of the most dramatic situations.

3.2.1. The physics of the ocean mixed layer

where we provide the basic physics that govern the upper layer of the ocean and the interaction with the atmosphere, all modulated by waves

The depth of the ocean mixed layer, also known as the ocean surface boundary layer (OSBL), is maintained by a number of processes, including most importantly buoyancy production through heating and cooling and shear production. It is however clear now that waves also play a role in the mixing of near-surface waters.

Breaking waves and whitecaps are the most visible manifestation of mixing close to the sea surface (Monahan, 1971; Wu, 1979; Scanlon et al., 2016). They increase the turbulence in the upper part of the ocean significantly (Craig and Banner, 1994; Craig, 1996, Gemmrich et al., 1994, Gemmrich and Farmer, 1999) and play a crucial role in homogenizing the uppermost part of the OSBL to a depth of the order of the significant wave height.

Through the interaction with the Coriolis effect, the Stokes drift velocity (Stokes 1847) associated with the wave field adds an additional term to the wave-averaged momentum equations. The effect was first presented by Hasselmann (1970) and has since been investigated for idealized cases by Weber (1983), Jenkins (1987), McWilliams and Restrepo (1999) and McWilliams and Sullivan (2000), among others. The force is known as the Stokes-Coriolis force or the Hasselmann force depending on whether it is considered to be purely an effect of the average Coriolis force acting on a particle with a Lagrangian velocity as given by the mean currents and the waves, or as a tilting of the planetary vorticity (Polton et al., 2005; Broström et al., 2014). The force does not directly modify the total mass transport, but it alters the distribution of momentum over the depth of the Ekman layer (McWilliams and Restrepo, 1999; Polton, 2009).

The Stokes drift decays rapidly with depth, but near the surface it can reach values close to 0.7 m s^{-1}. The full two-dimensional spectrum is in principle required to compute the Stokes drift velocity profile (Janssen et al., 2004; Janssen, 2012), but many simplified profiles (most commonly the monochromatic profile) are often used (see, e.g., Skyllingstad and Denbo, 1995; McWilliams and Sullivan, 2000; Carniel et al., 2016b; Polton et al., 2005; Saetra et al., 2007; Tamura et al., 2012). However, this underestimates the near-surface shear and overdoes the deep Stokes drift (Ardhuin et al., 2008). Recently, profiles that improve the shear and the deep flow still relying on the same integrated parameters (mean period, first order spectral moment and surface Stokes drift) have been proposed (Breivik et al., 2014, 2015).

The interaction between the wave-induced Stokes drift and planetary vorticity leads to Langmuir circulation, as was shown by Craik and Leibovich (1976). Skyllingstad and Denbo (1995) and McWilliams et al. (1997) were the first to identify the significant role of Langmuir *turbulence* in enhancing mixing in the upper ocean. Several studies have employed large eddy simulations (LES) to investigate the impact of

Langmuir turbulence in the upper ocean (Skyllingstad and Denbo, 1995; McWilliams et al., 1997; Teixeira and Belcher, 2002; Polton and Belcher, 2007; Harcourt and D'Asaro, 2008; Grant and Belcher, 2009), and in some cases even direct numerical simulations (DNS) have been employed. Most of these studies have found and confirm that waves do have a rather profound impact on the upper part of the ocean, but there is still considerable disagreement about which processes are more important. So far there have been few studies (see below) of the wave impact on three-dimensional ocean circulation models or fully coupled models of the ocean, the atmosphere and the oceanic wave field although the potential impact of waves on the climate system is recognized (Babanin et al., 2009; Cavaleri et al., 2007; Fan and Griffies, 2014; Li et al., 2016).

All these results have shown that wind-generated gravity waves have a profound effect on the OSBL, and may help explain the insufficient mixing found in Eulerian ocean models, especially in the extra-tropics. Langmuir turbulence, Stokes-Coriolis forcing and the direct injection of turbulence by breaking waves may substantially reduce the common shallow bias in the mixed layer depth predicted by most state-of-the-art climate models (Fan and Griffies, 2014). Furthermore, wave-turbulence interaction directly affects the evolution of weather systems and thus the predictability of forecast models (Breivik et al., 2015).

While the reality of the above mentioned processes is now qualitatively undisputed, having experimental proofs in the field is another matter. Indeed observing wave-induced turbulence is challenging for two distinct reasons. First, obtaining measurements of turbulent parameters in the wave zone means either placing instruments in the violent environment of breaking waves, or remotely measuring quantities in the wave-breaking zone. Secondly, the spectral gap between turbulent and wave-related scales is small, meaning that wave motion may easily be mistaken for turbulent activity. New instruments and methods for making Eulerian and Lagrangian measurements within the wave-breaking zone of the mixed layer are now becoming available. Examples of such instruments are the MATS turbulence profiler (Fer and Paskyabi, 2014) and the buoyant Air-sea Interaction Profiler (ASIP; see Ward et al., 2014). The SWIFT buoy used by Thomson (2012) appears as a promising solution for also the Arctic waters.

Of course theoretical estimates of the energy input into turbulence exist. As for Stokes drift and Langmuir circulation we use the wave spectrum, we can use the energy balance equation of the third generation wave models (Komen et al., 1994) to evaluate the momentum and turbulent kinetic energy fluxes into the ocean as respectively

$$\tau_{oc} = \tau_a - \rho_w g \int_0^{2\pi} \int_0^{\infty} \frac{k}{\varpi} \left(S_{in} + S_{ds} \right) d\omega \, df$$

And

$$\Phi_{oc} = -\rho_w g \int_0^{2\pi} \int_0^{\infty} \left(S_{in} + S_{ds} \right) d\omega \, df$$

hence directly from source terms.

The interplay between waves, ocean and atmosphere has different facets. While growing waves absorb energy and momentum from the wind field, in turn they release it when they break (Janssen et al., 2004; Rascle et al., 2006; Ardhuin and Jenkins, 2006; Janssen, 2012). This lowers or raises the stress on the water side (i.e., the stress below the oceanic wave field) relative to the air-side stress, depending on whether the sea state is growing or decaying. Only when the wave field is in equilibrium with the energy injected by the wind will the stress on the two sides of the surface be equal.

While wave breaking affects and mixes the upper few meters of the ocean, we still face (see above) the problem of a not sufficiently deep mixed layer in most of our model results. Indeed ocean models tend to mix too weakly (or have ad-hoc mixing parameterizations that actually overdo the mixing, see Breivik et al., 2015), producing warm biases which affect their heat uptake and deep-water formation (Babanin et al., 2009; Huang et al., 2011; Fan and Griffies, 2014). When coupled to meteorological models, this warm bias in turn affects the atmosphere by distorting the atmospheric deep convection and thus upsetting the delicate feedbacks in the climate system (Sheldon and Czaja, 2014). In the study by Fan and Griffies (2014) a significant change in the mixed layer temperature and its vertical extent was achieved with the introduction of Langmuir turbulence following the parameterizations by McWilliams and Sullivan (2000) and Smyth et al. (2002), as well as the parameterization of mixing by non-breaking waves suggested by Qiao et al. (2004). This latter mixing process appears similar to the mixing due to the high Reynolds numbers of the orbital motion of non-breaking waves explored by Babanin (2006) and Babanin and Haus (2009). The Qiao et al. (2004) approach is not yet universally accepted, but it is relatively easy to implement and has been used for a range of regional and global model experiments where it is found to make an impact. Using a climate model of intermediate complexity, Babanin et al. (2009) explored the effect of the three wave-related mixing processes, namely injection of turbulent kinetic energy from breaking waves, Langmuir circulation and the aforementioned mixing by non-breaking waves. They found that all three processes contribute to the depth and temperature of the mixed layer. Similarly, Huang et al. (2011) coupled WAVEWATCH III (Tolman et al., 2002) to a version of the Princeton Ocean Model (POM, Blumberg and Mellor, 1987) and demonstrated an improved summertime temperature profile using the non-breaking parameterization of Qiao et al. (2004).

Waves affect all the processes at the interface, and in particular the exchanges between ocean and atmosphere. These include aerosol production, heat transfer, radiation, albedo (and this is not an exhaustive list). Janssen and Viterbo (1996) showed how sensitive the atmosphere and its evolution can be to the sea albedo that is heavily affected by the presence of breaking waves.

Although relevant for climate, hence on very large scales, much of what said holds also for enclosed seas. Moreover, the smaller the spatial scale we consider, the shorter the involved time scale, hence more rapid the effects. This is particularly true when approaching the coastline in shallow water. A classical case, that we will illustrate with a couple of examples, is the combined wave set-up, surge and increased surface stress when wind and waves encounter a shallow coast. The bottom-induced breaking leads to wave set-up (see the example in Section 3.1 and in Fig. 3.9), while the dynamics of the basin and the local surface wind stress pile up water against the shore. Note that approaching the shore, because of momentum balance, the external forcing (radiation stress and surface wind stress) must be counterbalanced on smaller depth, which implies steeper sea level gradients towards the shore. Besides the rough surface due to wave breaking increases the surface drag, leading to an increased overall effect of the, albeit slightly reduced, wind speed. Of course this is reflected in a positive feed-back on the waves and the surge. This is negligible when breaking is only at the shore (but still relevant for coastal aerosol), but it may become relevant if the bottom slope is very mild and the bottom induced breaking appears kilometres offshore. See in this respect the example of Venice flooding in the following sub-section and in Fig. 3.12.

3.2.2. *Implementations with wave parameterizations illustrative examples of where in the world the just described couplings have been applied*

Having presented the main (but certainly not exhaustively) aspects of the physics involved in the full coupling of the ocean interior, surface waves and the atmosphere (with a keen eye on wave modelling), it is now time to present an overview of where and how such coupled systems have been applied for enclosed seas .

Several one-dimensional mixed layer models have appeared that incorporate wave-mixing parameterizations, in particular Stokes production and wave breaking (Rascle et al., 2006; Bakhoday-Paskyabi

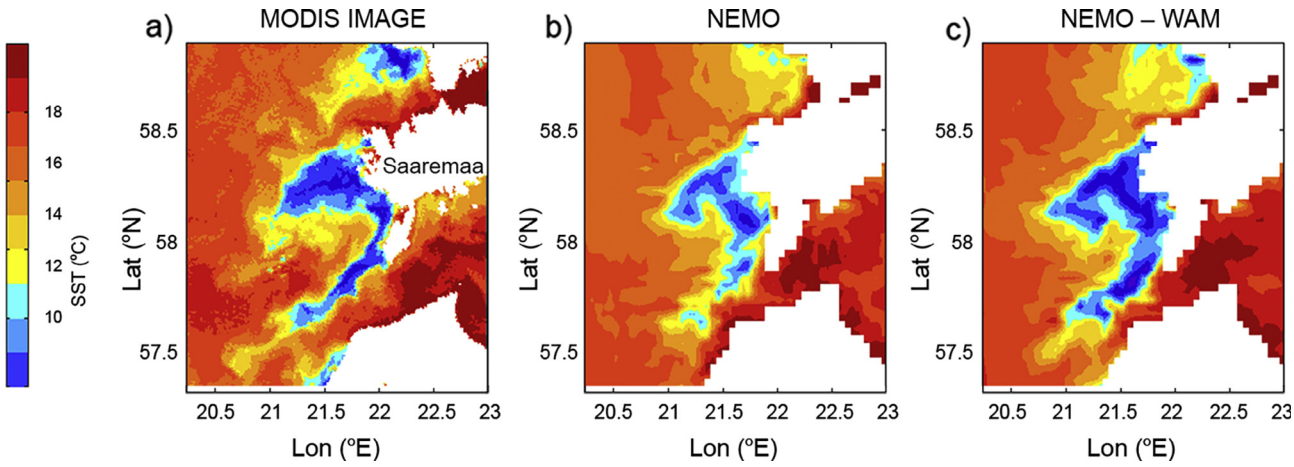

Fig. 3.11. Upwelling in the Baltic Sea, off the coast of Estonia. Panel (a) satellite Modis image, (b) and (c) uncoupled and fully coupled runs respectively.

et al., 2012; Janssen, 2012). Kantha and Clayson (2004) revised the second-moment turbulence closure model to account for Langmuir Circulation (LC) effects by adding the Stokes drift production term to the TKE equations, and Harcourt (2013, 2015) developed a second moment closure model of Langmuir turbulence.Despite extensive numerical investigations of Langmuir circulation and its turbulent mixing based on Large Eddy Simulations and one-dimensional ocean vertical mixing models, only a few studies have coupled and tested LC, breaking, and non-breaking wave effects on three-dimensional ocean models, let alone coupled models of the atmosphere and ocean (Li et al., 2016, 2017). Fan and Griffies (2014) implemented and assessed the impact of parameterized wave-induced mixing on global climate simulations. Li et al. (2016, 2017) incorporated WAVEWATCH-III into the Community Earth System Model (CESM) and found that implementing Langmuir turbulence improved the shallow bias of the mixed layer depth in long climate integrations. Recently, Breivik et al. (2015) implemented a fully coupled atmosphere-wave-ocean global numerical weather prediction model by coupling the operational ECWAM wave model (Janssen, 2004; Bidlot, 2012) to the NEMO ocean model component as part of the ensemble suite of the Integrated Forecast System (IFS) of ECMWF. They implemented mixing by wave breaking, Stokes-Coriolis forcing and wave-modulated stress in their model, and demonstrated the vital role of correctly including wave mixing for reducing the SST bias.

The wave-related processes described above are quite varied in their impact as well as the complexity involved in their implementation in ocean models. Two model systems in particular have been used to test these processes, namely the Regional Ocean Model System (ROMS, see Shchepetkin and McWilliams, 2005, Warner et al., 2008a; Warner et al., 2010) and the Nucleus of European Modelling of the Ocean (NEMO) model (see Madec, 2012). Other model systems also in regular use include POM (Blumberg and Mellor, 1987). ROMS has been extended to incorporate the vortex-force formalism by Uchiyama et al. (2010) and through the COAWST coupled WRF-SWAN-ROMS setup it has been used extensively for near-shore applications in which wave effects play an important role (Kumar et al., 2011, 2012). An implementation of the Stokes-Coriolis force in integrated form (impulse) was presented by Röhrs et al. (2012). A new fully coupled system for the U.K. has been recently completed by Lewis et al. (2018).

The NEMO model has also recently been extended (see Breivik et al., 2015; Mogensen et al., 2017) to include Stokes-Coriolis forcing as a body force in the momentum equations, a modification of the flux of turbulent kinetic energy following Craig and Banner (1994) and Mellor and Blumberg (2004), but with fluxes estimated from the EC-WAM wave model component of the forecast system of ECMWF (Janssen, 2004). The momentum flux from the atmosphere to the ocean is also modified by the wave field. The impact has been found to be quite significant regionally, up to 0.5 K, caused by the Stokes-Coriolis force and the momentum flux. The injection of turbulent kinetic energy has an even greater effect, although this is in part due to the fact that NEMO has too vigorous mixing in its default setup, and the impact when compared to a law-of-the-wall boundary condition is on the order of 0.5 K in the extra-tropics. Recently, Alari et al. (2016) have shown that the impact of these three wave effects is also significant in enclosed seas. In the case of the Baltic Sea the impact on upwelling and downwelling from Stokes-Coriolis forcing reached 0.3 K. The impact of the wave field on water level has also been found to be significant in storm events in the North Sea. Here the effect is mainly due to the increased stress from growing waves (rougher sea surface). This leads to enhanced drag and with it increased water level. This was first demonstrated by Mastenbroek et al. (1993) and recently demonstrated for two intense storms in the autumn of 2013 by Staneva et al. (2017) using a regional NEMO model.

Are we in the position to draw a solid conclusion on the basic physics of ocean, waves and atmosphere interactions? The situation is not yet crystal clear. Although as we have seen quite a number of studies have addressed the modelling and parameterizations of the coupled system (Babanin et al., 2009; Fan and Griffies, 2014; Breivik et al., 2014, 2015), it is still unclear which of the wave-related effects are the most important for the oceanic mixed layer. Recent investigations of the mixed layer depth biases have revealed that surface gravity waves do deepen the thermocline. The question is how. Wave-

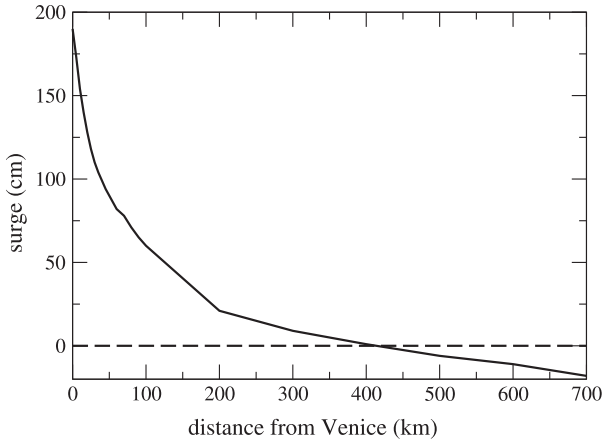

Fig. 3.12. Surge along the Adriatic Sea (see Fig. 2.3, panel b) at the peak of the storm of 4 November 1966. The horizontal scale shows the distance from the Venice coast. The estimate is 2 km offshore (6 m depth), at the end of the jetties bordering the entrance to the lagoon.

turbulence interaction, and in particular Langmuir mixing, breaking waves, and non-breaking gravity waves (Qiao et al., 2004; Babanin, 2006; Babanin et al., 2009; Huang et al., 2011) all appear to be candidate mechanisms for explaining the lack of mixing. These processes enhance the turbulent kinetic energy throughout the mixed layer and thus influence both the depth of the mixed layer and the near-surface temperature (Janssen, 2012; Breivik et al., 2015). Most likely all of them act in this direction, but their relative importance remains to be determined. It appears clear that more work is needed to get a proper representation of wave-induced effects in ocean models.

3.2.3. Practical examples

cases where the coupling turned and remain essential for the correct results

As in Section 3.1 we provided examples for the wave-current interaction, we describe here a few cases where the final results imply a more or less direct interaction with also the atmosphere.

3.2.3.1. Upwelling in the Baltic Sea. Towards the end of the previous section we cited how in the Baltic Sea (Alari et al., 2016) full consideration of the impact of the wave effects on the local circulation and atmospheric modelling led to a manifest upwelling in the coastal areas. The corresponding results are shown in Fig. 3.11. Panel (a) shows an upwelling, documented by a Modis image, off the coast of Estonia. Panel (b) is the control run without the coupling with waves and the atmosphere. The role of coupling is evident in (c), with a much stronger upwelling, much more similar to the one detected by the satellite.

3.2.3.2. Deep sea water formation due to cold outbreak. In the winter of early 2012 an exceptional inflow of very cold air hit the Northern Adriatic Sea (Fig. 2.3, panel b) with sustained north-east bora wind for more than one week. This gave the chance to investigate how, perhaps counter-intuitively; waves can play an important role in the definition of also deep water properties. In the Adriatic Sea the process is known. Therefore the forecast and the duration of the event led to the organization of a devoted campaign that, together with the oceanographic tower “Acqua alta” (panel d), provided a wealth of detailed and distributed data. At the same time a full two-way coupled wave, atmosphere and ocean model system was implemented using, and comparing the results with, all the measured data. Improvements in the turbulent heat fluxes forecast using the atmosphere-ocean coupled run were related with the dynamic sea surface temperature brought into the system by the ocean model, while full coupling with also surface waves further improved the simulations and the results with respect to the in-situ measured data acquired at the tower. Benetazzo et al. (2014) and Carniel et al. (2016b) provide a full description of the model set-up and related results. The coupling turned out essential from different points of view. Coupling waves and currents increased the latter by $0.15\,m\,s^{-1}$, in so doing slightly reducing the wave heights. At the same time the enhanced (because of waves) turbulent heat fluxes ($+45\,W\,m^{-2}$, about 10% of the average heat budget) led to an increased turbulence in the atmospheric surface layer. In turn (Abdalla and Cavaleri, 2002) the higher gustiness level led to a more effective and rapid growth of the wave field that, via the strong breaking, was fed again to the current. The evolution of the mean kinetic energy in the basin confirms that the explicit inclusion of wave effects in atmospheric-ocean interactions provide a different dynamical characterization of the overall basin. Coupling ocean, atmosphere and waves (at the limit also in only a sub-region of the model domain) may significantly modify the water circulation and characteristics in much larger areas in spite of their apparently small extent of influence. This can strongly affect the volume of water involved in the cooling process within a whole semi-enclosed basin, its density and kinetic energy, conditioning its potential contribution to deep-sea ventilation. In the event of winter 2012 the cold water produced in the northern part of the basin moved southwards in a narrow flow along the Italian peninsula, till reaching in the southern part the deep part of the basin, flowing then out through the Otranto Strait into the Ionian Sea (Fig. 2.3) to become part of the local deep water.

3.2.3.3. Cyclogenesis. A similar process, but on different scale and depth, happens especially in autumn in the north-western part of the Mediterranean Sea (Fig. 2.3, panel a). In this period of the year the first northerly storms bring cold energetic air over the still warm local water. Granted the differences between less (Northern Adriatic) and more deep (Gulf of Lyon) conditions, the process is similar to what just explained in the previous example. Very strong waves enhancing the current, very large turbulent heat fluxes with consequent gustiness (the local mistral winds are famous for their violence), hence increased active generation, more white-capping, feed-back on current, etc. Of course there is a strong cooling of the surface water and heating of the atmosphere. This is where, given the scale, the main difference arises. The strong heating of the lower layers of the atmosphere leads to the generation of an intense low pressure system (cyclogenesis) with further implications for the local wave and current fields. Incidentally, quite often these low pressure systems are the ones that give rise to the conditions favourable to the Venice floods in the Adriatic Sea (see below).

3.2.3.4. Medicanes. The high surface temperatures of the Mediterranean Sea can lead to the formation of intense low pressure systems with some of the characteristics of hurricanes, hence the name assigned to these systems: Medicanes. Although not particularly intense in terms of minimum central pressure, the associated wind speeds can be rather strong. A particularly intense one occurred between 4 and 7 November 2011 in the western part of the basin. The minimum pressure was estimated at 985 hPa with wind speeds up to $27\,m\,s^{-1}$. Ricchi et al. (2017) have done a careful analysis of the system. In particular they explored in detail how sensitive the results were to (1) the coupling, first between ocean and atmosphere, then also the inclusion of two-way wave effects, (2) different parameterizations of the sea surface roughness. The positive SST anomaly ($+1.5$–$3\,^{\circ}C$) in the area turned out essential in the development of the cyclone and in its evolution. This was crucially dictated, in the model results, by the SST evolution and consequently by the level of coupling. The comparison of the SST recorded on a buoy in the Gulf of Lyon shows clearly that the best result (i.e. the most intense cooling during the Medicane) was achieved when taking into account the increased heat transfer from the sea to the atmosphere due to the presence of waves. This corresponded also to the lowest modelled minimum pressure. Notwithstanding the increased strength of the system, this did not lead to also a further increase of the estimated wind speeds because of the increased friction at the surface. However, the combination led to larger wave heights.

A remarkable and instructive finding came from the use of three different parameterizations of the sea surface roughness, based respectively on wave steepness H_s/L_p and (two) on wave age u_*/c_p. While the related expressions (see Ricchi et al., op.cit., for a full discussion) have been derived in what, relatively speaking, we can call ‘normal conditions’, the use in a hurricane may lead to contrasting results. The reason is the strong spatial variability of the wind and wave conditions, and consequently the possible step, rather unnatural, distribution of the results. Ricchi et al. (op.cit.) even suggest to make some preliminary tests in practical applications to verify which a parameterization may appear as the most suitable for the situation of interest. This strongly suggest we still have a long way to go before having a good physical description of the interplay between wind and waves.

3.2.3.5. Hurricane Katrina. In the previous Section 3.1.4 we had shown, among other examples, the wave, wave set-up, and surge maximum conditions in a large area around and to the east of the Mississippi delta.

It is this last field (Fig. 3.8, panel c) that we recall to illustrate in a dramatic case one aspects of the physics we described at the end of Section 3.2.1. It is hard to imagine the wave conditions in the shallow zone just east of the delta, where maximum wind and waves pushed waters towards the coast. The crucial point is the roughness of the sea surface, the consequent increase of the surface wind stress, the increased local depth (surge), hence the higher waves closer and closer to coast and in the previously dry land.

3.2.3.6. Venice flood. In one of the examples in Section 3.1 we have shown the wave set-up during the 1979 storm whose flood ranks second in recorded history (since 1872). The number one was 4 November 1966. No measured data exist because the tower in Fig. 2.3, d was not yet there and all the tide gauges at the coast were destroyed (as most of the jetties). The official level was recorded as the floating mark left on the walls of Venice. Cavaleri et al. (2010) made a careful reconstruction of the event. The resulting profile of the sea level at the peak of the storm along the whole basin is in Fig. 3.12. The dramatic increase of the level when moving in shallower and shallower water, when approaching the northern end of the basin, is clear. Note that also here the target at the left was the entrance to the lagoon, the relevant information for Venice. Two kilometres further on, at the actual beaches, the level was estimated at least 0.5 m higher.

3.2.3.7. Unbalance in the Venice lagoon. Remaining in the same area, the Venice lagoon (Fig. 2.3, panel c) is 50 km long, 10 km wide, very shallow, with an average depth of slightly more than one meter, with sparse deeper canals. When the north-east bora wind blows with high speed, the water at the southern end of the lagoon, where a small town is located, is about one meter higher than in Venice. The reason is again the interaction of the short choppy waves with the atmosphere. In the lagoon the bora-induced waves are permanently very “young”, with vigorous breaking. Consequently there is a high drag, hence the pile-up at the southern end. This notwithstanding the (partially) reduced wind speed (because of the enhanced surface drag) as proved by direct comparison with the parallel data recorded at the external station close to the sea and most of all those from the oceanographic tower.

4. Wave data assimilation in enclosed seas

J.Portilla-Yandun, S.Abdalla, J.-R.Bidlot, Ø.Breivik, L.Cavaleri
j.portilla@ymail.com

where we outline the need for an effective and optimized data assimilation system in the coastal and enclosed seas, and we describe, on the base of the available information, the best approach for both long term and operational forecast activity

4.1. The situation to deal with

where, before going into the actual methodology, we frame the problem to be faced

We should never forget that the models we love and use so much are always, and still are, just models. Irrespective of the recent model improvements, they are still far from perfect. As such they provide estimates of the quantities of interest, estimates that by definition are prone to errors. Where possible, we make use of the corresponding measured values, where and when available, to get from the two combined information (measured data are estimates as well, see Section 2.5) the best overall estimate we can get. This is essential both for long term hindcast as for the best picture of the situation to start from for the next forecast.

Having outlined the general idea, we soon find that the practical application faces different problems in the open ocean and in the enclosed and coastal seas. From a very general point of view there is no doubt that the performance of open sea modelling has outpaced the one where the coasts play their role (after all, this is the reason for this paper). There are many reasons for this. The orography affects the local meteorology, hence the wind fields we depend upon (see Section 2.1). The geometry of the basin, limited depths, coastal currents, stronger coupling, etc., all contribute to make the task more complicated with likely greater errors. On the other hand this, the coastal environment, is where most of our interests are concentrated. Both these factors highlight the need for an approach capable to optimize the available information making use of the best practical and theoretical approaches. Of course this leads us to data assimilation as the natural approach to achieve this.

Open ocean, in practice global, wave modelling has made use for a quarter of a century of the information available via satellite altimetry. Within its limitation of providing only the H_s integral parameter, the ubiquitous information from altimeters has played, and still plays, a fundamental role in improving the quality of our model results in the open oceans. However, some of the characteristics of this ubiquity show their limit in enclosed seas. Fig. 4.1 shows the performance of the ECMWF wave forecast system for different environments.

In panel a there is an obvious difference between the wide open basins (e.g., INDIA and CRB) and the enclosed seas (e.g., MEDSEA and KOREA). The overall result is made even clearer in the other three panels, b, c, d, where we show the same results, but specified per altimeter, area and time. Panel b reports the performance on the globe (for all the available buoys), c only the tropical areas, d for a typical (North Sea) enclosed (but not so enclosed) basin. The different extent of the lasting information is evident. Of course this has to do with the time a wave system takes to cross a basin and with the dominance of wind sea and/or swell. However, a more fundamental role is played by the ‘only integral parameter’ information mostly available from altimeters and their discontinuous and selective passing over an area of interest. This becomes crucial in the coastal and enclosed sea environment.

Panel 4.1.a shows the percent reduction in standard deviation error, following assimilation of H_s data in different areas and basins. The reference corresponds to the ECMWF global wave model without any wave data assimilation. Three analysis experiments were carried out. (1) The periods from June to September 2014 and (2) from November 2014 to February 2015 assimilated Jason-2, Cryosat and Saral data and were based on the 40 km global model. (3) For the period June–July 2016 the 28 km model was used, assimilating also the Jason-3 data.

Luckily another source of information is frequently available. Wave measuring buoys, still within the limitations outlined in Section 2.5, provide the most complete information presently available. Besides making available, if arranged for, the actual time series of the single waves at the measuring position, they provide also the full 2D spectrum with all the information that can be derived. Besides wave buoys are available (see, e.g., Fig. 2.9) not only as large networks, but as specifically located instruments for a specific operational purpose wherever, e.g. harbours or operational rigs, the information needs to be available ‘now and there’. Both the volume of the available information (at least two orders of magnitude more than the single integral parameter) and the crucial role of good quality information that is often required for specific applications, imply a very sound and complete approach to data assimilation, capable to use not only the latest available information, but also the one associated to the geometry and characteristics of the basin. This is what we describe in the following sections.

4.2. State of the art

where we point out the limitations of the most used approaches

In their traditional approach, altimeter and, where available, buoy data have been used only with their synthetic information of significant wave height. Of course this approach hides the true information, i.e. the complexity of the actual distribution of energy among the various

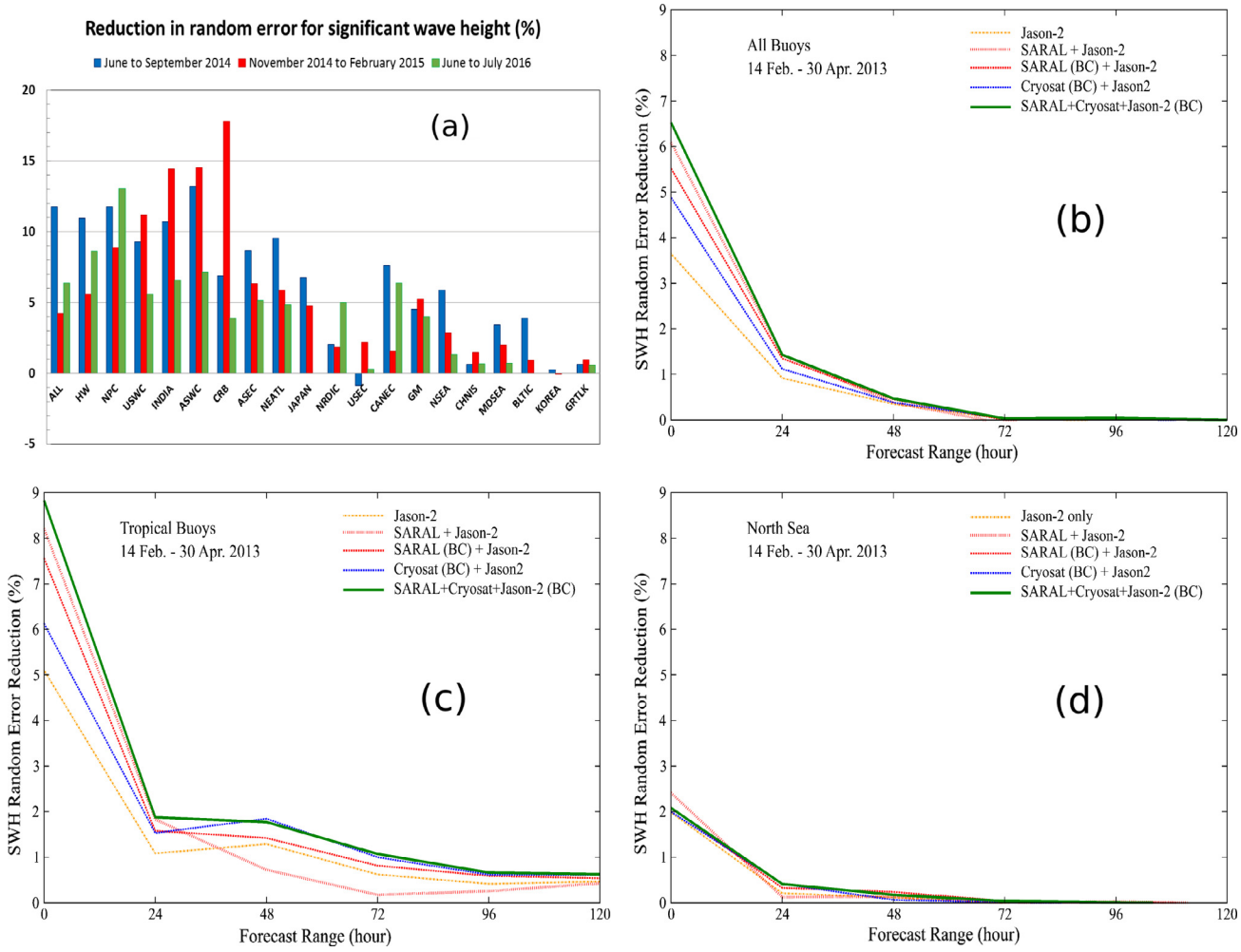

Fig. 4.1. (a) Standard deviation error of the ECMWF model significant wave height. Reduction of error (positive indicates improvement) following assimilation of buoy data. The various areas are detailed in Table 4.1. Panels b, c, d show the reduction of standard deviation error when assimilating different altimeters data for all buoys, tropical areas, and the North Sea respectively.

frequencies and directions. While in the inner seas a 2D spectrum will display in general less wave systems (typically wind sea and swell) than in the ocean, we need to consider that the smaller the basin the stronger will be in general the spatial and temporal gradients that characterize the environment. Time gradients, i.e. rapidly changing conditions (see Section 2.1), point to the need of a more detailed (in spectral space) and frequent information if this is to be provided to harbours or general users. Of course this pushes the choice towards devoted in situ measurements capable to provide the required full spectral (f-θ) information. This approach, in most of the cases a buoy, has several advantages. First, a good knowledge of the local wave climate (that we can derive from previous modelling) allows to choose strategically the right monitoring position that, granted the modern technology, can continuously supply data in real time. Second, in situ instruments have more flexibility in the variables to be measured. Nowadays regions with high marine activity, hence requiring effective forecast systems, are often covered by dense monitoring networks (see, among others, Bertotti et al., 2014; Alfieri et al., 2012; Alves et al., 2014; Landsea et al., 2012). Therefore the potential exists for fully exploiting the available information to improve the inner sea and coastal (albeit short term) forecasts.

During the last decades several attempts have been made to implement wave DA routines in enclosed seas and nearshore scenarios. Good examples are provided by Voorrips et al. (1997), Siddons et al. (2009), Portilla (2009), Veeramony et al. (2010), Waters et al. (2013), Rusu and Guedes Soares (2015), Wahle et al. (2015), Panteleev et al. (2015). In most of the cases the data have routinely been assimilated using a simple Optimal Interpolation scheme with static error covariance specification (e.g., Abdalla et al., 2010). In general there are a couple of bottlenecks in these developments. The first one relates to the fact that improvements in DA are understood (or misunderstood) as adopting more complex optimization algorithms (e.g., 3DVAR, 4DVAR, Optimal Interpolation, Kalman filters). However, environmental DA in general has to deal with a more basic issue which is how to combine a full 2D background field with single point measurements. In practice in DA one has to produce first the full 2D observational field that is then combined with the background field by the optimization algorithm. This first task is usually embedded in the whole DA algorithm as it will be illustrated below. As mentioned above, the second limitation is that the actual model variable is the wave spectrum. The significant wave height (or wave period) is only a bulk parameter, with a two-dimensional matrix reduced to a single scalar, and this is a very drastic reduction of information. In fact, for a given H_s there are infinite possibilities of energy distribution, and this produces uncertainties in both ways, first when obtaining the 2D H_s background field, and then when the analysed field is transferred to the analysed spectra. For DA in general, but also specifically for enclosed and coastal seas, a more complete information is required than what frequently used. We claim that only a fully spectral information can satisfy the practical requirements of coastal and inner seas managements and engineering. It is in

this direction that we concentrate our effort in this chapter. Here we advocate for a DA algorithm consistent with the modern third-generation spectral wave models and spectral observing techniques. This is explained in the following section.

4.3. Towards the development of a spectral data assimilation scheme

where we outline the best approach for the problem of interest

In a Bayesian framework, data assimilation is the process of combining modelled and observed data in such a way that the resulting output is more accurate than the two single or simply combined sources (see e.g., Evensen, 1994). A good wave DA system must be consistent with (a) the statistical properties of both observations and model output, (b) the model dynamics, and (c) the local wave conditions. These requirements are explained in more detail below.

(a) By statistical properties of the data, we mean their associated errors. We typically tend to regard observations as the ground truth, against which model is evaluated. In fact, observations can also be, and usually are, subject to different type of errors, like measuring errors as such, or instrument misrepresentation of the physical phenomena, or shortcomings of the methods for processing the signals, among others (see Section 2.5 for an extensive discussion). So more appropriately, measurements have to be regarded as a mere estimate of the truth with an associated standard deviation, exactly how model data have to be regarded (e.g., Janssen et al., 2007). Under this premise, the task of DA is statistically simple (in principle at least), and consists of producing a single output from the corresponding inputs and their (model and measurements) associated errors (e.g., Daley, 1993).

(b) For a DA system not to be too cumbersome, it needs to run along harmonically with the model dynamics. To achieve this, a few things need to be taken into account. The first is that the model variable to work with is not the significant wave height H_s, but actually the directional wave spectrum. Failing to consider this puts us in the very intricate situation of having to correct with a single parameter a variable that has typically a few hundreds degrees of freedom (typically nθ = 24 to 36 directions and between nf = 25 and 36 frequency bins). In doing so, we are most likely forced to make assumptions that override the physics represented by the model (e.g., Lionello et al., 1992). The second important consideration is related to the model structure. To avoid numerical instability, the advection terms in the action balance equation are run with a time step that is consistent with the speed of waves over the computational grid. On the other hand sink and source terms run sequentially, and with a different time step tuned to the typical rate of change of the parameterized physical processes (e.g., Komen et al., 1994; Holthuijsen, 2007). From this perspective, DA corrections behave to the model precisely as a sink-source term, so they have to be operated accordingly.

(c) A DA scheme can only be effective if it takes into account the physical processes involved in the wave evolution and propagation. In general, the wave climate can be characterized by the local wind-sea conditions and swells from distant storms. However, in enclosed seas, due to the limited dimensions of the basin, the distinction is often not so neat as in the open ocean. The time variability, recurrence, and magnitude of events are also fundamental aspects. In enclosed seas, wave conditions are typically low or moderate, but extreme events can be very destructive. They are episodic with recurrence generally associated to specific seasons or meteorological conditions (e.g., winter storms). Therefore, a precise knowledge of the local wave climate in terms of the 2D spectrum should be the starting point.

The large spatial gradients of wind and wave fields often found in enclosed seas, and in other specific near-shore scenarios, add other challenging features for local wave modelling. These large gradients arise for instance from very irregular bathymetries and topographies, with offshore, slanted, or funnelled winds (see Section 2.1). In this regard, it is important for the DA system to capture the geographical details of covariances between variables in complex topography, otherwise we would be trying to correct data at remote positions with unrepresentative measurements (Kalnay, 2003, pp. 156–157). These requirements are hard to assess when only integrated parameters of the spectrum are considered.

Finally it is worthwhile to mention that, for all the reasons till now discussed in this paper, it is frequent o have systematic errors in enclosed sea wave modelling. It is especially in these case that DA becomes an essential tool to improve the quality of the results and, last but not least, to help analysing the situation.

We illustrate some of these aspects by analysing the main components of a generalized 3DVAR algorithm, in which the DA task is set-up as an optimization problem, where the differences between model and observations are to be minimized (e.g., Kalnay, 2003, eq 5.5.8). This is expressed by the set of Eqs. from (4.1) to (4.3).

$$\nabla J(S_{f,\theta}) = B^{-1}(S_{f,\theta}-S^{B}_{f,\theta}) + H^{T}R^{-1}H(S_{f,\theta}-S^{B}_{f,\theta})-H^{T}R^{-1}\{S^{O}_{f,\theta}-H(S^{B}_{f,\theta})\} \tag{4.1}$$

$$\nabla J(S^{A}_{f,\theta}) = 0 \tag{4.2}$$

$$S^{A}(\psi)_{f,\theta} = \alpha S^{B}(\beta f,\theta \pm \delta) \tag{4.3}$$

where J represents the cost function to be solved, S is the wave spectrum, f and θ indicate that the differences are evaluated over the discrete spectral domain of frequency and direction, the superscript B indicates background (model) grid points corresponding to both observation and remote grid points inside the assimilation domain, O refers to observations, and A to analysis ($S^{A}_{f,\theta} = S_{f,\theta}(\psi)$), where ψ is the set of tuning parameters, composed of α, β and δ, with the aim of correcting energy, frequency (or period), and direction respectively. **H** is the observation operator, which interpolates and transforms gridded model variables to observed variables. **R** is the observation covariance matrix, considered diagonal here, meaning that observations errors are uncorrelated. In turn **B** defines the weighting factors over the spatial domain computed from the error correlations associated to $S^{B}_{f,\theta}$ (namely, the background error covariance matrix). In this scheme, the two most important components of the system are ψ and **B**. ψ indicates how the model spectrum is operated in order to obtain the "analysed" spectrum. **B** relates to the weight the single observations have at the remote surrounding points inside the assimilation domain.

Dealing with all the (nf × nθ) components of a 2D spectrum is not practical. A solution is suggested by the fact that these components are not independent. Indeed the wave conditions at given point and time are in general the superposition of different wave systems, each one generated at different time and in a different area, each one with its own typical (mean) frequency f_m and (mean) direction θ_m. In practice a 2D spectrum is the superposition of these, to a large extent, independent systems (or their numerical equivalent, partitions) that for many practical purposes can be represented by their characteristic f_m and θ_m, plus of course energy E_m. For many practical purposes, including DA, it turns out that, without any practical loss of accuracy, rather than the single $nf \times n\theta$ components it is convenient to consider a limited number of wave systems or spectral partitions. Given a long time series of spectra, hence of its partitions, it is possible to make a statistics of their basic characteristics, e.g. f_m and θm (plus E_m of course). This statistics, which too is defined on the (f-θ) space, leads to a distribution (occurrence probability) that will obviously reproduce the dominant, i.e. more frequent, wave systems at that location (examples will soon be given). In practice we obtain a representation of the local wave climate, a sort of signature of the long term wave climate at that position. Of course, if the spectra are available at each grid point, the

statistics, i.e. the occurrence probability, can be evaluated for each single point, which opens the way to related correlations. Portilla-Yandún et al. (2015) provide a detailed explanation of the procedure and of the information that can be derived.

The different physical characteristics of each system (or partition) imply that the relationship, between its value at the measurement location and the ones at the model grid points where data assimilation is to be performed, varies from system to system. In a more formal way each system will require not only different correction measures (ψ), but it will also have in general different spatial domains (**B**). The elements of **B** can be computed using the definition of the covariance (equation 4.4), by means of the computation of the correlation coefficient ρ, quantified here by means of the coefficient of determination R^2 (Eq. (4.5)), and the analysis model of Eq. (4.3). This approach is explained in detail in Portilla-Yandún and Cavaleri (2016).

$$\rho_{i,j} = \frac{\langle \sigma_i \sigma_j \rangle}{\sigma_i \sigma_j} \tag{4.4}$$

$$R^2_{i,j} = 1 - \frac{\int_\theta \int_f [s^T_{f,\theta} - s^A_{f,\theta}]^2 df\, d\theta}{\int_\theta \int_f [s^T_{f,\theta} - \overline{s^T_{f,\theta}}]^2 df\, d\theta} \tag{4.5}$$

Here the angle brackets indicate the error covariance between the assimilation point i and the remote point j, σ are the error standard deviations, and ρ is the error correlation coefficient. A typical approach is to use a sufficiently long hindcast (one or better a few years) of the spectral wave conditions in the area of interest to derive the information to be then used in operational forecast and DA. The error standard deviation in (4.4) can be estimated for instance by comparing independent wave data sets, e.g. via the triple co-location method, as shown, among others, by Janssen et al. (2007). R^2 is the coefficient of determination, the numerator quantifies the differences between the true spectrum T and the analysed spectrum A. The denominator is the normalizing factor in terms of the true spectrum. This procedure is illustrated with examples in the North Sea and Lake Michigan given in the two following sections.

4.4. Examples

where we provide two rather different, both representative, examples of the approach we suggest as the best solution

4.4.1. The North Sea case

The North Sea is a semi-enclosed basin about 1000 × 500 km across. It is widely open from the north flank to the North Atlantic, so swells originated in that area regularly enter the domain. Northerly winds are also very frequent, therefore the northerly wave systems are typically characterized by a mixture of locally generated waves and swell (Reistad et al., 2011; Aarnes et al., 2012; Semedo et al., 2015). Extreme conditions related to northerly waves might occur in combination with low pressure meteorological fronts leading also to storm surges. At its southwest corner, the North Sea is connected to the Atlantic through the English Channel. However, the channel is too narrow and partly shallow for ocean swells to penetrate, but the geography allows south-westerly winds to blow over a relatively long fetch, and consequently waves with this direction are also important in the domain. Other less frequent situations can be found specially related to wind blowing from different directions. In socio-economical terms, the southern North Sea is a very active region and hosts important maritime activities such as oil extraction and harbours as Rotterdam (see Section 2.6.3), Antwerp, and London. Waves in the area are forecast by different centres, and they are extensively monitored with buoys and radars networks (see, among others, Wolf et al., 2011; Maresca et al., 2014; Behrens, 2015).

For the present purposes and to illustrate the capability of the method we focus our attention on the area of the Dutch oil platform K13 in the southern North Sea. We use the data from the close-by buoy as potential source of information for operational application and, at the start, to define the wave climate of the area. The analysis of the locally recorded wave spectra leads to the results shown in Fig. 4.2. In panel a we see the local mean spectrum, dominated by a south going low frequency system (at 180°), and a north-east going system (50°) with a more wind sea appearance. The distinction between the two systems is even more evident in panel b, where (see the previous section) we report the related model derived occurrence probabilities. If the distribution of panel b were known at all grid points in the surrounding area, we could then establish for each point the corresponding cross assignment with the partitions at the K13 position. This would then allow to use the K13 buoy data for DA in operational applications. Obviously we do not have measured data at all the grid points. The solution is to use the output of a locally run wave model as a proxy for the ground truth. Note in this respect that, granted the unavoidable approximations, the model spectra are a more complete and suitable information than the one derived from a buoy (where approximations and sampling variability are always present). For the present example we use a one-year dataset of spectral output from the WaveWatchIII model (Tolman et al., 2013), which is used as a proxy for the ground truth.

The model data come from an *ad-hoc* implementation in which the spectral output has been saved for every model grid point at three hour interval. The model spatial resolution is 0.1°in latitude and longitude, the spectrum is discretized in 29 frequencies ranging from 0.035 to 0.5

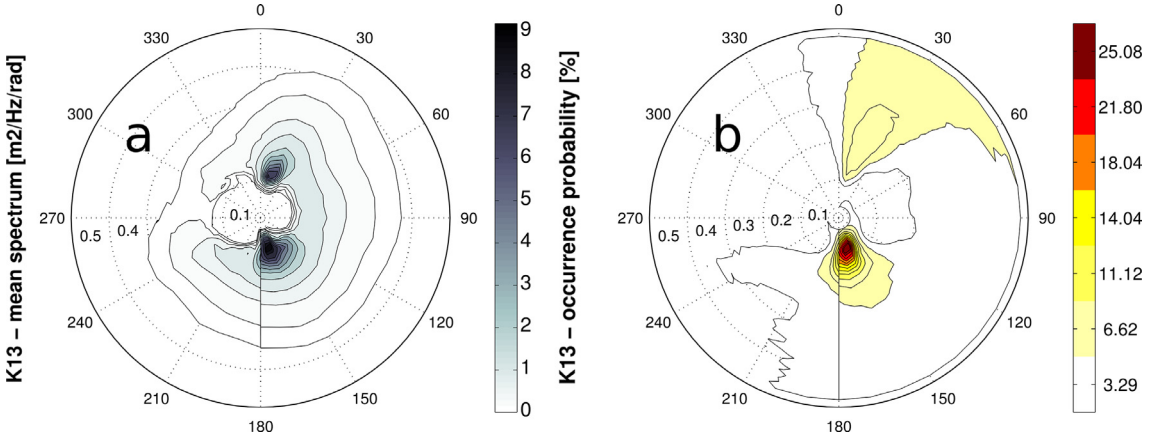

Fig. 4.2. (a) Mean spectrum (from buoy) and (b) occurrence probability (from model data) for the K13 buoy (53.2°N, 3.2°E; see for reference Fig. 4.3). Data are from 2003 to 2007. The radial axis indicates frequency in Hz. Waves are shown in the flow direction (oceanographic convention).

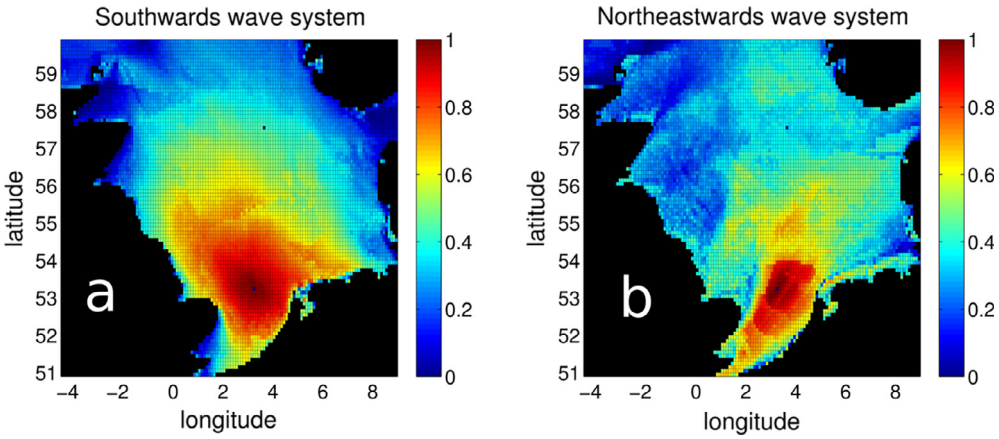

Fig. 4.3. Error correlations in the North Sea, for the two main wave systems shown in Fig. 4.2, for the assimilation point K13 (53.2°N, 3.2°E). (a) System flowing southwards, (b) system flowing north-eastwards.

in 1.1 geometric sequence, with 24 uniformly spaced directions. Bathymetric data are from the ETOPO databases (Smith and Sandwell, 1997). Ice coverage fields and forcing winds are from the NCEP-GFS archive with 0.5°resolution. Boundary conditions come from a 0.5° global grid spatial resolution, run together with the North Sea grid using the multigrid capabilities of WaveWatchIII.

Once a clean signal of the wave systems is obtained on the whole computational domain, we use the scheme given by Eqs. (4.1)–(4.5) to compute the error correlations. For the two main wave systems of K13, the results are shown in Fig. 4.3. It is immediately evident that the two systems have different structures, domains, and magnitudes of the error correlations. The wave system propagating southwards correlates strongly over a larger spatial domain and decorrelates smoothly with distance. Although the errors as such have been calculated on purely statistical bases, physically consistent patterns can be identified.

For instance around the Thames estuary, the correlation reduces sharply because waves from the North are blocked by the East Anglia peninsula. In the southern part around Belgium and the Netherlands, bathymetric effects can be appreciated although bathymetry as such is not explicitly considered in the computations. Its effects appear implicitly from the changes in the spectra, because everything derives from model data.

It is worth stressing that the methodology provides meaningful results also if, to go to the limits, the wave systems change direction, and possibly period, moving across the grid. This because the cross assignment algorithm searches for differentials from point to point. Thus this methodology overcomes the long standing issue on the complexity of cross-assigning wave systems from different sources (e.g., Gerling, 1992; Voorrips et al., 1997; Corbella et al., 2015).

For the system flowing to North-East, strong correlations are found over a narrow strip, oriented more or less along the coastline. The correlation structure in this case is a lot more irregular and decays slowly along the flow direction, showing large values even in front of the Danish and Norwegian coasts. This is because these wave conditions are more associated to the wind fields (i.e., they are wind waves). The spatial irregularities also suggest that for this less frequent wave system the dataset is too short for the purpose, and that we need longer time series to derive more robust results. In any case, these two images give a clear view of the error correlation structures showing that there can be, and are, major differences between the different wave systems. In turn this indicates that they cannot be assimilated considering the same correlation function.

4.4.2. *Lake Michigan case*

Differently from the North Sea, Lake Michigan is a fully enclosed mass of water with characteristic dimensions 500 × 200 km. Although the standard wave conditions range from low to mild, during the autumn months cold northerly and warm southerly fronts may give rise to extreme meteorological and wave conditions, commonly known as the *November gales*, which are in turn (the northerly ones) enhanced by the lake warm waters. Sustained westerly and northerly winds and low-pressure fronts, accompanied by surge, are also common. In socio-economical terms, the lake hosts many transportation, commercial, and recreational activities, and hosts large coastal cities like Chicago and Milwaukee located on the southern shore. For an indication of the wave climate, we use data from the NDBC buoy 45,007 (yellow circle in Fig. 4.5a), and from the ECMWF ERA-Interim reanalysis (Dee et al., 2011). The results of the analysis for both these sources are presented in Fig. 4.4 where some relevant differences between the buoy and model distributions can be seen. From the buoy data (panels a, b) we recognize the two cited main wave components, one flowing northwards, the other southwards. From the mean energy spectrum (panel a) the presence of waves flowing eastwards can also be appreciated, but these waves do not appear clearly in the probability density plot (panel b). This suggests that these waves are not so frequent, but experience indicates that they can be very energetic. On the contrary, in the model distribution these (easterly going wave conditions) are clearly depicted. As for the two main buoy systems, the southwards one appears to be flowing mainly at about 200° in the model (panel d).

For this example (Fig. 4.4 c and d) the model data have been taken from the cited ECMWF ERA-Interim archive, whose resolution (111 km), although here interpolated to 0.36°, is much coarser than desirable for the present purpose, i.e. for an enclosed relatively limited basin. Nevertheless useful results have been obtained. Those for the background error estimates are presented in Fig. 4.5. Here panel *a* shows the bathymetry, the points corresponding to the 0.36° interpolated ECMWF model grid (in magenta), and the location of the buoy NDBC 45,007 (in yellow), assumed as the assimilated observation. Panels *b, c*, and *d* are the computed correlation structures, with respect to the measurement point, for the three main wave systems flowing northwards, southwards, and eastwards respectively.

Several instructive aspects can be pointed out. In general the three wave systems have similar structures, the largest one being associated to one of the eastwards systems, with 0.5 values up to the very north part of the lake. Other physically consistent features can be observed. As expected the largest correlation values in the three cases (0.8 and higher) are observed in the region around the buoy, where this is also favoured by the rather homogeneous bathymetry (about 100 m). To the north of this region, a very shallow feature is present, followed by again deep water conditions (300 m). This discontinuity is clearly reflected into the correlation structure. In the north part the geographical configuration becomes even more complex, including the presence of a

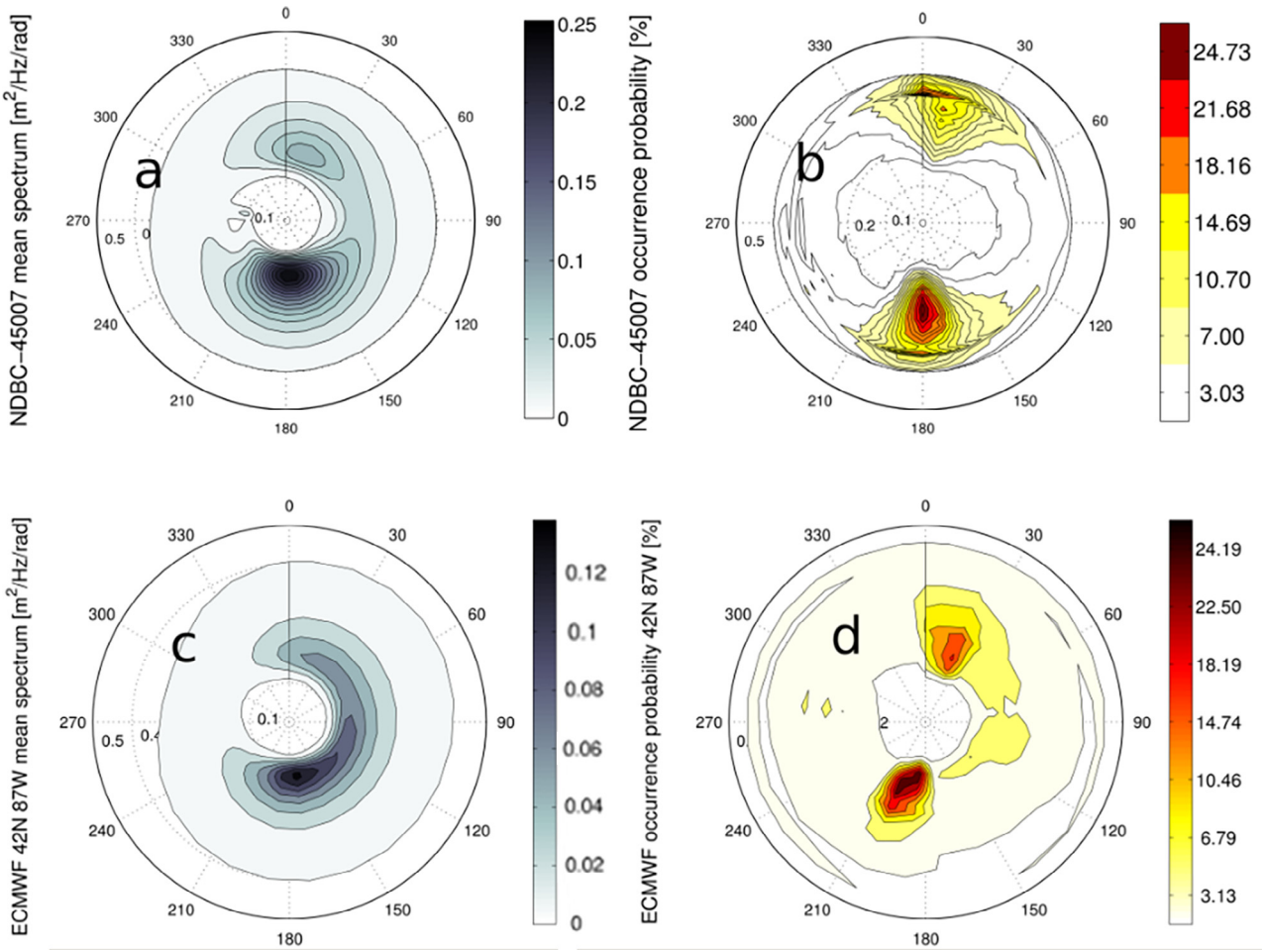

Fig. 4.4. (a) Mean spectrum and (b) occurrence probability for the NDBC 45,007 buoy (42.67°N, 87.0°W; see Fig. 4.5 for its position). Buoy data are from 1997 to 2014. (c) Mean spectrum and (d) occurrence probability for ERA-Interim model data at the buoy location. Model data are from 1979 to 2013. The radial axis indicates frequency from 0 to 0.5 Hz. Waves are shown in the flow direction (oceanographic convention).

mountain range, and this too affects the wind, hence wave, fields. Another orography derived feature is seen in *c,* where the correlation values in the easternmost part of the lake are very low because waves flowing southwards are blocked in the central eastern part of the lake.

This example has been purposely chosen to give an indication about the spatial resolution requirements, which for complex configurations, both geographical and meteorological, like the case of Lake Michigan, can be very demanding. This shows how for these situations a much higher resolution is required to carry out the data assimilation with the due efficiency and positive results. Note how a preliminary analysis of the background error and its variability in space can be very useful in planning the geometry of a network of stations to be then used in operational applications.

4.5. Discussion, perspectives, and conclusions

where we summarize our arguments framing the proposed approach within the various systems presently used

If data are locally available, DA provides the best approach to improve the estimate of the situation and of the following forecast in complex modelling situations in enclosed seas. This can be done without breaking the spirit of modern wave models that rely heavily on the physical understanding of the processes. First, we need to see DA as an extra source term that we must design fully on the combination of statistical and physical information and of principles. It is clear therefore that for consistent wave data assimilation, the spectral approach is the way to go. This is not only because wave spectra as such contain detailed information on the different physical processes, but also because, failing to consider the wave spectrum, corrections cannot be properly introduced. Most of the time DA systems based only on integral parameters tend to add noise to the models. Therefore the spectral DA approach implies also the design of DA system. The result is more consistent with the model than the present approaches, which are frequently mere adaptations of methods used in other fields of science as meteorology, where the description of processes and the nature of variables are completely different.

It is important to note that in the literature, when discussing DA in general, the point often arises of whether a particular DA scheme (e.g. OI, 3DVAR, 4DVAR) is superior to the other ones. Once we recognize the fundamental role of background errors in data assimilation, it is clear that this discussion is immaterial because, if the errors of the system and the spectral update approach have not been carefully designed, all these schemes would perform poorly. It is certain that the more requirements we introduce in the cost function, the more constrained the problem is, and therefore better results should be expected (if we have the proper information). Therefore, a more relevant question for operational use is how much we can improve the results by adding complexity (and therefore increasing the computational burden) of the DA scheme. All these difficulties and the advantage of a sound approach are even more manifest in the difficult environment of the enclosed seas.

Two common practices in wave DA implementations are (a) to assimilate integral parameters like H_s, and (b) to parameterize roughly

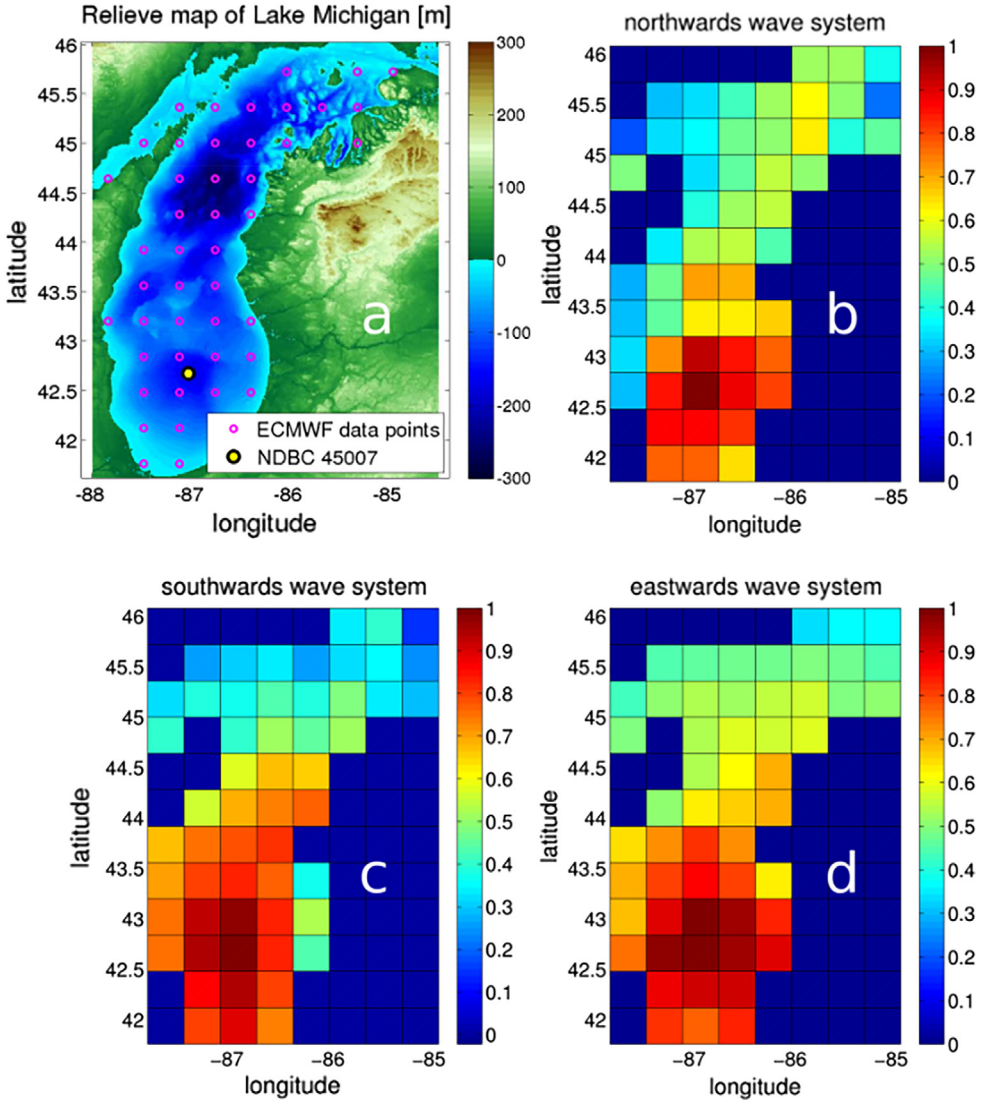

Fig. 4.5. (a) Lake Michigan depth, position of the reference buoy, and grid point distribution. (b, c, d) Background error correlations for the three main wave systems, seen in Fig. 4.4, flowing northwards, southwards, and eastwards respectively. The ECMWF data points in panel a have been interpolated from the original coarser ERA-Interim resolution.

the background error covariance matrix with circular or elliptic functions decaying exponentially with distance. As shown in the two examples, these practices have major shortcomings, because the H_s value as such does not give any specific information on the spectral wave systems active at that specific moment on the area we are considering. Besides, as we have shown, the correlation structures can be rather complex, inherently containing many physical characteristics of the system, which are not only a simple function of distance. Convenient also in the oceans, all this becomes mandatory in enclosed seas and coastal areas.

A common and relevant aspect we have mentioned in operational implementations is the computational cost of DA. Also for schemes like the OI, 3DVAR, and 4DVAR, with the described approach this is not an issue even if several wave systems are considered because the matrices **B** are precomputed and the optimization step is rather simple. Therefore the cost of these schemes will be a small fraction of the model computing requirements. That might not be the case for Adjoint or Kalman filtering schemes for which the costs are of the same order of, or larger than, those of the model, as on the other hand it is the case also for more conventional approaches. However, the wave model run as such is relatively cheap, so with the present computing capacities this aspect should not actually be a barrier. As with any DA system, a more critical requirement in this sense is the availability of near-real time observations.

Some parallel perspectives of wave DA are first the possible feedbacks that can be established with the meteorological model. Wave model errors are linked to a large extent to wind field errors, and this is more the case in the enclosed seas. Hence information about wave model performance brings, or could bring, immediately information on the driving wind fields. In turn this information can be useful not only for the wave model, but also to improve surge predictions. Second is the fact that DA systems, if properly used and interpreted, regularly help to point out deficiencies of the measured data, and this information can be useful to improve measuring methods and processing procedures as well.

5. Summary: the present and the future

L.Cavaleri, A.Sanchez-Arcilla
luigi.cavaleri@ismar.cnr.it

where we summarize the situation of wave modelling in enclosed and coastal seas and try to discuss what the future may hold

Ten years ago a similar paper was issued, discussing the evolving

situation in wave modelling, acknowledging the positive results, but also the problems. After fifty years of established background (the energy balance equation applied to wave modelling was made public in 1957), this branch of scientific engineering had reached, via a sometime discontinuous progress, a solid state of maturity. Of course problems were present and expectations were declared. As it is often the case in a mature science (but beware of unexpected steps in knowledge), much action was then put into applications, strongly driven by the social and economic interests in inner seas and close to coasts. In this paper we have focused on these last applications, pointing out the successes and the problems, the well-defined results and the ones we are still aiming to. Driven by both the wish/need for better results and the love for science, somehow our targets keep moving ahead as we progress. Ten years into this new path, it was time to think and define where we are and which our next actions are going to be. It is also instructive to compare the present achievements with the expectations of ten years ago. Although at the time we had a wider perspective (the open oceans) for most of our considerations, unavoidably our present inner and coastal sea focus has ample superposition with our previous interests, and a comparison is possible. In the following we will first frame and discuss the present situation, before venturing into the future trying to guess the developments we expect and would like to achieve in the next 10–20 years.

5.1. The present

where we frame the present situation, highlighting the advancements, but showing also as some of the expectations of ten years ago have not been achieved

It is clear we have done much progress in enclosed seas. Certainly linked to the strongly increased computer power (hence resolution), it is also associated to remarkable improvements in physics of the processes and modelling. In this respect probably the best step ahead has been the substantial level of coupling between waves and current. The better results in both these models allow an effective coupling with strongly improved results, especially in coastal zones. However, these progresses have been partly limited by the strongest level of interaction in the enclosed seas dictated by the shorter fetches available, hence by the on average higher frequency waves. While what has been achieved is not yet good enough, we have at least a much clearer idea of the situation. It is interesting that this development had been fully anticipated ten years ago. Another good guess was the development and now wide use of unstructured grids to move smoothly from the relatively coarse resolution offshore to the much more refined one where needed, mostly close to coasts. Differences of resolution up to three orders of magnitude between the two extremes are common (but beware of numerics, soon to be discussed).

We had some improvement in physics, but possibly less than expected, at least specifically for enclosed and coastal seas. In this respect it is the increased resolution that is forcing to consider some new aspects previously hidden by the coarser approach. Again the main result has been a much more detailed mutual interaction between waves and currents (the one between waves and wind was operational since the early '90s). Here part of the credit goes to the much improved quality of the meteorological input (an amply anticipated development). However, although here high resolution (order of 1 km or less) local models are potentially available, still in most of the cases potentially important details of coastal winds are not up to the level. Sometime we can guess in qualitative terms what the solution should be, but the model results simply do not provide the satisfactory quantitative reply we aim to.

Still on the physical side of the problem, there is concern about the modelling of the most intense storms. It is not the H_s in itself that is important, but the force with which wind acts on the waves, especially for a young sea. Citing a recurrent example, the extremely intense blowing of mistral or bora over a very young short fetch sea leads to conditions that, if witnessed, make one wonder about the validity of our present approach.

As anticipated ten years ago, there has been a strong development in numerics, and in particular of unstructured grids. This has been a consequence of the need of high resolution close to coasts, especially in case of a complicated geometry of the coastline and bathymetry. Indeed, all the complications of nesting progressively finer grids disappear with the unstructured solution. Of course this comes at a price: the numerics is more complicated and deserves particular attention. A strictly "best solution" does not necessarily exist, the most convenient solution often being case specific. The practical implications are not trivial and can lead to substantially different results. The problem is that in many cases this requires due attention by the user. However, in many cases a model user is just a user, often taking the model as a black box. While often self-organizing checks self-control the system, some sensitivity tests would be very useful, especially if the model value is taken at face value as exact.

Still within the numerical component, but not limited to unstructured grids, there is still an ample use of so-called "limiters" in the integration of the model equations. Their reason for existence is to avoid unphysical results of some of the integrated quantities. While properly used they are justified (a typical non-numerical example is the 0.73 upper limit for the ratio wave height/local depth), we should never forget that, however justified and well posed, the use of a limiter implies a lack of physics or proper numerics on our side.

Having listed the successes, it is only fair to see where our expectations were not, or were only partly, fulfilled.

Bottom processes are still a problem. A good example is given by the just cited (0.73) wave height limit on a certain depth. Much effort has been recently put to improve this limit or definition, now forty years old. However, not much improvement has been achieved. This suggests we really do not have a proper understanding of the related physics. However, for most of the cases the problem is not, within limits, the lack of physical knowledge. We know which are the basic processes at work, but we are not completely sure how they interact (e.g., wave and current induced bottom friction) and, most of all, we often lack the necessary information. This can vary from highly variable geometry and characteristics to, in case of sandy or muddy bottoms, the potentially quick changes of the bottom features. For practical purposes the solution, if such, seems to be a sort of ensemble approach, i.e. different solutions, based on different assumptions, providing the range of possible outputs.

The correct estimate of nonlinear interactions has not shown drastic advancements, more so in shallow water. It has been a repeated refrain that "next generation computers will be so fast that we will be able to use Exact-nl (the related full calculation) in our models". Without exploring the related quantification, the truth is that, whenever a "ten times faster" computer is available, the default action is to increase resolution. So we are still with DIA or similar solutions and there is no perspective of a change of attitude for "next time".

A somehow similar argument, but for different reasons, concerns the fundamentally statistical spectral approach. There has been much debate wondering if it makes sense, as we do with spectral models, to go to spatial resolution shorter than the wavelengths we want to describe. Of course in this case our estimated spectrum has a correspondence only in time, not in space. However, there had been much talking about, e.g. spectra and bispectra, to provide more physical results. While studies continue, for routine practical applications we are still on the traditional ground.

In enclosed and coastal seas, we face a problem with data assimilation. It is clear that the limited dimensions we deal with imply a shorter memory in the system. Therefore, most of the time the focus is on very short forecast ranges. This concerns the distributed information, i.e. satellite data (see Section 2.5). Buoys, mostly close to coast, are deployed either for verification of the incoming wave conditions or

on purpose for operational use (e.g., harbour and marine operations), i.e. for decision making. In general operators have a good feeling of their model performance and also a good interpretation of the discrepancies between model and observations. They do not follow any of the two sources blindly, but they subjectively assess the real situation according to the available information and their experience. Strictly speaking, this is human data assimilation. While the human value must not be underestimated, at the same time we should try to automatize the approach using sufficiently smart systems. The operational system of NOAA-NCEP cited at sub-section 2.6.1 is a good example in this respect. Use in the opposite direction, i.e. for offshore blowing wind, is limited for two reasons. On one hand, as we have seen in Section 2.1, the wind information close to coast is not accurate as offshore; on the other hand there is a limited correlation between short fetch conditions, especially the modelled ones, and the more developed ones in the rest of the basin.

A very positive aspect with respect to ten years ago is the convergence of the models towards a more unified and agreed upon physics. It is a recurring process. Of the various branches offering different approaches, in time one emerges as the best and most satisfactory, where everyone converges. But then we go into deeper details, with different approaches, and from the "winning" branch smaller branches sprout associated to different solutions, and the cycle repeats. This is a healthy process, exploring different grounds. This is the present situation, with substantially similar, but slightly different, physics (possibly coefficients), with a continuous mutual exchange of information and cross-comparison of results. This is a very satisfactory situation, forerunning further advancements.

We have devoted a strong effort to make clear to the user that the data we use to improve or validate our models are just estimates of the truth. Pretty good estimates in most of the cases, but with well-defined confidence limits. On one hand these derive from the random variability of the wavy process. To be practical, the significant wave height derived from a 20 min buoy record has an uncertainty of 6% at 90% confidence. On the other hand, an instrument provides the local truth only with errors, and these errors can be quite significant. This should be taken into account when judging the performance of a model. Incidentally this is one of the reasons while in practical terms the model root mean square error cannot be lower than a certain value.

Somehow this takes us to the last topic of this picture of the present. Most of the validations we do with our model results are based on integral parameters, typically H_s, T_m or T_p, θ_m (with their confidence limits). However, it is amply acknowledged that, although direct and intuitive, most of the time these parameters do not provide by themselves a satisfactory view of the situation. Clearly the best information is provided by the 2D spectrum. This has two drawbacks: (a) the spectrum is not always available, (b) if it is, it has very large (much more than the 6% for H_s) confidence limits, a hardly mentioned inconvenient truth. An intermediate solution is provided by the partition approach, i.e. by identifying in the 2D spectrum the different wave systems that compose it, and providing the integral parameters for each composing system. This will also be the background for the data assimilation that that we discuss in "The future" section.

5.2. The future

where we list the areas where developments and a more intense use of present facilities are expected and needed, and where, although presently not sufficiently considered, we need to put attention in the future

Our look into the future needs to be not only an extrapolation of, e.g., the last ten years. This would be, so to say, a passive attitude. Rather, our analysis of the present situation must also suggest where, following our perceptions of the future needs, we should drive, if however possible, the system in the future, all this within the limits of human attitude and interests.

By and large the basic physics of wave models is considered well established (but see comments below), and it would be natural to think that improvements in the near future will be quite marginal. There are some 'howevers'. First, we still have the problem of white-capping. Modellers may appreciate the availability of a "tuning knob" to drive the model to the best (on average) results. It is interesting that, if we had purely physically specified source functions and the results were not good, in principle we would not know where to act.

On the other hand the dramatic improvements in highly detailed computer simulations of the air-sea interaction processes hint to substantial advances in the understanding and quantification of the involved energy exchanges. Besides the great progresses in experimental and measured characteristics of, and energy involved in, white-capping with the consequent bubble plumes and spray suggest a possible future shift of some of the pressure for better knowledge on the wind input side, for long assumed a strong stronghold of the overall theoretical approach.

Still at a general level, and again not limited to enclosed and coastal seas, there are the attempts to solve the energy balance equation via a full evaluation of the nonlinear interactions with all the implications for the other source terms. While this does not seem to be a realizable target in the near future, it is something that, if happening, would shake heavily the whole system.

At a more fundamental level we should consider the hypotheses that are at the base of our wave energy or action balance equation and wonder if and how we need to modify it to go further. On a broad scale we can question, and explore the limits of, the validity of the linear wave theory at the base of our spectral approach (the fourth-order nonlinear wave-wave interactions are not the full solution). The first and relatively simplest correction can be for inhomogeneous media and to make the advection amplitude dependent. This is obviously also connected to what we call bound modes.

Again questioning the base of the wave action equation we need to realize that this equation is a good approximation to the truth only in deep water. Moving to shallow areas nonlinearities become more important, in reality more than most of us think. There is a diffused belief that, also when accordingly modified, the present formulation does not satisfy the needs in shallow water. Approaching this area the importance of triads progressively emerges. However, considered in SWAN, their present formulation is only a crude approximation to the truth. In our continuous quest for better results, this will have to be taken into consideration and given a workable solution.

Another fundamental advancement, on which work has been done for a number of years, concerns a generalized evolution equation for the transport of the coupled second order wave statistics of the surface elevation. If successful, this will bring the field beyond the present idea of energy spectrum. However, this approach is still at the experimental level and the practical implications for the real daily activities are not yet clear.

A process till now considered mainly from the theoretical point of view is Bragg resonance with the bottom spectrum. Apart from the involved computations, the point is that we mostly lack the necessary information (the 2D spectrum, in principle also time dependent). However, in some cases this process will have to be considered because its potential influence on the final results can be very large.

A further physical frontier we will need to deal with is a more detailed description of what is going on in the breakers zone on the shore. There is a tremendous amount of energy dissipated here in very short space and time. More importantly, this area is crucial for several relevant processes whose present solutions are not fully satisfactory. Physical and numerical advancements are here required.

Discussing "The present" situation we have mentioned that most of the physics in our wave models loses its validity under extreme conditions. Indeed, it is amazing, and it should be a valuable piece of information, that, notwithstanding such limitation, we get reasonably good results. In any case white-capping, together with its interaction

with wind, leads to spray that is considered as the most effective transfer of matter and heat to the atmosphere. This process is connected to the generation by wind. As a matter of fact, we are here at a choice: either we accept that in these strongly forced conditions the physics is different, or, if we consider our physics universally valid and we know the conditions are different, we must acknowledge that something is not fully correct in our present view of the generation/dissipation processes. It is worth to specify that these, if not extreme, highly pushed conditions, are possible and relatively frequent also in enclosed seas. We recall the cited 12 m significant wave height in the "small" Adriatic Sea and, for a different situation, the highly generative limited fetch conditions present in the Gulf of Lion and the Northern Adriatic Sea, respectively under mistral and bora wind.

Under what we can call "normal" conditions the physics of wave-current interactions is well developed, but some aspects still need to be improved. The question often is if the full necessary information is available. Especially close to coast, with a pronounced orography, the role of the wind field may be crucial, affecting both the local waves and current, with mutual interactions. In these highly variable conditions we frequently lack one of the implicit assumptions, i.e. that the current is vertically uniform, at least within the wave vertical range. Present wave models are not prepared for a vertically non-uniform current. More in general the overall view of the wave-current interactions will have to move towards a more 3D approach, and this is more true in coastal waters where both the fields, waves and current, are modified by the limited vertical scope.

This more intense interaction rises the problem of the calibration of the models we use. The expression for the various processes have by default been obtained in 'normal' conditions, i.e. in general without much influence by currents. It is meaningful to wonder if these calibrations still hold when there is a strong 3D interaction with current. This is an open problem that does not have an immediate solution.

The need for a deeper look to currents is also connected to their stratification and interaction with the atmosphere. A general problem of circulation modelling is the frequently too shallow thermocline. Waves have their role in this respect, as also has the Langmuir circulation whose generation requires the coupling of the full meteo-ocean system. More in general, as wave modellers acting frequently in coastal water conditions, to consider the interaction with currents is practically a "must". The problem is that circulation modellers still drive their currents with the wind stress, ignoring that most of the related energy and momentum transfers happen via wind waves. Things are progressively changing. There is a very widespread movement towards coupled modelling, see, among others, the cited example by Lewis et al. (2018). In the long term we will have to get used to talk about the wave-current system as a single, possibly also with wind, logical unit. This will be, and already is, crucial when dealing with coastal flooding under strong stormy conditions. What has been shown for Katrina and the Gulf of Mexico coast is a very convincing argument.

Computers will become faster and more powerful. This will push users towards higher resolutions. It is an interesting question why we like to think that, or act as, a higher resolution will always be "the solution". It is true that, as mentioned above, we often lack detailed information (a highly variable bathymetry, or think of the fractal conditions at the southern border of the Bothnian Sea), but (1) if we go to higher resolution, a meaningful job requires a correspondingly detailed information, (2) we must be sure that what we model is the truth, (3) there is the non-trivial problem of natural variability. When modelling an environment with a relatively coarse resolution, we implicitly produce results that represent, right or wrong, the average conditions at each mesh point (in space and time). However, as continuous high resolutions show, or as, within limits, seen in scatterometer and SAR images, nature performs with a high (conditions dependent) natural variability. If the physics of our model progresses with its resolution, this variability must and will appear also in the model results. However, we should never forget that, the more we go into resolution, the more our results, although partially deterministic in space, will be always only statistically valid in time. For obvious reasons we do not have the corresponding, in space and time, measured information. Note that this may be true also for full basins or full ocean (or global) meteorological models if pushed beyond a certain resolution. This does not mean this variability will be useless. Possibly fundamental for the local physics (e.g., integral fluxes), we will use it in statistical terms to achieve further knowledge in relatively high frequency processes, e.g. the characteristics of gustiness. Note that, within limits, this will be less the case for wave results because of their characteristics of being an integral in space and time of the driving wind field. Their variability may not be trivial for special cases, e.g. short fetch generation of very gusty winds (bora and mistral).

The high resolution leads us to talk about numerical grids. There is no doubt that unstructured grids will be the solution for improving the resolution where required in enclosed and coastal seas. On a wider scale, for a number of years there has been some interest in the capability of dynamically adapting the local conditions of the grid where required by, e.g., the stronger spatial gradients. A common problem reported from a similar approach in circulation modelling is the continuous interpolation required and the consequent progressive smoothing of the field. This may well be the case, however, on one hand the results will certainly be better than with a coarse (relatively speaking) resolution, on the other one new grid adaptations are not required at each time step and can be partly coincident with the previous one, in so doing strongly reducing the problem. Indeed this seems to be the only approach to a proper dealing of cases like hurricanes where, whichever the resolution of the global or, e.g., Atlantic, model, it will not be sufficient for a proper description of their central part. Note that purposely we do not touch here the corresponding meteorological problem.

Still related to grids, and pushed by the use of unstructured ones, numerics has become in our field a very dynamical subject where advancements and improvements are to be expected. We are presently well aware of the problems we are facing, the key point being that with the present numerical methods we cannot satisfy all the requirements of an ideal solution, both as computer and accuracy (not to mention the numerical details). New methods need to be developed, and this will be more and more the case as we move on one hand to more extreme conditions (this is possible also in the enclosed seas), on the other hand to more and more shallow water with higher and higher resolution. The link with the physics in the breakers zone is obvious. As with physics, there is a level of conservatism in our present approaches and solutions. The person considering physics or numerics as only tools to reach the real target, e.g. the maximum wave height in front of a harbour, may be happy to have the computer machine running smoothly. However, the specialist of the subject, in our case the numerical expert, may point out a number of potential, perhaps hidden, problems and push for a new solution. From a more general perspective, the existence of a discussion, not only of alternative solutions, suggests that the field is not yet sufficiently mature. Indeed, in other fields of science, including mathematics, there are more profound studies on the integration of partial differential equations. We should always be open to these new solutions, especially when their correct use could appreciably, if not more, change our results. This is a very general problem, i.e. the balance between specialized and focused knowledge, where, zooming more and more on a specific subject, we tend to ignore the useful progresses in parallel sciences. The interesting experiment of representing the spatial distribution of the wave fields in spectral mode (as in spectral meteorological models) is instructive in this respect.

Discussing numerics involves the use of limiters. Of course at present they are needed and useful. However, as just said, the fact that our machine is running smoothly and meaningful results pop out does not imply that what we are doing is correct. Every limiter implies something is wrong in our approach. In a way they are useful because they tell us where we need to act, let this be physics or numerics.

A final subject bordering between physics and numeric is the use of phase resolving models. The dream of a fully deterministic approach (assuming the corresponding input information is available) has lured engineers for decades. Without discussing the possible spatial extent of these simulations before the spatial resolution takes its toll, the present and for the foreseeable future drastic limit to their use is still the required computer time.

In “The present” we have mentioned what we can call the limitations of data assimilation in enclosed and coastal seas, i.e. its limited validity in time: the information, i.e. the waves, will rapidly reach the coast. With respect to the open ocean there is also a more pronounced asymmetry in the fields. This implies that the usual empirical default distributions of the range of influence of a give piece of information may not necessarily lead to a good job. Indeed, as we discussed in Chapter 4, a preliminary study is required for any area of interest, providing, for every point of the grid, hence for every measured datum available and for a given wave system, the corresponding map of influence. We believe this is the method that, valid also on the open ocean, will be more so in enclosed seas.

Much more attention needs to be paid to the errors of measured data. While we expect an improved quality in some aspects or types of instruments, there is a strong possibility that the one of the master reference in our field, i.e. buoys, is deteriorating because of the need to decrease their price and handling costs. A strong push should be done on management and manufacturers to make available, better if in real time, the raw original data. This would allow improved analyses of directional distributions, single, including freak, wave heights, and, where done, intercomparisons of different instruments. Campaigns in this last direction are strongly recommended. In any case comparison of model data versus measured ones must take the measurement errors into consideration. An open problem is that these errors are frequently not available.

Much expectation exists for satellite data close to coast. Indeed, the Sentinel 3 approach of slicing the explored area in 300 m long (in the direction of flight) and a few kilometres wide zones sounds very promising, especially if the flight direction is perpendicular to the coastline. However, for the time being and the immediate future the errors, instrumental and statistical, present in those data can be accepted using the data for some purposes, but their use for model validation remains at least debatable. Progresses are expected, but far from the accuracy of a local measurement.

Some of the refinements in the physics of wave models, especially in wave-current interactions or in some aspects of non-linearity (e.g., bound modes), badly need more information than the classical measurements. To a large extent, either shot views of a field or time measurements at a single point, all rely on or assume linear theory. However, in a way this is one of our present limits. Measurements as the cited stereo ones, providing both k and f directional spectra, are badly needed to progress further on a solid ground. Luckily this technology is now available and well described. Granted the availability of platforms and rigs, this technology is expected to have a large diffusion.

The uncertainty that characterizes every estimate, either as hindcast or forecast, and the need to provide also this information to the user will lead more and more towards the use of ensemble approaches. Already present at some of the forecasts centres, we expect their use will increase in the future, especially where and when the specific value of one or more parameters is of concern. The problem is that at present the ensemble is (mostly) only meteorologically driven, while the wave model (and current one as well), is (are) taken as deterministically correct. However, we know this is not true. We can make a model ensemble, but this is too limited. As in meteorological modelling, new tools need to be developed to have ensemble wave runs. Of course, at centres such as ECMWF the wave model has been for a long while two-way coupled to the meteorological one, so that the suggested flow seems natural. However, again this corresponds to taking into account the meteorological uncertainty, while the one in the wave model also needs to be considered.

The thin line between rigour and pragmatism concerns the approach to a specific problem, e.g. the forecast of the wave conditions at a certain harbour. It is clear that in general we pursue the solution of the general problem, i.e. wave conditions in enclosed seas. However, given a certain target, possibly limited in space, there will always be a greater level of empiricism if experience shows that a certain pragmatic solution provides the best results.

On a more general and final perspective, our aims and expectations of wave model improvements, however important, are not the whole purpose. It is clear that in general we are moving towards a fully coupled atmosphere–ocean system where the waves are the modulating interface. Indeed, both if we consider a developing cyclogenesis or work as far as climate models (but most of them ignore waves), waves are the key knob that modulates all the heat, matter, energy et al. transfers at the sea surface. This is another enormous field still in its initial stage, but that badly needs devoted activity and drastic developments. It is interesting, instructive and stimulating how, in solving a problem, we go from the focused attention of a technical detail to the ample view of the Earth system.

Acknowledgements

Judith Wolf and Jaak Monbaliu have devoted quite a bit of their time to go through and review the whole paper with valuable suggestions, pointing out where something had to be clipped and where more emphasis and data were requited for specific subjects. The paper has certainly improved thanks to their review. José-Henrique Alves, Sabique Langodan, Roberto Padilla-Hernandez, Kirti Samiksha Volvaiker contributed and provided material for this paper. They appear as co-authors in some of the Sections. Casey Dietrich, of North Carolina State University, has kindly provided the very effective maps of the flood due to Katrina, Fig. 3.8.

A decade ago a similar white-paper on wave modelling was published as a product of the WISE Group. In this period the Group has grown and in practice it is no longer possible to produce now a Group-paper. However, all of us who have actually worked on it must and are pleased to acknowledge that, at least in spirit, this is a community product, derived from much work from most of the authors, but also from the long term interactions and sometime hot discussions that are at the base of a community science where honesty, friendship and a love for nature are the keys to success. However, both for the benefit of us and the ones who will follow, it is necessary to frame every now and then the situation. Using an often used parallelism, it is like climbing a mountain. Every so often we need to put a pin in the rock of the cliff we are ascending to know better, and to be sure of, where we are and proceed further on solid ground.

L. Cavaleri, L. Bertotti, S. Carniel and A. Sanchez-Arcilla have been partially supported by the EU contract 730030 call H2020-EO-2016 ‘CEASELESS’.

Appendix A. Supplementary material

Supplementary data associated with this article can be found, in the online version, at http://dx.doi.org/10.1016/j.pocean.2018.03.010.

References

Aarnes, O.J., Breivik, Ø., Reistad, M., 2012. Wave extremes in the Northeast Atlantic. J. Clim. 25, 1529–1543. http://dx.doi.org/10.1175/JCLI-D-11-00132.1.

Abdalla, S., 2015. SARAL/AltiKa wind and wave products: monitoring, validation and assimilation. Mar. Geodesy 38, 365–380. http://dx.doi.org/10.1080/01490419.2014. 1001049.

Abdalla, S., Cavaleri, L., 2002. Effect of wind variability and variable air density on wave modelling. J. Geoph. Res. 107 (C7), 17-1–17-17.

Abdalla, S., De Chiara, G., 2017. Estimating random errors of scatterometer, altimeter and model wind speed data. J. Sel. Top. Appl. Earth Observ. Remote Sens. 10 (5), 2406–2414. http://dx.doi.org/10.1109/JSTARS.2017.2659220.

Abdalla, S., Janssen, P.A.E.M., 2017. Monitoring waves and surface winds by satellite altimetry: applications. In: Stammer, D., Cazenave, A. (Eds.), Satellite Altimetry Over Oceans and Land Surfaces. CRC Press, Taylor & Francis Group, USA, pp. 379–424.
Abdalla, S., Janssen, P.A.E.M., Bidlot, J.-R., 2010. Jason-2 OGDR wind and wave products: monitoring, validation and assimilation. Mar. Geodesy 33 (1), 239–255. http://dx.doi.org/10.1080/01490419.2010.48779".
Abdalla, S., Janssen, P.A.E.M., Bidlot, J.B., 2011. Altimeter near real time wind and wave products: random error estimation. Mar. Geodesy 34 (3–4), 393–406. http://dx.doi.org/10.1080/01490419.2011.585113.
Abdalla, S., Dinardo, S., Benveniste, J., Janssen, P.A.E.M., 2018;al., in press. Validation of Cryosat-2 SAR wind and wave data. Adv. Space Res. http://dx.doi.org/10.1016/i.asr.2018.01.044.
ACT - Alliance for Coastal Technologies, 2007. ACT Wave Sensor Technologies. In: Proceedings of a Workshop held by the Alliance for Coastal Technologies, March 7–9, 2007, St. Petersburg, FL, pp. 26. < http://www.act-us.info/Download/Workshops/2007/USF_NDBC_Wave/ > .
ACT - Alliance for Coastal Technologies, 2012. Wave measurement systems test and evaluation protocols in support of the National Operational Wave Observation Plan. In: Proceedings of a Workshop held by the Alliance for Coastal Technologies, February 22–24, 2011, St. Petersburg, FL, pp. 29. < http://www.act-us.info/Download/Workshops/2012/USFUM_Wave_Measurement/ > .
Adam, A., Buchan, A.G., Piggott, M.D., Pain, C.C., Hill, J., Goffin, M.A., 2016. Adaptive Haar wavelets for the angular discretisation of spectral wave models. J. Comput. Phys. 305, 521–538. http://dx.doi.org/10.1016/j.jcp.2015.10.046.
Agnon, Y., 1999. Linear and nonlinear refraction and Bragg scattering of water waves. Phys. Rev. E 59, 1319–1322. http://dx.doi.org/10.1103/PhysRevE.59.R1319.
Agnon, Y., Sheremet, A., Gonsalves, J., Stiassnie, M., 1993. A unidirectional model for shoaling gravity waves. Coastal Eng. 20, 29–58.
Alari, V., Staneva, J., Breivik, Ø., Bidlot, J.-R., Mogensen, K., Janssen, P.A.E.M., 2016. Surface wave effects on water temperature in the Baltic Sea: simulations with the coupled NEMO-WAM model. Ocean Dyn. 66, 917–930. http://dx.doi.org/10.1007/s10236-016-0963-x.
Alfieri, L., Salamon, P., Pappenberger, F., Wetterhall, F., Thielen, J., 2012. Operational early warning systems for water-related hazards in Europe. Environ. Sci. Policy 21, 35–49. http://dx.doi.org/10.1016/j.envsci.2012.01.008. ISSN 1462-9011.
Allender, J., Audunson, T., Barstow, S.F., Bjerken, S., Krogstad, H.E., Steinbakke, P., Vartdal, L., Borgman, L.E., Graham, C., 1989. The WADIC project: a comprehensive field evaluation of directional wave instrumentation. Ocean Eng. 16 (5/6), 505–536.
Alves, J.H., Chawla, A., Tolman, H., Schwab, D., Lang, G., Mann, G., 2014. The Operational Implementation of a Great Lakes Wave Forecasting System at NOAA/NCEP. Weath. Forecasting 29, 1473–1497. http://dx.doi.org/10.1175/WAF-D-12-00049.1.
Anderson, M.E., Smith, J.M., 2014. Wave attenuation by flexible, idealized salt marsh vegetation. Coastal Eng. 83, 82–92.
Appel, K.W., Riordan, A.J., Holley, T.A., 2005. An objective climatology of Carolina coastal fronts. Weath. Forecasting 20, 439–455.
Ardhuin, F., Herbers, T.H.C., 2002. Bragg scattering of random surface gravity waves by irregular sea bed topography. J. Fluid Mech. 451, 1–33. http://dx.doi.org/10.1017/S0022112001006218.
Ardhuin, F., Jenkins, A.D., 2006. On the interaction of surface wave and upper ocean turbulence. J. Phys. Oceanogr. 36, 551–557.
Ardhuin, F., Roland, A., 2012. Coastal wave reflection, directional spread, and seismoacoustic noise sources. J. Geophys. Res.: Oceans 117 (C11).
Ardhuin, F., Roland, A., 2013. The development of spectral wave model: coastal and coupled models. Coastal Dynamics, Arcachon, France, pp. 25–37.
Ardhuin, F., Herbers, T.H.C., van Vledder, G.Ph., Watts, K.P., Jensen, R., Graber, H.C., 2007. Swell and slanting-fetch effects on wind wave growth. J. Phys. Oceanogr. 37 (4), 908–931.
Ardhuin, F., Rascle, N., Belibassakis, K.B., 2008. Explicit wave-averaged primitive equations using a generalized lagrangian mean. Ocean Modell. 20, 35–60.
Ardhuin, F., Rogers, W.E., Babanin, A.V., Filipot, J.-F., Magne, R., Roland, A., Van der Westhuysen, A.J., Queffeulou, P., Lefevre, J.M., Aouf, L., Collard, F., 2010. Semi-empirical dissipation source functions for ocean waves. Part I: definition, calibration, and validation. J. Phys. Oceanogr. 40, 1917–1941.
Ardhuin, F., Roland, A., Dumas, F., Bennis, A.C., Sentchev, A., Forget, P., Wolf, J., Girard, F., Osuna, P., Benoit, B., 2012a. Numerical wave modelling in conditions with strong currents: dissipation, refraction, and relative wind. J. Phys. Oceanogr. 42 (12), 2101–2120.
Ardhuin, F., Dumas, F., Bennis, A.-C., Roland, A., Sentchev, A., Forget, P., Wolf, J., Girard, F., Osuna, P., Benoit, M., 2012b. Numerical wave modelling in conditions with strong currents: dissipation, refraction and relative wind. J. Phys. Oceanogr. 42, 2101–2120.
Ardhuin, F., Collard, F., Chapron, B., Ardhuin, F.-G., Guitton, G., Mouche, A., Stopa, J.E., 2015. Estimates of ocean wave heights and attenuation in sea ice using the SAR wave mode on Sentinel-1A. Geophys. Res. Lett. 42, 2317–2325. http://dx.doi.org/10.1002/2014GL062940.
Babanin, A.V., 2006. On a wave-induced turbulence and a wave-mixed upper ocean layer. Geophys. Res. Lett. 33, L20605. http://dx.doi.org/10.1029/2006GL027308.
Babanin, A.V., Haus, B.K., 2009. On the existence of water turbulence induced by non-breaking surface waves. J. Phys. Oceanogr. 39, 2675–2679.
Babanin, A.V., Makin, V.K., 2008. Effects of wind trend and gustiness on the sea drag: Lake George study. J. Geophys. Res. 113, C0215. http://dx.doi.org/10.1029/2007JC004233.
Babanin, A.V., Ganopolski, A., Phillips, W.R., 2009. Wave-induced upper-ocean mixing in a climate model of intermediate complexity. Ocean Model. 29 (3), 189–197. http://dx.doi.org/10.1016/j.ocemod.2009.04.003.
Babanin, A.V., Hsu, T.-W., Roland, A., Ou, S.-H., Doong, D.-J., Fan, Y.M., 2011. Spectral modelling of typhoon Krosa. Nat. Hazards Earth Syst. Sci. 11, 501–511. http://dx.doi.org/10.5194/nhess-11-501-2011.
Bakhoday-Paskyabi, M., Fer, I., Jenkins, A.D., 2012. Surface gravity wave effects on the upper ocean boundary layer: modification of a one-dimensional vertical mixing model. Continental Shelf Res. 38, 63–78.
Barthelmie, R.J., 1999. The effects of atmospheric stability on coast wind climates. Meteorol. Appl. 6, 39–47.
Barthelmie, R.J., Grisogono, B., Pryor, S.C., 1996. Observation and simulations of diurnal cycles of near-surface wind speeds over land and sea. J. Geophy. Res. 101 (D16), 21327–21337.
Battjes, J.A., 1994. Shallow water wave modelling. Proc. Int. Symp. Wave – Physical and Numerical Modelling. University of British Colombia, Vancouver Canada.
Battjes, J.A., Janssen, J.P.F.M., 1978. Energy loss and set-up due to breaking of random waves. In: Proc. 16th Int. Conf. Coastal Eng. ASCE, Hamburg, pp. 569–587.
Beardsley, R.C., Chen, C., Xu, Q., 2013. Coastal flooding in Scituate (MA): a FVCOM study of the 27 December 2010 nor'easter. J. Geoph. Res. Oceans 118, 6030–6045. http://dx.doi.org/10.1002/2013JC008862.
Becq-Girard, F., Forget, P., Benoit, M., 1999. Non-linear propagation of unidirectional wave fields over varying topography. Coastal Eng. 38, 91–113.
Behrens, A., 2015. Development of an ensemble prediction system for ocean surface waves in a coastal area. Ocean Dyn. 63 (4), 469–486.
Bender, L.C., Guinasso, N.L., Walpert, J.N., Howen, S.D., 2009. A comparison of two methods for determining wave heights form a discus buoy with a strapped-down accelerometer. In: Proceedings 11th International Workshop on Wave Hindcasting and Forecasting, Halifax, Canada.
Bender, L.C., Guinasso, N.L., Walpert, J.N., 2010. A comparison of methods for determining significant wave heights-Applied to a 3-m discus buoy during Hurricane Katrina. J. Atmos. Oceanic Technol. 27, 1012–1028.
Benetazzo, A., Fedele, F., Gallego, G., Shih, P.-C., Yezzi, A., 2012. Offshore stereo measurements of gravity waves. Coastal Eng. 64, 127–138.
Benetazzo, A., Carniel, S., Sclavo, M., Bergamasco, A., 2013. Wave-current interaction: effect on the wave field in a semi-enclosed basin. Ocean Modell. 70, 152–165. http://dx.doi.org/10.1016/j.ocemod.2012.12.009.
Benetazzo, A., Bergamasco, A., Donaldo, D., Falcieri, F.M., Sclavo, M., Langone, L., Carniel, S., 2014. Response of the Adriatic Sea to an intense cold air outbreak: dense water dynamics and wave-induced transport. Prog. in Oceanogr. 128, 115–138.
Benetazzo, A., Barbariol, F., Bergamasco, F., Torsello, A., Carniel, S., Sclavo, M., 2015. Observation of extreme sea waves in a space-time ensemble. J. Phys. Oceanogr. 45, 2261–2275. http://dx.doi.org/10.1175/JPO-D-15-0017.1.
Benoit, M., 1992. Practical comparative performance survey of methods used for estimating directional wave spectra from heave-pitch-roll data. In: Proceedings of the 23rd International Conference on Coastal Engineering. ASCE, pp. 62–75.
Benoit, M., Marcos, F. Becq, F., 1996. Development of a third generation shallow-water wave model with unstructured spatial meshing. In: Proc. 25th Int. Conf. on Coastal Engineering. pp. 465–478.
Berkhoff, J.C.W., 1972. Computation of combined refraction–diffraction. In: Proc. 13th Int. Conf. on Coastal Engineering ASCE, Vancouver, BC, 10–14 July 1972. ASCE, New York, NY, pp. 471–490.
Bertin, X., Li, K., Roland, A., Bidlot, J.-R., 2015. Contribution of short-waves in storm surges: two case studies in the Bay of Biscay. Continental Shelf Res. 2015. http://dx.doi.org/10.1016/j.csr.2015.01.005.
Bertotti, L., Cavaleri, L., 1985. Coastal set-up and wave breaking. Oceanologica Acta 8 (2), 237–242.
Bertotti, L., Canestrelli, P., Cavaleri, L., Pastore, F., Zampato, L., 2011. The Henetus wave forecast system in the Adriatic Sea. Nat. Hazards Earth Syst. Sci. 11, 2965–2979.
Bertotti, L., Cavaleri, L., Loffredo, L., Torrisi, L., 2013. Nettuno: analysis of a wind and wave forecast system in the Mediterranean Sea. Mon. Weather Rev. 141 (9), 3130–3141. http://dx.doi.org/10.1175/MWR-D-12-00361.1.
Bertotti, L., Cavaleri, L., Soret, A., Tolosana-Delgado, R., 2014. Performance of global and regional nested meteorological models. Continental Shelf Res. 87, 17–27. http://dx.doi.org/10.1016/j.csr.2013.12.013. ISSN 0278-4343.
Bidlot, J.-R., 2012. Present status of wave forecasting at ECMWF in Workshop on Ocean Waves, 25–27 June 2012, 15p. Available online at < http://www.ecmwf.int/publications/ > .
Bidlot, J.-R., 2017. Twenty-one years of wave forecast verification. ECMWF Newsl. 150, 29–32. http://dx.doi.org/10.18442/ECMWF-NL-201610.
Bidlot, J.-R., Hansen, B., Janssen, P.A.E.M., 1997. Wave modelling and operational forecasting at ECMWF. In: Stel, J.H. et al. (Eds.). Operational Oceanography: The Challenge for European Co-operation: Proceedings of the First International Conference on EuroGOOS 7–11 October 1996, vol 62. Elsevier Oceanography Series, The Hague, The Netherlands, pp. 206–213.
Birkemeier, W.A., Thornton, E.B., 1994. The DUCK94 Nearshore Field Experiment. In: Proc. Conference on Coastal Dynamics, 1994, pp. 815–821.
Bishop, C.T., Donelan, M.A., 1987. Measuring waves with pressure transducers. Coastal Eng. 11, 309–328.
Björkvist, J.-V., Tuomi, L., Fortelius, C., Pettersson, H., Tikka, K., Kahma, K., 2016. Improved estimates of near shore wave conditions in the Gulf of Finland. J. Mar. Syst. http://dx.doi.org/10.1016/j.jmarsys.2016.07.005.
Blain, C.A., Linzell, R.S., Chu, P., Massey, C., 2010. Validation Test Report for the Advanced CIRCulation Model (ADCIRC) v45.11. NRL/MR/7320—10-9205. Naval Research Lab, Stennis Space Center, MS, 109pp.
Blumberg, A.F., Mellor, G.L., 1987. A description of a three-dimensional coastal ocean circulation model in Three-Dimensional Coastal Ocean Models, N S Heaps (Ed.), AGU Coastal and Estuarine Series 4, American Geophysical Union, Washington DC.
Bolanos, R., Osuna, P., Wolf, J., Sanchez-Arcilla, A., 2011. Development of the POLCOMS-WAM current-wave model. Ocean Modell. 36, 102–115.

Bolanos, R., Brown, J.M., Souza, A.J., 2014. Wave-current interactions in a tide dominated estuary. Continental Shelf Res. 87, 109–123.
Booij, N., Holthuijsen, L.H., 1987. Propagation of ocean waves in discrete spectral wave models. J. Comput. Physic 68 (2), 307–326. http://dx.doi.org/10.1029/98JC02622.
Booij, N., Ris, R.C., Holthuijsen, L.H., 1999. A third-generation wave model for coastal regions, Part I, Model description and validation. J. Geophys. Res. Oceans 104, 7649–7666.
Bosart, L.F., 1975. New England coastal frontogenesis. Q. J. R. Meteorl. Soc. 101, 957–978.
Bottema, M., Van Vledder, G.Ph., 2008. Effective Fetch and non-linear four-wave interactions during wave growth in slanting fetch conditions. Coastal Eng. 55 (2008), 261–275.
Bredmose, H., Agnon, Y., Madsen, P., Schaffer, H., 2005. Wave transformation models with exact second-order transfer. Eur. J. Mech. (B/Fluids) 24 (6), 659–682.
Breivik, O., Janssen, P.A.E.M., Bidlot, J.-R., 2014. Approximate Stokes drift profiles in deep water. J. Phys. Oceanogr. 44, 2433–2445. http://dx.doi.org/10.1175/JPO-D-14-0020.1.
Breivik, O., Mogensen, K., Bidlot, J.-R., Balmaseda, M.A., Janssen, P.A.E.M., 2015. Surface wave effects in the NEMO ocean model: forced and coupled experiments. J. Geophys. Res. Oceans 120. http://dx.doi.org/10.1002/2014JC010565.
Bretherton, F.P., Garrett, C.J.R., 1968. Wavetrains in inhomogeneous moving media. Proc. R. Soc. Lond. A: Math. Phys. Eng. Sci. 302 (1471), 529–554.
Bretschneider, D.L., 1952. Revised wave forecasting relationships. In: Proceedings 2nd Conference on Coastal Engineering. ASCE, Council on Wave Research.
Bretschneider, C.L., 1958. Revisions in wave forecasting: Deep and shallow water. In: Proc. 6th Conf. On Coastal Eng. ASCE, Council on Wave Research.
Broström, G., Christensen, K.H., Drivdal, M., Weber, J.E., 2014. Note on Coriolis-Stokes force and energy. Ocean Dyn. 64 (7), 1039–1045. http://dx.doi.org/10.1007/s10236-014-0723-8.
Brown, J.M., Bolanos, R., Wolf, J., 2013. The depth-varying response of coastal circulation and water level in 2D radiation stress when applied in a coupled wave-tide-surge modelling system during an extreme storm. Coastal Eng. 82, 102–113.
Brown, J.M., Wolf, J., 2009. Coupled wave and surge modelling for the eastern Irish Sea and implications for model wind-stress. Continental Shelf Res. 29, 1329–1342.
Bunney, C., Saulter, A., 2016. An ensemble forecast system for prediction of Atlantic-UK wind waves. Ocean Modell. http://dx.doi.org/10.1016/j.ocemod2015.07.065.
Burke, J., 2008. The one I'll never forget, Bayview Yacht Club Report. < www.bycmack.com/history/1985_Port_Huron_to_Mack_Race_by_John_Burke_(2008).pdf > .
Carniel, S., Bonaldo, D., Benetazzo, A., Bergamasco, A., Boldrin, A., Falcieri, F.M., Sclavo, M., Trincardi, F., Langone, L., Sclavo, M., 2016a. Off-shelf fluxes across the Southern Adriatic margin: factors controlling dense-water-driven transport phenomena. Mar. Geol. 375, 44–63. http://dx.doi.org/10.1016/j.margeo.2015.08.016.
Carniel, S., Benetazzo, A., Bonaldo, D., Falcieri, F.M., Miglietta, M.M., Ricchi, A., Sclavo, M., 2016b. Scratching beneath the surface while coupling atmosphere, ocean and waves: analysis of a dense water formation event. Ocean Modell. 101, 101–112. http://dx.doi.org/10.1016/j.ocemod.2016.03.007.
Cavaleri, L., 1980. Wave measurements using a pressure transducer. Oceanologica Acta 3 (3), 339–346.
Cavaleri, L., 2000. The oceanographic tower Acqua Alta – activity and prediction of sea states at Venice. Coastal Eng. 39, 29–70.
Cavaleri, L., 2006. Wave modelling - where to go in the future. Bull. Amer. Meterol. Soc. 87 (2), 207–214.
Cavaleri, L., Zecchetto, S., 1987. Reynolds stresses under wind waves. J. Geoph. Res. 92 (C4), 3894–3904.
Cavaleri, L., Bertotti, L., 1997. In search of the correct wind and wave fields in a minor basin. Mon. Weather Rev. 125 (8), 1964–1975.
Cavaleri, L., Sclavo, M., 1998. Characteristics of quadrant and octant advection schemes in wave models. Coastal Eng. 34, 221–242.
Cavaleri, L., Bertotti, L., 2004. Accuracy of the modelled wind and wave fields in enclosed seas. Tellus 56A, 167–175.
Cavaleri, L., Bertotti, L., 2006. The improvement of modelled wind and wave fields with increasing resolution. Ocean Eng. 33 (5–6), 553–565.
Cavaleri, L., Alves, J.-H.G.M., Ardhuin, F., Babanin, A., Banner, M., Belibassakis, K., Benoit, M., Donelan, M., Groeneweg, J., Herbers, T.H.C., Hwang, P., Janssen, T., Janssen, P.A.E.M., Lavrenov, I.V., Magne, R., Monbaliu, J., Onorato, M., Polnikov, V., Resio, R., Rogers, W.E., Sheremet, A., McKee Smith, J., Tolman, H.L., van Vledder, G., Wolf, J., Young, I., 2007. Wave modelling – the state of the art. Progr. Oceanogr. 75 (4), 603–674. http://dx.doi.org/10.1016/j.pocean.2007.05.005.
Cavaleri, L., Bertotti, L., Buizza, R., Buzzi, A., Masato, V., Umgiesser, G., Zampato, M., 2010. Predictability of extreme meteo-oceanographic events in the Adriatic Sea. Q. Jour. R. Meteor. Soc. 400–413. http://dx.doi.org/10.1002/qj.567.
Cavaleri, L., Fox-Kemper, B., Hemer, M., 2012. Wind waves in the coupled climate system. Bull. Am. Meteorl. Soc. 93 (11), 1651–1661.
Chamberlain, P.G., Porter, D., 1995. The modified mild slope equation. J. Fluid Mech. 291, 393–407. http://dx.doi.org/10.1017/S0022112095002758.
Chawla, A., Kirby, J.T., 2002. Monochromatic and random wave breaking at blocking points. J. Geophys. Res. Oceans 107 (C7), 3067.
Chawla, A., Tolman, H.L., Gerald, V., Spindler, D., Spindler, T., Alves, Jose-Henrique G.M., Cao, Degui, Hanson, Jeffrey L., Devaliere, Eve-Marie, 2013. A multigrid wave forecasting model: a new paradigm in operational wave forecasting. Weather Forecasting 28 (4), 1057–1078.
Chelton, D.B., Ries, J.C., Haines, B.J., Fu, L.L., Callahan, P.S., 2001. Satellite altimetry. In: Fu, L.L., Cazenave, A. (Eds.), Satellite Altimetry and Earth Sciences: A Handbook of Techniques and Applications. Academic, San Diego, pp. 1–132.
Cipollini, P., Benveniste, J., Bouffard, J., Emery, W., Fenoglio-Marc, L., Gommenginger, C., Griffin, D., Hoyer, J., Kurapov, A., Madsen, K., Mercier, F., Miller, L., Pascual, A., Ravichandran M., Shillington, F., Snaith, H., Strub, P.T., Vandenmark, D., Vignudelli, S., Wilkin, J., Woodworth, P., Zavala-Garay, J., 2009. The role of altimetry in coastal observing systems. In: Proceedings of the OCEANOBS'09 Conference, WSA WPP-306, vol. 2(I), pp. 181–192.
COASTALT, 2011. Development of Radar Altimetry Data Processing in the Coastal Zone. < http://www.coastalt.eu/ > or < http://www.coastalaltimetry.org > .
Colby, F.P., 2004. Simulation of the New England sea breeze: the effect of grid spacing. Weath. Forecasting 19, 277–285.
Collins, J.I., 1972. Prediction of shallow water spectra. J. Geophys. Res. 77 (15), 2693–2707.
Collins III, C.O., Lund, B., Waseda, T., Graber, H.C., 2014. On recording sea surface elevation with accelerometer buoys: lessons from ITOP (2010). Ocean Dyn. 64 (6), 895–904.
Collins III, C.O., Rogers, W.E., Marchenko, A., Babanin, A.V., 2015a. In situ measurements of an energetic wave event in the Arctic marginal ice zone. Geophys. Res. Lett. 42. http://dx.doi.org/10.1002/2015GL063063.
Collins III, C.O., Vincent, C.L., Graber, H.C., 2015b. A statistical method for correlating paired wave spectra. J. Atmos. Oceanic Technol. 32, 2130–2146.
Corbella, S., Pringle, J., Stretch, D., 2015. Assimilation of ocean wave spectra and atmospheric circulation patterns to improve wave modelling. Coastal Eng. 100, 1–10. http://dx.doi.org/10.1016/j.coastaleng.2015.03.003. ISSN 0378-3839.
Courant, R., Friedrichs, K., Lewy, H., 1928. On the partial difference equations of mathematical physics. IBM J. Res. Dev. 11, 215–234.
Craig, P.D., Banner, M.L., 1994. Modelling wave-enhanced turbulence in the ocean surface layer. J. Phys. Oceanogr. 24 (12), 2546–2559. http://dx.doi.org/10.1175/15200485(1994) 024<2546:MWETIT>2.0.CO;2.
Craig, P.D., 1996. Velocity profiles and surface roughness under breaking waves. J. Geophys. Res. 101 (C1), 1265–1277. http://dx.doi.org/10.1029/95JC03220.
Craik, A., Leibovich, S., 1976. A rational model for Langmuir circulations. J. Fluid Mech. 73 (03), 401–426. http://dx.doi.org/10.1017/S0022112076001420.
Dabbi, E.P., Haigh, I.D., Lambkin, D., Hernon, J., Williams, J.J., Nicholls, R.J., 2015. Beyond significant wave height: a new approach for validating spectral wave models. Coastal Eng. 100, 11–25.
Daley, R., 1993. Atmospheric Data Analysis. Cambridge University Press, pp. 472 ISBN 9780521458252.
Dalrymple, R.A., Kirby, J.T., Hwang, P.A., 1984. Wave diffraction due to areas of energy dissipation. J. Waterw. Port Coast. Ocean Eng. 110, 67–79.
Dee, D.P., Uppala, S.M., Simmons, A.J., Berrisford, P., Poli, P., Kobayashi, S., Andreae, U., Magdalena, M.A., Balsamo, G., Bauer, P., Bechtold, P., Beljaars, A.C.M., van de Berg, L., Bidlot, J.-R., Borgmann, N., Delsol, C., Dragani, R., Fuentes, M., Geer, A.J., Haimberger, L., Healy, S.B., Holm, E.V., Isaksen, L., Källberg, P., Köhler, M., Matricardi, M., Mc Nally, A.P., Monte-Sanz, B.M., Morcrette, J.-J., Park, B.-K., Peubey, C., de Rosnay, P., Tavolato, C., Thépaut, J.-N., Vitart, F., 2011. The ERA-Interim reanalysis: configuration and performance of the data assimilation system. Q. J. R. Metrol. Soc. 137, 553–597. http://dx.doi.org/10.1002/qj.828.
Dietrich, J.C., Zijlema, M., Westerink, J.J., Holthuijsen, L.H., Dawson, C., Luettich Jr., R.A., Jensen, R.E., Smith, J.M., Stelling, G.S., Stone, G.W., 2011. Modelling hurricane waves and storm surge using integrally-coupled, scalable computations. Coastal Eng. 58, 45–65.
Dietrich, J.C., Tanaka, S., Westerink, J.J., Dawson, C.N., Luettich, R.A., Zijlema, M., Holthuijsen, L.H., Smith, J.M., Westerink, L.G., Westerink, H.J., 2012. Performance of the Unstructured-Mesh, SWAN+ADCIRC Model in Computing Hurricane Waves and Surge. J. Sci. Comput. 52 (2), 468–497.
Dietrich, J.C., Zijlema, M., Allier, P.E., Holthuijsen, L.H., Booij, N., Meixner, J.D., Proft, J.K., Dawson, C.N., Bender, C.J., Naimaster, A., Smith, J.M., Westerink, J.J., 2013. Ocean Modell. 70, 85–102.
Doble, M.J., Bidlot, J.-R., 2013. Wavebuoy measurements at the Antarctic sea ice edge compared with an enhanced ECMWF WAM: progress towards global waves-in-ice modelling. Ocean Modell. 70, 166–173. http://dx.doi.org/10.1016/j.ocemod.2013.05.012.
Dodet, G., Bertin, X., Bruneau, N., Fortunato, A.B., Nahon, A., Roland, A., 2013. Wave-current interactions in a wave-dominated tidal inlet. J. Geophys. Res. Oceans 118, 1587–1605. http://dx.doi.org/10.1002/jgrc.20146.
Donelan, M.A., Hamilton, J., Hui, W.H., 1985. Directional wave spectra of wind generated waves. Philos. Trans. R. Soc. Lond., Ser A 315, 500–562.
Donelan, M.A., Skafel, M., Graber, H., Liu, P., Schwab, D., Venkatesh, S., 1992. On the growth rate of wind-generated waves. Atmos.-Ocean 30, 457–478.
Donelan, M.A., Dobson, F.W., Graber, H.C., Madsen, N., McCormick, C., 2005. Measurement of wind waves and wave-coherent air pressures on the open sea from a moving SWATH vessel. J. Atmos. Oceanic Technol. 22, 896–908.
Doyle, J.D., Warner, T.T., 1993. Nonhydrostatic simulations of coastal mesobeta-scale vortices and frontogenesis. Mon. Wea. Rev. 121, 3371–3392.
Drennan, W.M., Donelan, M.A., Madsen, N., Katsaros, K.B., Terray, E.A., Flagg, C.N., 1994. Directional wave spectra from a swath ship at sea. J. Atmos. Oceanic Technol. 11, 1109–1116.
Drennen, W.M., Graber, H.C., Collins III, C.O., Herrera, A., Potter, H., Ramos, R.J., Williams, N.J., 2014. EASI: an air-sea interaction buoy for high waves. J. Atmos. Oceanic Technol. 31, 1397–1409.
Eldeberky, Y., Battjes, J.A., 1995. Parametrisation of triad interactions in wave energy model. In: Proc. Coastal Dynamics Conf. 1995, Gdansk, Poland, pp. 140–148.
Eldeberky, Y., Madsen, P.A., 1999. Deterministic and stochastic evolution equations for fully dispersive and weakly nonlinear waves. Coastal Eng. 38, 1–24.
Elgar, S., Herbers, T., Guza, R.T., 1994. Reflection of ocean surface gravity waves from a natural beach. J. Phys. Oceanogr. 24 (7), 1503–1511.
Elias, E.P.L., Gelfenbaum, G., van der Westhuysen, A.J., 2012. Validation of a coupled wave-flow model in a high-energy setting: the mouth of the Columbia River. J.

Geophys. Res. Oceans 117 (C9), 2156–2202. http://dx.doi.org/10.1029/2012JC008105.
Engelstad, A., Jansen, T.T., Herbers, T.H.C., van Vledder, G.Ph., Elgar, S., Raubenheimer, B., Trainor, L., Garcia-Garcia, A., 2013. Wave evolution across the Louisiana shelf. Continental Shelf Res. 52, 190–202.
Evensen, G., 1994. Sequential data assimilation with a nonlinear quasi-geostrophic model using Monte Carlo methods to forecast error statistics. J. geoph. Res. 99 (C5), 10143–10162.
Fan, Y., Griffies, S.M., 2014. Impacts of parameterized Langmuir turbulence and non-breaking wave mixing in global climate simulations. J. Climate 27, 4752–4775. http://dx.doi.org/10.1175/JCLI-D-13-00583.1.
Fan, Y., Ginis, I., Hara, T., Wright, C.W., Walsh, E.J., 2009. Numerical simulations and observations of surface wave fields under an extreme tropical cyclone. J. Phys. Oceanogr. 39, 2097–2116.
Fer, I., Paskyabi, M.B., 2014. Autonomous ocean turbulence measurements using shear probes on a moored instrument. J. Atmos. Oceanic Technol. 31, 474–490.
Ferrarin, C., Umgiesser, G., Cucco, A., Hsu, T.-W., Roland, A., Amos, C.L., 2008. Development and validation of a finite element morphological model for shallow water basins. Coastal Eng. 55 (9), 716–731. http://dx.doi.org/10.1016/j.coastaleng.2008.02.016.
Ferrarin, C., Roland, A., Bajo, M., Umgiesser, G., Cucco, A., Davolio, S., Buzzi, A., Malguzzi, P., Drofa, O., 2013. Tide surge wave modelling and forecasting in the Mediterranean Sea with focus on the Italian coast. Ocean Modell. 61, 38–48. http://dx.doi.org/10.1016/j.ocemod.2012.10.003.
Filipot, J.F., Ardhuin, F., Babanin, A.V., 2010. A unified deep-to-shallow water wave-breaking probability parameterization. J. Geophys. Res. 115, C04022. http://dx.doi.org/10.1029/2009JC005448.
Flamant, C., Pelon, J., Hauser, D., Quentin, C., Drennan, W.M., Gohin, F., Chapron, B., Gourrion, J., 2003. Analysis of surface wind and roughness length evolution with fetch using a combination of airborne lidar and radar measurements. J. Geophy. Res 108 (C3), 8058.
Forristal, G.Z., Reece, A.M., 1985. Measurements of wave attenuation due to a soft bottom: the SWAMP experiment. J. Geoph. Res. C90, 3376–3380.
Forristal, G.Z., Doyle, E.H., Silva, W., Yoshi, M., 1990. Verification of a soil wave interaction model (SWIM). In: In: Davies, A.M. (Ed.), Modelling Marine Systems Vol. II. CRC Press, Boca Raton, Florida, pp. 41–68.
Fredereickson, P.A., Davidson, K.L., 2003. Observational buoy studies of coastal air-sea fluxes. J. Climate 16, 593–599.
Freilich, M.H., Guza, R.T., 1984. Nonlinear effects on shoaling surface gravity waves. Phil. Trans. R. Soc. Lond. A 311, 1–41.
Freilich, M.H., Guza, R.T., Elgar, S.L., 1990. Observations of nonlinear effects in directional spectra of shoaling waves. J. Geophys. Res. 95 (C6), 9645–9656.
Fujita, T.T., 1981. Tornadoes and downbursts in the context of generalized planetary scales. J. Atmos. Sci. 38 (8), 1511–1534.
Garcia-Nava, H., Ocampo-Torres, F.J., Osuna, P., Donelan, M.A., 2009. Wind stess in the presence of swell under moderate to strong wind conditions. J. Geophy. Res 114 (C23008).
Gautier, C., Caires, S., 2015. Operational wave forecasts in the southern North Sea, IAHR 2015, The Hague, the Netherlands, 28 June–3 July, 4pp.
Geiser, J., 2012. Iterative splitting methods for solving time-dependent problems. Appl. Math. Lett. 25 (5), 793–797.
Gelci, R., Cazalé, H., 1962. Une equation synthétique de l'évolution de l'état del la mer. J. Mechan. Phys. Atmosphére Série 2 (4), 15–41.
Gemmrich, J., Farmer, D.M., 1999. Near-surface turbulence and thermal structure in a wind–driven sea. J. Phys. Oceanogr. 29, 480–499.
Gemmrich, J., Garrett, C., 2012. The signature of inertial and tidal currents in offshore wave records. J. Phys. Oceanogr. 42, 1051–1056.
Gemmrich, J.R., Mudge, T.D., Polonichko, V.D., 1994. On the energy input from wind to surface waves. J. Phys. Oceanogr. 24 (11), 2413–2417.
Gerling, T.W., 1992. Partitioning sequences and arrays of directional ocean wave spectra into component wave systems. J. Atmos. Oceanic Technol. 9, 444–458. http://dx.doi.org/10.1175/1520-0426(1992) 009<0444:PSAAOD>2.0.CO;2.
Gerritsen, H., de Goede, E.D., Platzek, F.W., Genseberger, M., van Kester, J.A.Th.M., Uittenbogaard, R.E., 2007. Validation Document Delft3D-FLOW. Report X0356, M3470, Delft Hydraulics, 109pp.
Gille, S.T., Llewellyn Smith, S.G., Statom, N.M., 2005. Global observations of the land breeze. Geophy. Res. Lett. 32, L05605.
Godunov, S., 1959. A finite-difference method for the numerical computation of discontinuous solutions of the equations of fluid dynamics. Mat. Sb. 47, 357–393.
Graber, H.C., 2005. The shoaling wave experiment. J. Atmos. Oceanic Technol. 22 797-797.
Graber, H.C., Terrary, E.A., Donelan, M.A., Drennan, W.M., van Leer, J.C., Peters, D.B., 2000. ASIS-A new air-sea interaction spar buoy: design and performance at sea. J. Atmos. Oceanic Technol. 17 (5), 708–720.
Grant, A.L., Belcher, S.E., 2009. Characteristics of Langmuir turbulence in the ocean mixed layer. J. Phys. Oceanogr. 39, 1871–1887. http://dx.doi.org/10.1175/2009JPO4119.1.
Groeneweg, J., van der Westhuysen, A.J., van Vledder, G.Ph., Jacobse, S., Lansen, J., van Dongeren, A.R., 2008. Wave modelling in a tidal inlet: performance of SWAN in the Wadden Sea. In: Proc. 31th Int. Conf. Coastal Eng., ASCE, pp. 411–423.
Groeneweg, J., van Gent, M., van Nieuwkoop, J., Toledo, Y., 2015. Wave propagation in complex coastal systems and the role of nonlinear interactions. J. Waterw. Port Coastal Ocean Eng. 141(5), 17. http://doi.org/10.1061/(ASCE)WW.1943-5460.0000300.
Hamilton, R.C., 1972. Ocean data gathering program report No. 7 covering hurricane Edith September 16, 1971, Baylor Company, Houston Texas.
Hanson, J.L., Phillips, O.M., 2001. Automated analysis ofocean surface directional wave spectra. J. Atmos. Oceanic Technol. 18, 277–293.
Harcourt, R.R., 2013. A second moment closure model of Langmuir turbulence. J. Phys. Oceanogr. 43, 673–697.
Harcourt, R.R., 2015. An improved second-moment closure model of Langmuir turbulence. J. Phys. Oceanogr. 45 (1), 84–103. http://dx.doi.org/10.1175/JPO-D-14-0046.1.
Harcourt, R.R., D'Asaro, E.A., 2008. Large-eddy simulation of Langmuir turbulence in pure wind seas. J. Phys. Oceanogr. 38 (7), 1542–1562. http://dx.doi.org/10.1175/2007JPO3842.1.
Hasselmann, K., 1970. Wave-driven inertial oscialltions. Geoph. Fluid Dyn. 463–502.
Hasselmann, K., 1971. On the mass and momentum transfer between short gravity waves and larger-scale motions. J. Fluid Mech. 50, 189–201.
Hasselmann, K., Collins, J.I., 1968. Spectral dissipation of finite-depth gravity waves due to turbulent bottom friction. J. Mar. Res. 26, 1–12.
Hasselmann, K., Barnett, T.P., Bouws, E., Carlson, H., Cartwright, D.E., Enke., K., Ewing, J.A., Gienapp., H., Hasselnamm, D.E., Kruseman, P., Meerburg, A., Muller., P., Olbers, D.J., Richter, K., Sell, W., Walden, H., 1973. Measurements of wind-wave growth and swell decay during the Joint North Sea Wave Project, (JONSWAP). Dtsch. Hydrogr. Z. Suppl. A 8(12), 95.
Hasselmann, S., Hasselmann, K., 1981. A symmetrical method of computing the nonlinear transfer in a gravity wave spectrum. Hamburger Geophysiklische Einzelschriften Reihe A: Heft 52.
Herbers, T.H.C., Jessen, P.F., Janssen, T.T., Colbert, D.B., MacMahan, J.H., 2012. Observing Ocean surface waves with GPS-tracked buoys. J. Atmos. OceanicTechnol. 29, 944–959.
Herbers, T.H.C., Lentz, S.J., 2010. Observing directional properties of ocean swell with an acoustic doppler current profiler (ADCP). J. Atmos. Oceanic Technol. 27, 210–225.
Herbers, T.H.C., Hendrickson, E.J., O'Reilly, W.C., 2000. Propagation of swell across a wide continental shelf. Geophy. Res. 105 (C3), 19729–19737.
Hersbach, H., Janssen, P.A.E.M., 1999. Improvement of the short-fetch behaviour in the Wave Ocean Model (WAM). J. Atmos. Oceanic Technol. 16, 884–892.
Herterich, K., Hasselmann, K., 1980. A similarity relation for the nonlinear energy transfer in a finite-depth gravity-wave spectrum. J. Fluid Mech. 97, 215–224.
Holland, K.T., Elmore, P.A., 2008. A review of heterogeneous sediments in coastal environments. Earth-Sci. Rev. 89 (3–4), 116–134.
Holland, K.T., Vinzon, S.B., Callian, L.I., 2009. A field study of coastal dynamics on a muddy coast offshore of Cassino beach, Brazil. Continental Shelf Res. 29 (3), 503–514.
Holthuijsen, L., 2007. Waves in Oceanic and Coastal Waters. Cambridge University Press, pp. 387 ISBN: 978-0521129954.
Holthuijsen, L.H., Tolman, H.L., 1991. Effects of the Gulf Stream on ocean waves. J. Geophys. Res. Oceans 96 (C7), 12755–12771.
Holthuijsen, L.-H., Herman, A., Booij, N., 2003. Phase-decoupled refraction-diffraction for spectral wave models. Coastal Eng. 49, 291–305.
Hope, M.E., Westerink, J.J., Kennedy, A.B., Kerr, P.C., Dietrich, J.C., Dawson, C., Bender, C.J., Smith, J.M., Jensen, R.E., Zijlema, M., Holthuijsen, L.H., Luettich, R.A., Powell, M.D., Cardone, V.J., Cox, A.T., Pourtaheri, H., Roberts, H.J., Atkinson, J.H., Tanaka, S., Westerink, H.J., Westerink, L.G., 2013. Hindcast and validation of Hurricane Ike (2008) waves, forerunner, and storm surge. J. Geoph. Res. Oceans 118, 4424–4460.
Hsu, T.W., Ou, S.H., Liau, J.M., 2005a. Hindcasting near shore wind waves using a FEM code for SWAN. Coastal Eng. 52, 177–195.
Hsu, T.W., Ou, S.H., Liau, J.M., Zanke, U., Roland, A., Mewis, P., 2005b. Verification and development of a spectral finite element wave model. In: Waves 2005, ASCE/COPRI, The Fifth International Symposium on Wave Measurement and Analysis. Billy Edge, Madrid, Spain.
Hsu, Y.L., Dykes, J.D., Allard, R.A., Wang, D.W., 2008. Validation Test Report for Delft3D. NRL/MR/7320—08-9079. Naval Research Lab, Stennis Space Center, MS, 42pp.
Huang, C.J., Qiao, F., Song, Z., Ezer, T., 2011. Improving simulations of the upper ocean by inclusion of surface waves in the Mellor-Yamada turbulence scheme. J. Geophys. Res. 116, C01007. http://dx.doi.org/10.1029/2010JC006320.
Huchet, M., Leckler, F., Filipot, J.-F., Roland, A., Ardhuin, F., Sikiric, M.D., Michaud, H., Delpey, M.T., Dodet, G., 2015a. On the high resolution coastal application with WAVWATCH III. In: Proc. 14th Workshop on Wave Hindcasting and Forecasting, Key West, Florida, USA.
Huchet, M., Leckler, F., Filipot, J-F., Roland, A., Ardhuin, F., DutourSikiric, M., Michaud, H., Delpey, M.T., Dodet, G., 2015b. High resolution modelling of nearshore wave processes using new implicit scheme of WAVEWATCH III. In: 14th International Workshop on Wave Hindcasting and Forecasting & 5th Coastal Hazard Symposium.
Hultquist, T.R., Dutter, M.R., Schwab, D.J., 2006. Reexamination of the 9–10 November 1975 "Edmund Fitzgerald" storm using today's technology, AMS. Bull. Am. Met. Soc. 87 (5), 607–622.
Hwang, P.A., Wang, D.W., Walsh, E.J., Krabill, W.B., Smith, R.N., 2000. Airborne measurements of the wave number spectra of ocean surface waves. Part I: spectral slope and dimensionless spectral coefficient. J. Phys. Oceanogr. 30, 2753–2767.
IOOS, 2009. A national operational wave observation plan. Integrated Ocean Observing System Program Office, Silver Spring, MD, 76pp. < http://www.ioos.noaa.gov/library/wave_plan_final_03122009.pdf > .
Isoguchi, O., Kawamura, H., 2007. Coastal wind jets flowing into the Tusushima strait and their effect on wind-wave development. J. Atmos. Sci. 64, 564–578.
Jacob, R., Larson, J., Ong, E., 2005. MxN communication and parallel interpolation in Community Climate System Model Version 3 using the model coupling toolkit. Int. J. High Perform. C. 19, 293–307.
Janssen, P.A.E.M., 1991. Quasi-linear theory of wind wave generation applied to wave forecasting. J. Phys. Oceanogr. 19, 745–754.
Janssen, P.A.E.M., 2004. The Interaction of Ocean Waves and Wind. Cambridge

University Press, pp. 300.
Janssen, P.A.E.M., 2008. Progress in ocean wave forecasting. J. Comput. Phys. 227 (7), 3572–3594. http://dx.doi.org/10.1016/j.jcp.2007.04.029.
Janssen, P.A.E.M., 2012. Ocean wave effects on the daily cycle in SST. J. Geophys. Res. 117, C00J32. http://dx.doi.org/10.1029/2012JC007943.
Janssen, P.A.E.M., Viterbo, P., 1996. Ocean waves and the atmospheric climate. J. Climate 9, 1269–1287.
Janssen, P.A.M.E., Hansen, B., Bidlot, J.-R., 1997. Verification of the ECMWF wave forecasting system against buoy and altimeter data. Weath. Forecasting 12, 763–784.
Janssen, P.A.E.M, Abdalla, S., Hersbach, H., 2003. Error estimation of buoy, satellite and model wave height data, Tech. Memorandum 402, European Center for Medium-Range Weather Forecasts, Reading UK.
Janssen, P.A.E.M., Saetra, Ø., Wettre, C., Hersbach, H., Bidlot, J.-R., 2004. Impact of the sea state on the atmosphere and ocean. Ann. Hydrogr. 3–772, 3.1–3.23.
Janssen, P.A.E.M., Abdalla, S., Hersbach, H., Bidlot, J.-R., 2007. Error estimation of buoy, satellite, and model wave height data. J. Atmos. Oceanic Technol. 24, 1665–1677. http://dx.doi.org/10.1175/JTECH2069.1.
Janssen, T.T., Herbers, T.H.C., 2009. Nonlinear wave statistics in a focal zone. J. Phys. Oceanogr. 39 (8), 1948–1964.
Janssen, T.T., Herbers, T.H.C., Battjes, J.A., 2008. Evolution of ocean wave statistics in shallow water: refraction and diffraction over seafloor topography. J. Geophys. Res. 113, C03024.
JCOMM, 2008. Final Report of the JCOMM Technical Workshop on Wave Measurements from Buoys, JCOMM-TR—047, WMO/TD-No. 1466, IOC-NO. 208. IOC Workshop Report No. 208, New York, NY, October 2008, < http://boram.lee.f.free.fr/data/J-TR-47-Wave-Buoy-Workshop/ > .
Jenkins, A.D., 1987. Wind and wave induced currents in a rotating sea with depth varying eddy viscosity. J. Phys. Oceanogr. 17, 938–951.
Jensen, R.E., Swail, V., Lee, B., O'Reilly, W.A., 2011. Wave measurement evaluation and testing. In: Proceedings of 12th International Workshop on Wave Hindcasting and Forecasting, Kohala Coast, Hawaii.
Jensen, R.E., Cialone, M.A., Chapman, R.S., Ebersole, B.A., Anderson, M., Thomas, L., 2012. Lake Michigan Storm: wave and water level modelling, Great Lakes Coastal Flood Study. In: 2012 Federal Inter-Agency Initiative, ERDC/CHL TR-12-26, USACE Engineer Research and Development Center, Vicksburg, MS, 330p.
Jensen, R.E., Swail, V.R., Buchard, R.H., Reily, R.E., Hesser, T.J., Blaseckie, M., MacIsaac. C., 2015. Field laboratory for ocean sea state investigation: FLOSSIE intra-measurement evaluation of 6N wave buoy systems. In: Proceedings of the 14th International Workshop on Wave Hindcasting and Forecasting, Key West, Florida, 8–13 November 2015.
Jiang, A., 2012. A linear theory of three-dimensional land-sea breezes. J. Atmos. Sci. 69, 1890–1909.
Jonsson, I.G., 1981. Booij's current–wave equation and the ray approximation. Technical report progress no. 54. Technical University of Denmark, Denmark, pp. 7–20.
Jonsson, I.G., 1990. Wave-current interactions. In: Le Mehaute, Hanes (Eds.), Chapter 3 in The Sea, Vol. 9, Part A. John Wiley & Sons, pp. 65–120.
Kahma, K.K., Calkoen, C.J., 1992. Reconciling discrepancies in the observed growth of wind-generated waves. J. Phys. Oceanogr. 22, 1389–1405.
Kaihatu, J.M., 2001. Improvement of parabolic nonlinear dispersive wave model. J. Waterw. Port Coastal Ocean Eng. 127 (2) 113-12.
Kaihatu, J.M., 2009. Application of a nonlinear frequency domain wave-current interaction model to shallow water recurrence effects in random waves. Ocean Modell. 26, 190–205.
Kaihatu, J.M., Kirby, J.T., 1995. Nonlinear transformation of waves in finite water depth. Phys. Fluids 8, 175–188.
Kalnay, E., 2003. Atmospheric Modelling, Data Assimilation and Predictability. Cambridge University Press, Cambridge, pp. 364 ISBN: 9780521796293.
Kantha, L.K., Clayson, C.A., 2004. On the effect of surface gravity waves on mixing in the oceanic mixed layer. Ocean Modell. 6 (2), 101–124.
Kennedy, A.B., Rogers, S., Sallenger, A., Gravois, U., Zachry, B., Dosa, M., Zarama, F., 2011. Building destruction from waves and surge on the Bolivar Peninsula during Hurricane Ike. J. Waterw. Port Coast. 137 (3), 132–141.
Kirby, J.T., 1984. A note on linear surface wave–current interaction over slowly varying topography. J. Geophys. Res. 162, 745–747. http://dx.doi.org/10.1029/JC089iC01p00745.
Kirby, J., 2003. Boussinesq Mmodels and applications to nearshore wave propagation, surf zone processes and wave-induced currents. In: Lakhan, C. (Ed.), Advances in Coastal Modelling. Elsevier Sciences, pp. 41.
Kirby, J.T., Chen, T.M., 1989. Surface waves on vertically sheared flows: approximate dispersion relations. J. Geophys. Res. Oceans 94, 1013–1027.
Kleijweg, J.C.M., Van Vledder, G.Ph., Steeghs, T.P.H., 2005. Integration of X-band remote sensing and numerical wave modelling of waves. In: Proc. Waves 2005, Madrid, Spain.
Kofoed-Hansen, H., Rasmussen, J.H., 1998. Modeling of nonlinear shoaling based on stochastic evolution equations. Coastal Eng. 33, 203–232.
Komen, G.J., Cavaleri, L., Donelan, M., Hasselmann, K., Hasselmann, S., Janssen, P.A.E.M., 1994. Dynamics and Modelling of Ocean Waves. Cambridge University Press, Cambridge.
Komen, G.J., Hasselmann, S., Hasselmann, K., 1984. On the existence of a fully developed wind-sea spectrum. J. Phys. Oceanogr. 14, 1271–1285.
Krogstad, H.E., Wolf, J., Thompson, S.P., Wyatt, L.R., 1999. Methods for intercomparison of wave measurements. Coastal Eng. 37, 235–257.
Kumar, N., Voulgaris, G., Warner, J.C., 2011. Implementation and modification of a three-dimensional radiation stress formulation for surf zone and rip-current applications. Coastal Eng. 58, 1097–1117. http://dx.doi.org/10.1016/ j.coastaleng.2011.06.009.
Kumar, N., Voulgaris, G., Warner, J.C., Olabarrieta, M., 2012. Implementation of the vortex force formalism in the coupled ocean-atmosphere-wave-sediment transport (COAWST) modelling system for inner shelf and surf zone applications. Ocean Modell. 47, 65–95.
Lai, R.J., Long, S.R., Huang, N.E., 1989. Laboratory studies of wave-current interaction: Kinematics of the strong interaction. J. Geophys. Res. Oceans 94, 16201–16214.
Landsea, C.W., Feuer, S., Hagen, A., Glenn, D.A., Sims, J., Perez, R., Chenoweth, M., Anderson, N., 2012. A reanalysis of the 1921–1930 Atlantic hurricane database. J. Climate 25, 865–885.
Langodan, S., Cavaleri, L., Anadhapalli, Y.V., Hoteit, I., 2014a. The Red Sea: a natural laboratory for wind and wave modelling. J. Phys. Oceanogr. 44, 3139–3159. http://dx.doi.org/10.1175/JPO-D-13-0242.1.
Langodan, S., Cavaleri, L., Viswanadhapalli, Y., Hoteit, I., 2014b. The Red Sea: a natural laboratory for wind and wave modelling. J. Phys. Oceanogr. 44, 3139–3159. http://dx.doi.org/10.1175/JPO-D-13-0242.1.
Langodan, S., Cavaleri, L., Viswanadhpaili, V., Hoteit, I., 2015. Wind-wave source functions in opposing seas. J. Geoph. Res. 6751–6768. http://dx.doi.org/10.1002/2015JC010816.
Lanser, D., Verwer, J.G., 1999. Analysis of operator splitting for advection-diffusion-reaction problems from air pollution modelling. J. Comput. Appl. Math. 111, 201–216.
Larson, J., Jacob, R., Ong, E., 2004. The model coupling toolkit: a new Fortran90 toolkit for building multiphysics parallel coupled models. Int. J. High Perform. C 19, 277–292.
Lax, P.D., Richtmyer, R.D., 1956. Survey of the stability of linear finite difference equations. Comm. Pure Appl. Math. 9, 267–293. http://dx.doi.org/10.1002/cpa.3160090206.
Lax, P.D., Wendroff, B., 1960. Systems of conservation laws. Commun. Pure Appl. Math. 13, 217–237.
Lesser, G.R., Roelvink, J.A., van Kester, J.A.T.M., Stelling, G.S., 2004. Development and validation of a three-dimensional morphological model. Coastal Eng. 51 (8–9), 883–915.
LeVeque, R.J., Yee, H.C., 1990. A study of numerical methods for hyperbolic conservation laws with stiff source terms. J. Comp. Phys. 86 (1), 187–210. http://dx.doi.org/10.1016/0021-9991(90)90097-K.
Lewis, H.W., Castillo Sanchez, J.M., Graham, J., Saulter, A., Bornemann, J., Arnold, A., Fallmann, J., Harris, C., Pearson, D., Ramsdale, S., Martínez-de la Torre, A., Bricheno, L., Blyth, E., Bell, V.A., Davies, H., Marthews, T.R., O'Neill, C., Rumbold, H., O'Dea, E., Brereton, A., Guihou, K., Hines, A., Butenschon, M., Dadson, S.J., Palmer, T., Holt, J., Reynard, N., Best, M., Edwards, J., Siddorn, J., 2018. The UKC2 regional coupled environmental prediction system. Geosci. Model Dev. 11, 1–42. http://dx.doi.org/10.5194/gmd-11-1-2018.
Li, J.-G., 2012. Propagation of ocean surface waves on a spherical multiple-cell grid. J. Comput. Phys. 231, 8262–8277.
Li, J.-G., Holt, M., 2009. Comparison of Envisat ASAR ocean wave spectra with buoy and altimeter data via a wave model. J. Atmos. Oceanic Technol. 26, 593–614.
Li, Q., Webb, A., Fox-Kemper, B., Craig, A., Danabasoglu, G., Large, W.G., Vertenstein, M., 2016. Langmuir mixing effects on global climate: WAVEWATCH III in CESM. Ocean Modell. 103, 145–160. http://dx.doi.org/10.1016/j.ocemod.2015.07.020.
Li, Q., Fox-Kemper, B., Breivik, Ø., Webb, A., 2017. Statistical models of global Langmuir mixing. Ocean Modell. 113, 95–114. http://dx.doi.org/10.1016/j.ocemod.2017.03.016.
Liau, J.-M., 2001. A Study of Wind Waves Hindcasting on the Coastal Waters (PhD Thesis). National, Cheng Kung University, Tainan, Taiwan.
Liau, J.-M., Roland, A., Hsu, T.-W., Ou, S.-H., Li, Y.-T., 2011. Wave refraction-diffraction effect in the wind wave model WWM. Coastal Eng. 58, 429–443.
Lionello, P., Günther, H., Janssen, P.A.E.M., 1992. Assimilation of altimeter data in a global third-generation wave model. J. Geophys. Res. 97 (14), 453–474. http://dx.doi.org/10.1029/92JC01055.
Liu, P.L.-F., 1990. Wave transformation. In: In: LeMehaute, B., Hanes, D.M.A. (Eds.), The Sea, vol. 9A. Wiley-Interscience, New York, NY, pp. 27–63.
Liu, Y., Yue, D.K.P., 1998. On generalized Bragg scattering of surface waves by bottom ripples. J. Fluid Mech. 356, 297–326.
Loescher, K.A., Young, G.S., Colle, B.A., Winstead, N.S., 2006. Climatology of barrier jets along the Alaskan coast. Part I: spatial and temporal distributions. Mon. Weather Rev. 134, 437–453.
Long, C.E., Oltman-Shay, J.M., 1991. Directional characteristics of waves in shallow water, US Army Corps of Engineers, Coastal Engineering Research Center, Technical Report CERC-91-1, USACE, Vicksburg, Mississippi, 152pp.
Longuet-Higgins, M.S., Stewart, R.W., 1960. Changes in form of short gravity waves on long tidal waves and tidal currents. J. Fluid Mech. 8, 565–583.
Longuet-Higgins, M.S., Stewart, R.W., 1961. The changes in amplitude of short gravity waves on steady non-uniform currents. J. Fluid Mech. 10, 529–549.
Longuet-Higgins, M.S., Stewart, R.W., 1962. Radiation stress and mass transport in gravity waves, with applications to "surf beats". J. Fluid Mech. 13, 481–504.
Longuet-Higgins, M.S., Stewart, R.W., 1964. Radiation stresses in water waves: a physical discussion, with applications. Deep Sea Res. 11, 529–562.
Luettich, R.A. Jr., Westerink. J.J., 2004. Formulation and Numerical Implementation of the 2D/3DADCIRC Finite Element Model Version 44.XX. < http://adcirc.org/adcirc_theory_2004_12_08.pdf > .
Luther, M.E., Meadows, G., Buckley, R., Gilbert, S.A., Purcell, H., Tamburri, M.N., 2013. Verification of wave measurement systems. Mar. Technol. Soc. J. 47 (5), 104–116.
MacIsaac, C., Naeth, S., 2013. TRIAXYS next wave II directional wave sensor. The evolution of wave measurements, MTS/EEE Oceans 2013, San Diego, California.
Madec, G., The NEMO team, 2012. NEMO Ocean Engine v3.4, Institut Pierre Simon Laplace, France, N.27, ISSN No. 1288-1619.
Madsen, O.S., Poon, Y.-K., Graber, H.C., 1988. Spectral wave attenuation by bottom friction: theory. In: Proc. 21th Int. Conf. Coastal Engineering, ASCE, pp. 492–504.

Madsen, P.A., Sørensen, O.R., 1992. A new form of the Boussinesq equations with improved linear dispersion characteristics. Part 2: a slowly-varying bathymetry. Coastal Eng. 18, 183–205.
Magne, R., Ardhuin, F., Rey, V., Herbers, T., 2005. Topographical scattering of waves: spectral approach. J. Waterw. Port Coastal Ocean Eng. 131 (6), 311–320.
Magnusson, A.K., Donelan, M.A., 2013. The Andrea wave characteristics of a measured north sea rogue wave. J. Offshore Mech. Arctic Eng. 135 (3), 031108-1.
Mahony, J., Pritchard, W., 1980. Wave reflexion from beaches. J. Fluid Mech. 101 (04), 809–832.
Makin, V.K., 2002. A note on the parametrisation of the sea drag. Boundary-Layer Meteorol. 106, 593–600.
Malardel, S., Wedi, N., Deconinck, W., Diamantakis, M., Kuhnlein, C., Mozdzynski, G., Hamrud, M., Smolarkiewicz, P., 2016. A new grid for the IFS, ECMWF Newsletter, No.146, pp. 23–28.
Malhadas, M., Neves, R., Leitao, P., Silva, A., 2010. Influence of tide and waves on water renewal in Obidos Lagoon, Portugal. Ocean Dynam. 60, 40–55.
Maresca, S., Braca, P., Horstmann, J., Grasso, R., 2014. Maritime surveillance using multiple high-frequency surface-wave radars. IEEE Trans. Geosci. Remote Sens. 52 (8), 5056–5071. http://dx.doi.org/10.1109/TGRS.2013.2286741.
Mase, H., 2001. Multidirectional random wave transformation model based on energy balance equation. Coastal Eng. J. 43, 317–337. http://dx.doi.org/10.1142/S0578563401000396.
Mass, C.F., Warner, M.D., Steed, R., 2014. Strong westerly wind events in the strait of Jan de Fuca. Weath. Forecasting 29, 445–465.
Masson, D., LeBlond, P.H., 1989. Spectral evolution of wind-generated surface gravity waves in a disperced ice field. J. Fluid Mech. 202, 43–81.
Mastenbroek, C., Burgers, G., Janssen, P.A.E.M., 1993. The dynamical coupling of a wave model and a storm surge model through the atmospheric boundary layer. J. Phys. Oceanogr. 23 (8), 1856–1866.
McWilliams, J.C., Restrepo, J.M., 1999. The wave-driven ocean circulation. J. Phys. Oceanogr. 29, 2523–2540.
McWilliams, J.C., Sullivan, P.P., 2000. Vertical mixing by Langmuir circulations. Spill Sci. Technol. Bull. 6 (3), 225–237. http://dx.doi.org/10.1016/S1353-2561.
McWilliams, J.C., Sullivan, P.P., Moeng, C.H., 1997. Langmuir turbulence in the ocean. J. Fluid Mech. 334, 1–30.
McWilliams, J.C., Restrepo, J.M., Lane, E.M., 2004. An asymptotic theory for the interaction of waves and currents in coastal waters. J. Fluid Mech. 511, 135–178.
Mellor, G., Blumberg, A., 2004. Wave breaking and ocean surface layer thermal response. J. Phys. Oceanogr. 34 (3), 693–698 doi:10/bftfk9.
Mellor, G., 2005. Some consequences of the three-dimensional current and surface wave equations. J. Phys. Oceanogr. 35 (11), 2291–2298.
Mellor, G., 2011. Wave radiation stress. Ocean Dyn. 61 (5), 563–568.
Mendez, F.M., Losada, I.J., 2004. An empirical model to estimate the propagation of random breaking and nonbreaking waves over vegetation fields. Coastal Eng. 51, 103–118.
Mentaschi, L., Besio, G., Cassola, F., Mazzino, A., 2013. Problems in RMSE-based wave model validations. Ocean Modell. 72, 53–58.
Miche, A., 1951. Le pouvoir reflechissant des ouvrages maritimes exposes a l'action de la houle. Annales des Ponts et Chaussees 121, 285–319.
Miles, J.W., 1957. On the generation of surface waves by shear flows. J. Fluid Mech. 3, 185–204.
Mogensen, K.S., Magnusson, L., Bidlot, J.-R., 2017. Tropical cyclone sensitivity to ocean coupling in the ECMWF coupled model. J. Geophys. Res. Oceans 122 (5), 4392–4412. http://dx.doi.org/10.1002/2017JC012753.
Monahan, E.C., 1971. Oceanic whitecaps. J. Phys. Oceanogr. 1, 139–144.
Monbaliu, J., Padilla-Henandez, R., Hargreaves, J.C., Albiach, J.C., Luo, W., Sclavo, M., Guenther, H., 2000. The spectral wave model, WAM, adapted for applications with high spatial resolution. Coastal Eng. 41, 41–62.
Mukai, A.Y., Westerink, J.J., Luettich, R.A., Mark, D., 2002. Eastcoast 2001, A tidal constituent database for western North Atlantic, Gulf of Mexico, and Caribbean Sea, ERDC/CHL TR-02-24, Vicksburg, MS, 194pp.
O'Reilly, W.C., 2007. An introduction to directional wave observations, Wave Sensor Workshop, Alliance for Coastal Technologies, St. Petersburg, Florida, March 7–9, 2007.
O'Reilly, W.C., Herbers, T.H.C., Seymour, R.J., Guza, R.T., 1996. A comparison of directional buoy and fixed platform measurements of Pacific swell. J. Atmos. Oceanic Technol. 13, 231–238.
Olabarrieta, M., Warner, J.C., Kumar, N., 2011. Wave-current interaction in Willapa Bay. J. Geophys. Res. Oceans 116 (C12014).
Oltman-Shay, J., Guza, R.T., 1984. A data-adaptive ocean wave directional-spectrum estimator for pitch and roll type measurements. J. Phys. Oceanogr. 14, 1800–1810.
Pallares, E., Sanchez-Arcilla, A., Espino, M., 2014. Wave energy balance in wave models (SWAN) for semi-enclosed domains – application to the Catalan coast. Continental Shelf Res. 87, 41–53.
Panteleev, G., Yaremchuk, M., Rogers, W.E., 2015. Adjoint-free variational data assimilation into a regional wave model. J. Technol. 32, 1238–1399. http://dx.doi.org/10.1175/JTECH-D-14-00174.1.
Pawka, S.S., 1983. Island shadows in wave directional spectra. J. Geophys. Res. 88, 2579–2591.
Pettersson, H., Graber, H.C., Hauser, D., Quentin, C., Kahma, K.K., Drennan, W.M., Donelan, M.A., 2003. Directional wave measurements from three wave sensors during the FETCH experiment. J. Geophys. Res. 108 (C3), 8061. http://dx.doi.org/10.1029/2001JC001164. 15pp.
Pettersson, H., Fortelius, C., Tikka, K., Björkqvist, J.-V., Kahma, K., 2014. Wave modelling in archipelagos. Coastal Eng. 83, 205–220.
Pezzutto, P., Saulter, A., Cavaleri, L., Bunney, C., Marcucci, F., Torrisi, L., Sebastianelli, S., 2016. Performance comparison of meso-scale ensemble wave forecasting systems in the Mediterranean Seat. Ocean Modell. 104, 171–186.
Phillips, O.M., 1977. The Dynamics of the Upper Ocean. Cambridge Univ. Press, Cambridge, pp. 336.
Pierson, W.J., 1983. The measurement of synoptic scale wind over the ocean. J. Geophy. Res. 88 (C3), 1683–1708.
Plant, W.J., Keller, W.C., Hayes, K., 2005. Simultaneous measurements of ocean winds and waves with an airborne coherent real aperture radar. J. Atmos. Oceanic Technol. 22, 832–846.
Polton, J.A., 2009. A wave averaged energy equation: Comment on "global estimates of wind energy input to subinertial motions in the Ekman-Stokes layer" by Bin Liu, Kejian Wu and Changlong Guan. J. Oceanogr. 65 (5), 665–668. http://dx.doi.org/10.1007/s10872-009-0057-1.
Polton, J.A., Belcher, S.E., 2007. Langmuir turbulence and deeply penetrating jets in an unstratified mixed layer. J. Geophys. Res. 112, C09020. http://dx.doi.org/10.1029/2007JC004205.
Polton, J.A., Lewis, D.M., Belcher, S.E., 2005. The role of wave-induced Coriolis-Stokes forcing on the wind-driven mixed layer. J. Phys. Oceanogr. 35 (4), 444–457. http://dx.doi.org/10.1175/JPO2701.1.
Pomaro, A., Cavaleri, L., Lionello, P., 2017. Characteristics and trends of the Adriatic Sea wind waves: analysis of a 37 year long instrument dataset. Int. J. Climatol. http://dx.doi.org/10.1002/joc.506.
Popinet, S., Gorman, R.M., Rickard, G.J., Tolman, H.L., 2010. A quadtree-adaptive spectral wave model. Ocean Modell. 34 (1), 36–49.
Portilla, J., 2009. Buoy data assimilation in nearshore wave modelling. PhD Dissertation. Katholieke Universiteit Leuven. pp. 193, ISBN: 9789460180743.
Portilla-Yandún, J., Cavaleri, L., 2016. On the specification of background errors for wave data assimilation systems. J. Geophys. Res. Oceans 120, 15. http://dx.doi.org/10.1002/2015JC011309.
Portilla-Yandún, J., Cavaleri, L., Van Vledder, G.Ph., 2015. Wave spectra partitioning and long term statistical distribution. Ocean Modell. 96 (P1), 148–160. http://dx.doi.org/10.1016/j.ocemod.2015.06.008.
Portilla, J., Ocampo-Torres, F.J., Monbaliu, J., 2009. Spectral partitioning and identification of wind sea and swell. J. Atmos. Oceanic Technol. 26, 107–122.
Portilla, J., Caicedo, A.L., Padilla-Hernandez, R., Cavaleri, L., 2015. Spectral wave conditions in the Colombian Pacific Ocean. Ocean Modell. 92, 149–168.
Prandle, D., Wyatt, L.R., 1999. Editorial Introduction to this special issue. Coastal Eng. 37, 193–199.
Qi, J., Chen, C., Beardsley, R.C., Perrie, W., Cowles, G., Lai, Z., 2009. An unstructured-grid finite-volume surface wave model (FVCOM-SWAVE): implementation, validations and applications. Ocean Modell. 28, 153–166.
Qiao, F., Yuan, Y., Yang, Y., Zheng, Q., Xia, C., Ma, J., 2004. Wave-induced mixing in the upper ocean: distribution and application to global ocean circulation model. Geophys. Res. Lett. 31, L11303. http://dx.doi.org/10.1029/2004GL019824.
Quinn, B.E., Toledo, Y., Shrira, V.I., 2017. Explicit wave action conservation for water waves on vertically sheared flows. Ocean Modell. 112, 33–47.
Rascle, N., Ardhuin, F., Terray, E.A., 2006. Drift and mixing under the ocean surface: a coherent one-dimensional description with application to unstratified conditions. J. Geophys. Res. 111, C03016. http://dx.doi.org/10.1029/2005JC003004.
Rasmussen, J.H., 1998. Deterministic and Stochastic Modelling of Surface Gravity Waves in Finite Depth. Ph.D. thesis. Technical University of Denmark.
Reistad, M., Breivik, Ø., Haakenstadt, H., Aarnes, O.J., Furevik, B.R., Bidlot, J.-R., 2011. A high-resolution hindcast of wind and waves for the North Sea, the Norwegian Sea and the Barents Sea. J. Geoph. Res. 116 (C5), C05019. http://dx.doi.org/10.1029/2010JC006402.
Ricchi, A., Miglietta, M.M., Barbariol, F., Bergamasco, A., Bonaldo, D., Benetazzo, A., Falcieri, F.M., Russo, A., Sclavo, M., Carniel, S., 2017. Sensitivity of a Mediterranean tropical-like cyclone to different model configurations and coupling strategies. Atmosphere 8 (5), 92. http://dx.doi.org/10.3390/atmos8050092.
Ricchiuto, M., Csík, A., Deconinck, A., 2005. Residual distribution for general time dependent conservation laws. J. Comput. Phys. 209 (1), 249–289.
Riley, R., Teng, C.-C., Bouchard, R., Dinoso, R., Mettlach, T., 2011. Enhancements to NDBC's digital directional wave module. In: Proceedings of MTS/IEEE Oceans 2011 Conference,Kona, Hawaii, September 2011.
Ris, R.C., Holthuijsen, L.H., Booij, N., 1999. A third-generation wave model for coastal regions: 2. Verification. J. Geoph. Res. Oceans 104 (C4), 7667–7681. http://dx.doi.org/10.1029/1998JC900123.
Rogers, W.E., Holland, K.T., 2009. A study of dissipation of wind-waves by mud at Cassino Beach, Brasil: prediction and inversion. Continental Shelf Res. 29, 676–690.
Rogers, W.E., Orzech, M.D., 2013. Implementation and testing of ice and mud source functions in WAVEWATCH III®. NRL Memorandum Report, NRL/MR/7320-13-9462, 31pp.
Rogers, W.E., Kaihatu, J.M., Petit, H.A.H., Booij, N., Holthuijsen, L.H., 2002. Diffusion reduction in a arbitrary scale third generation wind wave model. Ocean Eng. 29, 1357–1390.
Rogers, E.W., Hwang, P.A., Wang, D.W., 2003. Investigation of wave growth and decay in the SWAN model: three regional scale applications. J. Phys. Oceanogr. 33, 366–389.
Rogers, W.E., Kaihatu, J.M., Hsu, L., Jensen, R.E., Dykes, J.D., Holland, K.T., 2007. Forecasting and hindcasting waves with the SWAN model in the Southern California Bight. Coastal Eng. 54, 1–15.
Rogers, W.E., Babanin, A.V., Wang, D.W., 2012. Observation-consistent input and whitecapping-dissipation in a model for wind-generated surface waves: Description and simple calculations. J. Atmos. Ocean. Technol. 29, 1329–1346.
Röhrs, J., Christensen, K.H., Hole, L.R., Broström, G., 2012. Observation-based evaluation of surface wave effects on currents and trajectory forecasts. Ocean Dyn. 62 (10–12), 1519–1533. http://dx.doi.org/10.1007/s10236-012-0576-y.

Roland, A., 2008. Development of WWM II: Spectral wave modelling on unstructured meshes, PhD thesis. Inst. of Hydraul. and Water Resour. Eng., Tech. Univ. Darmstadt, Darmstadt, Germany.
Roland, A., 2014. Application of Residual Distribution (RD) schemes to the geographical part of the wave action equation, ECMWF Workshop on Ocean Waves, 25–27 June 2012, U.K. < https://www.ecmwf.int/sites/default/files/elibrary/2012/12002-application-residual-distribution-rd-schemes-geographical-part-wave-action-equation.pdf > .
Roland, A., Ardhuin, F., 2014. On the developments of spectral wave models: numerics and parameterisations for the coastal ocean. Ocean Dyn. 64, 833–846.
Roland, A., Mewis, P., Zanke, U., Ou, S.H., Hsu, T.W., Liau J.M., 2005. Verification and improvement of a spectral finite element wave model. In: Waves 2005, ASCE/COPRI, The Fifth International Symposium on Wave Measurement and Analysis. Billy Edge, Madrid, Spain.
Roland A., Zanke U., Hsu, T.W., Ou, S.H., Liau J.M., 2006. Spectral wave modelling on unstructured grids with the WWM (Wind Wave Model) – I: the deep water case. In: Third Chinese-German Joint Symposium on Coastal and Ocean Engineering (JOINT2006), Tainan, Taiwan.
Roland, A., Cucco, A., Ferrarin, C., Hsu, T.-W., Liau, J.-M., Ou, S.-H., Umgiesser, G., Zanke, U., 2009. On the development and verificationof a 2-D coupled wave-current model on unstructured meshes. J. Mar. Syst. 78, S244–S254.
Roland, A., Zhang, Y.J., Wang, H.V., Meng, Y., Teng, Y.C., Maderich, V., Brovchenko, I., Dutour-Sikiric, M., Zanke, U., 2012. A fully coupled 3D wave-current interaction model on unstructured grids. J. Geophys. Res. 117, C00J33. http://dx.doi.org/10.1029/2012JC007952.
Romeiser, R., 1993. Global validation of the wave model WAM over a one-year period using Geosat wave height data. J. Geophy. Res. 98 (C3), 4713–4726.
Ruessink, B.G., Walstra, D.J.R., Southgate, H.N., 2003. Calibration and verification of a parametric wave model on barred beaches. Coastal Eng. 48, 139–149.
Rusu, L., Guedes Soares, C., 2015. Impact of assimilating altimeter data on wave predictions in the western Iberian coast. Ocean Modell. 96 (P1), 126–135. http://dx.doi.org/10.1016/j.ocemod.2015.07.016.
Saetra, Ø., Albretsen, J., Janssen, P.A.E.M., 2007. Sea-state-dependent momentum fluxes for ocean modelling. J. Phys. Oceanogr. 37 (11), 2714–2725. http://dx.doi.org/10.1175/2007JPO3582.1.
Salmon, J.E., 2016. Surf wave hydrodynamics in the coastal environment. PhD thesis. Delft Univ. Tech., 155pp. Available at < http://repositery.tudelft.nl > .
Salmon, J.E., Holthuijsen, L.H., 2015. Modelling depth-induced wave breaking over complex coastal bathymetries. Coastal Eng. 105, 21–35.
Salmon, J.E., Holthuijsen, L.H., Zijlema, M., van Vledder, G.Ph., Pietrzak, J., 2015. Scaling depth-induced wave breaking in two-dimensional spectral wave models. Ocean Modell. 87, 30–47.
Salmon, J.E., Smit, P.B., Janssen, T.T., Holthuijsen, L.H., 2016. A consistent collinear triad approximation for operational wave models. Ocean Modell. 104, 203–212. http://dx.doi.org/10.1016/j.ocemod.2016.06.009.
Samiksha, S.V., Vethamony, P., Rogers, W.E., Pednekar, P.S., Babu, M.T., 2017. Wave energy dissipation due to mudbanks formed off southwest coast of India. Estuarine Coastal Shelf Sci. 196, 387–398.
Sanchez-Arcilla, A., Garcia-Leon, M., Gracia, V., 2014. Hydro morphodynamic modelling in Mediterranean storms. Errors and uncertainties under sharp gradients. Nat. Hazard Earth Syst. 2 (2), 1693–1728.
Saprykina, Y.V., Kuznetsov, I.V., Shugan, H.H., Hwun, W.Y., Hsu, Yan, R.Y., 2015. Discrete evolution of the surface wave spectrum on a nonuniform adverse current. In: Doklady Earth Sciences, vol. 464, no. 2. Springer Science & Business Media, p. 1075.
Scanlon, B., Breivik, O., Bidlot, J.-R., Janssen, P.A.E.M., Callaghan, A.H., Ward, B., 2016. Modelling whitecap fraction with a wave model. J. Phys. Oceanogr. http://dx.doi.org/10.1175/JPO-D-15-0158.1.
Sclavo, M., Cavaleri, L., Barstow, S.F., Athanassoulis, G.A., 2002. An efficient tool for wave climate analysis in European coastal waters, P.S.Z.N. Mar. Ecol. 23 (Suppl. 1), 361–369.
Sclavo M., Benetazzo, A., Carniel, C., Bergamasco, A., Falcieri, F.M., Bonaldo, D., 2013. Wave-current interaction effect on sediment dispersal in a shallow semi-enclosed basin. In: Conley, D.C., Masselink, P.E., Russell, O'Hare, T.J., (Eds.), Proc., 12th International Coastal Symposium (Plymouth, England), J. Coast. Res., Special Issue, vol. 65, pp. 1587–1592.
Semedo, A., Vettor, R., Breivik, Ø., Sterl, A., Reistad, M., Guedes Soares, C., Lima, D., 2015. The wind sea and swell waves climate in the Nordic seas. Ocean Dyn. 65 (2), 223–240. http://dx.doi.org/10.1007/s10236-014-0788-4.
Shchepetkin, A.F., McWilliams, J.C., 2005. The regional oceanic modelling system (ROMS): a split-explicit, free-surface, topography-following-coordinate oceanic model. Ocean Modell. 9 (4), 347–404. http://dx.doi.org/10.1016/j.ocemod.2004.08.002.
Sheldon, L., Czaja, A., 2014. Seasonal and interannual variability of an index of deep atmospheric convection over western boundary currents. Q. J. R. Meteorol. Soc. 140, 22–30. http://dx.doi.org/10.1002/qj.2103.
Shrira, V.I., Slunyaev, A.V., 2014. Nonlinear dynamics of trapped waves on jet currents and rogue waves. Phys. Rev. E 89 (4), 041002.
Shynu, R., Rao, V.P., Samiksha, S.V., Kessarkar, P.M., Vethamony, P., Naqvi, S.W.A., Babu, M.T., Dineshkumar, P.K., 2017. Suspended matter and fluid mud off Alleppey, southwest coast of India. Estuarine, Coastal Shelf Sci. 185, 31–43.
Siddons, L., Wyatt, L., Wolf, J., 2009. Assimilation of HF radar data into the SWAN wave model. J. Mar .Syst. V77 (I3), 312–324. http://dx.doi.org/10.1016/j.jmarsys.2007.12.017.
Skamarock, W.C., Klemp, J.B., Dudhia, J., Gill, D.O., Barker, D.M., Wang, W., Powers, J. G., 2005. A description of the advanced research WRF Version 2. NCAR Technical Note, NCAR/TN-468 + STR.
Skop, R.A., 1987. Approximate dispersion relation for wave-current interactions. J. Waterw. Port Coastal Ocean Eng. 113 (2), 187–195.
Skyllingstad, E.D., Denbo, D.W., 1995. An ocean large-eddy simulation of Langmuir circulations and convection in the surface mixed layer. J. Geophys. Res. 100 (C5), 8501–8522. http://dx.doi.org/10.1029/94JC03202.
Smedman, A., Larsen, X.G., Hogstrom, U., 2003. Effect of sea state on the momentum exchange over the sea during neutral conditions. J. Geophy. Res. 108 (C11), 3367. http://dx.doi.org/10.1029/2002JC001526. 13pp.
Smit, P.B., 2014. Deterministic and stochastic modelling of ocean surface waves. Ph.D. thesis. Delft University of Technology. The Netherlands, 155pp.
Smit, P.B., Janssen, T.T., 2013. The evolution of inhomogeneous wave statistics through a variable medium. J. Phys. Oceanogr. 43, 1741–1758.
Smit, P.B., Janssen, T.T., 2016. The evolution of nonlinear wave statistics through a variable medium. J. Phys. Oceanogr. 46 (2), 621–634.
Smit, P.B., Janssen, T.T., Holthuijsen, L.H., Smith, J.M., 2014. Non-hydrostatic modelling of surf zone wave dynamics. Coastal Eng. 83, 36–48.
Smit, P.B., Janssen, T.T., Herbers, T., 2015. Stochastic modelling of coherent wave fields over variable depth. J. Phys. Oceanogr. 45, 1139–1154.
Smith, R., 1975. Reflection of short gravity waves on a non-uniform cur- rent. Math. Proc. Cambridge Philos. Soc. 78, 517–525.
Smith, W.H.F., Sandwell, D.T., 1997. Global seafloor topography from satellite altimetry and ship depth soundings. Science 277, 1956–1962. <http://www.sciencemag.org/content/vol277/issue5334/>.
Smith, J.M., 2002. Wave pressure gauge analysis with current. J. Waterw. Port Coast. Ocean Eng. ASCE 128, 21–275.
Smith, J.M., Bermudez, H.E., Ebersole, B.A., 2000. Modelling waves at Willapa Bay, Washington. In: Proc. 27th International Conference on Coastal Engineering, pp. 826–839.
Smith, G.A., Babanin, A.V., Riedel, P., Young, I.R., Oliver, S., Hubbert, G., 2011. Introduction of a new friction routine into the SWAN model that evaluates roughness due to bedform and sediment size changes. Coastal Eng. 58, 317–326.
Smyth, W.D., Skyllingstad, E.D., Crawford, G.B., Wijesekera, H., 2002. Nonlocal fluxes and Stokes drift effects in the K-profile parameterization. Ocean Dyn. 52 (3), 104–115. http://dx.doi.org/10.1007/s10236-002-0012-9.
Sørensen, O.R., Schäffer, H.A., Sørensen, L.S., 2004. Boussinesq-type modelling using an unstructured finite element technique. Coastal Eng. 50, 181–198.
Soulsby, R.L., 1995. Bed shear-stresses due to combined waves and currents. In: Stive, M., Fredsøe, J., Hamm, L., Soulsby, R., Teisson, C., Winterwerp, J. (Eds.), Advances in Coastal Morphodynamics. Delft Hydraulics, Delft, The Netherlands, pp. 420–423.
Sportisse, B., 2000. An analysis of operator splitting techniques in the stiff case. J. Comput. Phys. 161 (1), 140–168.
Staneva, J., Wahle, K., Koch, W., Behrens, A., Fenoglio-Marc, L., Stanev, E.V., 2016. Coastal flooding: impact of waves on storm surge during extremes – a case study for the German Bight. Nat. Hazards Earth Syst. Sci. 16, 2373–2389. http://dx.doi.org/10.5194/nhess-16-2373-2016.
Staneva, J., Alari, V., Breivik, Ø., Bidlot, J.-R., Mogensen, K., 2017. Effects of wave-induced forcing on a circulation model of the North Sea. Ocean Dyn. 67, 81–101. http://dx.doi.org/10.1007/s10236-016-1009-0.
Steele, D.J., Dorling, S.R., Von Glasow, R., Bacon, J., 2013. Idealized WRF model sensitivity simulations o fsea breeze types and their effects on offshore windfields. Atmos. Chem. Phys. 13, 443–461.
Steele, K.E., Teng, C.-C., Wang, D.W.C., 1992. Wave direction wave measurements using pitch-roll buoys. IEEE J. Oceanic Eng. 19 (4), 349–372.
Steele, K.E., Wang, D.W., Earle, M.D., Michelena, E.D., Dagnall, R.J., 1998. Buoy pitch and roll computed using three angular rate sensors. Coastal Eng. 35, 123–139.
Steenburgh, W.J., Schultz, D.M., Colle, B.A., 1998. The structure and evolution of gap outflow over the Gulf of Tehuantepec, Mexico. Mon. Weather Rev. 126, 2673–2691.
Stiassnie, M., Drimer, N., 2006. Prediction of long forcing waves for harbor agitation studies. J. Waterw. Port Coast. Ocean Eng. 132 (3), 166–171.
Stockwell, R.G., Large, W.G., Milliff, R.F., 2004. Resonant inertial oscillations in moored buoy ocean surface winds. Tellus 56 (5), 536–547.
Stoffelen, E., 1998. Towards the true near-surface wind speed: Error modeling and calibration using triple collocation. J. Geoph. Res. 193 (C4), 7755–7766.
Stokes, G.G., 1847. On the theory of oscillatory waves. Trans. Cambridge Philos. Soc. 8, 441–455.
Suastika, I.K., 2012. A spectral model for blocking of random waves. Coastal Eng. J. 54 (02), 1250013 1-29.
Sullivan, P.P., McWilliams, J.C., 2010. Dynamics of winds and currents coupled to surface waves. Ann. Rev. Fluid Mech. 42, 19–42.
Sun, J., Vandermark, D., Mahrt, L., Vickers, D., Crawford, T., Vogel, C., 2001. Momentum transfer over the coastal zone. J. Geophy. Res. 106 (D12), 12437–12448. http://dx.doi.org/10.1029/2000JD900696.
Sutherland, J., Walstra, D.J.R., Chesher, T.J., van Rijn, L.C., Southgate, H.N., 2004. Evaluation of coastal area modelling systems at an estuary mouth. Coastal Eng. 51, 119–142.
Suzuki, T., Zijlema, M., Burger, B., Meijer, M.C., Narayan, S., 2011. Wave dissipation by vegetation with layer schematisation in SWAN. Coastal Eng. 59, 64–71.
Swail, V., Jensen, R.E., Lee, B., Turton, J., Thomas, J., Gulev, S., Yelland, M., Etala, P., Meldrum, D., Birkemeier, W., Burnett, W., Warren, G., 2009. Wave measurements, needs and developments for the next decade. In: Proceedings of OceanObs'09, vol. 2 II-1-87, pp. 999–1008.
Tamura, H., Miyazawa, Y., Oey, L.-Y., 2012. The Stokes drift and wave induced-mass flux in the North Pacific. J. Geophys. Res. 117, C08021. http://dx.doi.org/10.1029/2012JC008113.
Tatavarti, V., Huntley, D.A., Bowen, A.J., 1988. Incoming and outgoing wave interactions on beaches. Coastal Eng. Proc. 1 (21).

Teixeira, M., Belcher, S., 2002. On the distortion of turbulence by a progressive surface wave. J. Fluid Mech. 458, 229–267. http://dx.doi.org/10.1017/S0022112002007838.
Teng, C.-C., Bouchard, R.H., 2005. Directional wave measured from data buoys using angular rate sensors and magnetometers. In: 5th Ocean Wave Measurement and Analysis, ASCE, Madrid, Spain.
Thompson, E.T., 1977. Wave climate at selected locations along U.S. coasts, Technical Report, TR-77-1. USACE Coastal Engineering Research Center, Fort Belvoir, Va.
Thomson, J., 2012. Wave breaking dissipation observed with "SWIFT' drifters. J. Atmos. Oceanic Technol. 29, 1866–1882.
Timpe, G.L., Van de Voorde, N., 1995. NOMAD buoys: an overview of forty years of use, OCEANS'95, MTS/IEEE, Challenges of Our Changing Global Environment, vol. 1, 309-315, 9–12 October 1995, San Diego, California.
Toledo, Y., 2013. The oblique parabolic equation model for linear and nonlinear wave shoaling. J. Fluid Mech. 715, 103–133.
Toledo, Y., Agnon, Y., 2009. Nonlinear refraction–diffraction of water waves: the complementary mild-slope equations. J. Fluid Mech. 641, 509–520.
Toledo, Y., Agnon, Y., 2012. Stochastic evolution equations with localized nonlinear shoaling coefficients. Eur. J. Mech. (B/Fluids) 34, 13–18.
Toledo, Y., Hsu, T.-W., Roland, A., 2012. Extended time-dependent mild-slope and wave-action equations for wave-bottom and wave-current interactions. Proc. R. Soc. Lond. A 468, 184–205. http://dx.doi.org/10.1098/rspa. 2011.0377.
Tolman, H.L., 1991a. Effects of tides and storm surges on North Sea wind waves. J. Phys. Oceanogr. 21, 766–781.
Tolman, H.L., 1991b. A third-generation model for wind waves on slowly varying, unsteady, and inhomogeneous depths and currents. J. Phys. Oceanogr. 21, 782–797.
Tolman, H.L., 1992. Effects of numerics on the physics in a third-generation wind-wave model. J. Phys. Oceanogr. 22, 1095–1111.
Tolman, H.L., 2002a. Validation of WAVEWATCH III version 1.15 for a global domain, NOAA/NWS/NCEP/OMB Technical Note Nr. 213, 33pp.
Tolman, H.L., 2002b. Limiters in third-generation wind wave models. Global Atmos. Ocean Syst. 8, 67–83.
Tolman, H.L., 2003. Treatment of unresolved islands and ice in wind wave models. Ocean Modell. 5, 219–231.
Tolman, H.L., 2007. The 2007 Release of WAVEWATCH.10, International Workshop on Wave Hindcasting and Forecasting, North Shore, Oahu, Hawaii.
Tolman, H.L., 2009. User manual and system documentation of WAVEWATCH-III version 3.14.NOAA/NWS/NCEP/MMAB Technical Note 222, 220pp.
Tolman, H., Balasubramaniyan, B., Burroughs, L.D., Chalikov, D.V., Chao, Y.Y., Chen, H.S., Gerald, V.M., 2002. Development and implementation of wind-generated ocean surface wave models at NCEP. Weath. Forecasting 17 (2), 311–333. http://dx.doi.org/10.1175/1520-0434(2002) 017<0311:DAIOWG>2.0.CO;2.
Tolman, H.L., Banner, M.L., Kaihatu, J.M., 2013. The NOPP operational wave model improvement project. J. Ocean Modell. 70, 2–10. http://dx.doi.org/10.1016/j.ocemod.2012.11.011.
Trainor, L.T., 2009. Field observation and SWAN model Predictions of wave evolution in a muddy coastal environment. M.Sc. dissertation. Naval Post Graduate School, Monterey, 73pp.
Tsujimoto, K., Koike, T., 2013. Land-lake breezes at low latitudes: the case of Tonle Sap Lake in Cambodia. J. Geophy. Res: Atmos. 118, 6970–6980.
Tucker, M.J., 1991. Waves in ocean engineering: Measurement, analysis, interpretation. Ellis Horwood, pp. 431.
Tuomi, L., Kahma, K.K., Pettersson, H., 2011. Wave hindcast statistics in the seasonally ice-covered Baltic Sea, Boreal. Env Res. 16, 451–472.
Tuomi, L., Kahma, K., Fortelius, C., 2012. Modelling fetch-limited wave growth from an irregular shoreline. J. Mar. Syst. 105–108, 96–105. http://dx.doi.org/10.1016/j.jmarsys.2012.06.004.
Uchiyama, Y., McWilliams, J.C., Shchepetkin, A.F., 2010. Wave-current interaction in an oceanic circulation model with a vortex-force formalism: application to the surf zone. Ocean Modell. 34 (1–2), 16–35.
van Unen, R.F., vandBeuzekom, A.A., Forristall, G.Z., Mathisen, J.-P., Starke, J., 1998. Wacsis—Wave crest sensor intercomparisonstudy at the Meetpost Noordwijk measurement platform. Oceans '98, Nice, France. IEEE, pp. 192–197.
Veeramony, J., Walker, D., Hsu, L., 2010. A variational data assimilation system for nearshore applications of SWAN. Ocean Modell. V35 (I3), 206–214. http://dx.doi.org/10.1016/j.ocemod.2010.07.008.
Vignudelli, S., Scozzari, A., Woodworth, P., Wolf, J., Barbosa, S., Gomez-Enri, J., 2012. Development of radar altimetry data processing in the oceanic coastal zone, ESA/ESRIN Contract No. 21201/08/I-LG-CCN 3 (Phase 2), Report on validation of reprocessed height and waves, COASTALT2-EWP5-D52-v12b.doc. < http://www.coastalt.eu/files/results/COASTALT2-D52-12b.pdf > .
Voorrips, A.C., Makin, V.K., Hasselmann, S., 1997. Assimilation of wave spectra from pitch-and-roll buoys in a North Sea wave model. J. Geophys. Res. 102 (C3), 5829–5849. http://dx.doi.org/10.1029/96JC03242.
Voronovich, A.G., 1976. Propagation of internal and surface gravity waves in the approximation of geometrical optics. Atmos. Oceanic Phys. 12, 850–857.
Vrecica, T., Toledo, Y., 2016. Consistent nonlinear stochastic evolution equations for deep to shallow water wave shoaling. J. Fluid Mech. 794, 310–342.
Wadhams, P., 1973. Attenuation of swell by sea ice. J. Geoph. Res. 78 (18), 3552–3563.
Wahle, K., Staneva, J., Guenther, H., 2015. Data assimilation of ocean wind waves using Neural Networks. A case study for the German Bight. Ocean Modell. 96 (P1), 117–125. http://dx.doi.org/10.1016/j.ocemod.2015.07.007.
Walsh, E.J., Wright, C.W., Vandemark, D., Krabill, W.B., Garcia, A.W., Houston, S.H., Murillo, S.T., Powell, M.D., Black, P.G., Marks Jr., F.D., 2002. Hurricane directional wave spectrum spatial variation at landfall. J. Phys. Oceanogr. 32, 1667–1684.
WAMDI Group, 1988. The WAM model – a third generation ocean wave prediction model. J. Phys. Oceanogr. 18, 1775–1810.
Wang, D.W., Liu, A.K., Peng, C.Y., Meindl, E.A., 1994. Wave-current interaction near the Gulf Stream during the Surface Wave Dynamics Experiment. J. Geophy. Res 99 (C3), 5065–5079.
Ward, B., Fristedt, T., Callaghan, A.H., Sutherland, G., Sanchez, X., Vialard, J., ten Doeschate, A., 2014. The Air-Sea Interaction Profiler (ASIP): an autonomous upwardly rising profiler for microstructure measurements in the upper ocean. J. Atmos. Oceanic Tech. 31 (10), 2246–2267.
Warner, J.C., Armstrong, B., He, R., Zambon, J.B., 2010. Development of a Coupled Ocean–Atmosphere–Wave–Sediment Transport (COAWST) Modelling System. Ocean Modell. 35 (3), 230–244. http://dx.doi.org/10.1016/j.ocemod.2010.07.010.
Warner, J.C., Sherwood, C.R., Signell, R.P., Harris, C., Arango, H.G., 2008a. Development of a three-dimensional, regional, coupled wave, current, and sediment-transport model. Comput. Geosci. 34, 1284–1306.
Warner, J.C., Perlin, N., Skyllingstad, E.D., 2008b. Using the Model Coupling Toolkit to couple earth system models. Environ. Modell. Softw. 23, 1240–1249.
Waters, J., Wyatt, L., Wolf, J., Adrian, H., 2013. Data assimilation of partitioned HF radar wave data into Wavewatch III. Ocean Modell. 72, 17–31. http://dx.doi.org/10.1016/j.ocemod.2013.07.003.
Weber, J.E., 1983. Steady wind- and wave-induced currents in the open ocean. J. Phys. Oceanogr. 13, 524–530 doi:10/djz6md.
Weller, R.A., Donelan, M.A., Brisco, M.G., Huang, N.E., 1991. Riding the crest: a tale of two wave experiments. AMS Bull. 72 (2), 163–183.
Westerink, J.J., Luettich, R.A., Feyen, J.C., Atkinson, J.H., Dawson, C., Roberts, H.J., Powell, M.D., Dunion, J.P., Kubatko, E.J., Pourtaheri, H., 2008. A basin to channel scale unstructured grid hurricane storm surge model applied to Southern Louisiana. Mon. Weather Rev. 136 (3), 833–864.
Westhuysen, A.J. Van der, 2010. Modelling of depth-induced wave breaking under finite depth wave growth conditions. J. Geophs. Res 115, C01008. http://dx.doi.org/10.1029/2009JC005433.
Westhuysen, A.J. Van der, Van Dongeren, A.R., Groeneweg, J Van, Vledder, G.Ph., Peters, H., Gautier, C., Van Nieuwkoop, J.C.C., 2012. Improvements in spectral wave modelling in tidal inlets. J. Geophys. Res. 117, C00J28. http://dx.doi.org/10.1029/2011JC007837.
Westhuysen, A.J. Van der, Padilla-Hernandez, R., Santos, P., Gibbs, A., Gaer, D., Nicolini, T., Tjaden, S., Devaliere, E.M., Tolman, H.L., 2013. Development and validation of the Nearshore Wave Prediction System. In: Proc. 93rd AMS Annual Meeting, Am. Meteor. Soc., Austin, 2013.
Westhuysen, A.J. Van der, Taylor, A.A., Padilla-Hernandez, P., Gibbs, A., Santos, P., Gaer, D., Cobb III, H.D., Lewitsky, J.R., Rhome, J.R., 2014. Enhancements to the nearshore wave prediction system to provide coastal and overland hurricane wave guidance. In: Proc. 94th AMS Annual Meeting, Am. Meteor. Soc., Atlanta, 2014.
Whitham, G.B., 1974. Linear and Nonlinear Waves. John Wiley and Sons, New York, pp. 636.
Willebrand, J., 1975. Energy transport in a nonlinear and inhomogeneous random gravity wave field. J. Fluid Mech. 70, 113–126.
Winstead, N.S., Colle, B.A., Bond, N., 2004. Synthetic aperture radar and high-resolution MM5 simulations of barrier jets in coastal Alaska. In: Geoscience and Remote Sensing Symposium, IGARAS'04, Proceedings IEEE International, pp. 140–143.
Winterwerp, J.C., de Graaff, R.F., Groeneweg, J., Luijendijk, A.P., 2007. Modelling wave damping at Guyana mud coast. Coastal Eng. 54, 249–261.
Wolf, J., Brown, J.M., Howarth, M.J., 2011. The wave climate of Liverpool Bay - observations and modelling. Ocean Dyn. 61 (5), 639–665. http://dx.doi.org/10.1007/s10236-011-0376-9.
Wu, J., 1979. Oceanic whitecaps and sea state. J. Phys. Oceanogr. 9, 1064–1068. http://dx.doi.org/10.1175/1520-0485(1979) 0092.0.CO;2.
Wyatt, L.R., Green, J.J., Gurgel, K.-W., Nieto Borge, J.C., Reichert, K., Hessner, K., Gunther, H., Rosenthal, W., Saetra, Ø., Reistad, M., 2003. Validation and intercomparisons of wave measurements and models during the EuroROSE experiments. Coastal Eng. 48, 1–28.
Wyatt, L.R., Green, J.J., Middleditch, A., 2009. Signal sampling inpacts on HF radar wave measurements. J. Atmos. Oceanic Technol. 26, 793–805.
Wyatt, L.R., Liakhovetsk, G., Graber, H.C., Haus, B.K., 2005. Factors affecting the accuracy of SHOWEX HF radar wave measurements. J. Atmos. Oceanic Technol. 22, 847–859.
Yanenko, N.N., 1971. The Method of Fractional Steps. Springer-Verlag, pp. 150 ISBN 978-3-642-65108-3.
Yildirim, B., Karniadakis, G.-E., 2012. A hybrid spectral/DG method for solving the phase-averaged ocean wave equation: algorithm and validation. J. Comput. Phys. 231 (14), 4921–4953.
Young, I.R., 1999. Wind Generated Ocean Waves. Elsevier, pp. 288.
Young, I.R., Verhagen, L.A., 1996a. The growth of fetch limited waves in water of finite depth. Part I: total energy and peak frequency. Coastal Eng. 28, 47–78.
Young, I.R., Verhagen, L.A., 1996b. The growth of fetch limited waves in water of finite depth. Part II: spectral evolution. Coastal Eng. 28, 79–100.
Zieger, S., Babanin, A.V., Rogers, W.E., Young, I.R., 2015. Observation-based source terms in the third-generation wave model WAVEWATCH. Virtual Special Issue on Ocean Surface Waves. Ocean Modell. 96, 2–25. http://dx.doi.org/10.1016/j.ocemod.2015.07.014.
Zijlema, M., 2009a. Parallel, unstructured mesh implementation for SWAN. In: Smith, J. M. (Ed.), Proc. 31th Int. Conf. on Coast. Engng., Hamburg, Germany, 2009, pp. 470–482.
Zijlema, M., 2009b. Application of UnSWAN for wave hindcasting in the Dutch Wadden Sea. In: 11th Int. Workshop on Wave Hindcasting and Forecasting, Halifax, Canada, session M5.
Zijlema, M., 2010. Computation of wind-wave spectra in coastal waters with SWAN on

unstructured grids. Coastal Eng. 57, 267–277.
Zijlema, M., Van der Westhuysen, A.J., 2005. On convergence behaviour and numerical accuracy in stationary SWAN simulations of nearshore wind wave spectra. Coast. Eng. 52, 237–256.
Zijlema, M., Stelling, G.S., 2008. Efficient computation of surf zone waves using the nonlinear shallow water equations with non-hydrostatic pressure. Coastal Eng. 55, 780–790.
Zijlema, M., Stelling, G.S., Smit, P.B., 2011. SWASH: an operational public domain code for simulating wave fields and rapidly varied flows in coastal waters. Coastal Eng. 58, 992–1012.
Zijlema, M., Van Vledder, G.Ph., Holthuijsen, L.H., 2012. Bottom friction and wind drag for wave models. Coastal Eng. 65, 19–26.
Zingone, E., Hufford, G.L., 2006. Analysing surface wind fields near lower cook inlet and Kodiak waters using SAR. In: 14th Conference on Satellite Meteorology and Oceanography, Anchorage Alaska, Session J4-11, Anchorage, Alaska, NOAA/NWS, 30 Jan–2 Feb. 2006.
Zuh, M., Atkinson, B.W., 2004. Observed and modelled climatology of the land-sea breeze circulation over the Persian Gulf. Int. J. Climatol. 24, 883–905.